

UNIVERSITY OF SOUTHAMPTON

School of Civil Engineering and the Environment

**Performance of Granular Drainage Systems
Permeated by Low Organic Strength Leachate**

by

Ralitza Nikolova

Thesis for the degree of Doctor of Philosophy

April 2004

Acknowledgements

The work presented in this thesis was made possible with the support of many people. I would first like to acknowledge the generous guidance, encouragement and mentorship of my supervisor Prof. William Powrie. I am grateful for the informative discussions and suggestions of Dr. David Smallman and for his devotion keeping the experimental apparatus running while I was away. I am indebted to Dr. John Robinson from the University of London who shared his experience in the field of microbiology and for his and his wife Pamela's endless and unconditional support and being like father and mother to me here in England. I would like to acknowledge the support of Prof. Bill Keevil at the School of Biological Sciences for the fruitful discussions and technical guidance about biofilm imaging in the latest stages of the thesis. I am grateful to the technicians in the laboratory – Deryk Taylor, Harvey Skinner and Steve Wake for their technical assistance in maintaining the experimental apparatus.

I would like to thank my mother and father for their unconditional love and unwavering encouragement and for always being next to me. I am grateful to my father for sharing his life-long experience in the field of engineering and for always believing in me. I would also like to say special thanks to all my friends for their friendship and support.

The financial opportunity to study at the University of Southampton and undertake this research was possible through the sponsorship of British Nuclear Fuels Ltd.

Abstract

The research is concerned with the leachate collection systems for in-ground repositories for the disposal of low-level radioactive waste. The drainage system can become ineffective in the long-term due to clogging, which can be microbiological, chemical or physical in nature. The objectives of this research were to investigate the mechanisms and the potential for biological and chemical clogging. The role of the sulphates dissolved in the leachate and their contribution to the clogging process was also studied with a particular focus on the competition for organic substrate between the sulphate-reducing and methanogenic bacteria. In addition, a review of previous work was made with the aim of establishing a common framework explaining the significance of different factors on the microbially mediated clogging of landfill drainage systems in general.

Four permeameter columns modelling sections of the drainage system were set up. The columns were operated as saturated drainage layers and were permeated by two different types of synthetic leachate. The rate of clogging was monitored by measuring changes in the drainable porosity of the aggregate.

The results indicated that:

- The development of organic clog material reached a steady state at the low organic loading rate of 0.1 mgCOD/cm³.day, although the operational conditions employed were limited in terms of their time scale and physico-chemistry.
- The development of chemical clog material, which consisted of low solubility salts as FeS and CaCO₃ can be significant but only in the long term. The accumulation of FeS is influenced by the availability of iron species. The accumulation of CaCO₃ precipitates was significant but only occurred for Ca concentrations exceeding the aqueous solubility limit of the CaCO₃ salt.
- Polysaccharides, produced by the bacterial populations under nitrogen and phosphorus limited conditions in the columns, and entrapment of gas bubbles in the pore space played a significant role in the clogging of the drainage aggregate.
- Column dismantling revealed that the clog remains relatively porous and permeable when its nature is mainly biological but becomes cemented and impermeable if accumulation of CaCO₃ precipitates has occurred.
- The laboratory tests investigated the competition between the sulphate reducing and methanogenic bacteria when acetate is used as substrate. The results indicated that sulphate reduction preceded methanogenesis.

The overall results indicated that the clog material will be mainly organic in nature with the entrapment of gas bubbles. For the operational period and conditions employed in the laboratory column experiments the quantity of clog material will reach a steady state leaving the drainage system relatively permeable.

Contents

Acknowledgements	i
Abstract	ii
Contents	iii
LIST OF FIGURES	vi
LIST OF TABLES	viii
Chapter 1	1
Introduction	1
1.1. Background	1
1.2. Objectives.....	4
1.3. Thesis outline	4
Chapter 2	6
Basic mechanisms of anaerobic biodegradation	6
2.1. Biochemical stabilisation of organic matter in the leachate drainage system.....	6
2.1.1. Stage I: aerobic degradation	7
2.1.2. Stage II: hydrolysis and acidogenesis.....	7
2.1.3. Stage III: acetogenesis	8
2.1.4. Stage IV: methanogenesis	9
2.1.5. Stage V	11
2.2. Other bacterial reactions and their significance.....	11
2.2.1. Competition between sulphate reduction and methanogenesis.....	12
2.3. Nutritional Requirements.	14
2.3.1. Carbon, nitrogen, phosphate and sulphur nutrition.....	14
2.3.2. Micronutrients and Trace Elements.....	14
2.4. Mechanism of leachate production and leachate types.....	15
2.5. Landfill Gas.....	15
Chapter 3	17
Literature review on the mechanisms of clogging	17
3.1. Field studies.....	17
3.1.1. German experience as reported by Brune et al. (1991)	17
3.1.2. Canadian experience at Keele Valley Landfill, Maple, Ontario, Canada	22
3.1.3. Landfill in Florida, Craven et al.	26
3.2. Mesocosm experiments	27
3.2.1. Operational set up.....	27
3.2.2. Saturated layer.....	29
3.2.3. Unsaturated layer.....	30
3.2.4. Separator layer.....	30
3.2.5. Chemical analysis of leachate.....	31
3.2.6. Dismantling	32
3.3. Column experiments.....	32
3.3.1. Brune et al. (1991).....	32
3.3.2. Paksy et al. (1995 and 1998)	36
3.3.3. Column studies, Rowe et al. (2000a, b, 2001b and c)	42
3.4. Comparison between the column experiments carried out by Brune <i>et al.</i> (1991), Rowe <i>et al.</i> (2000a) and Paksy <i>et al.</i> (1999).....	54
3.4.1. 4 mm size particles	56

3.4.2.	6 mm size particles	57
3.4.3.	15 mm size particles	61
3.4.4.	20 mm size particles	63
3.4.5.	Common observations for all the groups	64
3.5.	Mechanism of clogging	65
3.5.1.	Microbiological clogging	65
3.5.2.	Bio-chemical clogging.....	66
3.5.3.	Development of clogging with time	68
3.6.	Scope for new research.....	70
Chapter 4.....	71	
Site Description and Test History	71	
4.1.	Site description	71
4.2.	Current leachate collection system	72
4.3.	Proposed future leachate collection system	72
4.4.	Test History	73
Chapter 5.....	74	
Materials and Methods	74	
5.1.	Column design.....	74
5.2.	Column operation	76
5.2.1.	Inoculation.....	76
5.2.2.	Continuous feeding regime (100% strength leachate).....	78
5.2.3.	Continuous feeding regime (200% strength leachate and high VFA, high SO ₄ ²⁻ type leachate) 80	
5.2.4.	Continuous feeding regime (low VFA, high SO ₄ ²⁻ type leachate with radionuclide analogues) 81	
5.3.	Analytical measurements.....	84
5.3.1.	VFA analysis	84
5.3.2.	Iron analysis	86
5.3.3.	Anion analysis (Cl, NO ₂ , NO ₃ , PO ₄ , SO ₄).....	87
5.3.4.	Cation analysis (Na ⁺ , NH ₄ ⁺ , K ⁺ , Mg ⁺ , Ca ²⁺)	87
5.3.5.	Gas analysis.....	88
5.3.6.	ICPMS analysis	88
5.3.7.	Carbon analysis	88
5.3.8.	Polysaccharide analysis	89
5.3.9.	XRF analysis	89
5.4.	Gas volume measurements	90
5.5.	Measurement of the rate of clogging.....	91
5.5.1.	Hydraulic gradient	91
5.5.2.	Drainable porosity	92
5.6.	Experimental design improvements	93
5.6.1.	Development of new method of gas measurement and installation of an overflow u-tube... 93	
5.6.2.	Power supply of the pressure transducers.....	93
5.6.3.	Lowering the leachate level in the column headspace.....	93
5.6.4.	Modification of the leachate inlet port.....	94
5.6.5.	Gas analysis.....	94
Chapter 6.....	96	
Results and Discussion	96	
6.1.	Columns supplied with leachate with high VFA (994 mg/l) and low SO ₄ ²⁻ (18 mg/l) concentrations, 50% and 100% strength leachate - columns 1 and 2	96
6.1.1.	VFA removal from the leachate	97
6.1.2.	pH measurements	101
6.1.3.	Iron concentrations	102
6.1.4.	Sulphate reduction	102
6.1.5.	Calcium concentrations	105
6.1.6.	Gas volume.....	106
6.1.7.	Gas composition	107
6.1.8.	Calculating the expected rate of gas generation on the basis of acetate and propionate degradation.	109
6.1.9.	Changes in hydraulic gradient	111
6.1.10.	Reduction in drainable porosity.....	111
6.2.	Column supplied with leachate with high VFA (1988 mg/l) and low SO ₄ ²⁻ (36 mg/l) concentrations – column 1, 200 % strength.....	116

6.2.1. VFA removal from the leachate	116
6.2.2. Sulphate reduction	118
6.2.3. Calcium concentrations	119
6.2.4. Gas volume	120
6.2.5. Calculating the expected rate of gas generation on the basis of acetate and propionate degradation	121
6.2.6. Reduction in drainable porosity	122
6.3. Columns supplied with leachate with low VFA (182 mg/l) and high SO_4^{2-} (1120 mg/l) concentrations (columns 3 and 4)	126
6.3.1. VFA removal from the leachate	126
6.3.2. pH measurements	127
6.3.3. Iron measurements	128
6.3.4. Radionuclide concentrations	129
6.3.5. Sulphate reduction	132
6.3.6. Calcium concentrations	134
6.3.7. Gas volume and composition	135
6.3.8. Changes in hydraulic conductivity	136
6.3.9. Reduction in drainable porosity	136
6.4. Column supplied with leachate with high VFA (994 mg/l) and high SO_4^{2-} (1120 mg/l) concentrations - column 4	140
6.4.1. VFA removal from the leachate	141
6.4.2. pH measurements	143
6.4.3. Sulphate reduction	144
6.4.4. Calcium concentrations	146
6.4.5. Gas volume	146
6.4.6. Reduction in drainable porosity	148
6.4.7. Comparison with the columns supplied with high VFA/low SO_4^{2-} and low VFA/high SO_4^{2-} type leachate	151
6.5. Summary of results regarding the clogging of the drainage aggregate	152
6.5.1. Measured inorganic constituents (Fe^{2+} , SO_4^{2-} , Ca^{2+})	152
6.5.2. Measured organic constituents	154
6.5.3. Volume of clog material	154
6.5.4. Comparison between the different operational regimes	156
6.6. Summary of results regarding the competition between SRB and methanogenic bacteria.	157
6.7. Summary of results regarding the adaptation of the bacterial populations to the increased nutrient concentrations	157
6.8. Comparison of the clogging rates with data from other researchers	158
6.9. Dismantling of Column 3	162
6.9.1. Dismantling procedure	162
6.9.2. Chemical analysis of the clog material	165
6.9.3. Optical images of fully hydrated biofilm	167
6.9.4. Polysaccharide and carbon analysis	173
6.10. Dismantling of Column 1	175
6.10.1. Dismantling procedure	176
6.10.2. Chemical analysis of the clog material	177
6.10.3. Findings from dismantling of columns 1 and 3	178
6.11. Conceptual model of clogging observed in the laboratory experiments	178
Chapter 7	180
Conclusions	180
References	184
Appendices	190
Appendix A - VFA, SO_4 , Ca, gas and drainable pore volume data for columns 1 and 4 (duplicates)	190
Appendix B - Total gas production in columns 1 and 2	195
Appendix C - Cumulative g VFA passed per litre pore volume in columns 1,2,3 and 4	201
Appendix D - Concentration of radionuclide analogues removed, inlet concentration - 20 $\mu\text{g/l}$, 200 $\mu\text{g/l}$, 2000 $\mu\text{g/l}$	210
Appendix E - XRF data for 10 samples of clean aggregate	217

LIST OF FIGURES

Figure 1-1: Typical containment measures (Daniel, 1993)	3
Figure 2-1: Sequence of use of electron acceptors in energy formation (From: Stumm and Morgan, 1996)	11
Figure 2-2: Competition between methanogenic and sulphate reducing bacteria	12
Figure 3-1: Mesocosm operational set up	28
Figure 3-2: Drainable porosity profiles: after 118 days at 1 litres/day and 104 days at 2 litres/day (left) and at column failure, 256 days at 1 litre/day and 216 days at 2 litres/day (right) (Rowe <i>et al.</i> , 2000b)	44
Figure 3-3: Drainable porosity profiles: after 165 -171 days (left) and at column failure (right) Rowe <i>et al.</i> (2000a)	46
Figure 3-4: Conceptual model showing the effect of different size particles on the clogging process	47
Figure 3-5: Dimensions of the experimental columns employed by the different researchers	55
Figure 3-6: Correlation between the volume of clog material and total COD removed for the 4 mm particle size group.	57
Figure 3-7: Correlation between the volume of clog material and total COD removed for the 6 mm particle size group	59
Figure 3-8: Amount of COD and inorganics needed to obtain equal volume of clogging in the 6 mm particle sizes group.	60
Figure 3-9: Correlation between the volume of clog material and total COD removed for the 15 mm particle sizes group	61
Figure 3-10: Correlation between the volume of clog material and total COD removed for the 20 mm particle size group	64
Figure 3-11: Correlation between the volume of clog material and total COD retained for all particle sizes	65
Figure 3-12: Model of the architecture of single-species biofilm (Costerton <i>et al.</i> , 1995)	66
Figure 3-13: Formation of incrustations (after Brune <i>et al.</i> , 1991); VFA - volatile fatty acids	67
Figure 3-14: Mechanism of clogging	69
Figure 5-1: The experimental column	75
Figure 5-2: The linear dependence of \log_{10} of the first hydrolysis constant on the ratio of the charge to the Metal-Oxygen distance (z/d) for four groups of cations	82
Figure 5-3: Initial experimental set up Figure 5-4: Experimental set up after modification of gas measuring system 95	
Figure 6-1: Acetic acid concentrations measured at the column inlet, tapping 2 and the column outlet since introduction of 50% strength leachate in column 2.	97
Figure 6-2: Propionic acid concentrations measured at the column inlet, tapping 2, tapping 3 and the column outlet since introduction of 50% strength leachate in column 2.	99
Figure 6-3: pH measurements in column 2	101
Figure 6-4: Iron concentrations in the inlet container for column 2, 100% strength leachate	102
Figure 6-5: Effect of pH on hydrogen sulphide equilibrium in an aqueous medium (Sawyer, 1978)	103
Figure 6-6: Sulphate concentrations measured at the column inlet, tapping 2 and column outlet since the introduction of 50% strength leachate in column 2.	104
Figure 6-7: Total calcium concentrations measured at the column inlet, tapping 2 and column outlet since the introduction of 50% strength leachate in column 2.	105
Figure 6-8: Measured cumulative volume of gas produced in column 2 since introduction of 100% strength leachate	106
Figure 6-9: Daily volume of gas produced in column 2	107
Figure 6-10: Measured and calculated cumulative volume of gas produced in column 2 since introduction of 100% strength leachate	110
Figure 6-11: Drainable porosity in column 2	112
Figure 6-12: The effect of gas bubbles on the drainable porosity in column 2, 100% strength	114
Figure 6-13: Growth curve of a bacterial culture (from Schlegel, 1987)	115
Figure 6-14: Acetate removal in column 1 since introduction of 200% strength leachate	116
Figure 6-15: Propionic acid removal in column 1, 200% strength leachate	118
Figure 6-16: Sulphate removal in column 1, 200% strength leachate	119
Figure 6-17: Calcium concentrations in column 1 since introduction of 200% strength leachate	120
Figure 6-18: Gas production in column 1 since introduction of 200% strength leachate	120
Figure 6-19: Daily gas production in column 1 since introduction of 200% strength leachate	121
Figure 6-20: Volume of calculated and measured cumulative volume of gas in column 1 since introduction of 200% strength leachate	122
Figure 6-21: Drainable porosity in column 1	123
Figure 6-22: Effect of gas bubbles on the drainable porosity in column 1 following introduction of 200% strength leachate	125

Figure 6-23: Acetic acid concentrations measured at the column inlet, tapping 2 and the column outlet since introduction of 50% strength leachate in column 3	126
Figure 6-24: pH measurements in columns 3 and 2	128
Figure 6-25: Iron concentrations in the inlet container for column 3, 100% strength leachate	129
Figure 6-26: Radionuclide concentration at column outlet at 20µg/l	130
Figure 6-27: Radionuclide concentration at column outlet at 200µg/l	130
Figure 6-28: Radionuclide concentration at column outlet at 2000µg/l	131
Figure 6-29: Sulphate concentrations measured at the column inlet, tapping 2 and column outlet since the introduction of 50% strength leachate in column 3	132
Figure 6-30: Total calcium concentrations measured at the column inlet, tapping 2 and column outlet since the introduction of 50% strength leachate in column 3	134
Figure 6-31: Relationship between CO ₂ and the three forms of alkalinity at various pH levels (Sawyer and McCarty, 1978).....	136
Figure 6-32: Drainable porosity in column 3.....	137
Figure 6-33: Effect of gas bubbles in column 3.....	139
Figure 6-34: Cumulative g VFA passed per litre pore volume required to clog the top section of columns 3 and 4	140
Figure 6-35: Acetic acid removal in column 4 since introduction of leachate containing high VFA, high SO ₄ ²⁻ concentrations	141
Figure 6-36: Propionic acid removal in column 4 since introduction of leachate containing high VFA, high SO ₄ ²⁻ concentrations	143
Figure 6-37: pH measurements in column 4 since introduction of high VFA, high SO ₄ ²⁻ type leachate.	144
Figure 6-38: Sulphate removal in column 4 since introduction of leachate containing high VFA, high SO ₄ ²⁻ concentrations.....	144
Figure 6-39: Calcium removal in column 4 since introduction of leachate containing high VFA, high SO ₄ ²⁻ concentrations.....	146
Figure 6-40: Gas production in column 4, high VFA, high SO ₄ ²⁻ type leachate.....	147
Figure 6-41: Inverted pipette method for gas measurements.....	147
Figure 6-42: Reduction in drainable porosity in column 4 since introduction of leachate containing high VFA, high SO ₄ ²⁻ concentrations	149
Figure 6-43: Effect of gas bubbles on the drainable porosity in column 4, high VFA, high SO ₄ ²⁻ type leachate	150
Figure 6-44: Schematic diagram showing the measured and calculated species.....	153
Figure 6-45: Amount of COD and inorganic substances needed to obtain 0.5 litres of clogging.....	160
Figure 6-46: Set up for column dismantling.....	163
Figure 6-47: 6 mm aggregate.....	163
Figure 6-48: 40 mm aggregate.....	164
Figure 6-49: Biofilm structure.....	167
Figure 6-50: Water channel	168
Figure 6-51: Finger of polysaccharide.....	168
Figure 6-52: Conceptual model of the architecture of single-species biofilm (From Costerton <i>et al.</i> , 1995)	169
Figure 6-53: Live bacteria cells.....	170
Figure 6-54: Dead bacterial cells.....	170
Figure 6-55: Live/Dead merged image.....	171
Figure 6-56: Nodules of precipitates	171
Figure 6-57: Water channels.....	172
Figure 6-58: Water channels.....	172
Figure 6-59: Water channels and individual bacterial cells.....	173
Figure 6-60: Cementation of the top column section (top-2)	176
Figure 6-61: Close-up of the top column section.....	176
Figure 6-62: Conceptual model.....	179

LIST OF TABLES

Table 2-1: Values for the energy released during anaerobic and aerobic degradation of organic matter (Tchobanoglous <i>et al.</i> , 2002).....	10
Table 3-1: Comparison of clog composition (% of total dry mass except for the Ca/CO ₃ ratio)	25
Table 3-2: Parameters relating to the column tests carried out by Brune <i>et al.</i> (1991) and supplied with highly loaded leachate	34
Table 3-3: Parameters relating to column tests carried out by Paksy <i>et al.</i> (1999).....	39
Table 3-4: Days in operation and leachate volume passed in columns supplied with 1 and 2 litres/day leachate.....	45
Table 3-5: Raw data relating to the results shown on Figure 3-3.	48
Table 3-6: Days in operation, litres of leachate passed and days in operation at the designed flow rate in columns containing 4, 6 and 15 mm beads.....	48
Table 3-7: Parameters regarding the column tests carried out by Rowe <i>et al.</i> (2000a) investigating the effect of different sizes particles on the clogging.	49
Table 3-8: Organic and inorganic loading for the 4 mm particle size group	56
Table 3-9: Organic and inorganic loading for the 6 mm particle size group	58
Table 3-10: Organic and inorganic loading for the 15 mm particle size group	62
Table 3-11: Organic and inorganic loading for the 20 mm particle size group	63
Table 5-1: Mass and height of the aggregates placed in the different columns	76
Table 5-2: Composition of the simulated Drigg waste/G6 sand layer.....	77
Table 5-3: Mass of the simulated waste layer (inclusive of the Drigg sand) placed in each permeameter column.....	77
Table 5-4: Composition of simulated leachates A and B (full strength).....	78
Table 5-5: Leachate constituents	79
Table 5-6: Hydraulic retention times and organic load for columns 1 to 4	80
Table 5-7: Composition of simulated leachates A (200%) and high VFA, high SO ₄ ²⁻ type leachate.....	80
Table 5-8: Radioactive elements and their analogues.....	81
Table 5-9: Compounds containing the radionuclide analogues of interest	82
Table 5-10: Background concentrations of the radionuclide analogues in the leachate supplied to column 3.	83
Table 5-11: Periods of each operational regime, flow rates and organic load for each permeameter column	85
Table 5-12: Air and Biogas component densities.....	91
Table 6-1: Composition of the gas produced (05/05/99 – commencement of full strength leachate) in column 2.....	107
Table 6-2: Drainable pore volumes on draining column 2	113
Table 6-3: Drainable pore volumes on filling column 2 in upward flow.....	115
Table 6-4: Drainable pore volumes on draining column 1	124
Table 6-5: Drainable pore volumes on filling column 1 in upward flow.....	125
Table 6-6: Masses of radionuclide analogues in mg removed at 20 µg/l	131
Table 6-7: Masses of radionuclide analogues in mg removed at 200µg/l	131
Table 6-8: Masses of radionuclide analogues in mg removed at 2000µg/l	132
Table 6-9: Amounts in mg of radionuclide sulphides formed at each operational regime - 20 µg/l, 200µg/l and 2000 µg/l of radionuclide analogues in column 3.....	134
Table 6-10: Headspace gas composition in columns 3 and 4.	135
Table 6-11: Drainable pore volumes on draining the column 3	138
Table 6-12: Drainable pore volumes on filling column 3 in upward flow.....	139
Table 6-13: Drainable pore volumes on draining column 4	149
Table 6-14: Drainable pore volumes on filling column 4 in upward flow.....	151
Table 6-15: Concentration of inorganic constituents and amounts removed from the leachate.	153
Table 6-16: Summary of changes in concentration of the organic constituents	154
Table 6-17: Volumes of the clog material	155
Table 6-18: Adaptation of the bacterial population.....	158
Table 6-19: Comparison between the leachate compositions, organic and inorganic load employed by Rowe <i>et al.</i> (2000a), Paksy <i>et al.</i> (1999) and this thesis.	159
Table 6-20: Ratio between carbon, nitrogen and phosphorus in the leachate medium used in this study. ...	161
Table 6-21: Samples taken at dismantling of column 3	164
Table 6-22: Amounts mg/kg of elements deposited on the drainage aggregate in column 3	165
Table 6-23: Amounts in mmol of elements deposited per kg of aggregate in column 3	166
Table 6-24: Amounts of metals retained for the whole column 3	166
Table 6-25: Total polysaccharide content expressed in terms of carbon (mg)	174
Table 6-26: Total amount of carbon in 15 ml extracted material	175

Table 6-27: Percent of polysaccharides	175
Table 6-28: Amounts mg/kg of elements deposited on the drainage aggregate in column 1	177
Table 6-29: Amounts in mmol of elements deposited per kg of aggregate in column 1	177

Chapter 1

Introduction

1.1. Background

All industrial activities produce wastes. Some of these wastes by the nature of the process, can be radioactive. It has been recognised that radioactive wastes are potentially hazardous and that special measures should be taken to ensure that they are disposed of in ways that protect human health and minimise their impact on the environment. Radioactive wastes are classified as high-level, intermediate-level and low-level, according to the amount of radioactivity in them (Clark, 1998).

This thesis concerns the low-level radioactive waste (LLW) only. LLW is generated from hospitals, laboratories and universities as well as nuclear power stations, nuclear fuel cycle facilities and isotope manufacturers. It typically contains protective clothing and gloves worn by the workers in nuclear plants, filters and other materials used to treat radioactive liquids, waste paper, packaging material, plastic sheeting and scrap metal (Clark, 1998). LLW can be classified, according to its composition, as:

- biodegradable - textiles, paper, timber, cardboard, rubber and plastics
- metals and steel
- inert - glass, concrete and excavation soil (British Nuclear Fuels Ltd., 2002).

Worldwide, LLW comprises 90% of the volume and only 1% of the radioactivity of all radioactive waste (Clark, 1998).

This thesis will focus on the in-ground disposal of LLW and the main hazards arising from it. Usually LLW is buried in shallow disposal sites. Following deposition, the organic fraction of a low level radioactive waste will begin to undergo chemical and microbiological degradation, resulting in the production of biochemical breakdown products including gases. The infiltration of rainfall, ground and surface waters into the waste mass, coupled with these breakdown products can produce leachate which contains waste particles, organic carbon and nitrogen compounds, heavy metals, radioactive elements and microorganisms (Clark, 1998). Uncontrolled release of leachate is one of the main potential hazard arising from the in-ground disposal of LLW, the others being contamination through airborne particles, ionising radiation and gases. Placement of LLW beneath a soil cover usually provides sufficient control to ensure that the risks to the general public from airborne contaminated particles and ionising radiation are kept to an acceptable level (Figure 1-1). The impact of gas can similarly be controlled by the provision of gas wells that allows any gas to be collected (Figure 1-1).

The control of leachate is usually more problematic and demands more consideration and engineering to find an acceptable long-term solution. In a LLW disposal site, the control of leachate is generally achieved through the combined strategies of:

- reducing infiltration into the waste to limit the potential volume of leachate generated
- providing a drainage system to remove leachate if generated
- placement of a low permeability layer beneath the drainage system to prevent residual leachate escaping from the site.

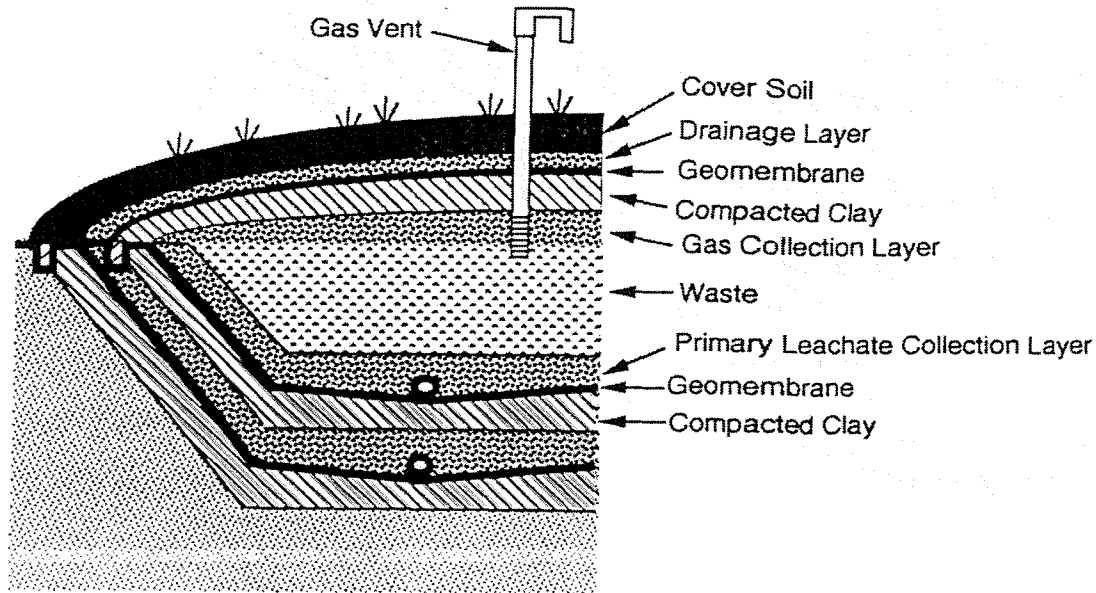


Figure 1-1: Typical containment measures (Daniel, 1993)

This project concerns the leachate drainage systems of LLW repositories and their long term performance bearing in mind the extended time period (up to 10,000 years) over which a repository may be required to function. Field observations in municipal landfill sites have indicated that leachate collection systems have a finite service life and can fail due to the build up of biofilm, chemical precipitates and small (e.g. silt and sand) particles (Fleming *et al.*, 1999). This build up is referred to as clogging and results in reduced hydraulic conductivity of the drainage layer leading to development of a leachate mound, which can subsequently result in increased advective migration of leachate through the barrier system into the ground or surface water (Fleming *et al.*, 1999). Laboratory studies investigating the mechanisms governing the clogging of leachate drainage systems have been carried out by various researchers but again always in the context of traditional municipal landfills (Brune *et al.*, 1991; Paksy *et al.*, 1998 and Rowe *et al.*, 2000a, b). A particular focus of their studies was the effect of CaCO_3 precipitation on clogging, while the contribution of the sulphates and metals on the clogging received rather less attention. Neither laboratory research, nor field investigations have been carried out to evaluate the performance of leachate collection systems in repositories containing LLW. Although LLW is superficially similar to domestic waste, the major differences are that the biodegradable fraction is limited to cellulose, resulting in leachate with considerably lower organic and occasionally high sulphate and metal contents (Humphreys *et al.*, 1996).

1.2.Objectives

The objectives of this research were:

- to investigate the potential for biological and chemical clogging of leachates representative of those emanating from low level radioactive waste disposal sites, which are characterised by lower organic, higher sulphate and possibly metal contents.
- to investigate the role of the sulphates and their contribution to the clogging process, with a particular focus on the competition for organic substrate between the sulphate-reducing and methanogenic bacteria and its implication for the clogging process.
- to review previous work, make comparisons and try to establish a common framework explaining the significance of different factors on microbially mediated clogging of landfill drainage systems in general.

1.3.Thesis outline

This thesis consists of seven chapters. Following this introduction, the second chapter introduces the basic mechanisms of the anaerobic biodegradation of waste that result in leachate production, highlighting the mechanisms that are also relevant to the processes that occur in the drainage system.

Chapter 3 incorporates a literature review of the mechanisms of leachate collection system clogging. The investigations carried out by the other researchers are divided into field observations, mesocosm and column studies. Finally a comparison between previous column experiments is made.

Chapter 4 provides information on the disposal site and the link between the field conditions and the laboratory set up.

Chapter 5 describes the design and operation of the experimental apparatus used in this study. Improvements in the design of the apparatus made during the study are outlined, and the analytical methods used are reviewed.

Chapter 6 examines the results in terms of reduction in the drainable porosity and the concurrent clogging of the drainage aggregate in the experimental columns. In addition the changes in the composition of the leachate during flow through the column with regard to the removal of the organic substrate and the reduction in sulphates are presented to allow investigation of the competition between sulphate-reducing and methanogenic bacteria. The volumes of the gas produced are reported and compared with the theoretical gas generation rates. The results are compared with those obtained by other researchers and a discussion on the further understanding of the mechanisms of clogging is made. In addition the chapter provides data on the chemical and microbiological composition of the clog material retrieved from the columns on their dismantling. On the basis of all the results, a conceptual model of the microbially mediated clogging is developed.

Chapter 7 presents the most important conclusions drawn from the work and outlines the future work.

Chapter 2

Basic mechanisms of anaerobic biodegradation

Following deposition the organic fraction of the waste will undergo microbial degradation. When water percolates through wastes that are undergoing decomposition, both biological and chemical (organic and inorganic) constituents will be leached in solution to form leachate. The dissolved organic constituents in the leachate will be degraded, as the leachate percolates downwards under the influence of gravity towards the leachate collection system, by the bacterial populations present in the waste. If decomposition is not completed within the waste body, degradation will continue in the drainage system. The following chapter makes a review of the basic mechanisms of the anaerobic biodegradation of waste that result in leachate production, highlighting the mechanisms that are also relevant to the processes that occur in the drainage system.

2.1. Biochemical stabilisation of organic matter in the leachate drainage system

Degradation of the organic fraction of the waste and the organic compounds within the leachate drainage system may be idealised as a five stage process. The first and fifth stages occur under aerobic conditions while stages 2 to 4 take place under predominantly anaerobic conditions. It should be noted that the literature review has focused on the degradation processes occurring under conditions encountered in landfill sites and leachate drainage systems. Although, the conditions encountered in LLW repository differ, mainly due to the low proportion of biodegradable material in LLW, the degradation processes that will occur in general will be similar.

2.1.1. Stage I: aerobic degradation

The first stage of the process is *aerobic degradation*, which occurs both during and for a period after waste placement and probably throughout the initial operation of the leachate drainage system. This stage is characterised with rapid metabolism of a proportion of the organic fraction of waste and dissolved organic substances in the leachate by aerobic microorganisms already present in the waste (Rovers and Farquhar, 1972). These microorganisms convert readily biodegradable carbohydrates to simple sugars, such as glucose, carbon dioxide and water.

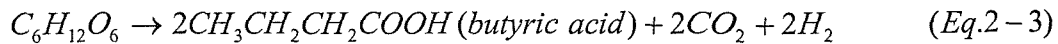
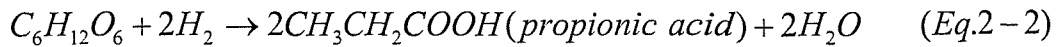
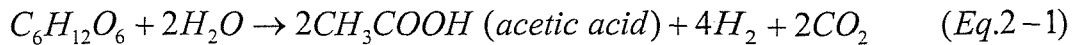
The duration of the aerobic stage depends on the availability of oxygen, which is influenced by management practices at the site such as the degree of waste compaction, the depth of the waste and the type of daily cover. Practices such as on-site compaction of deposited material and increasing the water content of the waste all reduce the pore space available for oxygen ingress. Furthermore as more waste is added to the site, oxygen flow into the underlying waste is impeded due to increased flow path, utilisation by near-surface waste and self-weight-compaction.

2.1.2. Stage II: hydrolysis and acidogenesis

As oxygen becomes depleted, further stages of degradation develop. The aerobic microorganisms are superseded by groups of micro-organisms which can tolerate low levels of oxygen (facultative anaerobes) and then, as anaerobic conditions develop, the obligate anaerobic micro-organisms which include the methane generating organisms (methanogens) become established. These processes are dynamic, each new stage being dependent on the creation of a suitable environment by the preceding stage.

In the second stage of the process, *hydrolysis and acidogenesis*, carbohydrates, lipids and proteins are first hydrolysed by appropriate microbial organisms to simple monomers. For example, cellulose is hydrolysed by cellulolytic organisms to yield simple sugars, protein is hydrolysed to amino acids, and lipid - to fatty acids and glycerol. These monomer derivatives are then fermented during the *acidogenic* phase to yield, as end products, a mixture of volatile fatty acids (VFA), hydrogen and ammonium. The spectrum of VFA

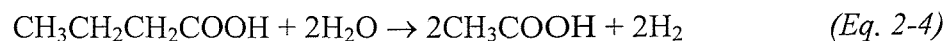
produced depends on the original substrate and prevailing digestion conditions but mainly consists of a mixture of acetic, propionic and butyric acids.



Other VFAs such as valeric and caproic acid can also be produced. *Acidogenesis* is the energy yielding stage for the hydrolytic and fermentative microorganisms.

2.1.3. Stage III: acetogenesis

In the third stage, *acetogenesis*, obligate hydrogen producing acetogenic bacteria (OHPA) convert the long-chain VFAs (propionic, butyric, valeric and caproic acids) to acetate, carbon dioxide and hydrogen. The long chain VFAs are degraded sequentially by subtraction of two-carbon fragments. VFAs with an even number of carbon atoms are degraded step-wise to form acetate: for example, one mole of butyric acid is degraded to form two moles of acetate:



VFAs with odd numbers of carbon atoms are degraded to form acetate and propionate: for example, one mole of valeric acid is degraded to one mole of acetate and one mole of propionate:



The propionate is then further broken down to acetate:



During this stage the gases generated from the waste mass are predominately carbon dioxide and hydrogen.

The conversion of the longer chain fatty acids to acetate requires energy input under standard conditions (25°C, 1 atmosphere pressure, pH=7.0). Acetogenesis must therefore be coupled with energy liberating reactions and to proceed hydrogen must be removed or

the concentration of hydrogen maintained at a very low partial pressure (Archer, 1988). If the hydrogen concentration remains greater than 10^{-4} atmospheres partial pressure the long-chain VFAs cannot be further degraded and under these circumstances propionic and butyric acids accumulate (acid souring). Consequently, *acetogenesis* can only be maintained if hydrogen utilising organisms such as methane-generating and sulphate-reducing bacteria are active. The relationship between the acetogenic and hydrogen removing bacteria is further explored in section 2.1.4.

2.1.4. Stage IV: methanogenesis

During *methanogenesis*, the methane-generating bacteria metabolise acetate, hydrogen and carbon dioxide produced during the previous degradation stages to form methane. Two main forms of methanogenic metabolisms have been found. These are:

- the hydrogen utilising metabolism, where the carbon dioxide and hydrogen, produced during acetogenesis provide the substrate for methane production.



This reaction releases very small amounts of free energy, which is just enough to sustain cell growth, resulting in very low growing rates (Rovers and Farquhar, 1972).

and

- the acetate utilising or aceticlastic metabolism, in which acetate is used for methane and carbon dioxide production.



This reaction releases slightly more energy and is energetically more favourable (Rovers and Farquhar, 1972). However, under field conditions no energetic advantage has been reported for either reaction (Archer, 1988).

The doubling time of methanogenic bacteria varies from 24 hours to several days (Tchobanoglous *et al.*, 2002). These slow rates of growth are due to the low biomass yield (Y) expressed in terms of the amount of biomass produced to the amount of substrate utilised under anaerobic conditions. Values for Y of only 0.046 g cells COD/g COD utilised was calculated for anaerobic systems, compared with 0.59 g cells COD/g COD utilised for aerobic (Tchobanoglous *et al.*, 2002). The biomass yield is directly related

with the free energy released, which is 3.57 kJ/electron equivalent during the methanogenic anaerobic process compared with 105 kJ/ electron equivalent for aerobic reactions as shown in Table 2-1. The significant difference in the energy released is because when CO₂ is used as a final electron acceptor, instead of O₂, a considerable amount of energy is needed to incorporate CO₂ into the bacterial cells (Tchobanoglous *et al.*, 2002). This results in much slower degradation of organic substances under anaerobic than aerobic conditions.

Reaction	Energy released (kJ/electron equivalent)
Aerobic degradation	
$\frac{1}{8}\text{CH}_3\text{COO}^- + \frac{3}{8}\text{H}_2\text{O} \rightarrow \frac{1}{8}\text{CO}_2 + \frac{1}{8}\text{HCO}_3^- + \text{H}^+ + e^-$	-27.66
$\frac{1}{4}\text{O}_2 + \text{H}^+ + e^- \rightarrow \frac{1}{2}\text{H}_2\text{O}$	-78.14
Total energy release	-105.82
Anaerobic degradation	
$\frac{1}{8}\text{CH}_3\text{COO}^- + \frac{3}{8}\text{H}_2\text{O} \rightarrow \frac{1}{8}\text{CO}_2 + \frac{1}{8}\text{HCO}_3^- + \text{H}^+ + e^-$	-27.66
$\frac{1}{8}\text{CO}_2 + \text{H}^+ + e^- \rightarrow \frac{1}{8}\text{CH}_4 + \frac{1}{8}\text{HCO}_3^-$	+24.11
Total energy release	-3.57

Note: The values for the energy released are obtained for the transfer of 1 mole of electrons in oxidation-reduction reactions. The negative sign shows release of energy.

Table 2-1: Values for the energy released during anaerobic and aerobic degradation of organic matter (Tchobanoglous *et al.*, 2002)

Methanogenic bacteria are very sensitive to hydrogen concentrations, being substrate for methane production, and pH, being most active in the pH range 6.8-7.4, and are dependant upon both. Thus, acetogenesis and methanogenesis form a symbiotic (mutually beneficial) relationship, where the methanogenic bacteria depend on the acetogenic bacteria to provide acetate and H₂ required for methane generation, and in turn the acetogenic bacteria depend on the methanogenic bacteria to remove H₂, accumulation of which leads to suppression of acetogenesis. As methanogenic bacteria are very slow growing bacteria, they are unlikely to be present in the early stages of refuse degradation. Their initial absence would lead to increased partial pressure of hydrogen, which would in turn result in inhibition of the acetogenesis and accumulation of long-chain VFAs thus lowering the pH, leading to further inhibition of methanogenesis.

2.1.5. Stage V

In the final stage of the process as the degradable components are exhausted, progressive re-establishment of aerobic conditions can occur.

2.2. Other bacterial reactions and their significance

Other types of anaerobic metabolism are possible when certain ions (NO_3^- , SO_4^{2-} , Fe^{3+}) are present in the leachate. Under these conditions the degradation of the available dissolved organic matter (CH_2O) is expected to follow the sequential use of alternative electron acceptors as shown in Figure 2-1 (Stumm and Morgan, 1996).

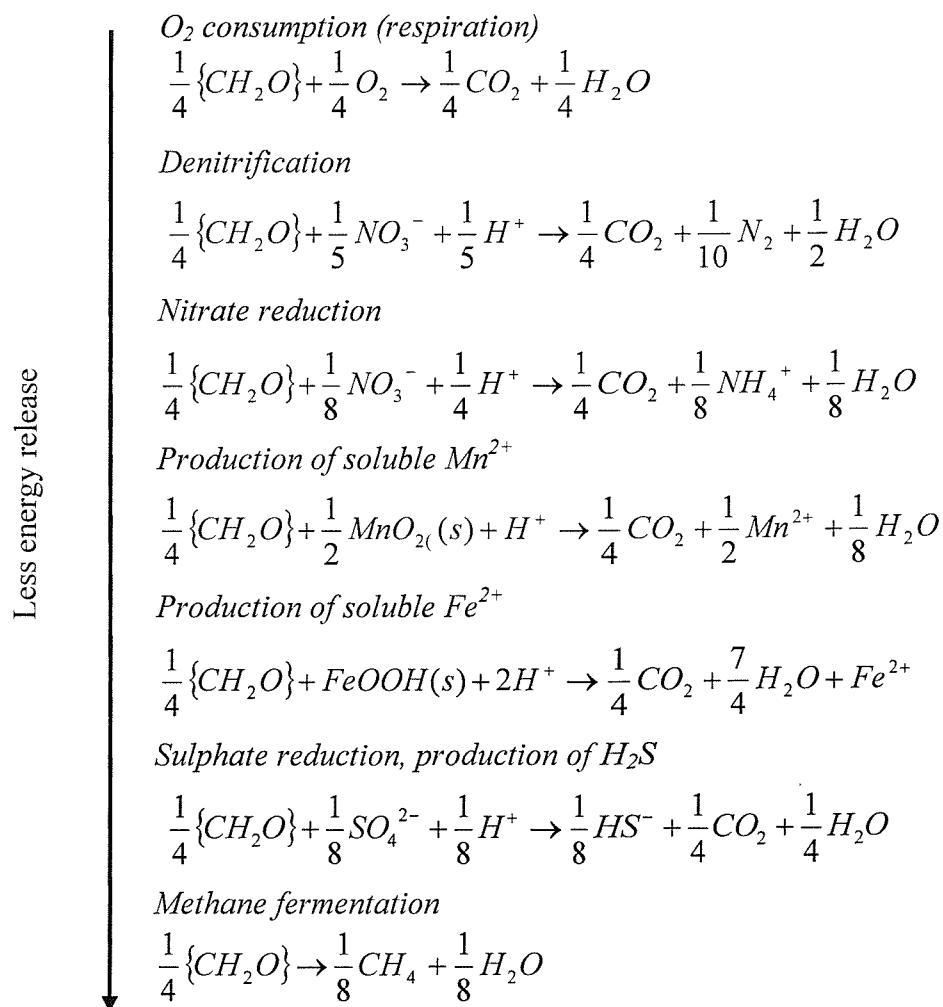
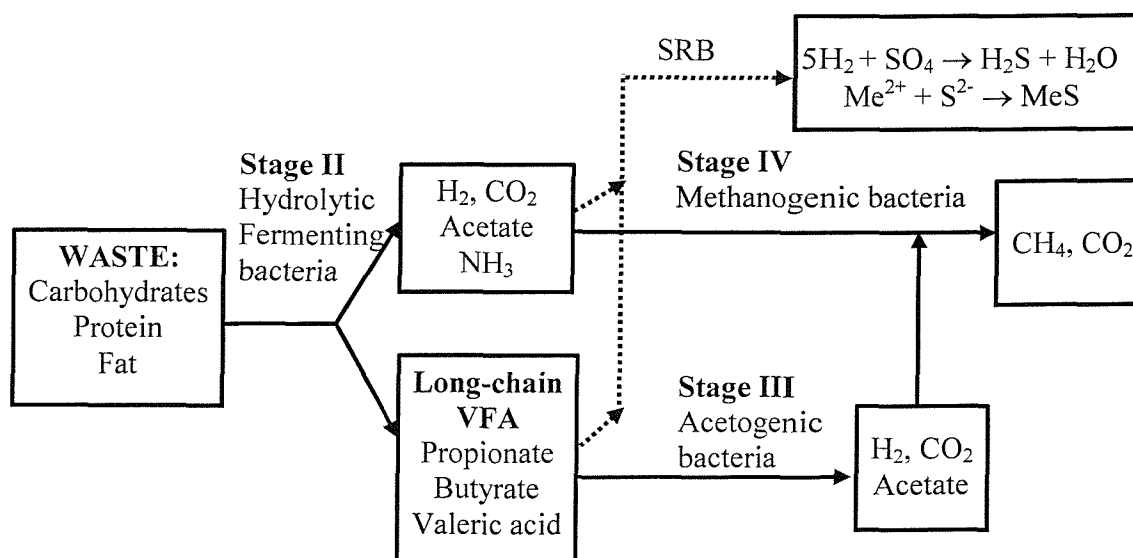


Figure 2-1: Sequence of use of electron acceptors in energy formation (From: Stumm and Morgan, 1996)

This is in descending order of the amount of energy released in each process and implies that denitrification will precede nitrate reduction, followed by the reduction of Fe^{3+} to Fe^{2+} then sulphate reduction. Methane production will occur last in the sequence due to the comparatively low amount of energy released. Due to the small difference in the energy released for the methanogenesis and sulphate-reduction, a competition between these two processes is possible. This competition has been investigated in the experimental work in this thesis.

2.2.1. Competition between sulphate reduction and methanogenesis

In sulphate fed anaerobic reactors, both sulphate reduction and methanogenesis can be final steps in the degradation process because SRB are capable of using many of the intermediates formed during methanogenesis (Figure 2-2).



Note: VFA – volatile fatty acids, SRB – sulphate reducing bacteria
 Me^{2+} - any metal

Figure 2-2: Competition between methanogenic and sulphate reducing bacteria

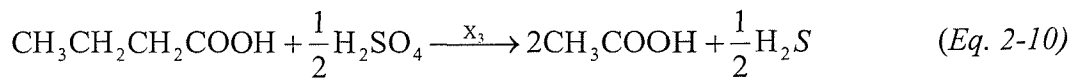
In general, substrate competition in such systems is possible on two levels: competition between SRB and acetogenic bacteria for VFA; and competition between SRB and methanogenic bacteria for acetate and hydrogen. Based on the kinetics of VFA (acetic, propionic and butyric acids) and hydrogen utilisation for SRB, acetogenic bacteria and methanogenic bacteria the SRB should be able to out-compete acetogenic and methanogenic bacteria (Oude Elferink *et al.*, 1994). This prediction has been confirmed

experimentally for hydrogen (Mulder, 1984) and for long chain VFA like propionic and butyric acids (Omil *et al.*, 1996, 1997 and Visser *et al.*, 1993). For utilisation of acetate in anaerobic reactors the situation is different. Various researchers have observed that during the breakdown of sulphate-containing waste water, SRB can indeed successfully compete with methanogenic bacteria for acetate (Visser, 1995), whereas others indicate that acetate is preferentially degraded to methane (Hoeks *et al.*, 1984 and Mulder, 1984). To explain these differences, factors other than pure bacterial kinetics should be taken into account. These include the COD/SO₄²⁻ ratio, the type of seed sludge, hydrogen sulphide inhibition, pH and nutrient limitation (Kalyuzhnyi *et al.*, 1998). Consequently, there is uncertainty regarding the competition between acetate utilising SRB and methanogenic bacteria, which has been investigated in the experimental work described in this thesis.

A. Stoichiometry

The simplified reactions of long chain-fatty acids degradation to acetate by acetogenic bacteria and SRB and consequently to H₂S and CH₄ by the SRB and methanogenic bacteria respectively, are as follows:

- *Acetogenesis*



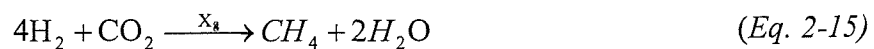
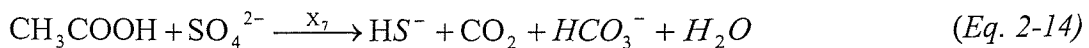
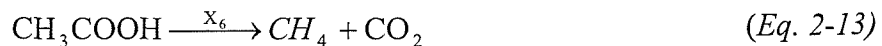
X₂ – all butyrate-degrading acetogenic bacteria

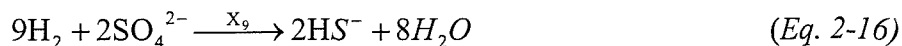
X₃ – all butyrate-degrading sulphate-reducing bacteria

X₄ – all propionate-degrading acetogenic bacteria

X₅ – all propionate-degrading sulphate-reducing bacteria

- *Methanogenesis and hydrogen sulphide production*





X₆ – all acetotrophic methanogenic bacteria

X₇ – all acetotrophic sulphate-reducing bacteria

X₈ – all hydrogenotrophic methanogenic bacteria

X₉ – all hydrogenotrophic sulphate-reducing bacteria

2.3. Nutritional Requirements.

For efficient anaerobic digestion, the nutritional requirements of the microbial populations present should be satisfied, as discussed below.

2.3.1. Carbon, nitrogen, phosphate and sulphur nutrition.

Carbon-containing compounds are required by microbes for energy metabolism and for the production of cellular biomass. Nitrogen is additionally required for protein synthesis during microbial growth. Phosphate is also an essential requirement for cell growth and energy metabolism. An optimal ratio between carbon, nitrogen and phosphorus of 100:24:4 is calculated using typical values for the composition of prokaryotic cells - 50% carbon, 22% oxygen, 12% nitrogen, 9% hydrogen and 2% phosphorus (Tchobanoglous *et al.*, 2002). Sulphur is also required for cell growth and during anaerobic digestion it can be supplied through the degradation of sulphur containing amino acids or through the reduction of sulphate to sulphide.

2.3.2. Micronutrients and Trace Elements.

Many micronutrients and trace elements are required for optimal microbial growth. The most important micronutrients required are calcium, magnesium, sodium and potassium. Trace elements needed for growth include nickel, selenium, manganese, iron and molybdenum, zinc and chromium as enzyme components, and cobalt, nickel, iron and copper in vitamins and co-enzymes (Tchobanoglous *et al.*, 2002).

2.4. Mechanism of leachate production and leachate types

In general, fresh refuse will contain some water but will not be saturated. After disposal, the water content of the waste may increase due to absorption of water by components such as paper, cardboard and textiles. Beyond a certain limit - known as the total absorptive capacity of the waste (field capacity) - the addition of further water would lead to the production of an equivalent volume of free-draining pore fluid called leachate (Powrie and Robinson, 2000). The leachate could contain waste particles and breakdown products generated in any of the stages I – V (section 2.1) as within the waste disposal site all the stages of degradation may be occurring at different stages at any one time. This is the result of different times of waste placement, different biodegradabilities and spatial variability in the physical and chemical environment of the waste material. In addition, leachate generation can occur long before the absorptive capacity has been exceeded as a result of channelling, the heterogeneous nature of the waste or because of high-intensity rainfall.

Acetogenic leachates are generated during the initial stages of refuse degradation (stages II and III), before stable methanogenic microflora have evolved. They are characterised by high concentrations of VFA, an acidic pH, a high BOD/COD ratio, and high levels of ammoniacal and organic nitrogen (Rovers and Farquhar, 1972).

Following the onset of methanogenesis, many of the VFA that are responsible for the acidic pH and high BOD are converted to methane and carbon dioxide resulting in emanation of methanogenic leachates. These leachates are characterised by low concentrations of fatty acids, a neutral to alkaline pH, lower levels of ammoniacal nitrogen and a low BOD/COD ratio, due in part to the existence of a stable microflora in the landfill but also due to waste stabilisation which had already occurred (Rovers and Farquhar, 1972). During the steady methanogenic stage, a dynamic equilibrium exists in which organic compounds are consumed as soon as they are produced.

2.5. Landfill Gas

During decomposition of the soluble organic matter in the drains various gases are generated. When the solubility limit of these gases in leachate is reached, gas bubbles will

be formed. These bubbles can become trapped in the network of pores and thus obstruct leachate flow, causing clogging of the leachate drainage system, as shown in this thesis.

The gas generated during the hydrolysis and fermentation degradation phase comprise of carbon dioxide and hydrogen. As the acetogenic and methanogenic stages develop the concentration of methane in the gas gradually rises. When a balance between the rate at which the organic fraction is leached in solution and the activity of the methanogens is reached, steady state methanogenic conditions occur resulting in a gas composition of about 66% methane and 34% carbon dioxide. As the concentration of dissolved organic substances in the leachate reduces, due to exhaustion of the degradable fraction within the waste, the methane and carbon dioxide generation declines (Rovers and Farquhar, 1972).

The gas generated may include hydrogen sulphide which is generated by the SRB. At sites with a high input of gypsum (CaSO_4) and plaster board, hydrogen sulphide concentrations of up to 30% by volume have been reported. For landfills which do not contain sulphate wastes, hydrogen sulphide concentrations rarely exceed 5 ppm because metallic sulphides are formed preferentially (Department of the Environment, 1995).

Chapter 3

Literature review on the mechanisms of clogging

The research conducted into the mechanisms causing the clogging of leachate collection systems has been divided into field observations, mesocosm and column studies. Brune *et al.* (1991) carried out a field investigation of a number of landfills in Germany where significant clogging had been observed. They also conducted a laboratory study in which they used column tests employing various drainage materials over a period of 16 months. Rowe *et al.* (1997) carried out a seven year study which involved exhuming the drainage system at the Keele Valley Landfill (Fleming *et al.*, 1999), large scale mesocosm experiments and anaerobic column studies (Rowe *et al.*, 2000a, b). Paksy *et al.* (1998) reported laboratory studies and Powrie *et al.* (1997) a field experiment. At the end of this chapter a comparison between the column experiments carried out by the researchers was made.

3.1. Field studies

3.1.1. German experience as reported by Brune et al. (1991)

Brune *et al.* (1991) reported findings from field investigations aimed at obtaining an understanding of the clogging processes in municipal landfill drainage systems. A survey of 29 German municipal landfill sites with leachate collection systems showed deposits of incrustation material in more than half of the cases investigated.

Clogging of the drainage pipes was ascertained by flushing and inspection. The extent of deposition ranged from just a layer of sludge on the bottom of the pipe to extensive incrustations which blocked the pipe cross section (Brune *et al.*, 1991).

Water discharge from the slope of the landfill, suggested by development of local damp spots and slope failure, was reported for 40% of the investigated sites. An accumulation of water on the bottom of the landfill was reported in 8 cases. In addition, accumulation of leachate within the body of the landfill was observed. The causes for it were not well understood but it was considered that this could have been due to impermeable layers within the waste body. It was suggested that installation of drainage at different horizons within the landfill can facilitate leachate collection.

At seven of the sites, parts of drainage systems were exhumed and it was revealed that layers of waste above the drainage system had become consolidated and impermeable to water. Brune *et al.* (1991) reported that the clogging could occur not only in the drainage system but also in the waste near the bottom of the landfill. However, this conclusion should be considered with caution as development of low permeability at the bottom waste layer can be due to compression and does not necessarily mean that clogging had taken place. According to those who conducted the excavations, a washing of fines from the refuse into the drainage system was not observed, even when coarse material was employed as drainage material (Brune *et al.*, 1991).

Although, the data provided by the landfill operators showed that incrustation processes occurred at most of the landfill sites, it was recognised that clogging could have not led to actual failure of the drainage system with subsequent accumulation of leachate. However, the scope of the investigation was not sufficient to establish any clear links. The data provided by the operators and on-site investigations clearly showed that incrustation processes occurred at most of the landfill sites and that together with insufficient drainage of the landfill body was one of the biggest problems facing the landfill operators. To be able to draw more definite conclusions, two German landfill sites (Altwarmbuchen and Venneberg), each typical of a particular method of landfill operation, were investigated in more detail.

A. Altwarmbuchen landfill

The Altwarmbuchen landfill site was deep (10-40 metres) and the rate of filling was very rapid (about 10-20 metres annually), which resulted in an intensive long lasting period of acidic fermentation and the production of an acetogenic leachate with a high pollution load (pH 5.9, COD = 51,200 mgO₂/l, BOD₅ = 23,300 mgO₂/l, BOD₅/COD = 0.46, Ca = 3,530 mg/l, Fe = 1,150 mg/l) and a temperature of 25-40°C in the drains. The high ratio of BOD₅ to COD in the samples collected from the drains suggests a high proportion of biodegradable substances and is indicative of a “young” or acetogenic leachate. Analysis of the gas phase in the drains revealed a composition of 60-65% methane and 30-35% carbon dioxide in most of the drains. Even drains with an acidic leachate had a similar ratio of methane to carbon dioxide indicating a presence of an active methanogenic population (Brune *et al.*, 1991).

At this landfill, clogging was particularly intense despite the fact that pipes were flushed at least once a year. Microscopic examination of leachate samples revealed high concentrations of bacteria (total direct counts of between 10⁶ and 10⁷ bacteria/ml). The most common bacteria found were methanogenic bacteria, SRB, fermentative bacteria, iron-reducing bacteria and manganese-reducing bacteria. On the basis of this, Brune *et al.* (1991) concluded that micro-organisms probably played an important role in causing precipitation and incrustation in the drainage system.

The structure of clogged drainage material recovered from the Altwarmbuchen landfill, ranged from a covering of individual grains of gravel with a thin layer of fine material to a complete filling of the pores between the gravel grains forming a concrete like structure. Chemical analysis showed that the main constituents of the clog material were carbonate (35%), calcium (20%), silica (13%), iron (9%), and sulphur (3%) by mass of dry solid matter. These inorganic constituents represented 80% of the clog material with the organic carbon accounting for only 3% of the total mass. While there were some variations in the composition of the deposits, with some having high iron and sulphur concentrations, calcium and carbonate concentrations were invariably very high.

It can be hypothesised that at the time of the investigation, carried out by Brune *et al.* (1991), the methanogenic bacteria were not present in the waste body. An interpretation of the data not done by Brune *et al.* (1991) suggests that methanogenic bacteria most probably

did not have time to develop due to the fast rate of tipping and the slow growth rates associated with these bacteria (section 2.1.4). This resulted in emanation of a strong acetogenic leachate from the deposited waste as suggested by the high BOD₅/COD ratio. In the drainage layer a population of methanogenic bacteria had developed, where they degraded the VFA to methane and carbon dioxide (as evidenced by the gas analysis). The concurrent increase in pH and availability of carbonate species and calcium enhanced the precipitation of calcium carbonates (to be discussed in section 3.1.2) which together with the increased bacterial activity contributed to enhanced clogging there.

B. Venneberg landfill

In contrast to the above example of extensive clogging, the Venneberg landfill showed very little clogging in the drain pipes between annual flushings (Brune *et al.*, 1991). The Venneberg landfill was relatively shallow (10 metres deep) and had been filled slowly (2 metres/annually). On one half of the landfill area the refuse had been subjected to uncontrolled pre-composting. Examination of the leachate sampled from the drains showed neutral to slightly alkaline pH values, COD = 1,000 mgO₂/l, BOD₅ = 40 mgO₂/l, BOD₅/COD = 0.04, Ca = 132 mg/l, Fe = 28 mg/l and a temperature between 15-20°C. The very low biodegradable content of the leachate (characterised by the BOD₅/COD ratio of 0.04) suggests “old” or methanogenic leachate. Analysis of the gas phase revealed a composition of 60-65% methane and 30-35% carbon dioxide in the drains. The relatively low temperature measured (15-20°C) was due to the lower intensity of exothermal processes as a result of the pre-composting and the smaller quantity of refuse deposited.

The researchers did not report the amount of waste deposited in the two investigated landfill sites. It could be argued that at the time of investigation the Altwarmbuchen site had received larger quantities of waste compared with the Venneberg site and that is why its drainage system clogged. However, the important point here, not discussed by Brune *et al.* (1991), is that the leachate emanating from the Altwarmbuchen landfill was “young” or acetogenic leachate while the leachate sampled from the drains at the Venneberg landfill site was “old” or methanogenic, indicated by the low BOD₅/COD ratio. The latter suggests that the organic portion of the refuse deposited at the Venneberg landfill was degraded to end products within the waste body, leading to emanation of leachate containing a very low concentration of degradable organic compounds (low BOD₅) and a relatively high concentration of recalcitrant substances (high COD). The bacteria responsible for this

degradation could have been either methanogenic bacteria, which had time to develop under the practice of slow tipping, or aerobic bacteria bearing in mind that the Venneberg landfill was shallow and slowly filled, implying that air had prolonged contact with the waste and thus favoured an aerobic rather than an anaerobic degradation of the waste. In general, the aerobic degradation process is faster than the anaerobic (section 2.1.4) thus facilitating occurrence of complete degradation within the waste body, rather than in the drainage system. In reality, probably both bacteria were present, the aerobic being in the refuse layers close to the surface and the methanogenic in the deeper layers. Bearing in mind that degradation of major part of the organic compounds occurred within the waste body, where clogging most likely would not be a problem due to the small organic and inorganic mass flux per unit area, suggests that the leachate reaching the drainage system contained small amounts of organics and inorganics, not sufficient to initiate extensive clogging there.

C. Conclusions

As a result of their field investigations Brune *et al.* (1991) concluded that:

1. metabolic activity of anaerobic bacteria is the main cause of clogging
2. the main components of the incrustation material are the cations of calcium and iron, combined with the anions of carbonate and sulphide
3. the highest concentrations of organic and inorganic substances in the leachate and the greatest annual amount of drain incrustation were associated with the landfill that was filled rapidly (10-20 metres annually).
4. low concentrations of organic substances and negligible drain incrustation were associated with the landfill that was filled slowly (2 metres annually) and had already reached a stable methane phase.

Brune *et al.* (1991) noted that the incrustation of a landfill drainage systems cannot be completely prevented but can be reduced by methods of landfill operation that create unfavourable conditions for the incrustation forming bacteria. The following recommendations to the landfill operators were made:

- the drainage aggregate should be as coarse as possible.
- the intensity and duration of the acidic phase needs to be reduced because of the associated high clogging rates of the drainage system. This can be achieved either by operational methods which result in reduction of the organic strength of the

leachate reaching the drainage system, such as slower filling of the landfill or the separate collection of organic waste and subsequent composting.

- the supply of inorganic incrustation forming substances containing iron and calcium needs to be reduced. The separate disposal of municipal and building waste was suggested, due to the higher organic content of the first and high calcium, iron and sulphate concentrations of the latter resulting in leachate with high incrustation potential (heavily loaded with easily biodegradable organic substances and a high iron and calcium concentration).
- the performance of the landfill drainage system is particularly impaired when leachate with a high incrustation potential coincides with a microflora in the stable methane phase. For this reason the establishment of a stable methane phase in only the lower waste layers should be avoided.

However, the researchers did not indicate how the last recommendation could be achieved. An interpretation of the data not done by Brune *et al.* (1991), as previously discussed, suggests that waste management practices to favour refuse degradation to end products within the waste body rather than in the drainage system are to be encouraged. This can be achieved in two ways. The first is to ensure that aerobic decomposition processes take place, which can be accomplished by either slow filling of the landfill as suggested by Brune *et al.* (1991) or by artificial introduction of air. The second way is by promoting the early establishment of methanogenic bacteria within the waste by co-disposal of sewage sludge and possibly pH control.

3.1.2. Canadian experience at Keele Valley Landfill, Maple, Ontario, Canada

The Keele Valley Landfill located north of Toronto, Canada became operational in 1983 and was constructed in four stages. In stages 1 and 2, the primary leachate collection system consisted of lateral French drains (50 mm nominal diameter stone) at a spacing of about 65 m sloping towards the main collection pipes (spacing 200 m). In stages 3 and 4, there was a 0.3 m thick continuous drainage blanket of uniformly graded crushed dolomitic stone with nominal size of 50 mm. The waste had an average depth of 30 metres, in places reaching up to 60 metres, and was placed directly on the drainage material. The landfill had an approximately 1.2 m thick compacted clay liner at the bottom

with a hydraulic conductivity of less than 10^{-10} m/s, overlain by about 0.3 m of fine to medium sand to provide protection against desiccation. This fine to medium sand was separated from the drainage stone by a geotextile.

A. Evidence of clogging in stages 1 and 2

Hydraulic pressure build up and temperature increases were monitored in the collection system and waste in stages 1 and 2, suggesting development of leachate mounding (Barone *et al.*, 1997). Subsequent exhumation in stage 1 was carried out to examine the performance of the clay liner after 4.25 years of landfilling (King *et al.*, 1993). It was revealed that the top 5 cm of the sand blanket, adjacent to the drainage layer, were black (presumably iron sulphide) and the bottom 10 cm of the sand layer, immediately above the clay liner, were lighter black to grey. It was suggested that this was due to chemical/biological clogging of the sand layer. This hypothesis was assessed by examining the dominant process governing the migration of a conservative tracer in the sand layer and making comparison with the clay liner. If the hydraulic conductivity of the sand had reduced significantly as a result of clogging, diffusion would be the major process governing the transport of the tracer.

The following experimental procedure was followed:

- samples were taken from the sand cushion and clay liner through hydraulic insertion of a 7.6 cm diameter tube
- pore water was extracted from different layers of the wet sand by high-speed centrifugation through filter paper overlying coarse glass beads. Pore water was obtained from slices of the clay liner samples by high pressure squeezing and consolidation at 30 MPa
- chemical analyses were carried out on the samples thereby obtained and pore water Cl, Na, K, Mg profiles along the depth of the sand and clay liner were presented.

The data showed that concentrations of chloride, which was considered to be a conservative tracer, were highest at the top of the sand layer and gradually diminished to zero at a depth of 0.6 m in the clay liner. The chloride concentrations measured in the sand cushion fitted very well the theoretical diffusion profiles for the clay layer, suggesting that diffusion was the dominant process governing the migration of contaminants. It was concluded that the sand cushion acted essentially as an additional 0.3 m thick diffusion

layer on top of the 1.2 cm thick compacted clay barrier, indicating that clogging processes in the sand layer had taken place. On this basis it can be speculated that clogging in the drainage layer must have also occurred. However, this was not subject to investigation by Barone *et al.* (1997).

B. Evidence of clogging in stages 3 and 4

A field investigation was carried out by Rowe *et al.* (1995) and Fleming *et al.* (1999) to examine parts of the leachate collection system in stage 4, which consisted of a continuous drainage blanket and had been in operation for 1, 3 and 4 years. Hydraulic head and temperature readings were taken at different locations throughout the landfill site, namely over the clay liner, within the sand and drainage layer and in the bottom waste layer. A hydraulic head build up of up to 5.5 m and a temperature increase of up to 30°C were measured in the bottom waste layer of the landfill. The temperature and the leachate mound tended to increase in parallel. This probably reflects the effect of increased heat-generating anaerobic activity after sufficient free water becomes available. This, in turn, tends to increase the amount of clogging, thus restricting drainage and leading to increased mounding of leachate, which further enhances anaerobic activity. Since the solubility of CaCO₃, one of the major components of the clog material, decreases with increasing temperature, the system can be seen to have several different mechanisms that reinforce each other, tending to accelerate both clogging and mound growth (Rowe *et al.*, 1995).

Field leachate samples showed an increase in leachate pH and a decrease in Ca content with decreasing the organic load. It was concluded that this was due to precipitation of inorganic minerals, namely CaCO₃. These field observations were compatible with the overall framework of the geochemistry of the leachate as described by Rittmann *et al.* (1996). The latter showed that most of the COD removal was due to the bacterial degradation of VFA to CH₄ and CO₂. The removal of the VFA by bacteria resulted in a significant pH and CO₂ partial pressure increase leading to a concurrent increase in the dissolved carbonate concentrations and their precipitation as CaCO₃, subject to availability of Ca species (Rittmann *et al.*, 1996).

The clog material included a significant portion of fine gravel, sand and other particles, not generally present in the clean drainage aggregate, which appeared to have been cemented by a calcite rich mixture of minerals derived from the leachate. It is

hypothesised that these particles were probably washed from the overlying waste, in the absence of a filter between the drainage blanket and the waste, and were trapped by the biofilm. The microbial digestion of the COD, by the bacteria present in the biofilm caused the precipitation of the calcite-rich mineral solids and the cementation of these particles.

A chemical analysis of the incrustation material showed 19-23% calcium, 30-32% carbonate, 1-3% iron, 0.2-0.9% sulphur, 20-30% silica content and only 1-4% organic matter. The average composition of the clog material (Table 3-1) was very similar to that given by Brune *et al.* (1991). However, Fleming *et al.* (1999) concluded that there were insufficient data to conclude whether this similarity represented a general case.

	Ca	CO ₃	Si	Mg	Fe	Total	Ca/CO ₃
Brune <i>et al.</i> , (1991) German landfill (field study)	20	35	13	1	9	78	0.57
Fleming <i>et al.</i> , (1999) Keele Valley Landfill (field study)	20	30	21	5	2	78	0.67

Table 3-1: Comparison of clog composition (% of total dry mass except for the Ca/CO₃ ratio)

The stone drainage blanket was found to contain significant quantities of soft black slime, coating individual 50 mm stones, and this often occupied most of the void space. The slime appeared more viscous in the upper part of the drainage layer, whereas below the pipe, in the zone of permanent saturation, the slime was more liquid. The degree of clogging was estimated visually to be 50-100% in the lower saturated zone of the drainage layer and was 30-60% in the upper unsaturated portion of the drainage layer.

The measured moisture content of the slime was in the range of 20%-78%, that is considerably lower than the typical value of 90% for bacterial biofilm, further confirming the presence of mineral precipitates (Fleming *et al.*, 1999). The pH of the slime ranged from 7.5 to 8.8. The measured density of the incrustation material ranged from 1.3 to 2.1 g/cm³ with an observed increase with time (Fleming *et al.*, 1999). Visual data suggested that “mature” clog, at the base of the biofilm, had achieved a greater density and increased solids content relative to the growing surface of the biofilm.

The clogging was generally greater in areas with larger leachate flows or where leachate ponding had occurred, and in older portions of the collection blanket. The amount of clogging was visibly more pronounced in and adjacent to the perforated collection pipes and in a zone of several meters around the pipes, where the leachate flow within the drainage blanket was highest (Fleming *et al.*, 1999 and Rowe *et al.*, 1995). It appears that the rate of clogging was strongly influenced by the leachate flow rate. At first sight this observation is surprising because as the leachate approaches the leachate drainage pipes its strength reduces due to degradation in the upper drainage layers leading to lower organic and inorganic loading. Apparently, this is more than compensated by the smaller surface area of the drainage material near the leachate drainage pipes resulting in higher hydraulic flux which in turn leads to higher organic and inorganic loading per unit area.

There was an approximately three orders of magnitude decrease in hydraulic conductivity in the lower saturated portion of the stone layer (initial - 0.3 m/s, measured in the laboratory after exposure to leachate - 1×10^{-4} m/s), although the stone still readily allowed transmission of leachate (Fleming *et al.*, 1997).

Within the perforated pipes, a significant accumulation of solid material had occurred and most of the 8 mm diameter perforations were blocked by clog material. This is why the use of greater than 8 mm perforations was suggested by Rowe *et al.* (1995). A conglomerate of clog material over 100 mm wide and 75 mm thick, consisting of cemented particles in a loose structure, was removed from one of the leachate collection pipes. This conglomerate was larger than the opening size of the perforated pipe suggesting that this structure must have grown inside the pipe by precipitation of leachate minerals, probably around a nucleus of silt, sand or other particles washed into the drainage system.

3.1.3. Landfill in Florida, Craven et al.

Craven *et al.* (1999) carried out a field study at a 6 year old landfill site. The site was chosen not because the landfill drainage material was believed to be clogged but because repair of one of the manholes was required, providing an opportunity to sample components of the leachate collection system. The leachate collection system consisted of French drains with High Density Polyethylene (HDPE) collection pipes, wrapped directly

with geofabric. The entire bottom of the landfill was overlain by 0.6 m of clean sand. Drainage samples were taken using direct and indirect procedures. The direct procedure was manual and might have resulted in collection of structurally disturbed samples, while the indirect procedure employed a horizontal coring device and was believed to result in less disturbance to the samples. The clean sand hydraulic conductivity was reported to be 1.85×10^{-2} cm/s. The hydraulic conductivity of the sand collected after 6 years of landfilling ranged from 1.83×10^{-2} to 9.72×10^{-3} cm/s (on average, a 33% reduction). None of the sand samples collected showed any visible sign of microbiological clogging or cementation. However, there was an increase in volatile solids content (as measured by ignition tests at 550°C) in the sand from 0.22% to 0.44% that might have been indicative of biomass growth but could also be a result of soluble organic matter in the leachate collected as part of the sample. Metal analysis (acid digestion procedure) showed the clean sand to contain Ca, Fe, Mg and K concentrations of 10.9, 142.7, 4.1 and 29.2 mg/kg respectively. Comparison with corresponding values of samples of sand from the drainage blanket show 881.7, 458.4, 101.9 and 96.0 mg/kg wet weight indicating that chemical precipitates, similar to the previous two field studies, had been deposited. Similarly to the volatile solids analysis, part of the metal concentration could be as a result of dissolved ions in the leachate collected as part of the sample. However, the drainage sand in some areas was visibly black, presumably indicating the presence of iron and SRB microbial activity. The geotextile that was wrapped around the leachate collection pipe had black slime and sand particles embedded in the woven material.

3.2. Mesocosm experiments

The field studies carried out by Rowe *et al.*, (1995) and Fleming *et al.*, (1999) prompted the initiation of mesocosm and column studies to investigate, in a more controlled environment, some of the parameters governing the clogging.

3.2.1. Operational set up

Rowe *et al.* (1995) and McIsaac *et al.* (2000) set up eighteen primary leachate collection system mesocosms to investigate the rate of clogging of leachate collection systems in full scale reactors, employing materials commonly used in waste management practice in Canada. The full scale reactors were 0.25 m wide, 0.6 m high and 0.7 m long and were

operated under conditions representative of a section of a continuous granular blanket adjacent to a leachate collection pipe at the Keele Valley Landfill, Ontario, Canada. The mesocosms, whose design mimicked field drainage system design, consisted of a waste layer, overlying a 0.30 m thick drainage layer comprising uniformly graded crushed dolomitic limestone with a nominal size of either 19 mm or 38 mm, overlying a geotextile/sand cushion which sloped at 1.5% to a half section of a PVC perforated pipe. Eight mesocosms had selected filter/separator layers between the waste and the drainage stone, namely non-woven needle punched polypropylene geotextile, woven slit-film geotextile, an additional “sacrificial” layer of coarse gravel placed between the non-woven geotextile and waste and a graded granular filter consisting of 4 cm deep layers of well graded concrete sand and 6 mm pea gravel. Ten mesocosms contained no separator between the waste and the coarse gravel drainage layer and acted as controls.

Flow rates through the mesocosms were designed to mimic field hydraulic conditions in two dimensions. Real leachate from the Keele Valley Landfill (pH 5.9-8.1; COD 10,000-25,000 mgO₂/l; BOD₅ 4,000-16,000; BOD₅/COD = 0.40-0.60; Ca 600-2,000 mg/l; Fe 50-350 mg/l) was pumped at a flow rate of 2.6 litres/day from one end of the mesocosms, in horizontal flow, simulating conditions immediately adjacent to the collection pipes. Leachate was also added to the surface of the waste at a very low flow rate (100 ml/day) to simulate the infiltration of moisture from the waste mass (0.2 m³/m²/annum). The mesocosms were operated with an overflow leachate level of 10 cm above the base of the stone. This flow regime resulted in the generation of two distinct layers – a saturated (bottom 10 cm of the drainage aggregate) and an unsaturated (the remaining 20 cm of the aggregate) layer. The mean residence time was 3 days (based on the initial unclogged porosity). The mesocosms were operated at a temperature of 27°C.

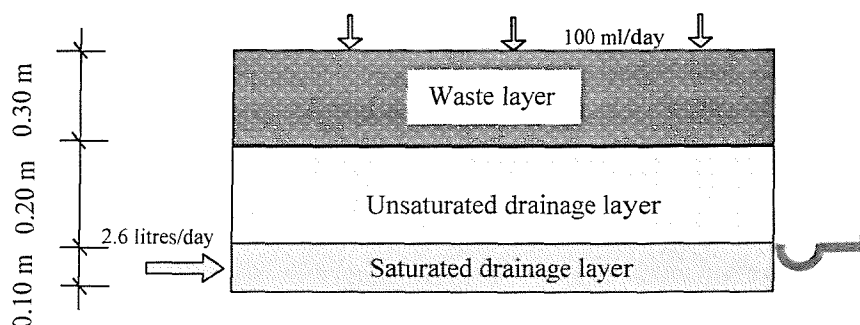


Figure 3-1: Mesocosm operational set up

Rowe *et al.* (1995) assessed the performance of the mesocosms generally and focused on the saturated drainage layer, while McIsaac *et al.* (2000) reported observations regarding the unsaturated layer in the mesocosm comprising 38 mm gravel and the performance of the different separator layers placed between the waste and the unsaturated layer.

3.2.2. Saturated layer

The performance of the 38 mm drainage stone compared with that of 19 mm stone and of the saturated drainage layer compared with the unsaturated layer with respect to the rate of clogging in the mesocosms was investigated by Rowe *et al.* (1995). Only interim results, regarding the porosity change of the two different sizes aggregate, were presented. These data showed a porosity reduction in the 19 mm stone from an initial value of 0.42 to 0.28, resulting in a void volume occupancy (VVO) of 33%. The porosity of the 38 mm aggregate was reduced from the initial value of 0.48 to 0.27, i.e. a VVO of 43%. The 19 mm and 38 mm diameter gravel had reached similar porosities after 2 years of operation, which resulted in greater VVO for the bigger aggregate due to the higher initial porosity. This is somewhat in contradiction with what was observed by Brune *et al.* (1991) (to be discussed in section 3.3.1.) under the unsaturated conditions in their column experiments and prompted further investigation in smaller scale column studies (see section 3.3.4.). When some of the mesocosms were terminated after six years of operation, the greatest clogging was observed in the saturated layer, where the porosity had reduced from 0.48 to about 0.15 with a VVO of about 70%. This is consistent with the 50-80% VVO noted in the exhumation of the 4 years old system at Keele Valley Landfill. For the unsaturated systems, the greatest clogging was for the 19 mm gravel where the maximum VVO was observed to be 20%. The saturated stone layer showed more clogging than the unsaturated, probably as a result of the larger leachate retention time in the saturated case. The latter resulted in clogging of the drains from the bottom up, with the saturated (bottom) drainage layer clogging first, followed by the unsaturated (top) layer. Rowe *et al.* (1995) suggested that:

- keeping the drainage system substantially unsaturated by maximising the slope between and perpendicular to the collection pipes, and
- reducing the flow by reducing the spacing between the pipes,

would result in a longer service life for the leachate collection system. These features would decrease the saturated fraction of the drain, and shorten the drainage path and the hydraulic retention time, thus slowing down the development of clogging.

However, the first suggestion and the conclusion regarding the accumulation of less clog material under unsaturated conditions should be considered with caution due to the difference in the flow rates employed in the mesocosm tests carried out by Rowe *et al.* (1995). The saturated layer had 25 times a higher flow rate (2.6 litres/day) than the unsaturated (100 ml/day), resulting in higher organic and inorganic loading for the saturated layer. Although the operational set up represents real landfill conditions, with a small flow rate through the unsaturated waste with the flow rate increasing as the leachate approaches the drainage system, it is impossible to conclude that the unsaturated layer will not clog as much as the saturated given that equal flow rates were used.

3.2.3. *Unsaturated layer*

McIsaac *et al.* (2000) presented preliminary findings concerning clog development within the unsaturated portion of the drainage layer in the mesocosm comprising 38 mm gravel. The researchers indicated that the clog material present in the unsaturated drainage stones was predominantly biological in nature with no evidence of formation of solid inorganic clog material. Furthermore, a distinct vertical distribution of the biofilm was observed, with more biofilm growth in the lower layers of the unsaturated stone, which were closer to the saturated drainage layer and thus had higher moisture content. The contact points between stones seemed to be a starting point for biofilm growth, probably due to the fact that the capillary fringe around the contact zones would create an environment favourable for biofilm development. The larger the capillary fringe around the contact points (i.e. the smaller the void space between contact points), the larger was the extent of the biofilm coverage on the stones.

3.2.4. *Separator layer*

McIsaac *et al.* (2000) investigated the effect of different separator layers placed between the waste and the unsaturated drainage layer. It was concluded that the presence of a separator minimised the occlusion of voids within the drainage material. The presence of a

geotextile decreased the amount of fines, sand sized particles and biofilm growth within the unsaturated zone. The non-woven geotextile visually performed best, with the smallest amounts of biofilm growth on the geotextile surface and the drainage stone beneath it. The biofilm that did develop was viscous and moist to the feel with no signs of accumulation of fines (McIsaac *et al.*, 2000). The mesocosm designed with a woven geotextile as a separator visually contained larger amounts of biofilm and fines on the unsaturated stones beneath it, compared with the non-woven geotextile. The filter separator, consisting of 4 cm thick layers, each of well graded concrete sand underlain by pea gravel (6 mm), experienced substantial clogging. It was hypothesised that capillary action within the granular filter (the void spaces between the sand grains were less than 2 mm) allowed retention of leachate due to capillary action and thus provided a moist environment conducive to biological growth. The sand had partially infiltrated into the pea gravel layer at the sand/pea gravel interface and this created an environment favourable to the bio-concretous processes that essentially cemented the top layer of pea gravel together. Beneath this, 15 cm thick, top layer the pea gravel was relatively clean with no sign of cementation. The pea gravel filter experienced less bioslime development most probably due to its roundness and lack of large, flat, lateral, vertical-facing surfaces. Waste intrusion was observed into the unsaturated gravel layer in all of the mesocosms where the waste was directly placed on the unsaturated gravel. The waste occluded the majority of the voids for a depth up to 2 stone diameters (38 mm drainage gravel) (McIsaac *et al.*, 2000).

3.2.5. Chemical analysis of leachate

Chemical analysis of leachate samples taken from the mesocosm inlet and outlet ports showed a decrease in COD and calcium concentrations as reported by Rowe *et al.* (1995) and Fleming *et al.* (1999). Rittmann *et al.* (1996) explained the chemistry behind these observations (discussed in 3.1.2.). Rowe *et al.* (1995) and Fleming *et al.* (1999) also noted a linear relationship between the total COD and dissolved calcium suggesting a constant value for the “yield coefficient” of mineral deposits in the clogging material, defined as the mass of calcium removed from solution per unit mass of COD removed.

3.2.6. *Dismantling*

Dismantling of one of the mesocosms revealed a complex clustering of microbial consortia, which included SRB, denitrifying bacteria (DN), methanogenic bacteria (MTB) and iron related bacteria (IRB). There was a concentric pattern, with the MTB dominating the core of the mesocosm, surrounded by focused sites of high SRB and/or high DN. IRB tended to be observed around the discharge ports of the mesocosms (Fleming *et al.*, 1999).

The mesocosm studies showed that:

- the larger particle sizes experienced greater void volume occupancy
- the saturated layer experienced more severe clogging than the unsaturated layer
- the unsaturated layer clogged from the bottom-up
- the non-woven geotextile performed better than the woven geotextile and sand/pea gravel filter as a separator layer between the waste and the unsaturated drainage aggregate.

The mesocosm studies reported by Rowe *et al.* (1995) and McIsaac *et al.* (2000) were comprehensive. However, the extensive clogging observed in the saturated section of the mesocosms could have been a function of the higher flow rate and not necessarily because of the saturated/unsaturated conditions. In addition, some of the conclusions, especially the one reached by McIsaac *et al.* (2000) on the performance of the different filter/separators were based mainly on visual observations and were qualitative rather than quantitative.

3.3. Column experiments

3.3.1. *Brune et al. (1991)*

In parallel with their field investigations, Brune *et al.* (1991) conducted laboratory tests to investigate the influence of leachate quality and drainage aggregate size on the incrustation process. The experiments were carried out in 12 plastic columns with a diameter of up to 200 mm and a height of approximately 1000 mm, each containing a layer of 30 cm depth of drainage aggregate overlain by a 15 cm layer of composted waste,

and operated in downward flow at a temperature of 30°C. The composted waste was introduced to represent real landfill conditions and simulate wash-out of suspended solids from the waste mass. Originally all the columns were operated in unsaturated conditions, with some columns becoming saturated as clogging developed. A column was considered to have clogged when leachate build up of more than 30 cm had developed. The effect of the following parameters on the clogging rate was investigated:

- Particle sizes - five different drainage aggregate grain sizes were employed in the experiment – 1-32 mm, 2-4 mm, 2-8 mm, 8-16 mm and 16-32 mm.
- Flow rate - real leachate was supplied to the columns and permeated the unsaturated layers of composted waste and drainage material with flow rates ranging from 6.8 litres/day to 9.8 litres/day in 11 of the columns, with one being supplied with 15.2 litres/day of leachate.
- leachate strength - nine of the columns were fed with leachate containing high concentrations of organic and inorganic substances, typical of landfill in the acidic phase of fermentation (pH 7.2-7.8; COD 1630–8890 mg/l; BOD₅ 400-4365 mg/l; Ca 130-380 mg/l; Fe 8-85 mg/l; SO₄ 1-121 mg/l), and three of the columns with leachate, which was lightly loaded with organic and inorganic compounds, typical of landfill in the stable methanogenic phase of decomposition (pH 7.4-7.9; COD 1450-2070 mg/l; BOD₅ 57-930 mg/l; Ca 70-120 mg/l; Fe 10-28 mg/l; SO₄ 29-115 mg/l).
- The effect of the presence or absence of a geotextile separator between the composted waste and drainage gravel was also examined.

The column tests can be divided in two main groups on the basis of the strength of their leachate.

A. Columns supplied with high strength leachate

Parameters relating to the column tests carried out by Brune *et al.* (1991) and supplied with highly loaded leachate are shown in Table 3-2. The coarse drainage material (16-32 mm) experienced a 5% porosity reduction and retained its permeability far longer than finer (2-4 mm, 2-8 mm) and well graded drainage materials (1-32 mm), both of which suffered almost complete loss of permeability, indicated by an increasing build up of leachate in the columns and concurrent 20% reduction in porosity, to reach a final porosity of 0.1-0.2. The medium size drainage material (8-16 mm) experienced a 8-10% porosity

reduction. Piezometers were installed at various heights in the columns, however no values were reported on the magnitude of head losses in any of the columns.

Column test / Particle size (mm)	1-32	2-4	2-8	8-16	16-32
Bed dimensions i.d. x height (cm)	20 x 30	20 x 30	20 x 30	20 x 30	20 x 30
Cross sectional area (cm ²)	314.16	314.16	314.16	314.16	314.16
Volume of the column (litres)	9.425	9.425	9.425	9.425	9.425
Initial pore volume (litres)	1.41	3.77	2.64	3.77	4.24
Flow rate (litre/day)	6.8	9.5	9.1	7.4	9.4
Litres passed	1700	3420	3094	3418.8	4342.8
Volume of clog material (litres)	0.565	1.885	1.508	0.566	0.471
Period over which it was observed (days)	250	360	340	462	462
COD concentration in leachate (mg/l)	5260	5260	5260	5260	5260
COD concentration removed per litre of leachate (mg/l)	3156	3156	3156	3156	3156
Total COD removed (kg)	5.37	10.79	9.76	10.79	13.71
Organic loading rate by volume (mg COD/cm³.d)	2.28	3.18	3.05	2.48	3.15
Organic loading rate by pore volume (mg COD/cm³.d)	15.18	7.95	10.88	6.20	7.00
Ca concentration in leachate (mg/l)	255	255	255	255	255
Ca concentration removed per litre of leachate (mg/l)	153	153	153	153	153
Fe concentration in leachate (mg/l)	47	47	47	47	47
Fe concentration removed per litre of leachate (mg/l)	18.8	18.8	18.8	18.8	18.8
SO ₄ concentration in leachate (mg/l)	61	61	61	61	61
SO ₄ concentration removed per litre of leachate (mg/l)	24.4	24.4	24.4	24.4	24.4
Total inorganics (Ca, Fe, SO ₄) removed (kg)	0.33	0.67	0.61	0.67	0.85
Inorganic loading rate by volume (mg/cm³.d)	0.14	0.20	0.19	0.15	0.20
Inorganic loading rate by pore volume (mg/cm³.d)	0.94	0.49	0.68	0.39	0.44
Hydraulic surface loading (ml/cm ² .day)	21.65	30.24	28.97	23.55	29.92
Hydraulic volumetric loading (ml/cm ³ .day)	0.72	1.01	0.97	0.79	1.00
Hydraulic pore volumetric loading (ml/cm ³ .day)	4.81	2.52	3.45	1.96	2.22
Suspended solids (mg/l)	present	present	present	present	present

Table 3-2: Parameters relating to the column tests carried out by Brune *et al.* (1991) and supplied with highly loaded leachate

Dismantling of the columns revealed that the pores were clogged with a black, tar-like incrustation material. The term “tar-like incrustation material” used by Brune *et al.* (1991) is somewhat confusing as “tar” implies a liquid substance and “incrustation” means formation of solid crust and should be considered with caution. It was observed that the

small voids in the fine drainage aggregate (2-4 mm, 1-32 mm) were filled with incrustation material and there were hardly any free pores. The 8-16 mm gravel was extensively covered with thick biofilm and was locally clumped together but the coarser pores were still permeable. The larger voids (16-32 mm) had some incrustation depositions but were not clogged and maintained their permeability, although the researchers did not report values regarding their hydraulic conductivity.

A transition zone, of about 3 cm, was observed between the compost layer and the coarse drainage aggregate (16-32 mm), where black compost and incrustation material had settled between the particles of gravel and caused some silting. The geotextile, used in some of the columns to separate the waste from the drainage aggregate, was completely sealed by the “tar-like incrustation material”, while the gravel beneath was quite loose and covered with only a slight film of thin, black slime. It was concluded on the basis of visual observations that a zone of reduced permeability was formed in the compost layer above the geotextile. A similar observation was made by McIsaac *et al.* (2000) regarding the underlying stone when a protector geotextile was used. However, no ponding of leachate was observed by McIsaac *et al.* (2000) probably due to the low leachate flow rates (100 ml/day), compared with 8-9 litres/day used by Brune *et al.* (1991), which resulted in development of less clogging.

B. Columns supplied with low strength leachate

The drainage aggregate used in the columns supplied with lightly loaded leachate was medium size (8-16 mm) and coarse (16-32 mm) drainage aggregate. The data showed no significant reduction in the porosity and permeability during the course of the experiment. Leachate build up did not occur in any of the columns. (Brune *et al.*, 1991).

C. Conclusions

The column experiments have provided several conclusions of practical significance for drainage layer design:

- firstly, the tests suggested that highly loaded leachate induced extensive clogging of the drainage material, whilst the lightly loaded leachate caused almost no incrustations. It was concluded that the clogging is proportional to the loading rate of organic substrate and inorganic salts.

- secondly, coarse drainage material (16-32 mm) experienced less reduction in drainable porosity and consequently retained its permeability far longer than finer (2-4 mm, 2-8 mm) and well graded drainage materials (1-32 mm).
- thirdly, the column tests showed that the geotextile separator placed between the waste and drainage aggregate could also clog, although the latter observation was only assessed visually.

D. Inconsistencies in Brune's column studies

The column experiments were carried out essentially in unsaturated conditions. Saturated conditions were only established after sufficient clogging had developed to cause a leachate mound to build up. In addition the tests were operated with a composted waste layer overlaying the drainage layer. The microbial population present in the waste would consume some of the organic substances, supplied with the leachate, before they had reached the drainage layers leading to an unrealistically high value of COD required to achieve certain clogging. On the other hand wash out of suspended particles from the composted waste would possibly contribute to clogging which is not COD related. The laboratory study carried out by Brune *et al.* (1991) was somewhat descriptive and qualitative. The chemical analysis of the leachate focused on the COD, Ca and Fe at the column inlet and outlet. The change in leachate composition and the corresponding reduction in the drainable porosity along the height of the experimental column were not presented. The effect of mass loading, by doubling the flow rate, was investigated but results showing its impact on the clogging were not reported.

Brune *et al.* (1991) carried out experiments using lightly loaded leachate but only with medium (8-16 mm) and coarse (16-32 mm) particle sizes. The researchers did not investigate the rate of clogging using lightly loaded leachate and small particle sizes, which Brune *et al.* (1991) showed to be most susceptible to clogging.

3.3.2. Paksy *et al.* (1995 and 1998)

Paksy *et al.* (1995) suggested that landfill drainage can act as a fixed bed bioreactor in which organic compounds are removed from the leachate by means of anaerobic degradation. In this respect a landfill drainage system could form part of a low-cost preliminary leachate treatment process. It was recognised that clogging, due to microbial

growth and chemical precipitates, might become a problem in the long term and would influence the effectiveness of a landfill drainage system as a bioreactor. To investigate this problem Paksy *et al.* (1998) and Peeling *et al.* (1999) carried out laboratory studies to examine the effect on the clogging rates of:

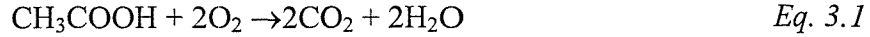
- flow rate: 0.4 –7 ml/min
- leachate composition:
 - strong leachate – BOD = 13 465 - 23 205 mgO₂/l, Total VFA = 16 500 mg/l, Ca = 200 mg/l, pH 5.4-6.2, Fe = 100 mg/l, SO₄ = 135 mg/l
 - weak leachate – BOD = 4 323 - 6 758 mgO₂/l, Total VFA = 3 000 mg/l, Ca = 200 mg/l, pH 5.5, Fe = 50 mg/l, SO₄ = 27 mg/l
- saturation conditions: saturated / unsaturated
- mineralogy of the aggregate: limestone, Thames gravel
- particle size of the drainage material: 5-10 mm, 10-20 mm, 20-40 mm.

Laboratory columns were constructed (diameter = 230 and 350 mm; height = 900 mm) to simulate a vertical section of a landfill drainage system and were operated in downward flow under saturated conditions. A reduction in the drainable porosity of 1-12% occurred after periods of 400-800 days, which was attributed to the growth of biomass in the pore space. Parameters relating to the column tests carried out by Paksy *et al.* (1998) are shown in Table 3-3.

A. Biological load (flow rate and leachate composition)

The biological load was defined as the mass of nutrient reaching a unit area of the column in unit time and is given by the cross-sectional product of the infiltration rate and the total fatty acids concentration in the influent leachate (mgVFA/cm² per day). On increasing the biological load, either by increasing the flow rate or VFA concentration, a corresponding increase in the amount of clogging was observed (up to a 4% reduction in the drainable porosity from the total value). However, the experiments designed by Paksy *et al.* (1995) investigated too many variables at the same time, leading to difficulty in assessing the effect of single factors, such as the leachate flow rate, strength and composition on the clogging rates. Data were re-evaluated in later version of the thesis (Paksy, 2002) and are not reviewed here.

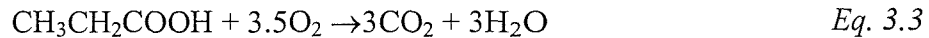
To make comparison with other column tests easier, the acetate, propionate and butyric acid concentration in the leachate were converted to COD concentration. COD is determined by measuring the amount of oxygen needed to chemically oxidise the organics in the leachate. Bearing this in mind, the acetate was converted using the following formula:



Equation 3.1 shows that each mole of acetate requires 2 moles of oxygen for oxidation (Kiely, 1996).

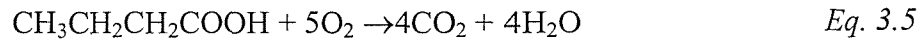
$$\text{COD} = \frac{2 \text{ moles of } \text{O}_2}{1 \text{ mole of } \text{CH}_3\text{COOH}} = \frac{2 \times 32}{1 \times 92} = 0.7 \quad \text{Eq.3.2}$$

If the acetate concentration was 1000 mg/l then the equivalent COD concentration would be 700 mg/l. For propionate the formula is:



$$\text{COD} = \frac{3.5 \text{ moles of } \text{O}_2}{1 \text{ mole of } \text{CH}_3\text{COOH}} = \frac{3.5 \times 32}{1 \times 106} = 1.06 \quad \text{Eq.3.4}$$

For butyric acid the formula is:



$$\text{COD} = \frac{5 \text{ moles of } \text{O}_2}{1 \text{ mole of } \text{CH}_3\text{COOH}} = \frac{5 \times 32}{1 \times 120} = 1.33 \quad \text{Eq.3.6}$$

The leachate composition varied during the operational period and this was taken into account when calculating the equivalent COD concentration.

B. Saturation conditions: saturated/unsaturated

In columns operated in saturated conditions, the increase in clogging was generally most significant in the zone closest to the inlet. In unsaturated conditions, the increase in clogging rate became more pronounced towards the outlet. The average clogging rates were slightly greater in saturated than unsaturated conditions with the greatest degree of clogging observed for sections of the column subjected to alternating periods of saturated and unsaturated flow. Paksy *et al.* (1999) concluded that in practice it is probably preferable to operate the drainage system saturated because this condition is easier to maintain with confidence than a continuous and uniform state of non-saturation.

Column test	B6	A1	B1	B2	B3	B4	B5	B7	B8	C1	C2	D1
Particle size (mm)	5-10	5-10	10-20	10-20	10-20	10-20	10-20	10-20	10-20	20-40	20-40	20-40
Bed dimensions i.d. x height (cm)	22 x 91	23 x 60	22 x 91	22 x 91	22 x 91	22 x 91	22 x 91	22 x 91	22 x 91	35 x 88	35 x 88	30 x 88
Cross sectional area (cm ²)	380.13	415.48	380.13	380.13	380.13	380.13	380.13	380.13	380.13	962.11	962.11	706.86
Volume of the column (litres)	34.59	24.93	34.59	34.59	34.59	34.59	34.59	34.59	34.59	84.67	84.67	62.20
Initial pore volume (litres)	12.43	10.55	13.20	12.75	12.75	12.96	15.30	13.22	12.71	34.55	34.61	21.91
Flow rate (litre/day)	1.15	1.28	0.62	0.52	0.62	1.10	0.62	0.62	1.11	0.62	4.82	6.90
Litres passed	587.46	479.58	230.02	547.28	239.32	407.60	230.02	230.02	563.08	222.58	2050.52	1815.00
Volume of clog material (litres)	1.164	0.556	0.387	0.742	0.390	0.696	0.723	0.599	0.406	0.724	0.196	0.311
Period over which it was observed (days)	510	409	371	442	386	370	371	371	509	359	425	263
COD concentration in leachate (mg/l)	20011.95	20210.94	13515.00	20713.09	13515.00	19077.95	13515.00	13515.00	20068.16	16673.02	2370.48	2225.21
COD concentration removed per litre of leachate (mg/l)	14108.19	7124.98	12529.35	18157.07	12071.70	9249.26	13633.60	13820.54	7030.97	15917.87	604.24	1557.64
Total COD retained (kg)	8.29	3.42	2.88	9.94	2.89	3.77	3.14	3.18	3.96	3.54	1.24	2.83
Organic loading rate by volume (mg COD/cm³.d)	0.47	0.37	0.23	0.27	0.22	0.30	0.24	0.25	0.23	0.12	0.03	0.17
Organic loading rate by pore volume (mg COD/cm³.d)	1.31	0.86	0.59	0.74	0.59	0.79	0.55	0.65	0.61	0.29	0.08	0.49
Ca concentration in leachate (mg/l)	200	200	200	200	200	200	200	200	200	200	200	200
Ca concentration removed per litre of leachate (mg/l)	100	100	100	100	100	100	100	100	100	100	100	100
Fe concentration in leachate (mg/l)	100	100	100	100	100	100	100	100	100	100	100	100
Fe concentration removed per litre of leachate (mg/l)	40	40	40	40	40	40	40	40	40	40	40.000	40
SO ₄ concentration in leachate (mg/l)	101.38	71.13	79.11	107.23	88.55	89.00	79.11	79.11	100.04	81.68	27.00	27.00
SO ₄ concentration removed per litre of leachate (mg/l)	40.55	28.45	31.64	42.89	35.42	35.60	31.64	31.64	40.02	32.67	10.80	10.80
Total inorganics (Ca, Fe, SO ₄) removed (kg)	0.11	0.08	0.04	0.10	0.04	0.07	0.04	0.04	0.10	0.04	0.31	0.27
Inorganic loading rate by volume (mg/cm³.d)	0.006	0.009	0.003	0.003	0.003	0.006	0.003	0.003	0.006	0.001	0.009	0.017
Inorganic loading rate by pore volume (mg/cm³.d)	0.017	0.020	0.008	0.007	0.009	0.015	0.007	0.008	0.016	0.003	0.021	0.047
Hydraulic surface loading (ml/cm ² .day)	3.03	3.08	1.630	1.370	1.63	2.90	1.63	1.63	2.91	0.64	5.01	9.76
Hydraulic volumetric loading (ml/cm ³ .day)	0.033	0.051	0.018	0.015	0.018	0.032	0.018	0.018	0.032	0.007	0.057	0.111
Hydraulic pore volumetric loading (ml/cm ³ .day)	0.093	0.121	0.047	0.041	0.049	0.085	0.041	0.047	0.087	0.018	0.139	0.315
Suspended solids (mg/l)	n/a	n/a	n/a	n/a	n/a	n/a	n/a	n/a	n/a	n/a	n/a	n/a

Table 3-3: Parameters relating to column tests carried out by Paksy *et al.* (1999)

C. Aggregate mineralogy

Two different types of material were used as drainage materials in the columns: limestone chippings and Thames gravel. These materials differ significantly in terms of both their physical and chemical characteristics. Limestone was considered initially as a worst case, as it can be expected to disintegrate under the influence of a leachate of pH 5.5 – 7.0. However, no significant difference in performance was apparent. The researchers suggested that the physical and/or chemical properties of the drainage material may have had little effect on the clogging process. After a biofilm had developed on the aggregate, the properties of the original material may be practically irrelevant.

D. Particle size

The typical particle size D_{10} of the drainage material was identified as one of the factors governing the rate of clogging, as has also been observed by Brune *et al.* (1991). Paksy *et al.* (1999) reported that the smaller particle sizes experienced greatest accumulation of clog material and recommended a D_{10} of at least 10 mm to guard against long-term clogging. However, a later discussion with the researchers (personal communication) identified that the data did not necessarily give enough evidence to support the above conclusion. It was recognised that carefully planned experiments using different particle sizes and equivalent quantities of organics passed should be carried out to enable comparison.

Paksy *et al.* (1995) suggested that the microbial growth may not continue indefinitely as the sustainable extent of the biomass would be expected to be limited by the availability of nutrients as determined by the leachate flow rate and composition. As part of the same study Peeling *et al.* (1999) reported a maximum specific rate of VFA removal of 3270 mg/litre bed volume per day. This implies that any excess of VFA will remain unutilised and the clogging should reach steady state porosity. The researchers recognised the beneficial implications this would have on the long-term viability of the landfill drainage systems, which can then be used with confidence as a low-cost preliminary leachate treatment system. However, they recognised that further tests are needed to investigate the reliability and generality of the hypothesis of limiting biomass growth.

E. Field experiments at Risley 3 landfill site, Risley, Warrington, Cheshire.

Powrie *et al.* (1997) investigated the clogging rates in three columns that had been previously operated by Paksy *et al.* (1998) with the only difference being that the leachate was supplied from the bottom and moved upwards through the column in contrast to the downward flow employed by Paksy *et al.* (1998). The reactors were supplied with real leachate, containing a high concentration of suspended solids (30-1900 mg/l, average 526 mg/l), high concentrations of ammonia (100-1100 mg/l, average 468 mg/l) and sulphate (20-1800 mg/l, 484 mg/l) and low concentrations of VFA (50-8000 mg/l, average 1472 mg/l). The leachate composition varied over time, but this is to be expected in view of the fact that the leachate was collected from an active landfill site. Saturated conditions were maintained in the columns. The columns were installed in a heated cabin (within which the temperature varied between 15-25°C) at Risley 3 landfill site, Risley, Warrington, Cheshire. Two of the columns were 350 mm in diameter and one was 300 mm in diameter. The leachate flow rate was 20 litres/day for the 350 mm diameter columns and 13 litres/day for the 300 mm diameter column.

Generally the porosity reduction in each column over the 6-month duration of the field trial was about 4% (from 38-40% initial to 34-36% final), except in the bottom sections, which was near the column inlet, where the reduction in drainable porosity was approximately 20% (from 40% to 20%). These values may be compared with up to 2.5% reduction in the drainable porosities measured in one of the columns operated previously by Paksy *et al.* (1998) in downward flow and supplied with synthetic leachate over a period of 14 months, and a reduction of 2% measured in a column supplied with real leachate over a period of 6-7 months, again operated previously by Paksy *et al.* (1998) in downward flow. The reason for the dramatic increase in clogging at the base of the columns during the Risley field trial was probably because of the suspended solids in the leachate, which were not present in the synthetic leachate used in the laboratory tests. The fact that similarly high rates of clogging were not observed in the columns operated with real leachate by Paksy *et al.* (1998) may have been due to the operation of the columns at Risley in upward flow. Suspended solids will tend to accumulate at the bottom of the column. In upward flow the density effect will contribute to clogging of the bottom section, while in downward flow (depending on the permeability of the system) some of the suspended solids will be transported downwards and accumulate at the column outlet or be flushed out. If this is the case, a real landfill drainage system might not clog as

quickly, as extrapolation of the Risley tests would suggest, provided that the flow pattern in reality is such that the suspended solids are flushed through and out of the drain.

In addition, experiments were carried out in a 35m³ skip, which incorporated three separate drainage channels (14 mm graded limestone, 10-20 mm gravel, 20-40 mm gravel) overlain by partly degraded waste. Leachate was introduced at the top of the skip by gravity flow through a network of pipes to ensure even distribution of leachate. For the first nine months the skip was operated in single pass flow at a flow rate of 0.3 m³/day, for the next 10 months the leachate was recirculated through the waste and the rate of leachate supply was higher at 3-5 m³/day. An elevated saturation level (30 cm above the drainage layer) was maintained by means of an inverted U-shaped outflow pipe. This resulted in vertical flow, saturated or unsaturated (depending on the depth) within the refuse, and horizontal, saturated flow within the drainage layer. The skip was operated at ambient temperature, which varied between 5 and 25°C.

The porosity of the 14 mm limestone decreased by 4 % (from 0.44 to 0.40, VVO=9%), by 7 % for the 10-20 mm gravel (from 0.41 to 0.36, VVO=12%) and by 11 % for the 20-40 mm gravel (from 0.41 to 0.30, VVO=27%). The greatest clogging was experienced by the largest particle sizes over a certain period of time. This unexpected result was attributed to contamination of the drainage material with soil, which had a small particle size and consequently contributed to the observed greater degree of clogging. However, this result is not abnormal in view of the data reported by Rowe *et al.* (2000a) to be discussed in detail in section 3.3.3.B.

3.3.3. Column studies, Rowe *et al.* (2000a, b, 2001b and c)

A series of Anaerobic Fixed Film Reactors (AFFR) column tests were carried out to evaluate the effect of flow-rate (1, 2 and 4 litre/day), nominal grain size (4 mm, 6 mm, 15 mm), temperature (10°C, 21°C and 27°C), leachate characteristics (real and synthetic) and particle shape on the rate and extent of clogging (Rowe *et al.*, 2000 a, b). The columns were 50 mm wide and 700 mm long and contained glass beads. Glass beads were used instead of natural materials to ensure that all 4-mm beads were in fact 4 mm in diameter so that the effect of the particle size would be clear in order to be able to validate the results of clogging computer models. Concern that the glass beads behaved in a different way

compared with natural granular materials initiated tests using pea gravel having a similar nominal size to allow for comparison. However, the results from these tests have not been reported. Real leachate was supplied to the columns at a flow rate of $0.51 \text{ m}^3/\text{m}^2/\text{d}$ (equivalent to 1 litre/day), except in the columns where the effect of the flow rate on the clogging rate was investigated. The columns were operated in upward flow to facilitate the maintenance of saturated conditions similar to those experienced at the bottom of the leachate collection system. The real leachate had the following characteristics - pH 6.92-7.00, COD = 8,628 - 13,615 mgO_2/l ; Ca = 536 mg/l ; TN = 1,065 mg/l ; Fe = 205 mg/l ; S = 46 mg/l .

A. Effect of flow rate (1, 2 and 4 litres/day)

Rowe *et al.* (2000b) investigated the effect of different flow rates, resulting in different mass loadings, on the clogging rates in columns containing 6 mm size aggregate and operated at temperature of 27°C . A column was defined as having “clogged” when it was not possible to transmit more than 10% of the daily design flow rate under a head of 2.4 m, relative to the base of the column. Drainable porosity data were given only for the columns with flow rates of 1 litre/day and 2 litres/day, so this review will focus only on these two columns.

The columns had initial drainable porosities of 0.375. The porosity profiles (Figure 3-2) revealed that the two columns developed different porosity profiles with time.

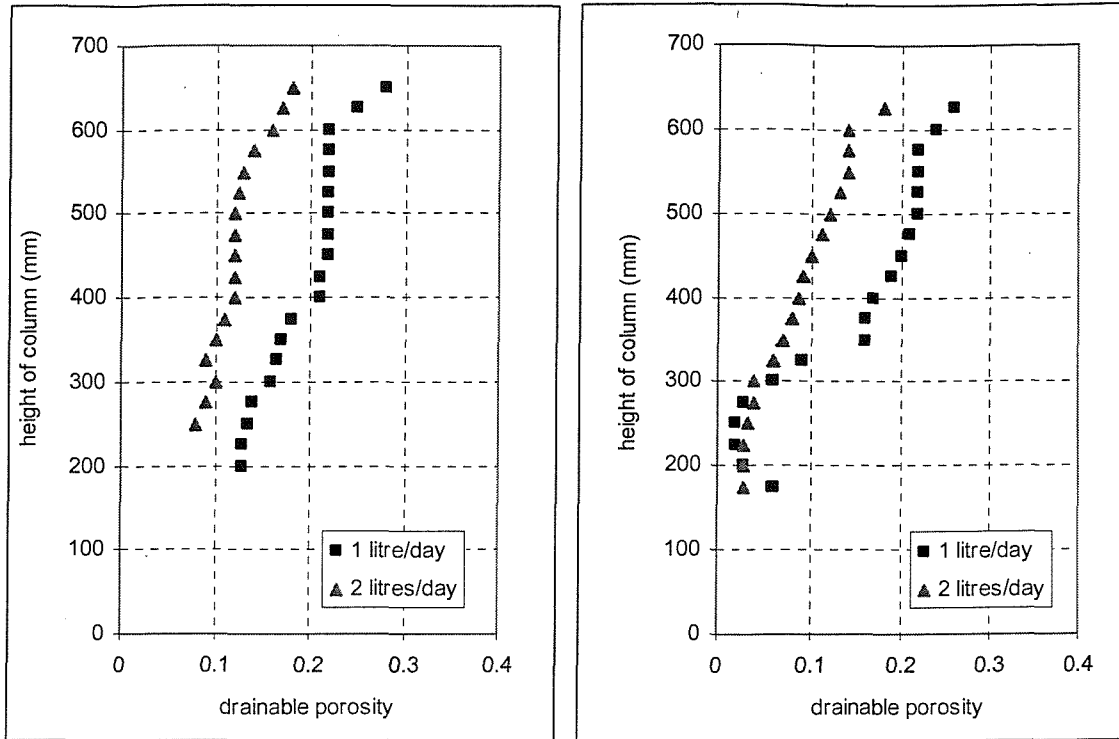


Figure 3-2: Drainable porosity profiles: after 118 days at 1 litres/day and 104 days at 2 litres/day (left) and at column failure, 256 days at 1 litre/day and 216 days at 2 litres/day (right) (Rowe *et al.*, 2000b)

The column supplied with leachate at a flow rate of 1 litre/day clogged due to the accumulation of clog material in the lower half of each column. The column supplied with 2 litres/day of leachate experienced more consistent accumulation of clog material along the entire column length. It was found that while higher flow rates gave rise to less efficient bioreactors (i.e. with a smaller reduction in organic and inorganic loading per unit volume of leachate passed) due to the shorter hydraulic retention time, this was more than compensated for by the increase in mass loading associated with the higher flow rates, leading to more deposition of CaCO_3 (and other inorganics) in a given period of time. This resulted in a greater reduction in drainable porosity in a shorter time for the column supplied with leachate at a flow rate of 2 litres/day, which however occurred after the passage of larger quantities of leachate (Table 3-4). In other words, increasing the flow rate, which resulted in increased mass loading on the columns, increases the rate of clogging.

Column type	Elapsed time (days)	Theoretical volume of leachate passed (litres)	Measured volume of leachate passed (litres)
1 litre/day	259	259	176
2 litres/day	216	432	262

Note: The discrepancy between the theoretical and measured volume of leachate passed is due to the fact that the designed flow rate became impractical to maintain as clogging developed.

Table 3-4: Days in operation and leachate volume passed in columns supplied with 1 and 2 litres/day leachate.

Additionally, the high flow rates seem to have provided more nutrients along the entire length of the column resulting in a more uniform development of biofilm and mineral clog along the height of the experimental apparatus as evidenced by the drainable porosity measurements and by data obtained upon column disassembly (Rowe *et al.*, 2000b). The researchers concluded that since the rate of clogging can be related to the mass loading, reducing the distance between the leachate collection pipes would decrease the total volume of leachate collected for one individual pipe and hence reduce the mass loading and rate of clogging in the gravel layer around the pipe.

These results prompt an interesting question concerning the clogging rate, which has not been investigated by Rowe *et al.* (2000b). What would the difference in clogging rates be whilst having a strong leachate pumped at a low flow rate and a dilute leachate supplied at a higher flow rate resulting in the same nutrients loading? If this experiment shows that the column supplied with dilute leachate at a higher flow rate experienced more uniform clogging along the entire length of the column with the top layer remaining permeable then having large quantities of a dilute leachate (essentially a flushing bioreactor) would most probably result in longer service life of the drainage system.

B. Effect of particle size (4 mm, 6 mm, 15 mm)

Rowe *et al.*, (2000a) investigated the effect of different particle sizes on the clogging rates in columns operated at a temperature of 27°C and a flow rate of 1 litre/day. The columns had initial drainable porosities of 0.37 (4 mm aggregate), 0.38 (6 mm aggregate) and 0.50 (15 mm aggregate). The porosity profiles (Figure 3-3) indicated that the columns containing 4 mm and 6 mm beads failed due to accumulation of clog material in the lower

half of each column, near the column inlet. The column containing 15 mm beads appeared to have failed due to a more consistent accumulation of clog material along the entire column length.

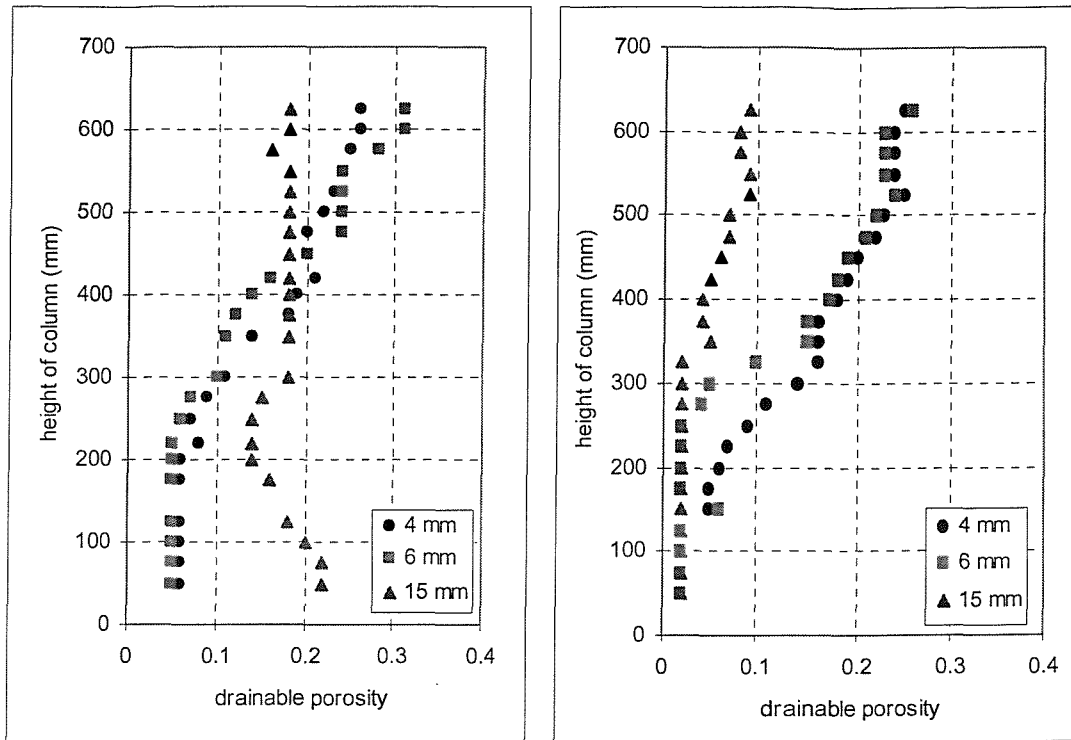
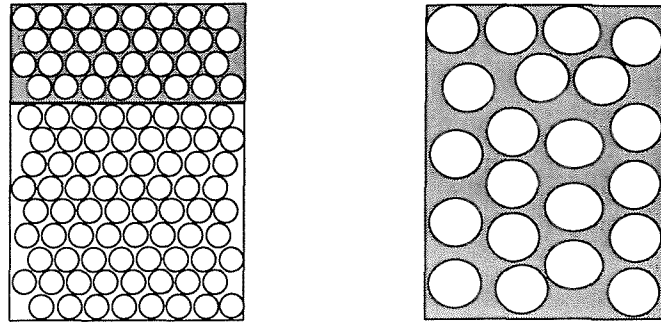


Figure 3-3: Drainable porosity profiles: after 165 -171 days (left) and at column failure (right) Rowe *et al.* (2000a)

The results summarised above were attributed to the combined effect of a number of factors:

- First, the surface area of the beads in the first 130 and 200 mm of the columns packed with 4mm and 6 mm beads respectively, was approximately equal to the total surface area (column length = 700 mm) of the column packed with 15 mm beads. The large surface area of the smaller beads allowed more biofilm growth near the inlet port for the 4 mm and 6 mm beads than for the 15 mm beads during the early stages of the test.
- Second, the size of the pores is in direct ratio to the particle size. Thus, for a given build up of clog material on a bead, the available opening size should be greater for the larger particles. This suggests that the 15 mm beads created a more permeable system, for a given growth of biofilm and mineral clog that still allowed leachate through to the upper portions of the column. For the columns with 4 mm and 6 mm beads, clogging in the lower portion of the column began to reduce the nutrients

and CaCO_3 available to the upper portion of the column, leading to extensive clogging only at the base of the column. This concept is shown on Figure 3-4, where the grey area indicates a similar surface area over which the clog material developed.



Column packed with small particles Column packed with big particles

Note: The area marked with grey shows area occupied by clog material

Figure 3-4: Conceptual model showing the effect of different size particles on the clogging process.

It was shown that larger particle diameters gave bioreactors as efficient as smaller particle diameters (i.e. similar reduction in organic and inorganic loading in a given time). This appears to have been because the clogging focused over a similar surface area – near the inlet of the columns for the smaller particles and over the entire column for the larger particles.

The experiments showed that at column failure the column containing 15 mm beads had a greater decrease in porosity, when averaged for the whole bed volume. This reduction in porosity had occurred after passage of a larger volume of leachate, larger amounts of COD and over a much longer period of time (Table 3-5). The more uniform distribution of the clogging throughout the height of the reactor packed with 15 mm beads contributed significantly to this observation. The smaller particle sizes, experienced a smaller reduction in the drainable porosity when averaged over the whole bed volume, but the clogging was more pronounced in the section nearest to the inlet, where the permeability was reduced relatively fast thereby restricting the supply of nutrients to the other column sections.

After 165-171 days (Figure 3-3 on the left)					At column failure (Figure 3-3 on the right)			
Particle size	Days of operation (litres passed)	Initial porosity	Porosity averaged for the bed volume	Volume of clog material (litres)	Particle size	Days of operation (litres passed)	Porosity averaged for the bed volume	Volume of clog material (litres)
4 mm	165 (137)	0.37	0.14	0.27	4 mm	252 (159)	0.14	0.27
6 mm	165 (159)	0.38	0.13	0.29	6 mm	259 (176)	0.12	0.30
15 mm	171 (166)	0.50	0.17	0.38	15 mm	383 (310)	0.04	0.54

Table 3-5: Raw data relating to the results shown on Figure 3-3.

These results are similar to those of the mesocosm tests carried out by Rowe *et al.* (1995) and Powrie *et al.* (1997) and indicate that it is not that the larger particle size aggregate experiences less clogging as suggested by Brune *et al.* (1991) and Paksy *et al.* (1998) but that the larger particles retain their permeability over a longer period of time, implying a longer service life when used for leachate collection systems, as shown in Table 3-6.

Column type	Days in operation	Litres of leachate passed	Days in operation at designed (full) flow rate (effective service life)
4 mm beads	252	159	132
6 mm beads	259	176	140
15 mm beads	383	310	329

Table 3-6: Days in operation, litres of leachate passed and days in operation at the designed flow rate in columns containing 4, 6 and 15 mm beads.

Table 3-7 shows parameters relating to the column tests carried out by Rowe *et al.* (2000a).

Column test / Particle size (mm)	4	6	15
Bed dimensions i.d. x height (cm)	5 x 59.1	5 x 59.1	5 x 59.1
Cross sectional area (cm ²)	19.630	19.630	19.630
Volume of the column (litres)	1.160	1.160	1.160
Initial pore volume (litres)	0.463	0.475	0.625
Flow rate (litre/day)	1.0	1.0	1.0
Litres passed	159	176	310
Volume of clog material (litres)	0.263	0.298	0.536
Period over which it was observed (days)	252	259	383
COD concentration in leachate (mg/l)	10756	10756	10756
COD concentration removed per litre of leachate (mg/l)	7959.44	7959.44	7959.44
Total COD removed (kg)	1.270	1.400	2.470
Organic loading rate by volume (mg COD/cm³.d)	6.859	6.859	6.859
Organic loading rate by pore volume (mg COD/cm³.d)	17.208	16.755	12.734
Ca concentration in leachate (mg/l)	536	536.000	536.000
Ca concentration removed per litre of leachate (mg/l)	396.64	396.64	396.64
Fe concentration in leachate (mg/l)	205	205	205
Fe concentration removed per litre of leachate (mg/l)	82	82	82
SO ₄ concentration in leachate (mg/l)	89	89	89
SO ₄ concentration removed per litre of leachate (mg/l)	35.60	35.60	35.60
Total inorganics (Ca, Fe, SO ₄) removed (kg)	0.08	0.09	0.16
Inorganic loading rate by volume (mg/cm³.d)	0.44	0.44	0.44
Inorganic loading rate by pore volume (mg/cm³.d)	1.11	1.08	0.82
Hydraulic surface loading (ml/cm ² .day)	50.93	50.93	50.93
Hydraulic volumetric loading (ml/cm ³ .day)	0.86	0.86	0.86
Hydraulic pore volumetric loading (ml/cm ³ .day)	2.16	2.11	1.60

Table 3-7: Parameters regarding the column tests carried out by Rowe *et al.* (2000a) investigating the effect of different sizes particles on the clogging.

C. Effect of temperature (10°C, 21°C, 27°C)

Experiments were carried out to investigate the effect of the temperature on the clogging rates at a constant flow rate of 1 litre/day in columns containing 6 mm size aggregate. Increased biological activity was evident with increasing temperature, as indicated by the enhanced COD removal. Associated with this greater microbial activity was an increased rate of CaCO₃ precipitation and consequently greater clogging at higher temperatures. In addition, the deposition of CaCO₃ was further enhanced by its having a lower solubility at high temperatures (Rowe *et al.*, 2001c)

D. Effect of leachate characteristics (real and synthetic)

Tests were carried out using both actual and synthetic Keele Valley Landfill leachate in columns containing 6 mm size aggregate, which were operated at a flow rate of 1 litre/day and a temperature of 27°C. The synthetic leachate composition was similar to that of the

actual leachate but did not contain suspended solids. These column experiments were carried out to evaluate the extent of clogging due to microbiological growth and chemical precipitation by isolating the effect of the suspended solids. Average drainable porosities (over the entire bed volume) of 0.33, 0.25 and 0.21 were measured for the columns supplied with synthetic leachate after approximately 120, 260 and 330 days respectively compared with 0.23, 0.14 and 0.10 for the columns supplied with real leachate. The results indicated that the “real” leachate columns tended to have a greater amount of clogging relative to the synthetic leachate due to the increased suspended solids load and the continuous microbial addition associated with the real leachate (Rowe *et al.*, 2001b).

There was, however a significant variation between the chemical composition of the synthetic and real leachate. The differences in the COD and Ca concentrations, which were considered the most important factors affecting the clogging rates, were taken into account by comparing the porosity not simply against time but against the equivalent cumulative mass of COD and CaCO₃ retained in the columns. However, discrepancies between the two essential microbial growth elements nitrogen and phosphorus, with the phosphate being a 7-8 times higher and the nitrogen 1000 times lower in the synthetic leachate, probably also affected the rate of biomass growth. Higher sulphate contents (40 times higher) and lower iron (280 times lower) concentrations were also observed in the synthetic leachate. These inconsistencies in leachate composition make it difficult to draw any definite conclusions from the experiments.

E. Common observations for all column tests carried out by Rowe et al. (2000a and b)

The column experiments carried out by Rowe *et al.* (2000a and b) showed a very clear variation in drainable porosity with distance along the column, indicating that the clogging will be greater where the leachate loading per unit area is greatest, which is near the inlet of the columns.

Yield coefficients (Y_c) of CaCO₃ were calculated, with units of milligrams of CaCO₃ removed from the leachate per milligram of COD removed. Y_c lay in the range of 0.14 to 0.20 mg CaCO₃/mg COD, with the most common value being 0.15 mg CaCO₃/mg COD. Since carbon accounts for only 0.12 mg per mg of CaCO₃

$\left(\frac{\text{atomic weight of C}}{\text{molecular weight of CaCO}_3} = \frac{12}{40+12+(16 \times 3)} = 0.12 \right)$, and the yield coefficient is

approximately 0.15 mg CaCO₃/mg COD, this gives 0.018 mg C in CaCO₃ per mg of COD consumed (0.12 × 0.15 = 0.018). The Keele Valley leachate COD comprised primarily 43% acetic, 35% propionic and 22% butyric acids, giving 0.46 mg C per mg COD. This simple calculation shows that the carbon attributable to the carbonate deposited within the columns would account for approximately 4% ($\frac{0.018}{0.46} \times 100\%$) of the total carbon removed from the leachate, in terms of COD removed. The remainder of the carbon is primarily released as by-products of microbiological processes in the form of carbon dioxide and methane. Thus the amount of carbon in CaCO₃ is only a small proportion of the available carbon and hence the availability of calcium rather than carbon is likely to be the factor limiting CaCO₃ deposition (Rowe *et al.*, 2000a, b).

An empirical relationship between the hydraulic conductivity and drainable porosity as clogged material accumulated on the glass beads was obtained (Rowe *et al.*, 2000a, b):

$$k = Ae^{bn_d} \quad n \geq 0.03 \quad (\text{Eq. 3-1})$$

where

- k - is hydraulic conductivity (m/s)
- A - is a fitting coefficient, ranging from 1.7×10^{-7} to 1.17×10^{-9} (m/s)
- b - is a fitting parameter and ranges from 39.1 to 50.47
- n_d - is the drainable porosity

It can be seen that the hydraulic conductivity drops with decreasing porosity and that there is a seven to eight order of magnitude drop in hydraulic conductivity by the time the drainable porosity drops to about 10% of the initial value. However, because of the small flow rate (1 litre/day) and the challenge of measuring small head differences in a biologically active environment that had to be maintained in anaerobic conditions, it was not practical reliably to detect a change in hydraulic conductivity until it had decreased by between four to five orders of magnitude and as such had caused a measurable head difference between the two piezometers.

The columns were found to be colonised by a diverse consortia of bacteria, including MTB, SRB and DN that are typically found in landfill waste and leachate. The SRB and

DN were present at all levels within the column while the MTB population was large near the column inlet and small near the column outlet but not present in between. The very high activity and large population size of methanogens near the column inlet indicates that the bacteria are not only colonising the columns but have also developed niches which allow these specialised bacteria to grow and thrive. However, Rowe *et al.* (2000b) did not give an explanation of this observation. It is surprising that a population of MTB developed extensively near the column inlet while DN and SRB populated the entire length of the column, given that methanogenesis is less favourable in terms of energy release compared with both sulphate reduction and denitrification.

Further analyses were carried out on dismantling the AFFR columns to obtain the density of the active and inactive portions of the biomass, to identify the type of bacteria present and to estimate the biofilm thickness (Rowe *et al.*, 2000a, b). The bulk wet density of the clog material (ρ_c) was measured to range from 1.5 to 2.0 Mg/m³ and the percentage of calcium (f_{Ca}), on a dry weight basis, was about 26%. These values allowed the calculation of the volume of the clog material and estimation of the service life of a leachate collection system. This was achieved by relating the volume of clog material to the calcium concentrations in the leachate thus using calcium carbonate as a “surrogate” for the complex bulk clog material (Eq. 3-2).

$$Y_t(t) = \frac{C_{Ca}(t)}{\rho_c f_{Ca}} \quad \text{Eq.3-2}$$

where,

Y_t – volumetric yield of clog per unit volume of leachate

C_{Ca} – concentration of Ca in mg/l

ρ_c – bulk (wet) density of the clog material

f_{Ca} – percentage of calcium in the clog material

Thus the volume of pore space occupied at some time is given by:

$$\frac{dV(t)}{dt} = QY(t) \quad \text{Eq.3-3}$$

where,

$V(t)$ – is the volume of pore space occupied

Q – the leachate flow per unit width of drainage blanket

Y_t - volumetric yield of clog per unit volume of leachate

A solution for constant and varying concentrations of Ca can be found in Rowe and Fleming (1998). A modification of this equation to accommodate for the fact that the clogging will not be uniform and there will be concentration of clogging towards the leachate collection pipes has been made and is shown in detail in Rowe and Fleming (1998).

F. Conclusions arising from Rowe's column studies

The results of the column studies described above have led to several conclusions of practical significance relating to the design and operation of leachate collection systems.

- Firstly, since the rate of clogging has been shown to be related to mass loading, reducing the distance between the leachate collection pipes would decrease the total volume of leachate collected for one individual pipe and hence reduce the mass loading and rate of clogging in the gravel layer around the pipe.
- Secondly, increasing the diameter of the granular material (D_{10}) and adopting relatively uniform grading with minimal fines for the material used in a leachate collection system may increase the life span of a leachate collection system, with all other factors being equal.
- Thirdly, this study has found bulk wet densities of the clog material, ρ_c , between 1.5 and 2.0 Mg/m³. This combined with the observed total calcium fraction of 26% of total clog material ($f_{Ca} \approx 0.26$) can be used in simple engineering calculations such as those proposed by Rowe and Fleming (1998) to estimate the rate of clogging of different collection system designs.

G. Inconsistencies in Rowe's column studies

The column studies by Rowe *et al.* (2000a, b) were carried out in laboratory columns with an internal diameter of only 50 mm, which could result in significant error in carrying out the drainable porosity measurements due to the small volumes involved. In addition the edge effect, bearing in mind the small diameter of the experimental columns, resulted in higher porosity for the columns packed with 15 mm particles ($n=0.50$) compared with $n=0.38$ and $n=0.39$ for the columns packed with 4 mm and 6 mm particles, respectively. Channelling along the column wall probably also occurred due to the absence of baffles. The glass beads used in the experiment had a smooth surface and a regular shape and may

have different clogging potential than natural materials. The leachate was passed through in the columns in upward flow and as such did not represent real conditions, leading to possibly higher clogging rates due to the following reasons:

- Gas bubbles, which (as will be shown in section 6.1.10 and 6.8) can block leachate flow, would tend to escape under the hydraulic conditions employed by Rowe *et al.* (2000a and b), while they would tend to become trapped in the matrix of polysaccharides and bacteria in downward flow.
- As clogging develops the pore space becomes occupied leading to an increase in velocity and possible shearing and transportation of the biofilm to lower sections in downward flow. This will not occur in upward flow hydraulic conditions, in which the biofilm will tend to accumulate near the inlet and possibly give rise to an enhanced degree of clogging.
- The suspended solids present in any real leachate will also tend to accumulate at the bottom of the column, contributing to even higher clogging in the section near the inlet in upward flow and increasing the clogging in the bottom section in the case of downward flow.

3.4. Comparison between the column experiments carried out by Brune *et al.* (1991), Rowe *et al.* (2000a) and Paksy *et al.* (1999)

The column experiments set up by Brune *et al.* (1991), Paksy *et al.* (1998) and Rowe *et al.* (2000a, b) were carried out in different sized columns (Figure 3-5), which were supplied with leachates with varying concentrations of VFA, Ca and Fe at different flow rates. The experimental columns were packed with different sizes of particles and were operated in saturated or unsaturated conditions.

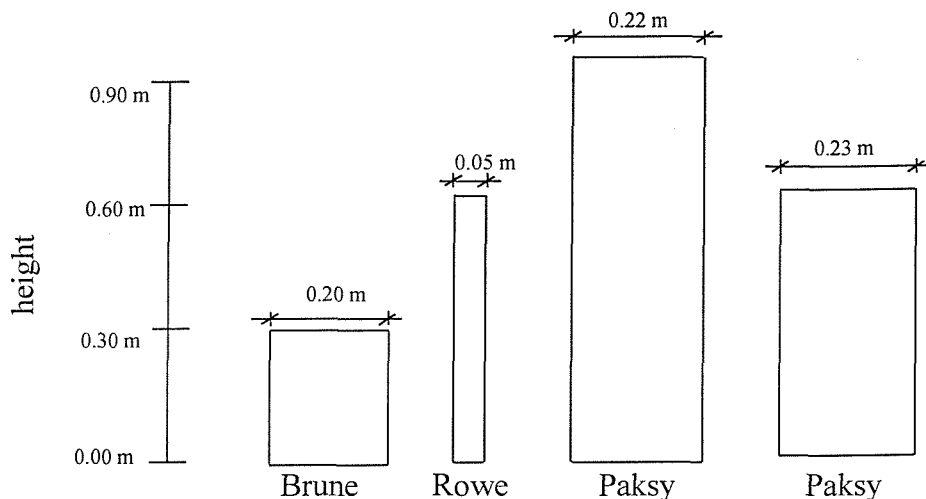


Figure 3-5: Dimensions of the experimental columns employed by the different researchers

To make comparison possible, the columns were divided into groups with similar particle sizes, as follows:

- **4 mm size particles**, including the columns packed with 1-32 mm and 2-4 mm particles (Brune *et al.*, 1991) and 4 mm particles (Rowe *et al.*, 2000a)
- **6 mm size particles**, including the columns packed with 2-8 mm particles (Brune *et al.*, 1991), 5-10 mm particles (Paksy *et al.*, 1998) and 6 mm particles (Rowe *et al.*, 2000a)
- **15 mm size particles**, including the columns packed with 8-16 mm particles (Brune *et al.*, 1991), 10-20 mm particles (Paksy *et al.*, 1998) and 15 mm particles (Rowe *et al.*, 2000a)
- **20 mm size particles**, including the columns packed with 16-32 mm particles (Brune *et al.*, 1991) and 20-40 mm particles (Paksy *et al.*, 1998).

Within these groups, the different experimental columns were compared on the basis of their organic and inorganic loading rates by volume and by pore volume, which had units of $\text{mg}/\text{cm}^3 \cdot \text{day}$. Calculation of the organic and inorganic loading rates allowed equilibration of the different leachate characteristics and flow rates over the different

column cross sections. The loading rates were calculated by dividing the total COD or inorganics passed by the equivalent days at full flow rate and by the total volume or the pore volume of the columns. The equivalent days at full flow rate were determined by dividing the total litres passed to the flow rate. The organic loading rate was classified as follows:

- **high** organic loading in the range of 10-20 mg COD/cm³ pore volume.day
- **medium** organic loading – from 1 to 10 mg COD/cm³ pore volume.day
- **low** organic loading – less than 1 mg COD/cm³ pore volume.day.

3.4.1. 4 mm size particles

Experimental set up details and leachate characteristics for the 4 mm particle size group are shown in Table 3-8.

Column test / Particle size (mm)	Brune <i>et al.</i> 1-32 mm	Brune <i>et al.</i> 2-4 mm	Rowe <i>et al.</i> 4 mm
Bed dimensions i.d. × height (cm)	20 x 30	20 x 30	5 x 59.1
Cross sectional area (cm ²)	314.16	314.16	19.63
Volume of the column (litres)	9.425	9.425	1.160
Initial pore volume (litres)	1.414	3.770	0.463
Flow rate (litre/day)	6.8	9.5	1.0
Litres passed	1700	3420	159
Equivalent days at full flow rate (days)	250	360	159
Period over which it was observed (days)	250	360	252
Volume of clog material (litres)	0.565	1.885	0.270
COD concentration in leachate (mg/l)	5260	5260	10756
COD concentration removed per litre of leachate (mg/l)	3156	3156	7959.44
Total COD removed (kg)	5.37	10.79	1.27
Organic loading rate by volume (mg COD/cm³.d)	2.28	3.18	6.86
Organic loading rate by pore volume (mg COD/cm³.d)	15.18	7.95	17.21
Ca concentration in leachate (mg/l)	255	255	536
Ca concentration removed per litre of leachate (mg/l)	153.0	153.0	396.6
Fe concentration in leachate (mg/l)	47	47	205
Fe concentration removed per litre of leachate (mg/l)	18.8	18.8	82
SO ₄ concentration in leachate (mg/l)	61	61	89
SO ₄ concentration removed per litre of leachate (mg/l)	24.4	24.4	35.6
Total inorganics (Ca, Fe, SO ₄) removed (kg)	0.33	0.67	0.08
Inorganic loading rate by volume (mg/cm³.d)	0.14	0.20	0.44
Inorganic loading rate by pore volume (mg/cm³.d)	0.94	0.49	1.11
Hydraulic surface loading (ml/cm ² .day)	21.65	30.24	50.93
Hydraulic volumetric loading (ml/cm ³ .day)	0.72	1.01	0.86
Hydraulic pore volumetric loading (ml/cm ³ .day)	4.81	2.52	2.16
State of clogging	Completely clogged	Completely clogged	Completely clogged

Table 3-8: Organic and inorganic loading for the 4 mm particle size group

The COD, Ca, Fe and SO_4 concentrations removed per litre of leachate are calculated using average % of removal for the duration of the experiment. The column packed with 1-32 mm particles operated by Brune *et al.* (1991) and the one packed with 4 mm particles operated by Rowe *et al.* (2000a) had very high organic loading rates (respectively 15.18 and 17.20 $\text{COD}/\text{cm}^3\cdot\text{d}$) and clogged relatively fast (respectively after 250 and 252 days of operation). The column packed with 2-4 mm particle sizes operated by Brune *et al.* (1991) had a medium organic loading rate (7.95 $\text{COD}/\text{cm}^3\cdot\text{d}$) and required a longer period of time (360 days) to reach complete clogging.

The cumulative amount of COD removed, expressed in kg, correlates well with the volume of clog material in litres as shown in Figure 3-6. As might be expected the higher the amount of COD removed, the bigger the volume of the clog material.

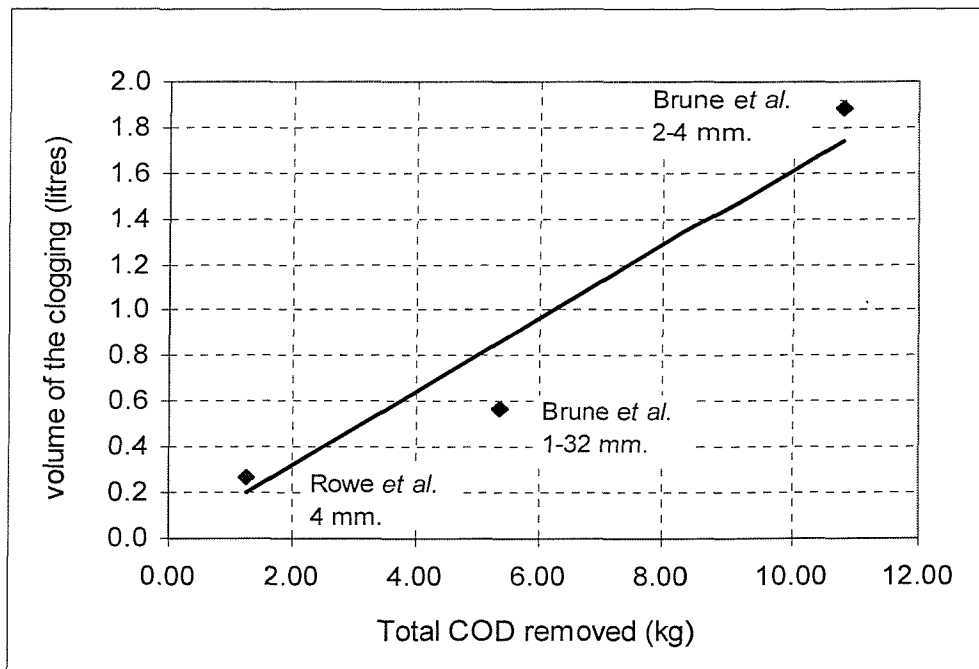


Figure 3-6: Correlation between the volume of clog material and total COD removed for the 4 mm particle size group.

3.4.2. 6 mm size particles

Experimental set up details and leachate characteristics for the 6 mm size particles group are shown in Table 3-9. The data shows that although Paksy *et al.* (1998) and Rowe *et al.* (2000a) used similar flow rates expressed in litres/day it resulted in different hydraulic

fluxes per unit volume due to differences in the total and pore volume of the columns. Similarly, comparable concentrations of organic and inorganic substances in the leachate resulted in different organic and inorganic loading rates per unit total or pore volume.

Column test / Particle size (mm)	Brune <i>et al.</i> 2-8 mm	Paksy <i>et al.</i> 5-10 mm	Paksy <i>et al.</i> 5-10 mm	Rowe <i>et al.</i> real 6 mm	Rowe <i>et al.</i> synthetic 6 mm
Bed dimensions i.d. × height (cm)	20×30	22×91	23×60	5×59.1	5×63.7
Cross sectional area (cm ²)	314.160	380.130	415.480	19.630	19.63
Volume of the column (litres)	9.425	34.590	24.930	1.160	1.25
Initial pore volume (litres)	2.640	12.430	10.550	0.441	0.475
Flow rate (litre/day)	9.10	1.15	1.28	1.00	1.00
Litres passed	3094	587.46	479.58	176	327.20
Equivalent days at full flow rate (days)	340	510	375	176	327
Period over which it was observed (days)	340	510	409	259	355
Volume of clog material (litres)	1.508	1.164	0.556	0.306	0.300
COD concentration in leachate (mg/l)	5260	20011.95	20210.94	10756	16860
COD concentration removed per litre of leachate (mg/l)	3156	14108.19	7124.98	7959.44	5058
Total COD removed (kg)	9.76	8.29	3.42	1.40	1.65
Organic loading rate by volume (mg COD/cm³.d)	3.05	0.47	0.37	6.86	4.04
Organic loading rate by pore volume (mg COD/cm³.d)	10.88	1.31	0.86	18.06	10.65
Ca concentration in leachate (mg/l)	255	200	200	536	1040
Ca concentration removed per litre of leachate (mg/l)	153	100	100	396.64	582.40
Fe concentration in leachate (mg/l)	47	100	100	205	0.74
Fe concentration removed per litre of leachate (mg/l)	18.80	40.00	40.00	82.00	0.29
SO ₄ concentration in leachate (mg/l)	61.00	101.38	71.13	89.00	127.00
SO ₄ concentration removed per litre of leachate (mg/l)	24.40	40.55	28.45	35.60	50.80
Total inorganics (Ca, Fe, SO ₄) removed (kg)	0.61	0.11	0.08	0.09	0.21
Inorganic loading rate by volume (mg/cm³.d)	0.19	0.01	0.01	0.44	0.51
Inorganic loading rate by pore volume (mg/cm³.d)	0.68	0.02	0.02	1.17	1.33
Hydraulic surface loading (ml/cm ² .day)	28.97	3.03	3.08	50.93	50.93
Hydraulic volumetric loading (ml/cm ³ .day)	0.97	0.03	0.05	0.86	0.80
Hydraulic pore volumetric loading (ml/cm ³ .day)	3.45	0.09	0.12	2.11	2.11
State of clogging	Extensively clogged	Moderate clogging	Moderate clogging	Completely clogged	Completely clogged

Note: Rowe *et al.* real – stands for column experiments using real leachate, Rowe *et al.* synthetic – stands for column experiments using synthetic leachate.

Table 3-9: Organic and inorganic loading for the 6 mm particle size group

At first sight, it is surprising that the columns operated by Paksy *et al.* (1998) did not clog completely bearing in mind the relatively high COD concentrations (in the range of 20,000 mg/litre) in their leachate, while the columns operated by Brune *et al.* (1991) and Rowe *et al.* (2000a) clogged extensively despite the smaller COD concentrations (from 5,000 to 16,860 mg/litre) in their leachate. However, the column operated by Brune *et al.* (1991) had a high hydraulic flow rate (9.1 litres/day) and the column used by Rowe *et al.* (2000a) had a very small pore volume (0.440 litres), resulting in very high organic loading rates for these columns, causing the observed fast occlusion of the pore space in these columns.

The columns operated by Paksy *et al.* (1998) had a very large pore volume (10.55 and 12.43 litres) leading to a 10 to 20 times lower organic loading rate, which resulted in development of only moderate clogging. Theoretically these columns would eventually clog as well but they would need a much longer period of time. However, Paksy *et al.* (1998) stopped the experiments prematurely due to time constraints, though it could be expected that the occlusion of the pore space probably would have developed even further if the researchers had continued operating the tests.

The cumulative amount of COD removed in the columns, expressed in terms of kg correlates well with the volume of clog material in litres as shown in Figure 3-7. Similarly, the higher the amount of COD removed, the bigger the volume of the clog material.

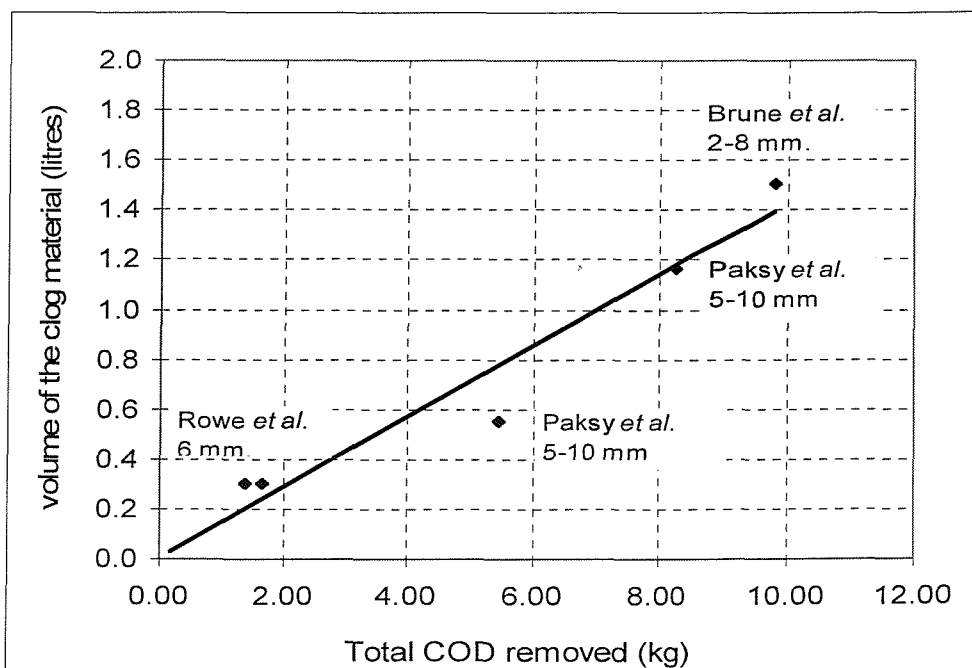
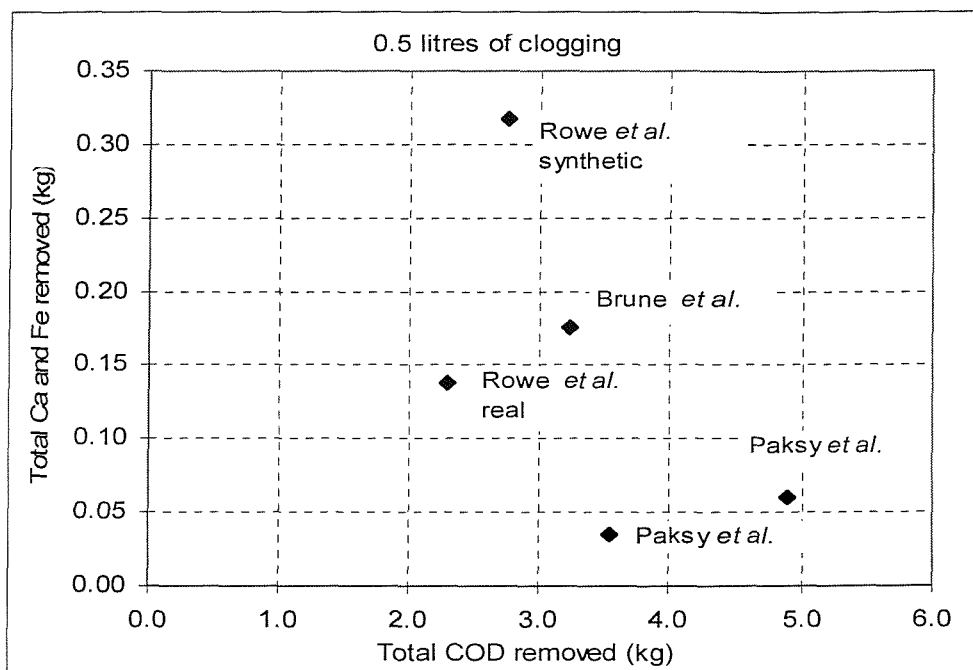


Figure 3-7: Correlation between the volume of clog material and total COD removed for the 6 mm particle size group

Figure 3-8 shows the amount of COD and inorganic substances required to accumulate 0.5 litres of clog material. The calculations were made by extrapolating the existing volume of clog material to 0.5 litres assuming a linear relationship between the volume of clog material and the quantity of organic and inorganic substances needed to sustain it. A comparison between the columns operated by Rowe *et al.* (2000a), supplied with synthetic and real leachate reveals that higher quantities of COD and inorganic substances are required in the column supplied with synthetic leachate to compensate for the absence of suspended solids (see 3.3.4.D).



Note: Rowe *et al.* real – stands for column experiments using real leachate, Rowe *et al.* synthetic – stands for column experiments using synthetic leachate.

Figure 3-8: Amount of COD and inorganics needed to obtain equal volume of clogging in the 6 mm particle sizes group.

The relatively higher amount of organics and inorganic substances required to accumulate the same amount of clog material in the experiments carried out by Brune *et al.* (1991) probably accounts for the fact that the leachate in these column tests was initially passed through a layer of composted waste, located above the drainage aggregate, where part of the organics were consumed without contributing to the clogging process in the drainage aggregate. In addition, the experiment carried out by Brune *et al.* (1991) was essentially conducted in unsaturated conditions. An analogy between the tests supplied with synthetic leachate carried out by Rowe *et al.* (2000a) and Paksy *et al.* (1998) suggests that although

organic concentrations induce significant biofilm growth, if the inorganic precipitates are not present to cement the clog material and make it impermeable, higher COD concentrations are needed to reach comparable clogging rates.

3.4.3. 15 mm size particles

Experimental set up details and leachate characteristics for the 15 mm particle size group are shown in Table 3-10. The column experiments carried out by Rowe *et al.* (2000a) had very high organic loading rates and clogged completely within a year of operation. The tests carried out by Brune *et al.* (1991) had a medium organic loading rate and this resulted in the development of moderate clogging during the operating period. The column experiments conducted by Paksy *et al.* (1998) had a low organic loading rate and negligible clogging over the period they were operated.

There is no apparent trend for the cumulative amount of COD removed and the volume of clog material as shown in Figure 3-9.

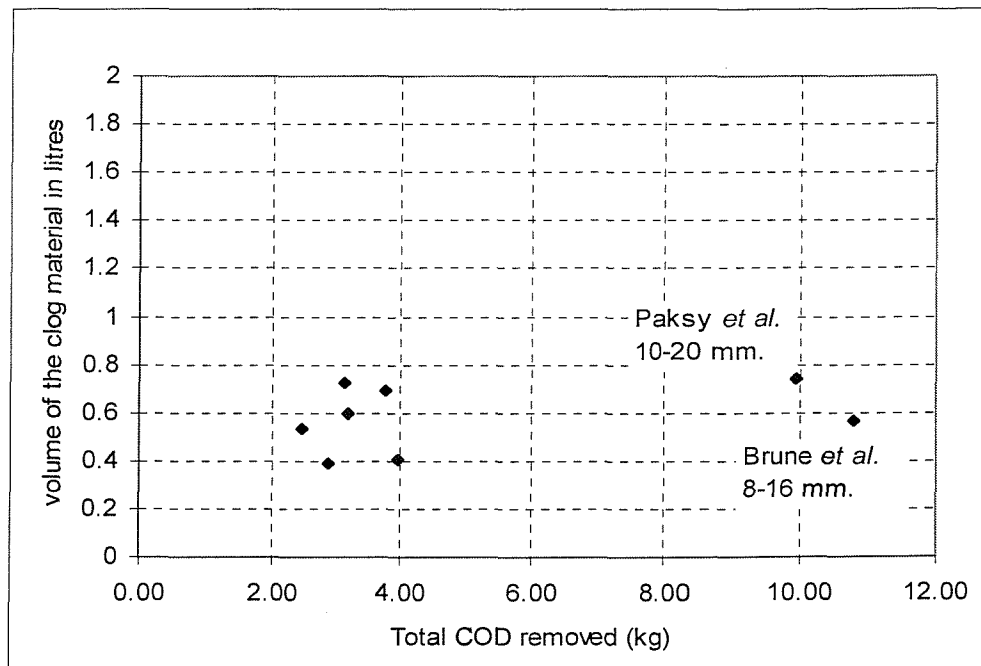


Figure 3-9: Correlation between the volume of clog material and total COD removed for the 15 mm particle sizes group

Column test / Particle size (mm)	Brune <i>et al.</i> 8-16 mm	Paksy <i>et al.</i> 10-20 mm	Paksy <i>et al.</i> 10-20 mm	Paksy <i>et al.</i> 10-20 mm	Paksy <i>et al.</i> 10-20 mm	Paksy <i>et al.</i> 10-20 mm	Paksy <i>et al.</i> 10-20 mm	Paksy <i>et al.</i> 10-20 mm	Rowe <i>et al.</i> 15 mm
Bed dimensions i.d. × height (cm)	20 x 30	22 x 91	22 x 91	22 x 91	22 x 91	22 x 91	22 x 91	22 x 91	5 x 59.1
Cross sectional area (cm ²)	314.16	380.13	380.130	380.13	380.130	380.13	380.13	380.13	19.63
Volume of the column (litres)	9.425	34.59	34.590	34.590	34.590	34.590	34.590	34.590	1.160
Initial pore volume (litres)	3.77	13.20	12.75	12.75	12.96	15.30	13.22	12.71	0.63
Flow rate (litre/day)	7.40	0.62	1.24	0.62	1.10	0.62	0.62	1.11	1.00
Litres passed	3418.80	230.02	547.28	239.32	407.60	230.02	230.02	563.08	310.00
Equivalent days at full flow rate (days)	462	371	442	386	370	371	371	509	383
Period over which it was observed (days)	462	371	442	386	370	371	371	509	383
Volume of clog material (litres)	0.57	0.39	0.74	0.39	0.70	0.72	0.60	0.41	0.54
COD concentration in leachate (mg/l)	5260	13515	20713.1	13515.0	19078	13515	13515	20068.2	10756
COD concentration removed per litre of leachate (mg/l)	3156	12529.4	18157.1	12071.7	9249.3	13633.6	13820.5	7031	7959.4
Total COD removed (kg)	10.79	2.88	9.94	2.89	3.77	3.14	3.18	3.96	2.47
Organic loading rate by volume (mg COD/cm³.d)	2.48	0.23	0.65	0.22	0.30	0.24	0.25	0.23	6.86
Organic loading rate by pore volume (mg COD/cm³.d)	6.20	0.59	1.76	0.59	0.79	0.55	0.65	0.61	12.73
Ca concentration in leachate (mg/l)	255	200	200	200	200	200	200	200	536
Ca concentration removed per litre of leachate (mg/l)	153	100	100	100	100	100	100	100	396.64
Fe concentration in leachate (mg/l)	47	100	100	100	100	100	100	100	205
Fe concentration removed per litre of leachate (mg/l)	18.80	40	40	40	40	40.	40	40	82
SO ₄ concentration in leachate (mg/l)	61.00	79.11	107.23	88.55	89.00	79.11	79.11	100.04	89
SO ₄ concentration removed per litre of leachate (mg/l)	24.40	31.64	42.89	35.42	35.60	31.64	31.64	40.02	35.60
Total inorganics (Ca, Fe, SO ₄) removed (kg)	0.67	0.04	0.10	0.04	0.07	0.04	0.04	0.10	0.16
Inorganic loading by volume (mg/cm³.d)	0.154	0.003	0.007	0.003	0.006	0.003	0.003	0.006	0.443
Inorganic loading by pore volume (mg/cm³.d)	0.385	0.008	0.014	0.009	0.015	0.007	0.008	0.016	0.823
Hydraulic surface loading (ml/cm ² .day)	23.55	1.63	3.26	1.63	2.90	1.63	1.63	2.91	50.93
Hydraulic volumetric loading (ml/cm ³ .day)	0.785	0.018	0.036	0.018	0.032	0.018	0.018	0.032	0.862
Hydraulic pore volumetric loading (ml/cm ³ .day)	1.963	0.047	0.097	0.049	0.085	0.041	0.047	0.087	1.600
Suspended solids (mg/l)	Moderate clogging	Negligible clogging	Negligible clogging	Negligible clogging	Negligible clogging	Negligible clogging	Negligible clogging	Negligible clogging	Completely clogged

Table 3-10: Organic and inorganic loading for the 15 mm particle size group

3.4.4. 20 mm size particles

Experimental set up details and leachate characteristics for the 20 mm size particles group are shown in Table 3-11. The column experiments carried out by Brune *et al.* (1991) had a medium organic loading rate. However, they did not experience even moderate clogging because of the large initial pore volume and the relatively short period of operation. The column experiments conducted by Paksy *et al.* (1998) had a very low organic loading rate resulting in negligible clogging over the operation period.

Column test / Particle size (mm)	Brune <i>et al.</i> 16-32 mm	Paksy <i>et al.</i> 20-40 mm	Paksy <i>et al.</i> 20-40 mm	Paksy <i>et al.</i> 20-40 mm
Bed dimensions i.d. × height (cm)	20 x 30	35 x 88	35 x 88	30 x 88
Cross sectional area (cm ²)	314.16	962.11	962.11	706.86
Volume of the column (litres)	9.425	84.666	84.666	62.204
Initial pore volume (litres)	4.241	34.550	34.610	21.910
Flow rate (litre/day)	9.40	0.62	4.82	6.90
Litres passed	4342.8	222.58	2050.52	1815
Equivalent days at full flow rate (days)	462	359	425	263
Period over which it was observed (days)	462	359	425	263
Volume of clog material (litres)	0.47	0.72	0.20	0.31
COD concentration in leachate (mg/l)	5260	16673	2370.5	2225.2
COD concentration removed per litre of leachate (mg/l)	3156	15917.9	604.2	1557.6
Total COD removed (kg)	13.71	3.54	1.24	2.83
Organic loading rate by volume (mg COD/cm³.d)	3.15	0.12	0.03	0.17
Organic loading rate by pore volume (mg COD/cm³.d)	7.00	0.29	0.08	0.49
Ca concentration in leachate (mg/l)	255	200	200	200
Ca concentration removed per litre of leachate (mg/l)	153	100	100	100
Fe concentration in leachate (mg/l)	47	100	100	100
Fe concentration removed per litre of leachate (mg/l)	18.80	40	40	40
SO ₄ concentration in leachate (mg/l)	61	81.68	27	27
SO ₄ concentration removed per litre of leachate (mg/l)	24.40	32.67	10.80	10.80
Total inorganics (Ca, Fe, SO ₄) removed (kg)	0.85	0.04	0.31	0.27
Inorganic loading rate by volume (mg/cm³.d)	0.196	0.001	0.009	0.017
Inorganic loading rate by pore volume (mg/cm³.d)	0.435	0.003	0.021	0.047
Hydraulic surface loading (ml/cm ² .day)	29.92	0.64	5.01	9.76
Hydraulic volumetric loading (ml/cm ³ .day)	0.997	0.007	0.057	0.111
Hydraulic pore volumetric loading (ml/cm ³ .day)	2.216	0.018	0.139	0.315
State of clogging	Negligible clogging	Negligible clogging	Negligible clogging	Negligible clogging

Table 3-11: Organic and inorganic loading for the 20 mm particle size group

There is no apparent trend for the cumulative amount of COD removed and the volume of clog material as shown in Figure 3-10.

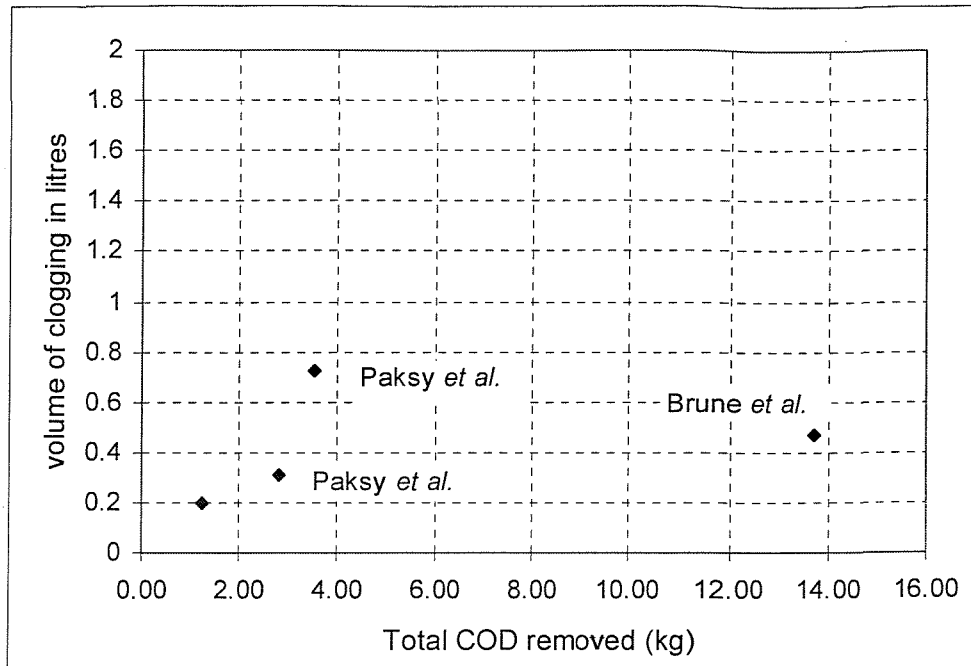


Figure 3-10: Correlation between the volume of clog material and total COD removed for the 20 mm particle size group

3.4.5. Common observations for all the groups

A correlation exists between the amount of COD removed from the leachate and the volume of clog material that developed (Figure 3-11). The data from the columns tests carried out by Brune *et al.* (1991) were disregarded as previously explained (section 3.4.2.). This correlation does not appear to depend on the particle size of the drainage aggregate, indicating that the total volume of the clog material will depend mainly on the amount of organics in the leachate. However, the particle sizes play a major role in the distribution pattern of the clogging. Rowe *et al.* (2000a) suggested that clogging occurred over a similar surface area – the top 20 cm for the small particles, which had a large surface area per unit volume and over the entire column ($h = 70$ cm) for the larger particles. After similar amounts of COD had been removed, the columns packed with small particles clogged faster because the clogging occurred in a small section near the column inlet which rapidly lost its permeability thereby preventing leachate reaching the lower sections of the columns. The larger particles allowed a more uniform distribution of the clogging throughout the experimental reactor thus providing a larger pore space resulting in a longer period of time over which the system was permeable.

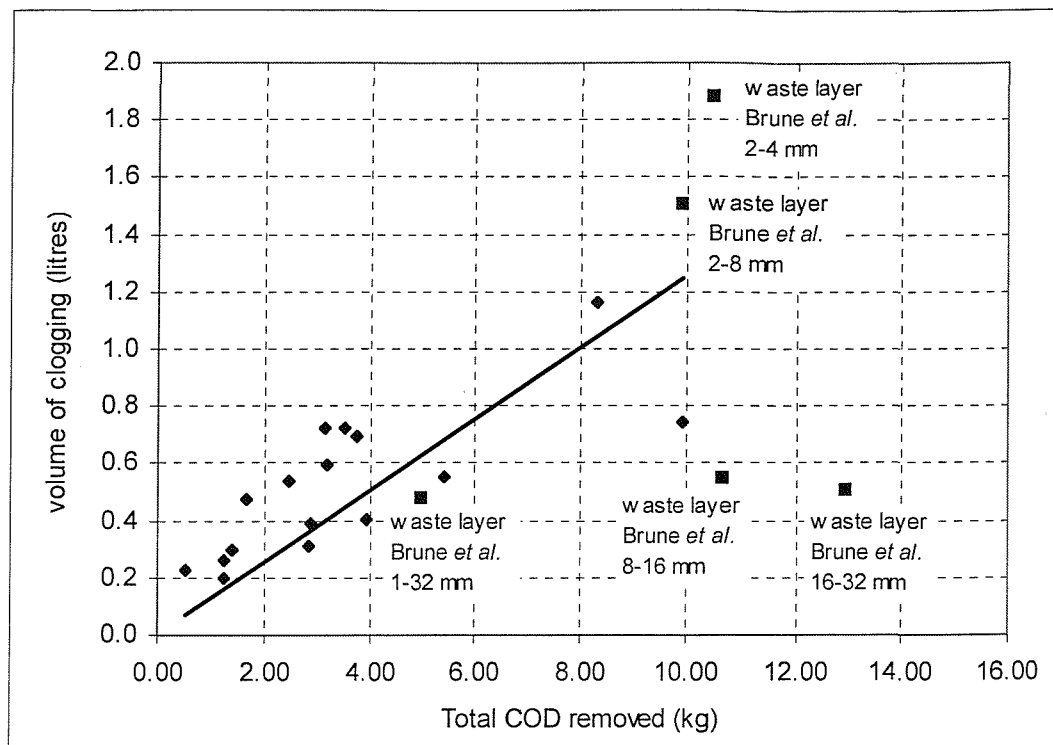


Figure 3-11: Correlation between the volume of clog material and total COD retained for all particle sizes

3.5. Mechanism of clogging

It has been shown that clogging can be caused by growth of bacteria, referred to as microbiological clogging, by precipitation of low solubility inorganic salts, referred to as bio-chemical clogging, or by suspended solids transported from the waste mass with the leachate, referred to as physical clogging. The mechanisms of the first two types of clogging has been investigated by Brune *et al.* (1991), Fleming *et al.* (1999) and Costerton *et al.* (1995) and will be discussed in more detail.

3.5.1. Microbiological clogging

Microbiological clogging is caused by the growth of bacteria in the leachate drainage system. Following adhesion to a surface, a bacterial cell undergoes a change that alters many of its structural molecules and induces synthesis of exopolysaccharides (EPS) (Costerton *et al.*, 1995). EPS provide the means by which the bacterial cell attaches to the surface of the drainage aggregate and other bacterial cells to form biofilms. Brune *et al.*

(1991) observed that the microorganisms colonized the surface of the gravel in the form of a highly porous 3-dimensional network of aggregates of bacteria. Costerton *et al.* (1995) used confocal scanning laser microscopy to study the biofilm structure and suggested that cell division coupled with exopolysaccharide synthesis leads to the development of micro-colonies enclosed in dense slime which are attached to the colonised surface. Some micro-colonies have simple conical structures, while others are mushroom-shaped (Figure 3-12). Water channels within the bacterial micro-colonies have been observed and there is evidence that advective flow occurs within the channels, which can provide a network that carries the bulk fluid containing nutrients throughout the vertical length of the biofilm. Thus the water channels act as a nutrient transportation system (Costerton *et al.*, 1995). However, McCarty *et al.*, 1984 and Costerton *et al.*, 1995 have show that molecular diffusion acts as a transport mechanism as well indicating that both diffusion and advection play a part in the transport of nutrients within the biofilm.

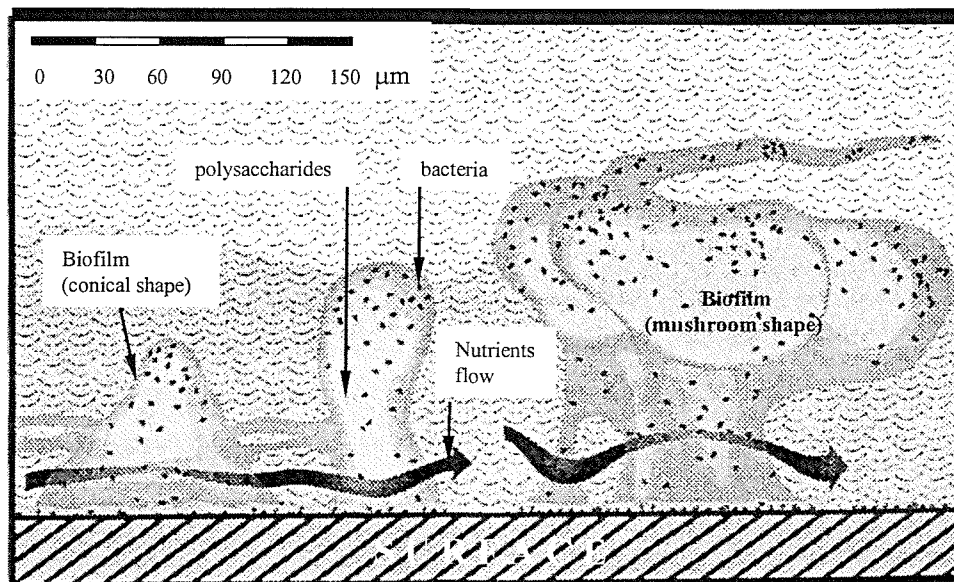


Figure 3-12: Model of the architecture of single-species biofilm (Costerton *et al.*, 1995)

3.5.2. Bio-chemical clogging

A. Mechanism.

Clogging is caused not only by the accumulation of microbial biofilms but also by mineral precipitates, composed mainly of carbonates and sulphides (Brune *et al.*, 1991). Biochemical precipitation is essentially caused by two processes:

1. Iron reducing bacteria solubilise Fe^{3+} by reducing it to Fe^{2+} , while SRB reduce sulphate to sulphide. This bioreduction of sulphate causes the milieu in the vicinity of the SRB to become alkaline which results in sulphur precipitating as insoluble ferrous sulphide.
2. Fermentative organisms produce organic acids, lowering the pH of the leachate and thus mobilise the calcium. Precipitation of calcium carbonate on the surface of the methane producing and sulphate-reducing bacteria probably results from their metabolic consumption of hydrogen ions causing a local elevation of the pH (Brune *et al.*, 1991).

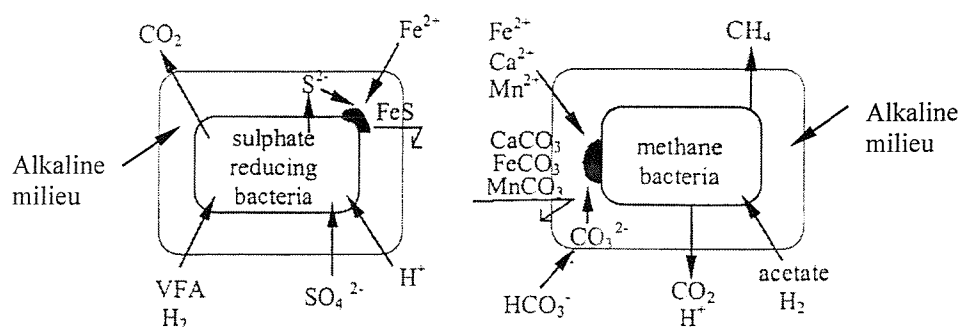


Figure 3-13: Formation of incrustations (after Brune *et al.*, 1991); VFA - volatile fatty acids

Rittmann *et al.* (1996) showed that CaCO_3 is precipitated not only by localised pH increases but also by global changes in the environment of the leachate drainage system, such as increased pH and dissolved carbonates, as a result of degradation of the VFAs present in the leachate.

B. Location of the inorganic precipitates

Metal sulphides and carbonates precipitate around nuclei, which can be provided by the fixed bacteria (Brune *et al.*, 1991), colloids or any other microscopic imperfections on the clean aggregate surface (Bordier and Zimmer, 1999). Brune *et al.* (1991) observed that the precipitates of inorganic material appeared as pimples on the surface of the microorganisms and their excretion products (slime fibrils) but never on the uncolonised spaces in between. However, observations by Brune *et al.* (1991) were made on the basis of on-growth experiments, which were carried out by placing sterilised glass microscope slides for varying periods of time in landfill drain pipes. The glass slides are perfectly smooth while natural granular materials used in leachate collection systems are imperfect

and numerous microscopic “peaks” can be found which can act as precipitation nuclei. Bordier and Zimmer (1999) carried out tests to elucidate the question of where the mineral precipitates form. The researchers distinguished pure mineral deposits (with minerals as precipitation nuclei), from organo-mineral deposits (with bacteria as precipitation nuclei) by staining the bacteria with acridine orange and subsequently observing the clogged material with scanning electron microscopy (SEM) coupled with X-ray electron diffraction spectroscopy (EDS). A high concentration of zinc, contained in the acridine orange and detected by the SEM/EDS analysis, would suggest that deposits were formed around a bacterial nucleus. The results showed precipitates forming not only on bacterial nuclei but also on mineral nuclei as well, indicating that precipitates can be found even on the clean surface of the drainage media.

3.5.3. Development of clogging with time

Brune *et al.* (1991) named the initial deposits “primary” and noted that subsequently they increased in size (secondary growth) and fused together. The large surface area thus created provided very favourable conditions for renewed colonization (Brune *et al.*, 1991). Cooke *et al.* (1999) developed the concept further by suggesting the existence of two types of biofilm layers – active and inactive. The active biofilm becomes inactive as growth proceeds outward and consists of inert biomass (non-degradable organic solids produced as part of dead biomass degradation) and mineral precipitates (Cooke *et al.*, 1999).

Rowe *et al.* (1995) suggested that clogging occurs in two stages. Initially, during a period which could be termed the “soft slime” stage, the leachate collection system is colonised by an anaerobic mixed bacterial culture causing the growth of a thick continuous biofilm over the surface of the drainage stone. The soft slime may occlude much of the pore space, but has been observed to exhibit some permeability and does not represent a permanent “clog”. It was reported that this process may take up to several years, as was evidenced by the soft black viscous slime observed during excavations of 1 to 4 years old areas of drainage blanket at the Keele Valley Landfill. This stage is presented in Figure 3-14 and is marked as 1.

In the second “mineral precipitation” stage of clogging, the biochemical processes within the biofilm and bulk liquid cause the deposition of mineral precipitates, chiefly calcium

carbonate, with lesser amounts of magnesium and iron carbonates and iron sulphide. These precipitates accumulated around surface-active nucleation sites provided by individual bacterial cells and extra-cellular polymers, entrapped soil particles and other mineral grains. This stage is marked as 2 in Figure 3-14 and is consistent with field observations, where it was observed that mineral deposits were concentrated at the base of the biofilm adjacent to the solid drainage stone. This is presumably where conditions differ most from those in the bulk liquid (increased pH) (Rowe *et al.*, 1995). Harper and Sudan (1991) indicate that in some types of biofilms, a pH higher than 10 can be expected a few micrometres within the biofilm surface.

As clogging develops and as the concurrent extensive occlusion of the free pore space continues, the leachate flow is forced through the biofilm. This will cause mineralization to develop throughout the volume of the biofilm mediated by the already established high pH conditions within the whole system, making the clog impermeable. This stage is marked as 3 in Figure 3-14.

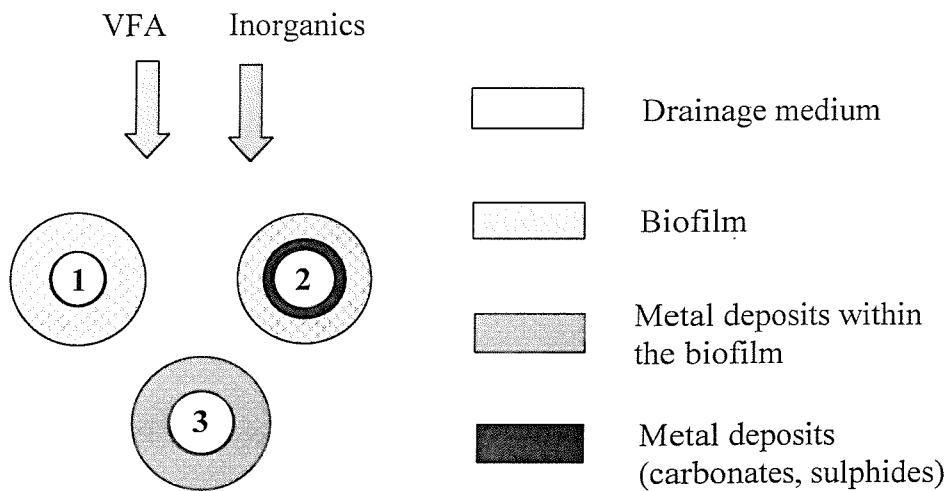


Figure 3-14: Mechanism of clogging

3.6. Scope for new research

The literature review has shown that various experiments have been conducted using municipal solid waste (MSW) type leachate containing a relatively high organic content. No research has been carried out on the clogging potential of leachate with lower organics but higher sulphate and possibly metal concentrations, which is representative of the leachate emanating from a low level radioactive waste. Whether the low organic content can induce sufficient microbiological and biochemical clogging or if certain combinations between organic and inorganic constituents are required are an issue, which has been investigated in this thesis.

The experiments conducted by Rowe *et al.* (2001a) emphasised the correlation between COD removal and CaCO_3 precipitation, Paksy *et al.* (1999) stressed the importance of the organics. Brune *et al.* (1991) mentioned that depositions of ferrous sulphide contributed to clogging, but did not measure sulphate concentration or removal, nor relate sulphate removal to COD consumption. It appears that the effect of the sulphate on the clogging process has received little attention. This work has therefore focused on the sulphates and their contribution to the clogging process. The experiments also explored the factors affecting the rates of sulphate reduction and methanogenesis, the relationship between the two, and the correlation with VFA removal and clogging.

Chapter 4

Site Description and Test History

This chapter provides information on the low level radioactive waste disposal site and the link between the field conditions and the laboratory experimental set up.

4.1. Site description

The Drigg site, owned and operated by BNFL, is the UK's principal site for the disposal of LLW. The site has been in operation since 1959 and receives wastes from a wide range of sources including: nuclear power stations, nuclear fuel cycle facilities, isotope manufacturers, universities, hospitals, general industry and from the remediation of historically contaminated sites. Only LLW is accepted for disposal at the Drigg site. This is defined as wastes containing radioactive materials other than those acceptable for disposal with ordinary refuse, but not exceeding 4GBq/t alpha emitting radionuclides and 12 GBq/t all other radionuclides (British Nuclear Fuels Ltd., 2002).

Since the start of the disposal operations at the site in 1959, waste disposal practices have varied to meet operational and regulatory requirements and to reflect developments in waste management. The initial disposal techniques involved loose tipping of waste into a series of trenches excavated into the glacial sediments beneath the consented area. In the late 1980s, trench disposal has been phased out in preference to emplacement of containerised waste in reinforced concrete vaults. The containerised waste consists of highly compacted (or non-compactable) waste immobilised in 20m³ steel containers by the addition of cementitious grout. Larger items of wastes are grouted directly, *in-situ* in the vault (British Nuclear Fuels Ltd., 2002).

The current project involved laboratory tests using leachate representative of the trench disposals only. Trench waste is typically made up of paper, packaging material, plastic sheeting, protective clothing and scrap metal. Although the waste has a superficial similarity to domestic waste, a major difference is that the putrescible fraction is limited to cellulose originating from paper products and wood.

4.2. Current leachate collection system

Leachate from the trenches is collected by a series of interceptor drains from the trenches drainage systems. The leachate flows under gravity from the interceptor drains through a drain to the marine holding tanks. The marine holding tanks then discharge through a pipeline to a series of diffusers off-shore in the Irish Sea (British Nuclear Fuels Ltd., 2002).

It is anticipated that the present arrangement of marine discharge will continue until the construction of the final engineering about 2100, whereupon the marine discharge facilities will be decommissioned and alternative discharge route made. Decommissioning of the marine outfall route is required, as the overland and sub-sea pipe-work is not considered to provide a viable long-term leachate disposal route because it is:

- remote from the site
- vulnerable to physical disruption and intrusion
- liable to blockage and clogging.

Damage of clogging of the marine outfall system could result in the backup of leachate within the pipe-work and the uncontrolled release of leachate into the near surface waters at some intermediate point between the site and the Irish Sea (British Nuclear Fuels Ltd., 2002).

4.3. Proposed future leachate collection system

The site closure concept plans for the replacement of the engineering pipeline with a passive alternative. Hydrological studies have demonstrated the continuity of the regional aquifer and the general south-westerly flow directions and discharge off-shore. A controlled discharge of leachates into the regional aquifer will therefore operate in a

similar way to the existing marine pipeline but will provide a robust long-term, alternative disposal route to an off-shore discharge location. This will be achieved through the engineering of high capacity vertical drain (British Nuclear Fuels Ltd., 2002).

Currently, the design of the vertical drain is at a conceptual stage and the choice of drainage material is under consideration. It was recognised that the long-term performance of the vertical drain will depend not only on careful installation and operation but also on careful planning at the design stage. The correct choice of drain materials, particle sizes and thickness are crucial in minimising the susceptibility of any drainage system to physical, microbiological and chemical clogging, thus ensuring its satisfactory long-term performance. Some of the factors influencing the microbiological and chemical clogging were investigated in this thesis. The physical clogging was studied by previous researchers and provided guidance for selection of particle sizes for the drainage and filter material and thicknesses employed in the experiments described in this thesis.

4.4. Test History

A series of experiments was conducted by other researchers to investigate the parameters governing the physical clogging of the vertical drain due to migration of fines from the soil only, as it is intended that the vertical drain will in reality be installed in natural ground. The overall aim was to obtain experimental data to guide the selection of the filter and drain materials and thicknesses to guard against clogging by soil fines.

The experimental data suggested that a filter of 6mm size aggregate and a thickness of 300mm and a drain of 40mm size aggregate and a thickness of 300mm. will not be susceptible to clogging due to migration of fines from the natural soil. These values were used to set up the experimental columns where the factors governing the microbiological and chemical clogging were investigated.

Chapter 5

Materials and Methods

This chapter describes the design and operation of the experimental apparatus used in this study. Improvements in the design of the apparatus made during this study are outlined, and the analytical methods used are also reviewed.

5.1. Column design

The laboratory tests which were part of this study were carried out in four permeameter columns (Figure 5-1). The columns were made from clear Perspex tube of internal diameter 257mm, 1000mm in height. They contained a layer of 30cm depth of 40mm aggregate, representing a main drainage layer, overlain by a 30cm depth layer of 6mm aggregate, representing a filter layer. To minimise preferential flow of leachate along the wall of the permeameter, the particle size of the drainage aggregate has to be twenty times less than the diameter of the column (Peeling *et al.*, 1999). The particle sizes of the filter layer complied with this rule but the particles of the drainage layer did not. For this reason baffles were installed through the main drainage layer to compensate for edge effects and channelling along the wall of the permeameter. Leachate inlet and gas outlet ports were incorporated into the lid. The leachate flow rate through the columns was regulated using a Watson Marlow pump (model 505S equipped with a 304MC pump head and 1.65mm bore marprene tube). PVC tubes were used for leachate supply and gas removal. PVC was chosen as a material because of its low air diffusion coefficient thus allowing maintenance of anaerobic conditions within the system. An overflow pipe was used to maintain a constant leachate level within each column.

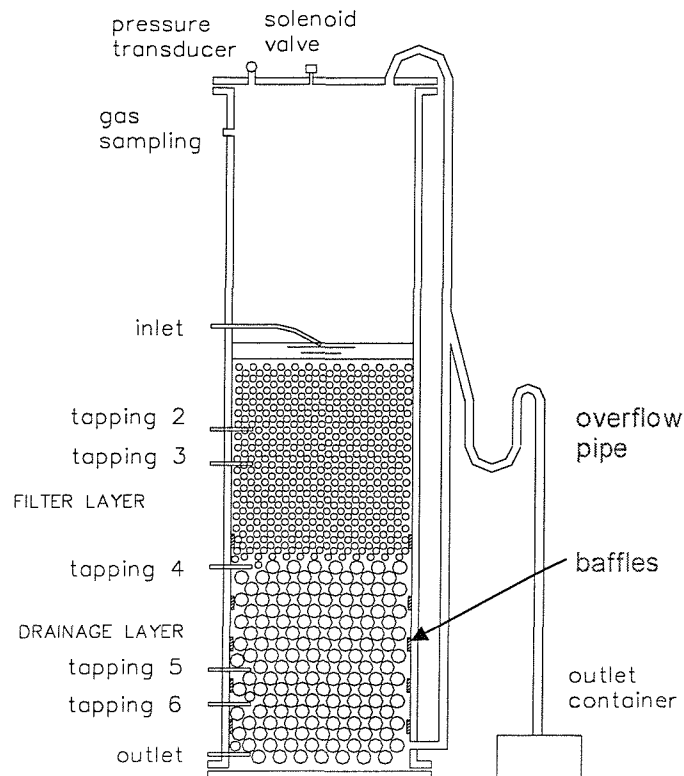


Figure 5-1: The experimental column

Six tappings along the vertical length of each column were used to sample leachate and measure drainable pore volumes (DPV) at various depths within the column. The columns were operated in a temperature-controlled environment, at a temperature of 22-23°C. This temperature was considered appropriate in view of the low organic content and shallow depth of the wastes. The lower the organic content the less enhanced the microbiological activity would be, resulting in lower energy and heat generation rates bearing in mind that part of the energy released by the bacterial cells is converted to heat (Tchobanoglous *et al.*, 2002). In addition, in shallow disposal sites the rate of heat loss to the environment is greater.

The general procedure followed in setting up each permeameter column was as follows.

1. The drainage and filter layer aggregates were washed with distilled water to remove fines and oven dried at 105°C overnight.
2. Particle size distribution analyses, according to BS1377 (1990), were carried out on representative samples of the filter, the main drain and the Drigg sand. The aggregates were dry sieved and the Drigg sand wet sieved. The main drainage aggregate was

found to consist of material in the size range 28-37.5 mm and the top filter layer 5-6.3 mm.

3. The main drain and the filter media were placed in the column from the top.

The total mass of each aggregate material placed in each permeameter was recorded and the data are presented in Table 5-1.

Column No.	Drainage layer		Filter layer	
	Mass (kg)	Initial height (mm)	Mass (kg)	Initial height (mm)
1	21.251	300	21.242	300
2	21.541	300	21.586	300
3	21.468	300	20.956	300
4	22.065	300	20.689	300

Table 5-1: Mass and height of the aggregates placed in the different columns

4. The lid of the column was replaced and the column sealed. Any air bubbles were flushed out with filtered rainwater from the inlet/outlet ports and manometer tubes. As an additional precaution against trapped air the apparatus was left undisturbed for 24 hours before testing was initiated.

5.2. Column operation

5.2.1. Inoculation

In order to generate a bacterial population on the drainage aggregate quickly, a simulated low level radioactive waste was used to inoculate permeameters 1 to 4. The simulated waste was mixed with natural soil (Drigg sand) in the ratio 40%/60% by dry mass to produce a representative mix of materials. It is anticipated that the vertical drain will in reality be installed in the natural ground outside the low level radioactive waste disposal, so that leachate entering the drains will have passed through both the waste and natural soil. A mixture of new and old waste is usually used for inoculation in clogging studies of this nature. The old waste is used to provide landfill bacteria and the new waste to supply nutrients for microbiological growth. In these experiments only new waste was employed because degrading waste was not available. The Drigg sand mixed with the new waste was the main source of bacterial inoculum (apart from unavoidable environmental

contamination). The composition of the inoculum is detailed in Table 5-2.

Material	% by dry mass
Drigg Sand	60.0
PVC Sheeting	6.4
Rubber gloves	4.8
Paper Sacks	4.4
Tissue	4.4
Wood Shaving	4.4
Metal Shavings	3.2
Electrical Cable	2.8
Glass Beads	2.8
Hayes Absorbent Granules	2.8
Polythene Bottles	2.0
Polythene Sacks	2.0

Table 5-2: Composition of the simulated Drigg waste/G6 sand layer

The waste layer was placed above the aggregate and the columns topped up with rainwater which was recirculated through the waste to encourage a microbial population to develop on the surface of the aggregate. Recirculation was in downward direction. The passage of water through the waste produces a solution termed an “endogenous leachate”. No filter was used to separate the waste from the drainage aggregate. This may have led to some physical clogging of the aggregate during the early stages of the experiments as a result of the washing out of particulate matter from the inoculum.

The depth of the waste layer was approximately 200 mm. The exact amounts used in each permeameter column are given in Table 5-3.

Column No	Mass (kg)	Initial height (mm)
1	3.084	200
2	2.461	190
3	2.012	200
4	1.784	200

Table 5-3: Mass of the simulated waste layer (inclusive of the Drigg sand) placed in each permeameter column

5.2.2. Continuous feeding regime (100% strength leachate)

Following the establishment of an active bacterial population (evident from the observed removal of VFA from the endogenous leachate) the columns were drained under nitrogen gas and the waste layer removed. Synthetic leachate was then supplied continuously at the top of the column in what is referred to as a continuous feeding regime. The columns were operated as saturated drainage layers and permeated with two different types of leachates, A and B. Leachate A had a relatively high VFA concentration but a low sulphate content (Table 5-4) and was supplied to columns 1 and 2. Leachate B had lower VFA but higher sulphate concentrations (Table 5-4) and was supplied to columns 3 and 4. The leachate compositions were based on chemical analytical data from samples obtained from vent bore holes in the low level radioactive waste repository and are believed to represent two possible leachate types present at the site (Paul Humphreys, BNFL, personal communication). It is thought that the high sulphate concentrations probably originated from construction waste.

Volatile fatty acids	Leachate A (mg/l)	Leachate B (mg/l)	Inorganic constituent	Leachate A (mg/l)	Leachate B (mg/l)
Acetic Acid	770	170	Calcium	170	160
Propionic Acid	95	5	Magnesium	82	50
n-Butyric acid	40	0	Sodium	127	62
Iso-butyric acid	20	0	Potassium	57	19
n-Valeric acid	7	0	Chloride	634	202
Iso-valeric acid	35	7	Bicarbonate	53	27
n-Caproic acid	7	0	Nitrate	20	16
Caprylic acid	20	0	Sulphate	18	1120
			Phosphate	0	0
TOTAL VFA	994	182	pH	6.6	7.1

Table 5-4: Composition of simulated leachates A and B (full strength)

The synthetic leachates were prepared by dissolving known quantities of the following components (Table 5-5) in 25 litres of distilled water.

Leachate A	Leachate B	Constituents
G /25 litres	g /25 litres	Inorganic constituents:
15.6250	14.7000	CaCl ₂ .2H ₂ O
2.7250	0.9075	KCl
17.3500	n/a	MgCl ₂ .6H ₂ O
1.8250	0.9300	NaHCO ₃
0.6850	0.5475	NaNO ₃
1.5925	n/a	Na ₂ SO ₄ .10H ₂ O
2.4880	n/a	NaCl
n/a	12.8250	MgSO ₄ .7H ₂ O
		VFAs:
19.2500	4.2500	Acetic acid
2.3750	0.1250	Propionic acid
1.0000	n/a	n-Butyric acid
0.5000	n/a	Iso-butyric acid
0.1750	n/a	n-Valeric acid
0.8750	0.1750	Iso-Valeric acid
0.1750	n/a	n-Caproic acid
0.5000	n/a	Caprylic acid
		Further constituents:
n/a	25.2840	98% H ₂ SO ₄
25	25	Iron Filings
Add, using pH probe to determine pH.		NaOH
6.6	7.1	pH

Table 5-5: Leachate constituents

Sodium hydroxide (NaOH) was added to adjust the pH to the required value. 25 g of iron fillings were added to the synthetic leachate to simulate metals which are present as discrete chunks in the waste body at Drigg.

To allow a gradual adaptation of the microbial population in the columns, the strength of the synthetic Drigg leachate was increased in steps of 25% until the full strength was reached.

The hydraulic retention times for columns 1 to 4 are given in Table 5-6. The hydraulic retention time is calculated by dividing the drainable pore volume by the flow rate and is an approximate measure of the average length of time that an element of fluid takes to pass through the column.

Column No	Hydraulic Retention Time (days)
Column 1	10.02
Column 2	9.85
Column 3	10.04
Column 4	9.95

Table 5-6: Hydraulic retention times and organic load for columns 1 to 4

5.2.3. Continuous feeding regime (200% strength leachate and high VFA, high SO_4^{2-} type leachate)

The overall concentration of the constituents in the leachate supplied to column 1 was doubled to investigate the effect these would have on the clogging. The switch to 200% strength leachate was commenced after steady state conditions under the previous operating regime (100% strength leachate) were achieved. The composition of the 200% strength leachate is shown in Table 5-7.

Volatile Fatty Acids	Leachate A (200%) mg/l	high VFA, high SO_4^{2-} mg/l	Inorganic Constituent	Leachate A (200%) mg/l	high VFA, high SO_4^{2-} mg/l
Acetic Acid	1540	770	Calcium	340	160
Propionic Acid	190	95	Magnesium	164	50
n-Butyric acid	80	40	Sodium	254	62
Iso-butyric acid	40	20	Potassium	114	19
n-Valeric acid	14	7	Chloride	1260	202
Iso-valeric acid	70	35	Bicarbonate	106	27
n-Caproic acid	14	7	Nitrate	40	16
Caprylic acid	40	20	Sulphate	36	1120
			Phosphate	0	0
TOTAL VFA	1988	994	pH	6.6	7.1

Table 5-7: Composition of simulated leachates A (200%) and high VFA, high SO_4^{2-} type leachate

The VFA concentration in column 4 (which had previously been supplied with low VFA, high SO_4^{2-} leachate) was increased to that originally supplied to columns 1 and 2 (high VFA, low SO_4^{2-}). This was to enable the interaction of VFA and SO_4^{2-} concentrations to be investigated, by comparing the performance of columns supplied with high VFA/high SO_4^{2-} and high VFA/low SO_4^{2-} (column 4 and column 1), and columns supplied with high VFA/high SO_4^{2-} and low VFA/high SO_4^{2-} (column 4 and column 3). The composition of the high VFA, high SO_4^{2-} leachate medium is shown in Table 5-7.

5.2.4. Continuous feeding regime (low VFA, high SO_4^{2-} type leachate with radionuclide analogues)

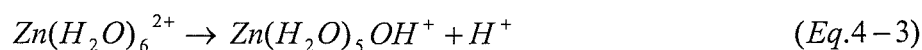
A. Background

Low level radioactive compounds are present in the low-level radioactive waste disposal site at Drigg, which could represent a risk to health if released into the environment. This test was recommended by BNFL and its purpose was to examine the transport behaviour of certain radioactive elements under the conditions likely to be encountered in the Drigg drainage system, in particular their sorption onto the biofilm and their potential to precipitate. Sorption tests, using radionuclide analogues simulating the radioelements suggested by BNFL, were carried out in the laboratory columns. Table 5-8 shows the radioactive elements of interest and their analogues.

Category	Example Radioelement	Analogue
AnO^{2+} , An^+	Cs, Np, U, Pu	Stable Cs
AnO^{2+} , An^+	Sr, Ni, Co, Ca, Ra, U	Ni, Co, Ba (for Ra), Rb
An^{3+}	Am, Eu	Eu
An^{4+}	Pu, Th U, Np	Ce
AnO^4	Tc (reduces to Tc^{4+})	Ru

Table 5-8: Radioactive elements and their analogues

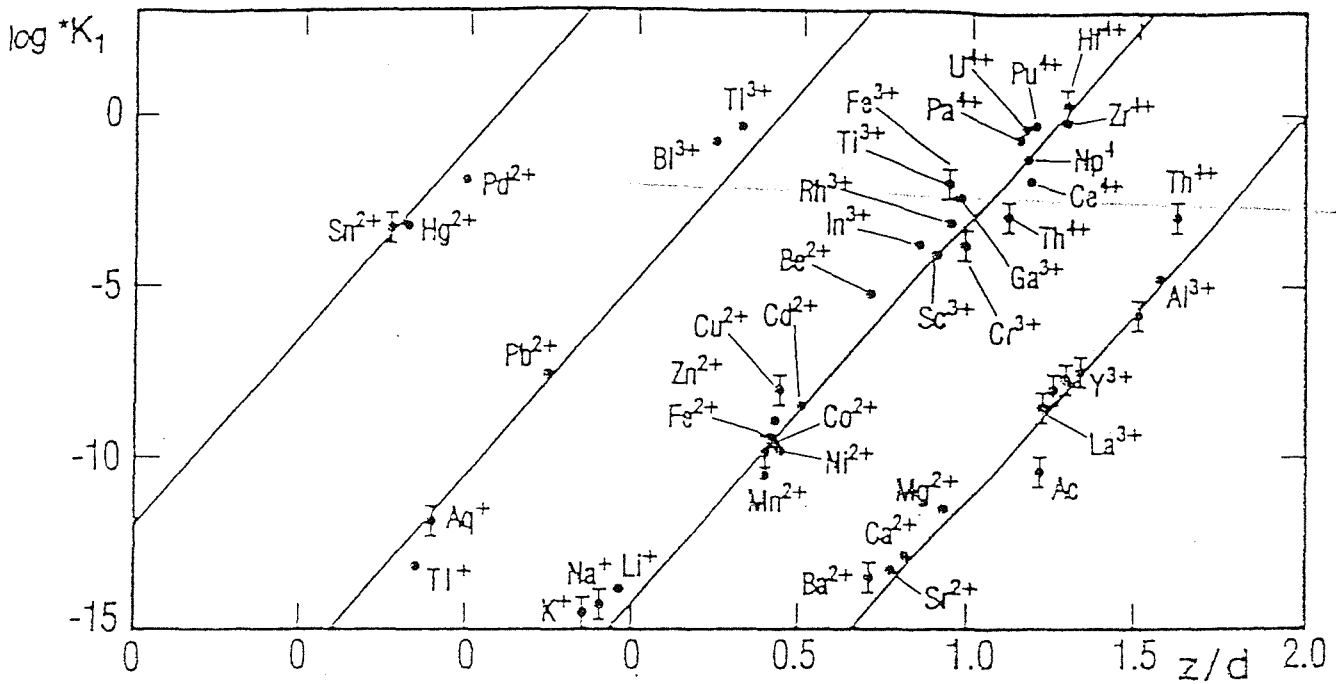
The analogues were chosen on the basis of their similarity in the behaviour of the cation of the respective radioactive element, in particular the first hydrolysis constant K_{11} and the ratio of the charge of the ion to the Metal-Oxygen distance (z/d) (Figure 5-2). All metal



cations in solution are hydrated. They co-ordinate four to six water molecules per ion forming aqueous ion-complexes.

The first hydrolysis constant is defined as:

$$K_{11} = \frac{[Zn(OH^+)] [H^+]}{[Zn^{2+}]} \quad (Eq.4-4)$$



Note: Note the change of abscissa zero for different groups

Figure 5-2: The linear dependence of \log_{10} of the first hydrolysis constant on the ratio of the charge to the Metal-Oxygen distance (z/d) for four groups of cations

The following compounds were chosen as analogues (Table 5-9) and introduced in the simulated leachate medium.

Element	Compound
Cs - caesium	CsCl
Ni - nickel	NiCl ₂ .6H ₂ O
Co - cobalt	CoSO ₄
Ba - barium	BaCl ₂ .2H ₂ O
Eu - europium	Eu ₂ (SO ₄) ₃ .xH ₂ O
Ce - cerium	CeCl ₃ .7H ₂ O
Rb - rubidium	Rb ₂ CO ₃
Ru - ruthenium	RuCl ₃

Table 5-9: Compounds containing the radionuclide analogues of interest

B. Concentrations of the radionuclide analogues.

No information was available regarding the concentrations of the radionuclide analogues expected to be found in the Drigg leachate. In order to decide on the concentration range to be employed in the experiment, first the background concentration of the radionuclide analogues potentially present due to impurities of the inorganic salts and organic acids used in the preparation of the simulated leachate medium was determined. Samples were collected from the outlet column 3 (low VFA, high SO_4^{2-} type leachate) and analysed for background concentrations of the radionuclide analogues by ICPMS (VG Elemental Plasma Quad PQ2+ ICP-MS) (Table 5-10).

Element	Compound	Column 3 (Leachate B - low VFA, high SO_4)
Cs – caesium	CsCl	0.005 ppb ($\mu\text{g/l}$)
Ni – nickel	$\text{NiCl}_2 \cdot 6\text{H}_2\text{O}$	0.170 ppb
Co – cobalt	CoSO_4	0.040 ppb
Ba – barium	$\text{BaCl}_2 \cdot 2\text{H}_2\text{O}$	0.320 ppb
Eu – europium	$\text{Eu}_2(\text{SO}_4)_3 \cdot x\text{H}_2\text{O}$	0.005 ppb
Ce – cerium	$\text{CeCl}_3 \cdot 7\text{H}_2\text{O}$	0.005 ppb
Rb – rubidium	Rb_2CO_3	0.030 ppb
Ru – ruthenium	RuCl_3	0.030 ppb

Table 5-10: Background concentrations of the radionuclide analogues in the leachate supplied to column 3.

On the basis of the background concentrations it was decided to start the test with the concentration of each of the analogues in the synthetic leachate B initially being 20 $\mu\text{g/l}$. Later on the concentration was increased to 200 $\mu\text{g/l}$ and then 2000 $\mu\text{g/l}$.

C. Investigation into the solubility of the cocktail of radionuclide analogues.

When other ions are present in the solution, the solubility of a compound can be different from its value in pure water. A series of experiments was carried out to investigate whether the solubility of the radionuclide analogues decreased when introduced into the synthetic leachate and when all the analogues were present in the solution. Each compound (Table 5-10) was dissolved, first separately and then as part of a mixture, into the synthetic leachate to give a concentration of 2000 $\mu\text{g/l}$ of each radionuclide analogue (the highest to be used in the column tests). No precipitation was observed after the addition of each of the eight radionuclide analogues in the synthetic leachate media either separately or as a mixture.

D. Experimental set up

The clogging test using radionuclide analogues was carried out in one of the duplicate columns (column 3) supplied with low VFA, high SO_4^{2-} type leachate. A mixture of each analogue dissolved in the simulated leachate medium was introduced into the column in a continuous feeding mode through the modified uppermost tapping similarly to the continuous feeding regime of the conventional clogging test (5.2.2.).

Periods and conditions of each operational regime, flow rates and organic load are given in Table 5-11. The organic load is expressed as mg VFA per litre DPV per day (mg VFA / litre DPV×day) where the concentration of VFA is multiplied by the flowrate and then divided by the initial (calculated) drainable pore volume (DPV).

5.3. Analytical measurements

5.3.1. VFA analysis

A. Sample preservation

The rate of removal of the VFA in the leachate was determined by measuring concentration changes in 1 ml samples collected from each of the tapping points along the height of the column. The samples were immediately preserved by the addition of 100 μl of 100% formic acid and stored in plastic vials in refrigerator at 4°C for up to a month (Banfield *et al.*, 1978).

B. Measurement

Concentrations of VFA were determined by gas chromatography using a Varian 3400CX Gas Chromatograph and flame ionisation detection (FID) in conjunction with an SGE BP21 megabore analytical column (25 m × 0.53 mm i.d., film thickness 8 mm). The method utilised an on-column injection technique (0.5 μl volumes) and a dual temperature ramping programme (60 – 100°C at 5°C per minute and 100 – 210°C at 10°C per minute) for the column oven. The injection temperature was 120°C and the detector temperature

Operational regime	Column 1 - Leachate A			Column 2 - Leachate A			Column 3 - Leachate B			Column 4 - Leachate B		
	Period of operation	Flow rates ml/min	Organic load (mg VFA litreDPV ⁻¹ day ⁻¹)	Period of operation	Flow rates ml/min	Organic load (mg VFA litreDPV ⁻¹ day ⁻¹)	Period of operation	Flow rates ml/min	Organic load (mg VFA litreDPV ⁻¹ day ⁻¹)	Period of operation	Flow rates ml/min	Organic load (mg VFA litreDPV ⁻¹ day ⁻¹)
Inoculation	Endogenous leachate May-June 96 – 21/11/97	0.5		Endogenous leachate May-June 96 – 21/11/97	0.5		Endogenous leachate May-June 96 – 21/11/97	1.0		Endogenous leachate May-June 96 – 21/11/97	1.0	
25% strength synthetic leachate	Leachate A 24/12/97 – 27/03/98	1.0	24.80	Leachate A 24/12/97 – 27/03/98	1.0	25.24	Leachate B 24/12/97 – 27/03/98	1.0	4.53	Leachate B 24/12/97 – 27/03/98	1.0	4.57
50% strength synthetic leachate (inoculum removed in August 1998)	Leachate A 27/03/98 – 05/05/99	1.0	49.61	Leachate A 27/03/98 – 19/04/99	1.0	50.48	Leachate B 27/03/98 – 20/04/99	1.0	9.07	Leachate B 27/03/98 – 04/05/99	1.0	9.14
100 % strength	Leachate A 05/05/99-01/06/01	1.0	99.22	Leachate A 19/04/99 still ongoing	1.0	100.96	Leachate B 04/05/99-06/03/01	1.0	18.14	Leachate B 04/05/99-30/05/01	1.0	18.28
200% strength	Leachate A 01/06/01-09/01/03	1.0	198.44									
high VFA, high SO ₄ ²⁻										30/05/01-08/02/03	1.0	99.83

Table 5-11: Periods of each operational regime, flow rates and organic load for each permeameter column

was 150°C. Hydrogen was used as the carrier gas (6 ml/min). An Autosampler Varian 8200 was used.

C. Calibration

A calibration procedure was carried out using a mixture of VFA (acetic, propionic, iso and n-butyric, iso- and n- valeric, n-caproic and caprylic acids, shown in order of elution) with concentration levels of 100 mg/l, 250 mg/l, 500 mg/l and 1000 mg/l. The results showed a linear correlation for each of the analytes in question.

5.3.2. Iron analysis

A. Sample preservation

The dissolved iron concentrations were determined by taking 5 ml samples every 2-3 days from the inlet leachate container. The samples were immediately preserved by the addition of 100 µl of 100% nitric acid (HNO₃) and stored in plastic vials in a refrigerator at 4°C prior to analysis.

B. Measurement

Iron analysis was carried out using a Atomic Absorption Spectrophotometer (Spectr AA-200, Varian, Australia). A hollow-cathode lamp for analysing Fe was used at a wavelength of 248.3 and the slit width was 0.2 mm. The lamp current was 5 mA. The sample was burnt in a acetylene/air flame where the air flow rate was 13.50 litres/min and the acetylene 2.0 litres/min.

C. Calibration

A calibration procedure was carried out using FeCl₃ as a standard. A linear correlation was obtained for standard solutions containing 1, 2, 5, 10 and 15 mg Fe/l. The standard solutions were preserved by addition of nitric acid following the same procedure as for the leachate samples.

5.3.3. Anion analysis (Cl , NO_2 , NO_3 , PO_4 , SO_4)

A. Sample preservation

5 ml sample volumes were collected from each tapping along the height of the column and immediately frozen.

B. Measurement

Anion analysis was carried out using a Dionex-500 IC/HPLC using an AS9 anion column in conjunction with an ASRS-1 anion suppressor (Dionex Ltd.) 25 μ l volume injections were applied to the column using a Dionex AS40 autosampler, incorporating a rheodyne valve. Column temperature was maintained at ambient. Detection was by a Dionex ED-40 electrochemical detector operating in conductivity mode. The mobile phase consisted of 1.8 mM sodium carbonate and 1.7 mM sodium bicarbonate pumped at a flow rate of 2.0 ml/min.

C. Calibration

A calibration procedure was carried out using a mixture of NaCl, NaNO₂, KNO₃, KH₂PO₄, MgSO₄·7H₂O with concentration levels of 100, 200, 250, 400, 500, 700, 900, 1000 μ M/l. The results showed a linear correlation for each of the anions in question.

5.3.4. Cation analysis (Na^+ , NH_4^+ , K^+ , Mg^+ , Ca^{2+})

A. Sample preservation

The sample preservation was the same as for the anion analysis.

B. Measurement

Cation analysis was carried out using a Dionex-500 IC/HPLC using a CS12A cation column in conjunction with a CGII cation suppressor (Dionex Ltd.). 25 μ l volume injections were applied to the column using a Dionex AS40 autosampler, incorporating a rheodyne valve. Column temperature was maintained at ambient temperature. Detection was by a Dionex ED-40 electrochemical detector operating in conductivity mode. The mobile phase consisted of 20 mM methanesulphonic acid pumped at a flow rate of 1.0 ml/min.

C. Calibration

A calibration procedure was carried out using a mixture of NaCl, NH₄NO₃, KH₂PO₄, MgSO₄·7H₂O, CaCl₂·2H₂O with concentration levels of 100, 200, 250, 400, 500, 700, 900, 1000 µM/l. The results showed a linear correlation for each of the cations in question.

5.3.5. Gas analysis

A. Sample preservation

Samples were collected using hypodermic syringes which were inserted through the butyl rubber stoppers installed in the column wall (see section 5.6.5). The samples were immediately analysed.

B. Measurement

Gas composition was measured using a Varian GC 3800 operating isothermally at 50°C, incorporating molecular sieve 13X, 60-80 mesh (1.5 mm × 4 mm i.d.) and HaysepC 80-100 mesh (1.5mm × 4 mm id) columns operating in back-flush mode in conjunction with a TCD detector. The injection volume was 0.25 ml. The injection temperature was 80°C and the detection temperature was 150°C. The carrier gas was argon at a flow rate of 6 ml/min.

5.3.6. ICPMS analysis

5 ml leachate sample volumes were collected from each tapping along the height of the column, acidified with 2% HNO₃ (Aristar, VWR) and analysed at the Southampton Oceanography Centre on a VG Elemental PlasmaQuad PQ2+ ICP-MS.

5.3.7. Carbon analysis

A. Measurement

A Dohrman DC-190 (Dohrman, USA) was used to measure the total carbon. The equipment contains a vertical quartz combustion tube packed with cobalt catalyst. Air flows through it at a rate of 200 ml/min. The furnace was operated at 800°C. The boat sampling mode was utilised due to the high concentrations of suspended solids in the samples. The samples were analysed twice and the average value taken.

B. Calibration

The equipment utilised single point calibration. Only one standard was required which was prepared by using Glycine at a concentration level of either 1000 mgC/l or 500 mgC/l depending on the concentration range of the samples.

5.3.8. Polysaccharide analysis

A. Measurement

The phenol-sulphuric method (Dubois *et al.*, 1956) was used to determine the polysaccharide content of the samples containing extracted biofilm material. The method utilised two reagents - phenol dissolved in water (5% weight/volume) and concentrated sulphuric acid. 1 ml sample, standard solution and blank was mixed with 1.0 ml phenol reagent and 5.0 ml concentrated sulphuric acid. The mixtures were left undisturbed for 10 min before being shaken vigorously and left for further 30 min. The absorbance was determined on spectrophotometer at wavelength of 490 nm.

B. Calibration

A calibration procedure was carried out using glucose as a standard with concentration levels of. A linear correlation was obtained for standard solutions containing 50, 100, 500, 1000 and 2000 $\mu\text{M/l}$.

5.3.9. XRF analysis

Aggregate samples from each column section were taken. Each sample had a dry weight of 10 g and was ground using high purity grinding barrels to obtain a sample with a consistency of powder. The powdered sample was mixed with 1 ml of 8% w/v polyvinyl alcohol, which acted as a binder. Then, the mixture was pressed to 25 tonnes using an hydraulic press to produce a 40 mm diameter pellet. The pellet was dried overnight at room temperature and then analysed using a Philips MAGIX-PRO fully automatic wavelength dispersive XRF.

5.4. Gas volume measurements

The amount of gas produced in each permeameter was initially monitored using a Triton gas flow meter (model No.8), connected directly to the outlet at the top of each column. Gas was allowed to flow into collection vessels and then through a 2.5% zinc acetate solution before passage through the flow meter to remove any hydrogen sulphide, which could damage the meter.



Subsequent sulphide analysis of the zinc acetate 'trapping solution' indicated that there was little hydrogen sulphide actually being released from the columns. Difficulties were encountered with the Triton flowmeter when single pass flow was commenced due to their method of measuring gas flow, which requires a pressure build up within the measuring vessel. With the overflow method utilised in the continuous flow regime (see Figure 5-3) it was found that this pressure build up was sufficient to force liquid out of the column via the overflow rather than operating the meter.

A different technique for measuring the volume of biogas has been developed since commencement of 100% strength leachate flow. Instead of trying to vent the gas generated into a measuring vessel it was decided to allow biogas to build up in the headspace of the column to a small pressure of 0.3 kPa above ambient. On reaching this pressure the biogas is vented automatically to the atmosphere by means of a solenoid valve. The volume of gas that must be generated (V_G) to trigger the solenoid operated release valve can be calculated using the Boyle-Marriott Law.

$$P_1 \times V_1 = P_a \times V_a \quad (\text{Eq. 5-6})$$

$$V_G = V_a - V_1 \quad (\text{Eq. 5-7})$$

P_1 – pressure build up = 100.3 kPa

V_1 – volume of the gas at pressure 100.3 kPa = volume of the column headspace

P_a – atmospheric pressure = 100 kPa

V_a – the volume of the gas at atmospheric pressure

V_G – volume of biogas generated

The solenoid valve outflow pipe was submerged in a beaker of water to a depth of 1mm to prevent air entering the column with the valve in the open position, which could otherwise occur as a result of the density difference between methane and air (Table 5-12). The head space pressure was measured by means of piezo-resistive gauge pressure transducers which were powered by a 12v D.C. battery (RS, U.K.). It was found that even this small pressure increase in the column headspace would push the leachate out of the system through the overflow pipe. As a result fluctuations in the leachate levels in the columns were observed, which could have been aided by variations in the ambient atmospheric pressure. To prevent this, the overflow pipe was connected to the column headspace. In this way the pressures exerted on the leachate in the column and in the overflow pipe were kept equal and consequently the levels constant. To stop any gas escaping from the system a U tube was incorporated into the overflow pipe, as shown in Figure 5-3 and 5-4 (page 95).

Gas	Density (kg/m ³)
Air	1.2928
Methane (CH ₄)	0.7167
Nitrogen (N ₂)	1.2507
Carbon dioxide (CO ₂)	1.9768
Hydrogen sulphide (H ₂ S)	1.5392

Table 5-12: Air and Biogas component densities

5.5. Measurement of the rate of clogging

The rate of clogging of the drainage material was assessed by monitoring:

- any change in the hydraulic gradient along the height of the column; and
- the reduction in the DPV of each column section, between adjacent tappings.

5.5.1. Hydraulic gradient

The hydraulic gradient along the height of the column was calculated on the basis of any measured head losses between adjacent tappings. The different tappings on the side of the columns were connected to a switched manifold and the head was measured at each tapping in turn by means of piezo-resistive gauge pressure transducers (0-1 psi, RS)

5.5.2. Drainable porosity

The DPV of each section (between adjacent tappings) was measured periodically by draining the pore fluid into a vessel containing nitrogen gas. The headspace and one of the side tappings of the column were connected to the measuring vessel, allowing the leachate draining into it to be replaced by nitrogen from the vessel thereby maintaining anaerobic conditions in the column. The measurements were carried out section by section, starting at the top by draining pore fluid from the saturation level to the level of tapping 2 (Paksy *et al.*, 1998). On completion of the measurement the drained pore fluid was either reintroduced into the column during the recirculation regime or fresh synthetic leachate was introduced from the bottom of the column during the continuous feeding regime.

The drainable porosity was calculated using Eq. 5-8.

$$n = \frac{V_d}{V_t} \quad (\text{Eq. 5-8})$$

where,

n – drainable porosity

V_d – drainable pore volume of the section under investigation, ml

V_t – total volume of the column section under investigation, ml

Three consecutive measurements of the drainable porosity in one of the experimental columns were carried out to establish the experimental error of the DPV measurement method. The error was estimated to be +/- 0.017 expressed in terms of porosity, as indicated by the vertical error bars in Figure 6-11 and Figure 6-32.

Owing to the method of measurement, at least some of the reductions in drainable pore volumes will be due to the presence of gas. As gas will tend to inhibit leachate flow, it was considered appropriate to attempt to separate the component of DPV reduction due to gas from that due to invasion of the pore space by biomass, exopolyaccharides and precipitates. It was therefore decided to measure not only the volume of leachate drained out of the column section but also the volume required to fill it again from the bottom up. The latter measurement would be less affected by gas bubbles. This technique was adopted after a total of 34.8 g of VFA per litre pore volume had passed (which corresponds to date 05/09/00) in columns 1 and 2, supplied with high VFA and low SO_4^{2-}

type leachate, and after a total of 19.0 g of VFA per litre pore volume had passed (which corresponds to date 20/09/00) in columns 3 and 4, supplied with low VFA and high SO_4^{2-} type leachate.

5.6. Experimental design improvements

Some changes were made during the columns operation, which improved the overall performance of the experimental apparatus. These amendments are detailed below and illustrated in Figure 5-3 and Figure 5-4.

5.6.1. Development of new method of gas measurement and installation of an overflow u-tube.

The development of this new method and the associated modifications to the experimental set up were explained in section 5.4.

5.6.2. Power supply of the pressure transducers

Problems were encountered with the pressure transducers used for measuring the headspace gas pressure in the columns. Gas pressure data were needed to calculate the gas generation rates in the laboratory columns as explained in section 5.4. It is believed that these problems were due to mains noise, which resulted in an unstable output signal. By using a battery to supply power (12V d.c.) to the pressure transducers a more stable output signals were obtained.

5.6.3. Lowering the leachate level in the column headspace

Analysis showed that most of the VFA were being removed from the leachate in the 10cm liquid layer above the aggregate. It was decided to keep the leachate levels just above the aggregate in the columns in order to confine the microbial processes to the aggregate layers. The overflow pipe that controls the leachate level was shortened to achieve this.

5.6.4. Modification of the leachate inlet port.

Originally the leachate inlet port was in the top column platen. The 30 cm distance between the inlet port and leachate level suggested creation of turbulent conditions at the point of contact of the incoming leachate with the saturated leachate level. To minimise turbulence, the first tapping, which became above the saturation level after lowering the leachate level, was modified to serve as an inlet port. The tapping was lengthened to reach the centre of the column and slightly bent downwards to touch the liquid layer overlying the aggregate, thereby minimising any disturbance.

5.6.5. Gas analysis

Butyl rubber stoppers were installed in the Perspex wall at the headspace section of each column to enable gas sampling by means of a hypodermic syringe.

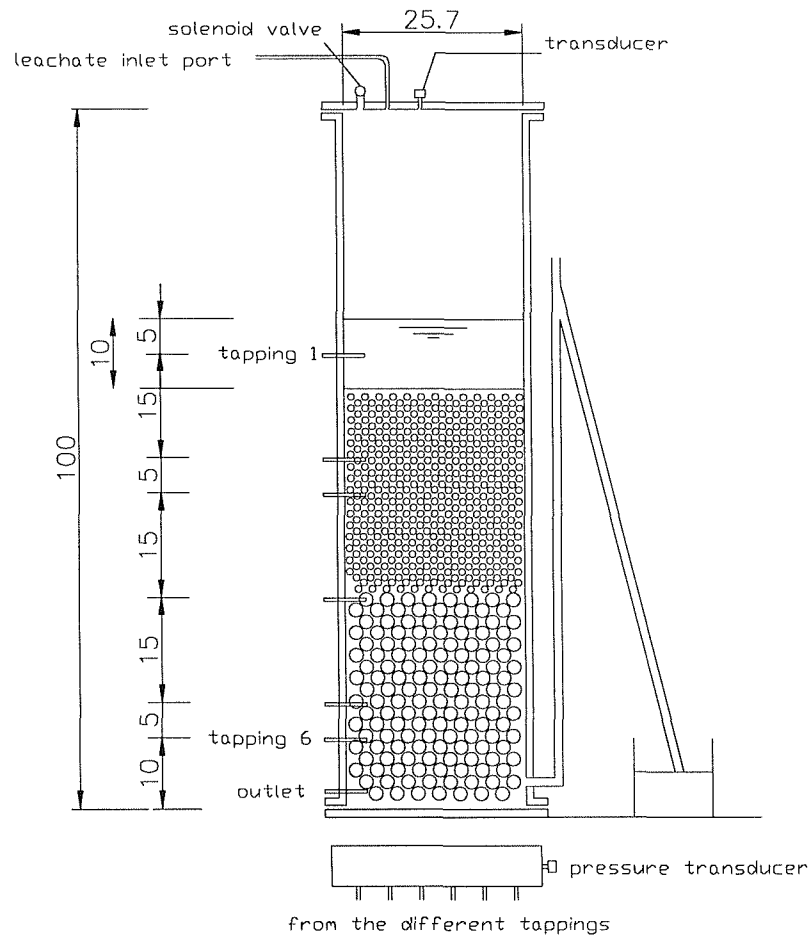


Figure 5-3: Initial experimental set up

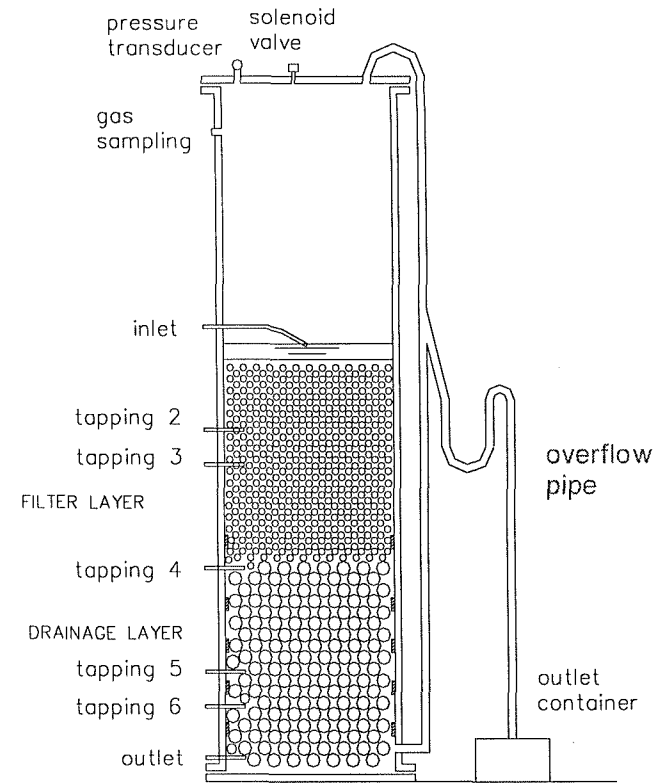


Figure 5-4: Experimental set up after modification of gas measuring system

Chapter 6

Results and Discussion

This chapter examines the results in terms of reduction in the drainable porosity and the concurrent clogging of the drainage aggregate in the experimental columns. In addition the changes in the composition of the leachate during flow through the column with regard to the removal of the organic substrate and the reduction of sulphates are presented to allow the inter-relationship between sulphate-reducing and methanogenic bacteria to be established. The volumes of the gas produced are reported and compared with the theoretical gas generation rates. The results are compared with those obtained by other researchers and a discussion on the further understanding of the mechanisms of clogging is made. In addition, data on the dismantling of columns 1 and 3 and on the chemical and microbiological composition of the clog material retrieved from these columns are provided. On the basis of all the results, a conceptual model of the microbially mediated clogging is developed.

6.1. Columns supplied with leachate with high VFA (994 mg/l) and low SO_4^{2-} (18 mg/l) concentrations, 50% and 100% strength leachate - columns 1 and 2

These experimental tests were carried out in duplicate. The results for column 2 are presented in this section. Data for the duplicate column (column 1) are given in Appendix A (Figure 1 to Figure 6).

6.1.1. VFA removal from the leachate

Eight VFAs were supplied to these columns – acetic (CH_3COOH), propionic ($\text{CH}_3\text{CH}_2\text{COOH}$), n- butyric ($\text{CH}_3\text{CH}_2\text{CH}_2\text{COOH}$), iso-butyric ($\text{CH}_3\text{CH}(\text{CH}_3)\text{COOH}$), n- valeric ($\text{CH}_3\text{CH}_2\text{CH}_2\text{CH}_2\text{COOH}$), and iso-valeric ($\text{CH}_3\text{CH}(\text{CH}_3)\text{CH}_2\text{COOH}$), n-caproic ($\text{CH}_3\text{CH}_2\text{CH}_2\text{CH}_2\text{CH}_2\text{COOH}$) and caprylic ($\text{CH}_3\text{CH}_2\text{CH}_2\text{CH}_2\text{CH}_2\text{CH}_2\text{CH}_2\text{COOH}$) acids. Only the removal rates of acetic and propionic acids since introduction of 50% strength leachate are shown. The other VFAs were present in small concentrations and graphs showing their removal are not presented owing to the difficulty of reliable measurement at the low concentrations utilised.

The data (Figure 6-1) show that doubling the acetate concentration on switching from 50% to 100% strength leachate initially inhibited or killed part of the population of acetate utilising bacteria. Immediately after introducing full strength leachate the acetate utilising bacteria were able to remove only 100 mg/l whereas previously they had been removing 385 mg/l when supplied with 50% strength leachate. This is consistent with observations made by Brune *et al.* (1991) who reported that microbial populations in the experimental columns were killed on accidentally increasing the leachate strength by up to 300% owing to a change in the leachate source.

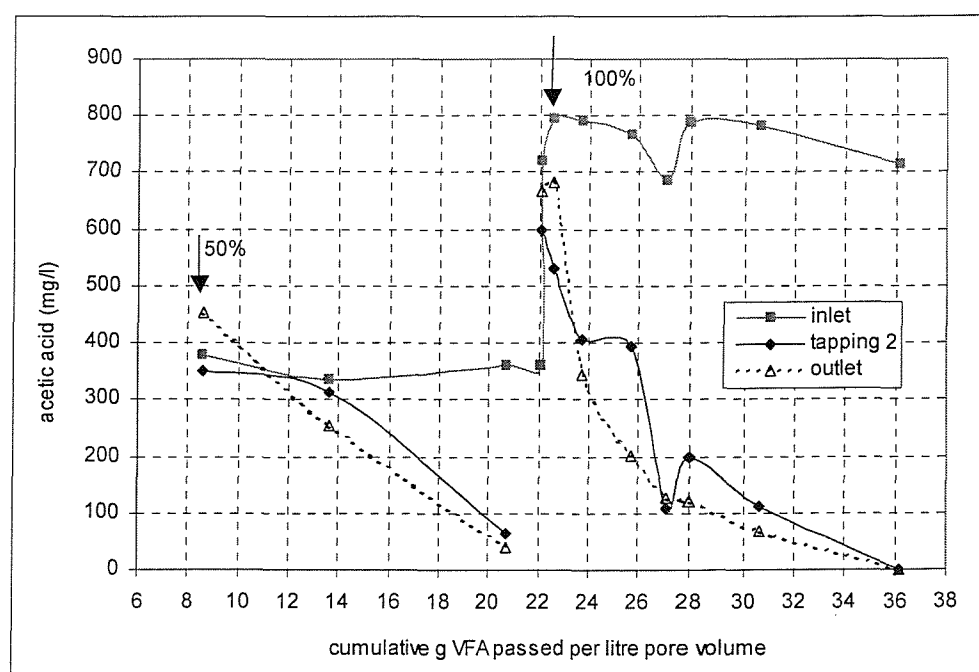


Figure 6-1: Acetic acid concentrations measured at the column inlet, tapping 2 and the column outlet since introduction of 50% strength leachate in column 2.

However, Brune *et al.* (1991) did not investigate the capacity of the bacteria to adapt to the increased biological load which has been addressed by the research carried out in this study. Gradually the bacterial population was observed to acclimatise/adapt to the increased acetate concentration by either cell growth or an increased metabolic rate. The acetate utilising bacteria were able to degrade completely the doubled acetate concentration after the passage of approximately 14 g VFAs per litre pore volume (187 days).

The acetate was removed mainly in the section between the inlet and tapping 2. The acetate concentrations at tappings 3, 4, 5 and 6 are not shown because no significant removal was observed in the lower sections of the column. This indicates that the acetate utilising bacteria in the top sections became acclimatised to the increased acetate concentrations due to either faster growth rates or a more active cell metabolism. The bacterial population in the lower sections did not develop, probably due to depletion of organic nutrients and/or other essential growth nutrient within the top sections. This observation is consistent with the fact that there was almost no reduction in drainable porosity in the lower sections (Figure 6-11, section 6.1.10).

The variation in the acetate inlet concentration was probably caused by bacterial activity within the storage container. The outlet concentrations immediately after the introduction of full strength leachate were higher than the concentrations at tapping two due to the nature of the experimental procedure. On switching to 100% strength leachate the column was initially instantly saturated with 100% strength leachate medium. The bacteria at the bottom sections were not very active or had not developed at all resulting in the measurement of initially higher concentrations.

In theory, additional acetate would be expected to be generated by the degradation of longer chain fatty acids introduced in the synthetic leachate :

- 81.79 mg/l of acetate from the degradation of 60 mg/l butyric acid, on the basis of Eq. 2-4.
- 24.70 mg/l acetate and 30.47 mg/l propionate from the degradation of 42 mg/l valeric acid (Eq. 2-5). The further degradation of propionate will result in the generation of an extra 24.70 mg/l of acetate (Eq. 2-6).
- 10.8 mg/l from the degradation of 7 mg/l n-caproic acid (Eq. 2-4)

- 33.4 mg/l of acetate from the degradation of 20 mg/l caprylic acid (Eq. 2-4).

The total amount of acetate that would be expected to be generated from the breakdown of the higher chain fatty acids is therefore 175.39 mg/l. Apparently, the acetate utilising bacteria removed this extra amount of acetate without any noticeable inhibition, in contrast to what has been observed by Nikolova (1997) and Rowe (personal communication).

Figure 6-2 shows the propionic acid concentrations at different tappings along the height of the column at 50% and 100% strength leachate. The variation in the inlet propionate concentrations was probably caused by bacterial activity within the storage container. The propionate utilising bacteria reacted in a slightly different way from the acetate utilising bacteria to the doubling of the substrate concentration. On introducing the 100% strength leachate the bacterial population in the top section (inlet - tapping 2) continued to remove 40-50 mg/l for the first 0.4 g VFA passed per litre pore volume (22.2-22.6 of total g VFA per litre pore volume passed), as it had been doing during the flow of 50% strength leachate, indicating that their metabolic activity was initially not affected.

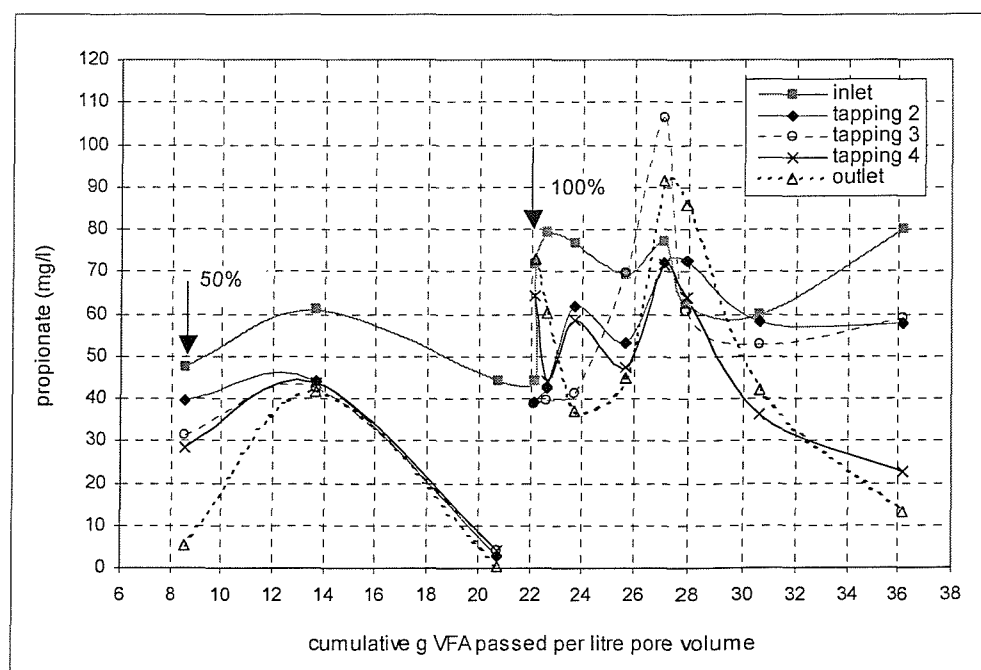


Figure 6-2: Propionic acid concentrations measured at the column inlet, tapping 2, tapping 3 and the column outlet since introduction of 50% strength leachate in column 2.

This was followed by the removal of approximately 25-30 mg/l between 22.6 – 25.6 of total g VFA per litre pore volume passed, reducing to negligible removal between 27-28 of total g VFA per litre pore volume passed, suggesting that almost complete inhibition or death of the propionate utilising bacteria had occurred there. Very little propionate was removed in the lower sections. It appears that the propionate utilising bacteria initially resisted the shock loading, followed by the gradual inhibition and/or death of part of the bacterial population, which corresponded to the passage of approximately 5 g VFA per litre pore volume (22.6 - 28 of total g VFA per litre pore volume passed).

While a concentration of 600 mg/l of acetate was already being removed after a total of 11 g VFA per litre pore volume had passed through the column, only small amounts of propionate were being removed at this stage indicating that the propionate utilising bacteria were inhibited for a longer time and needed more time for adaptation than the acetate utilising bacteria.

A concentration of 20 mg/l of propionate was being removed within the column after a total of 30 g VFA per litre pore volume had passed through the column, all between tapping 3 and the column outlet. Only a very small amount of propionate was being removed between the inlet and tapping 3. After a total of 36 g VFA per litre pore volume had passed through the column, 71% of the propionate supplied to the column (57 mg/l) was being removed by the column outlet – 22 mg/l between the inlet and tapping 2, almost nothing in section 2-3, and 35 mg/l in section 3-4. This shows that a gradual increase in the rate of removal of propionate occurred after a total of 14 g VFA per litre pore volume had passed, indicating a process of acclimatisation for the bacterial population there. No removal of propionic acid was observed in the lower sections (tapping 4 - outlet). The propionate-utilising bacteria had probably not developed there due to depletion of an essential growth nutrient.

The propionate utilising bacteria would require the passage of more than 14 g of VFA per litre pore volume (22-36 total g VFA per litre pore volume passed) to remove completely the doubled propionate concentration. The data suggest that there was a delay in the inhibition of the propionate utilising bacteria followed by longer inhibition and recovery periods than the acetate utilising population, suggesting that the rate of metabolism and growth of the propionate utilising bacteria was probably slower. The same observation has

been made by Peeling *et al.* (1999)

It appears that the rate of propionate removal was higher in section 3-4 than in the top sections (inlet – tapping 2, tapping 2 – tapping 3) between the passage of 13-21 total g VFA per litre pore volume. However, it could be that the degradation of valeric acid, which would produce propionate (30.47 mg/l) as an intermediate product, occurred between the inlet and tapping 3. This may explain the fact that there was apparently little or no net removal of propionic acid in these sections (inlet – tapping 2, tapping 2–3). This hypothesis is further supported by the generation of 20-28 mg/l of propionate between sections 2-3 and 4-outlet between 9-12 total g VFA per litre pore volume had passed through the column.

6.1.2. pH measurements

Figure 6-3 shows the pH at different tappings along the height of the column after VFA and SO_4^{2-} removal had reached a steady state. The measurement was carried out after a total of 38.5 g VFA per litre pore volume had passed through the column, which corresponds to day 395 after the introduction of 100 % strength leachate. The pH of the simulated leachate medium increased (i.e. it became less acidic) between the inlet and tapping 2. This is consistent with the effect of degradation of VFA to methane and carbon dioxide in this section.

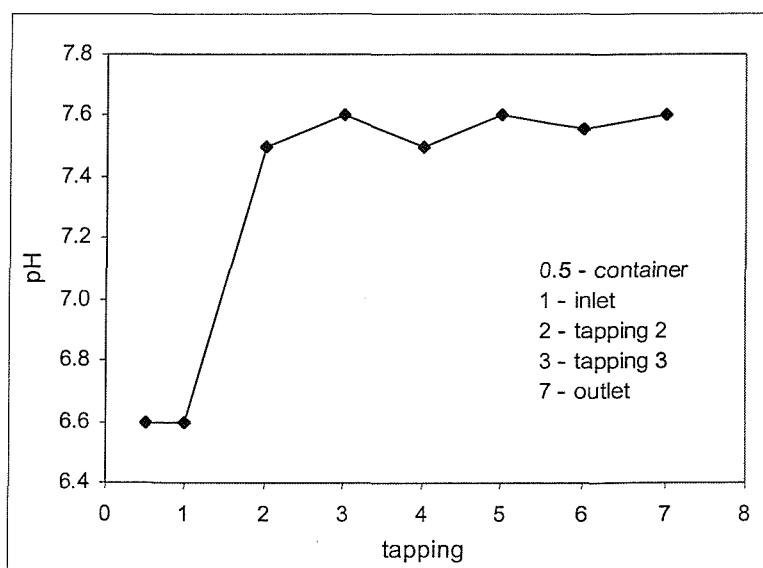


Figure 6-3: pH measurements in column 2

6.1.3. Iron concentrations

25 g of iron filings were introduced in the 25 litre inlet container where the simulated leachate medium was kept. This resulted in a gradually increasing dissolved iron concentrations in the inlet containers which reached a maximum value of 12 mg Fe/l (Figure 6-4) after nine days. The 25 litre container was kept at 4°C and retained sufficient leachate to supply the experimental column for 14 days, which is why the concentration of Fe is shown for this period of time.

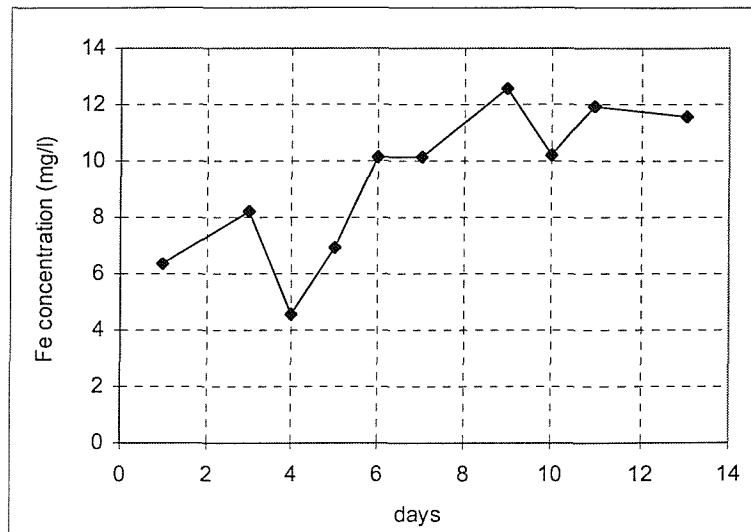


Figure 6-4: Iron concentrations in the inlet container for column 2, 100% strength leachate

The iron concentrations in samples collected from the column outlet were below 1 mg/l, which indicated almost complete removal of the dissolved iron species within the column. Taking this into account and that the average concentration of Fe available was 8.25 mg/l (Figure 6-4) gives a total amount of iron removed since introduction of 100% strength leachate of 13.25 g Fe ($8.25 \text{ mg/l} \times 1605.6 \text{ litres} = 13.25 \text{ g Fe}$). This value will be used to calculate the total amount of MeS deposited (section 6.1.4)

6.1.4. Sulphate reduction

As previously discussed, in the presence of high concentrations of sulphate, SRB oxidise the long chain fatty acids and reduce the sulphate to hydrogen sulphide (Eq. 5-1).



Hydrogen sulphide gas can exist in various forms ($\text{H}_2\text{S}_{\text{gas}}$, $\text{HS}^-_{\text{aqueous}}$, $\text{S}^{2-}_{\text{aqueous}}$) depending on the pH (Figure 6-5). The dissolved hydrogen sulphide species ($\text{HS}^-_{\text{aqueous}}$, $\text{S}^{2-}_{\text{aqueous}}$) will then react with the available reduced metal species (mainly iron) and precipitate in the form of ferrous sulphide (Eq. 5-2) (Sawyer, 1978).

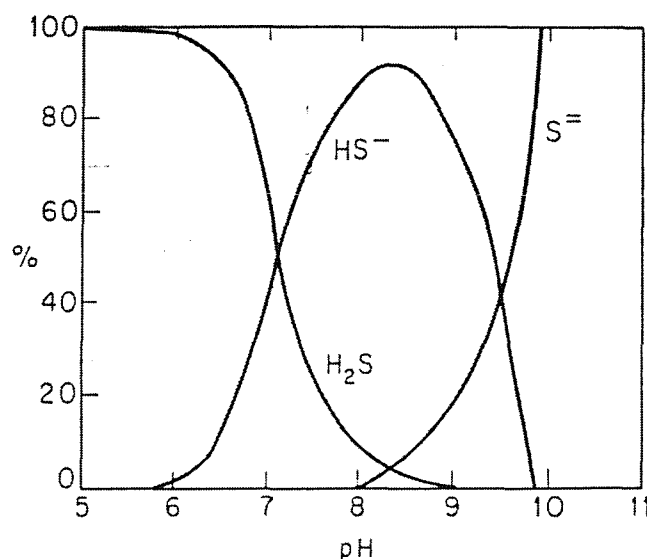


Figure 6-5: Effect of pH on hydrogen sulphide equilibrium in an aqueous medium (Sawyer, 1978)

Chemical analysis of leachate samples collected from the different tappings along the height of the columns shows that all of the sulphate was removed in the uppermost section of the column (inlet - tapping 2) (Figure 6-6). The resulting hydrogen sulphide would be expected to be present in the form of free H_2S (30%) and as HS^- ion (70%) at the pH range of 7.4-7.6 measured in the column (Sawyer, 1978). The resultant dissolved sulphides can then react with any available reduced metal species (mainly iron) and precipitate on the aggregate in the form of black precipitates, presumably iron sulphide. The development of black deposits was observed, which appeared first in the liquid layer overlying the aggregate and then spread downwards to occupy the filter layer. To prove the nature of this deposit, XRF analysis has been carried out on dismantling the column (chapter 6).

Theoretical stoichiometric calculations on the basis of Eq. 2-14 indicate that a concentration of 11.22 mg/l acetate is needed to reduce fully the 18 mg/l SO_4^{2-} supplied with the full strength leachate. On the basis of this, the simple correlation: acetate concentration (mg/l) = $0.62 \times$ sulphate concentration (mg/l) can be used to calculate the concentration of acetate required to reduce a known concentration of sulphate.

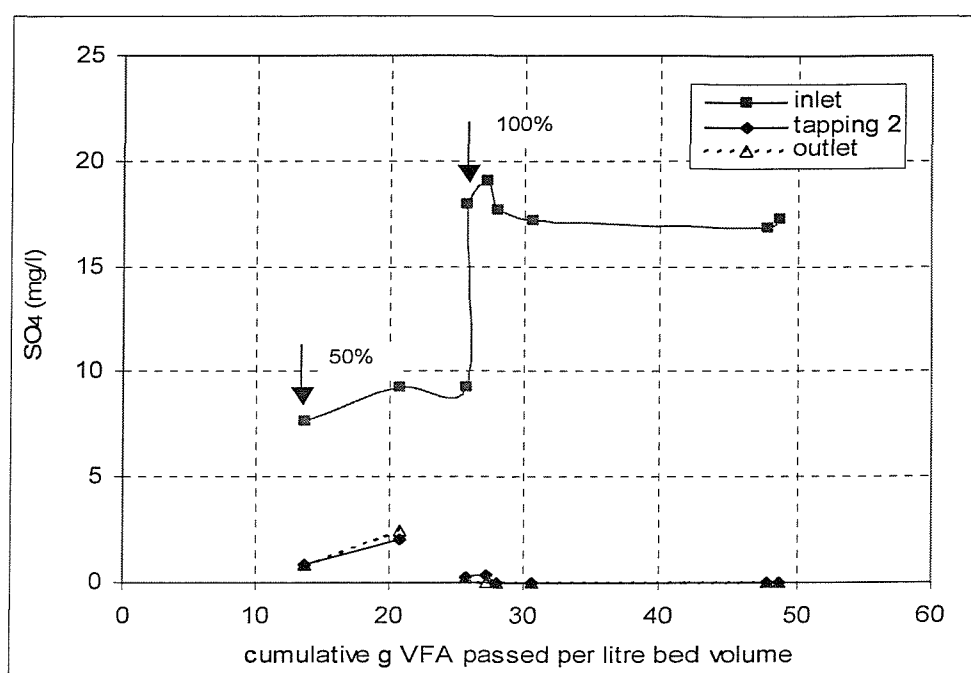


Figure 6-6: Sulphate concentrations measured at the column inlet, tapping 2 and column outlet since the introduction of 50% strength leachate in column 2.

Based on Figure 6-6, the mass of sulphur removed was 9.30 g as S^{2-} since the introduction of 100% strength leachate. The total mass of iron removed since the introduction of 100% strength leachate was 13.25 g Fe. Precipitation of the sulphur as FeS would have required 16.20 g Fe - more than was available. The available Fe would have reacted with 7.60 g S^{2-} to form 20.86 g of FeS precipitates. Assuming a bulk (wet) density of the clog material of 1.6 g/cm^3 as measured by Rowe *et al.* (2000a, b) gives a total volume of 13.04 ml for the FeS precipitates. This accounts for only 3.0 % of the total volume of accumulated clog material, which was 435 ml. The sulphur could have precipitated as FeS_2 , which would have required 8.09 g Fe to form 17.40 g or 10.88 ml of FeS_2 . This accounts for only 2.5 % of the total volume of accumulated clog material. These calculations suggest that FeS or FeS_2 precipitates had a relatively small contribution to the clogging processes taking place in the experimental columns 1 and 2.

6.1.5. Calcium concentrations

Figure 6-7 shows that there has been little removal of Ca^{2+} from the leachate since introduction of 100% strength leachate.

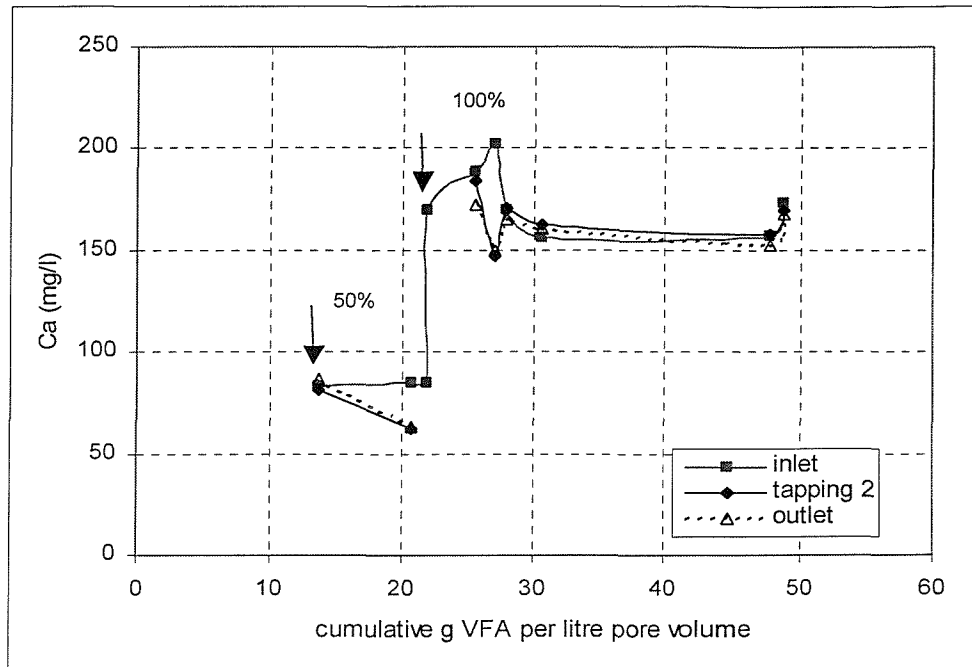


Figure 6-7: Total calcium concentrations measured at the column inlet, tapping 2 and column outlet since the introduction of 50% strength leachate in column 2.

At first sight, it is surprising that the Ca was not precipitated as it has a low solubility as the calcium carbonate (CaCO_3) salt. However, the solubility of CaCO_3 depends on the pH which in turn governs the distribution of dissolved carbonate species (CO_3^{2-} , HCO_3^-) in the system. At lower pH the dissolved carbonate species will be predominantly in the form of the bicarbonate ion (HCO_3^-). Without the availability of carbonates (CO_3^{2-}), calcium carbonate cannot be formed and calcium will stay in solution in the form of soluble calcium bicarbonate [$\text{Ca}(\text{HCO}_3)_2$]. At higher pH, CO_3^{2-} species will predominate leading to the formation and precipitation of CaCO_3 . This explains why the molar solubility of CaCO_3 ranges from 0.02 at pH 6.0 to only 0.0011 at pH 8.0 which corresponds to 2000 mgCaCO_3/l or 800 mgCa/l at pH 6.0 and 110 mgCaCO_3/l or 44 mgCa/l at pH 8.0 (Bialkowski, 2000). At pH 7.6, as measured in the experimental column, and assuming a linear relationship between pH 6 and pH 8.0 the solubility for Ca is 233 mg/l . The Ca concentrations in the leachate did not exceed the solubility product, which is why precipitation did not occur.

6.1.6. Gas volume

The cumulative volume of gas produced since the introduction of 100% strength leachate is shown in Figure 6-8. Various techniques for measuring gas were attempted (section 5.4), which is why data are not reported for the 50% strength leachate and why the datum was reset when full strength leachate was introduced.

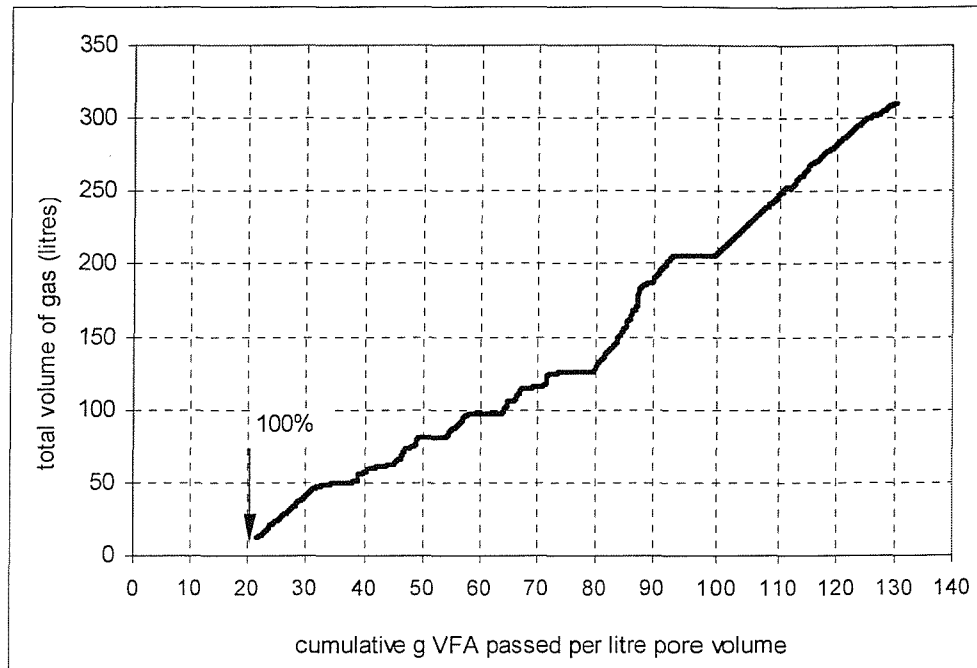


Figure 6-8: Measured cumulative volume of gas produced in column 2 since introduction of 100% strength leachate

The daily volume of gas produced varied between zero and 2.0 litres (Figure 6-9). The most likely reason for this variation is that gas was released into the column headspace periodically through ebullition of trapped gas in the aggregate of the column. A similar observation for gassing waste was made by Hudson *et al.* (2001).

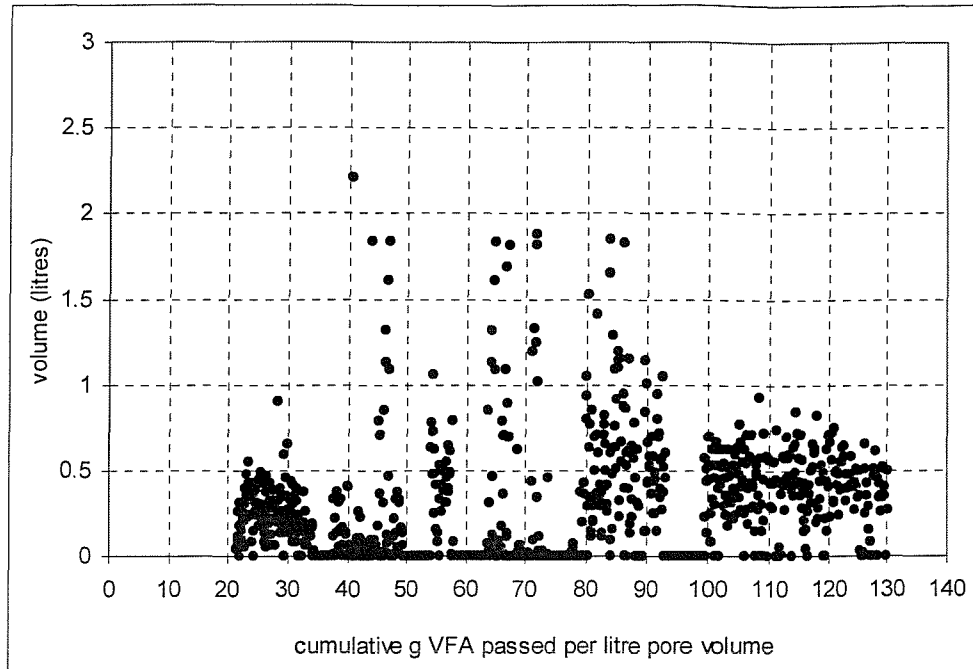


Figure 6-9: Daily volume of gas produced in column 2

6.1.7. Gas composition

The gradually increasing proportion of methane in the gas generated (Table 6-1) is consistent with the gradual adaptation/growth of the microbial population of methanogenic bacteria in response to the increased leachate strength (Figure 6-1 and Figure 6-2). An infrared analyser (Geotechnical instruments, GA24) was used for analysis of the samples from 05/05/99 until 10/06/99. Only carbon dioxide, methane and oxygen could be analysed in this way, which is why there are no data regarding the nitrogen content in these samples.

Date	CH ₄ (%)	CO ₂ (%)	N ₂ (%)
05/05/99	33.62	-	-
10/05/99	41.03	0.53	-
20/05/99	54.27	-	-
10/06/99	64.69	0.24	-
15/05/01	85.00	5.50	9.50
06/07/01	88.00	6.00	6.00

Table 6-1: Composition of the gas produced (05/05/99 – commencement of full strength leachate) in column 2.

Typical values for landfill gas composition from biodegradable organic waste in the methanogenic phase are 60% methane and 40% carbon dioxide by volume (Kiely, 1997). In this respect the percentage of carbon dioxide measured is very low, probably due to it being dissolved in the leachate at the pH measured of 7.4-7.6, as shown with the calculations below.

The CO₂ gas dissolves in water to give carbonate and bicarbonate species. Their concentration was not measured. However, an estimation of their concentration has been done by knowing the partial pressure of CO₂ in the gas space. The concentration of the dissolved CO₂ species (HCO₃⁻, CO₃²⁻) can be calculated using Henry's law (Eq. 5-3)

$$x_g = \frac{P_T}{H} p_g \quad (\text{Eq. 5-3})$$

where,

x_g - is the molar concentration of the gas species in water, mole species/mole water

$$= \frac{\text{mole gas species } (n_g)}{\text{mole gas species } (n_g) + \text{mole water } (n_w)}$$

P_T - is total pressure, usually 1 atm.

H - Henry's law constant, atm.

p_g - mole fraction of the species in the gas phase, mole gas species/mole gas

The partial pressure of CO₂ is 6/100 = 0.06 atm. The Henry's law constant for CO₂ at 20°C is 1420 atm (Tchobanoglous, 2002). Thus, the equilibrium molar concentration of CO₂ in water is:

$$x_g = \frac{1}{1420} 0.06 = 4.23 \times 10^{-5} \text{ mole gas species / mole water} \quad (\text{Eq. 5-4})$$

One litre of water contains 1000g/(18g/mole) = 55.6 moles of water, thus

$$\frac{n_g}{n_g + n_w} = 4.23 \times 10^{-5} \quad (\text{Eq. 5-5})$$

$$\frac{n_g}{n_g + 55.6} = 4.23 \times 10^{-5} \quad (\text{Eq. 5-6})$$

because the number of moles of dissolved gas in a litre of water is much less than the number of moles of water $n_g + 55.6 \approx 55.6$. Substituting into Eq. 5-6 gives

$$n_g \approx 55.6 \times 4.23 \times 10^{-5} \quad (\text{Eq. 5-7})$$

$$n_g \approx 2.3 \times 10^{-3} \text{ mole CO}_2/\text{litre} \quad (\text{Eq. 5-8})$$

Multiplying by the molecular weight of CO₂ (44 g/mole) gives the saturation concentration of CO₂ in water as 103.37 mg/l. The number of moles of dissolved CO₂ gas produced since the introduction of 100% strength leachate is then:

$$2.3 \times 10^{-3} \text{ mole CO}_2/\text{litre} \times 1605.6 \text{ litres (since 100\% strength leachate)} = 3.77 \text{ moles CO}_2 \quad (\text{Eq. 5-9})$$

One mole of gas occupies 22.4 l at standard temperature and pressure (0°C or 273.2K and 760 mm Hg) and 24.12 litre at 21°C (294.2K) and 760 mm Hg. Thus the dissolved CO₂ species would have contributed to generation of $3.77 \times 24.12 = 90.93$ litres of CO₂.

Performing the same calculations for CH₄ ($p_g = 0.88$, $H = 37\,600$ atm) gives a saturation concentration in water of only 20.82 mg CH₄/litre (1.3×10^{-3} mole CH₄/litre) because of the low solubility of CH₄ in water. The number of moles of dissolved CH₄ gas generated since the introduction of 100% strength leachate is then:

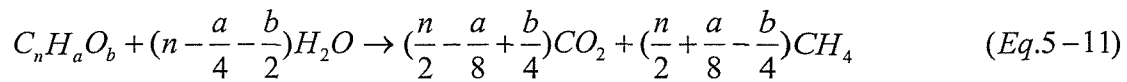
$$1.3 \times 10^{-3} \text{ mole CH}_4/\text{litre} \times 1605.6 \text{ litres} = 2.09 \text{ moles CH}_4 \quad (\text{Eq. 5-10})$$

The dissolved CH₄ species would have contributed to generation of $2.09 \times 24.12 = 50.39$ litres of CH₄.

On the basis of these calculations, the total amount of CH₄ produced was 272.80 litres released in the headspace (0.88×310 litres of gas measured) plus 50.39 litres dissolved gives in total 323.19 litres CH₄. The total amount of CO₂ produced was 18.60 litres released in the headspace (0.06×310 litres of gas measured) plus 90.93 litres dissolved gives in total 109.53 litres CO₂. The amount of N₂ in the column headspace was 18.60 litres. The total volume of the gas released in the column headspace and dissolved in the leachate was 451.32 litres. The proportion of CH₄ in this mixture was 71.6% and of CO₂ – 24.3%. These values are closer to those reported by Kiely, 1997.

6.1.8. Calculating the expected rate of gas generation on the basis of acetate and propionate degradation.

In principle, the volume of biogas produced can be calculated using the Buswell equation (Buswell and Hatfield, 1939)



Calculations showing in detail how the theoretical volume of gas was calculated are shown in Appendix B, Tables 1, 2 and 3. On this basis the total expected daily gas generation due to the degradation of 1108.8 mg of acetate ($770 \text{ mg/l} \times 1.44 \text{ litres/day}$) and 136.80 mg propionate ($95 \text{ mg/l} \times 1.44 \text{ litres/day}$) passed per day is 523.22 ml CH_4 /day and 500.95 ml CO_2 /day. However, initially the microbial population did not utilise all the acetate and propionate available in the leachate because it needed time to acclimatise. Performing the same calculations but with the actual concentrations of nutrients being removed (Tables 1, 2 and 3, Appendix B) gives the theoretical amount of gas produced since the introduction of 100% strength leachate as 516.11 litres CH_4 and 502.10 litres CO_2 . The total theoretical amount of the gas produced is 1018.21 litres.

Analysis (section 6.1.7) indicated that the headspace gas was mainly methane. Almost no CO_2 -gas was present, probably due to its dissolution in the leachate in the form of bicarbonates. There is a discrepancy between the calculated methane production (516.11 litres CH_4) and the measured total gas production in column 1 (310.0 litres) (Figure 6-10).

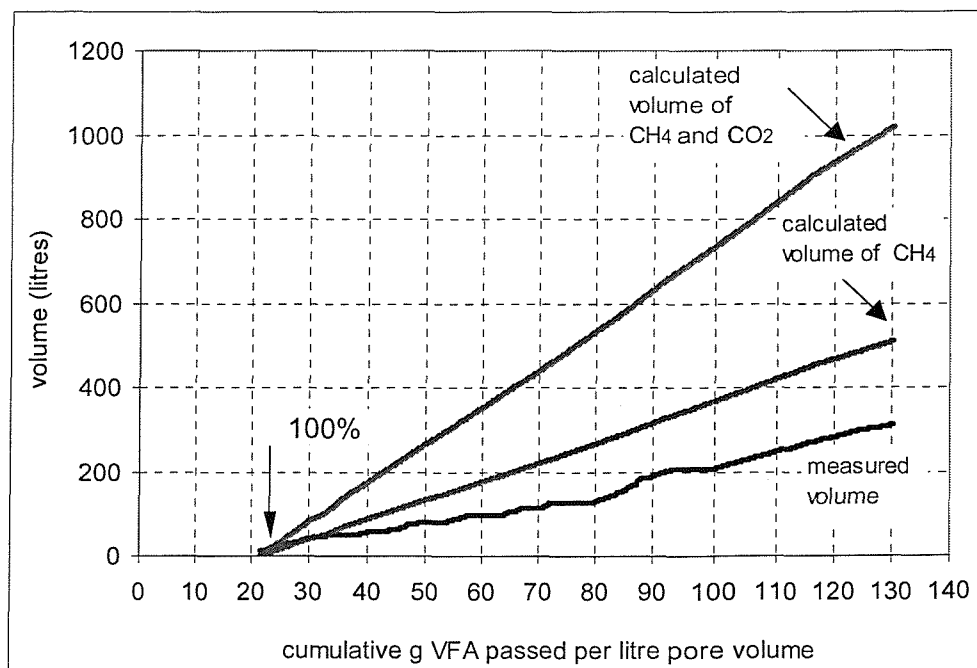


Figure 6-10: Measured and calculated cumulative volume of gas produced in column 2 since introduction of 100% strength leachate

The difference is probably due to the fact that some carbon is utilised by the bacteria for cell growth, polysaccharide production (discussed in section 6.8 and 5.6.) rather than gas generation, and that some is dissolved in the leachate ($50.39 \text{ CH}_4 + 90.93 \text{ CO}_2 = 141.32$ litres lost due to being dissolved in the leachate).

6.1.9. Changes in hydraulic gradient

No apparent head losses with depth within the columns were observed during the period of operation. This indicates that clogging was not sufficient to affect significantly the permeability of the drainage media. However with a pumped flow rate of 1 ml/min, Darcy's law suggests that head losses exceeding 1mm would only be generated when the permeability of the clogged gravel reached that of a fine sand ($\approx 2.0 \times 10^{-4}$ m/s). Increasing the pumped flow rate to 1 litre/min would give more easily measurable head losses, but at the risk of disturbing any biofilm which had developed within the column.

A reduction in gravel permeability is unlikely to be detected, at least in the early stages of clogging. The main technique used to detect clogging was therefore drainable pore volume measurement. Analysis of the clogged gravel using Differential Interference Contrast (DIC) microscope provided supplementary information on the structure and thickness of the deposited material at the conclusion of the experiment (section 6.9).

6.1.10. Reduction in drainable porosity

Relating the reduction in drainable porosity simply to the elapsed time does not reflect the differences in the leachate flow rates or composition. Figure 6-11 shows the reduction in drainable porosity against the cumulative quantity of VFA passed per unit volume. The latter was calculated by multiplying the total number of litres passed by the concentration of VFA, and dividing by the pore volume. Detailed data on the cumulative g VFA passed per litre pore volume are given in Appendix C, Table 1.

Reductions in the drainable porosities in the top sections (tappings 1-4) were observed, with up to a 7-8% decrease occurring in the very top section of the columns (tappings 1-2) and 3-4% in the sections between tappings 2-3 and 3-4. This reduction was considered to have been due to microbial growth and the accumulation of exopolysaccharides,



precipitates and gas bubbles within the pore space. Microbial activity was evidenced by the removal of VFA from the synthetic leachate, as discussed in section 5.1.1, and the observed production of gas, reported in section 6.1.6. The accumulation of precipitates was suggested by the development of black deposits, which were first observed in the liquid layer overlying the aggregate, and later spread into the filter layer. It was thought that these deposits probably comprised iron sulphides, indicating the presence not only of methanogenic bacteria but also of SRB in these columns. To verify this, X-ray Fluorescence (XRF) analysis was carried out after dismantling the columns (section 6-10). The presence of polysaccharides was confirmed at column dismantling by carrying out polysaccharide measurements (chapter 6). The accumulation of gas bubbles is discussed later on in this section. Almost no reduction in porosity occurred in the lower sections (tappings 4-5, 5-6 and 6-out). This was probably due to the decreasing concentrations of nutrients being unable to sustain the development of a significant microbial population in the lower parts of the columns.

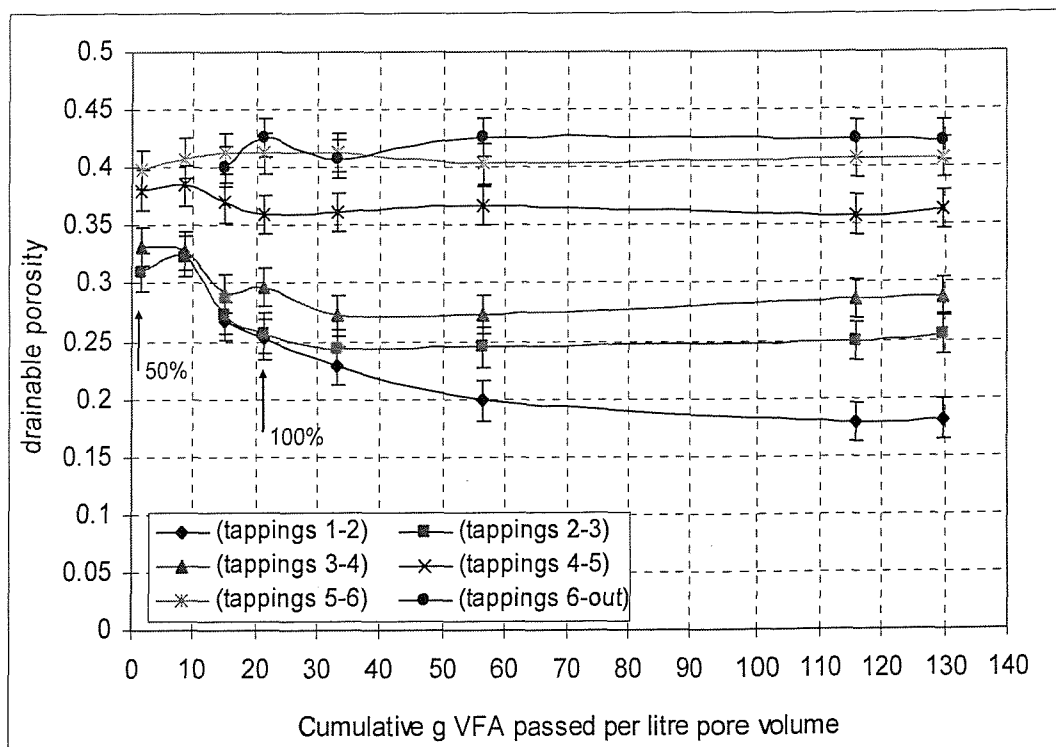


Figure 6-11: Drainable porosity in column 2.

The values for the drainable porosity plotted in Figure 6-11 were calculated by dividing the measured drainable pore volume (Table 6-2) by the total volume for each section.

leachate strength	25%	50%			
date	20/03/1998	29/04/1998	09/09/1998	10/12/1998	
g VFA / l.p.v.	48.88	1.71	8.59	15.04	
tapping (1-2)	2.304	2.266	2.299	1.386	
tapping (2-3)	0.823	0.805	0.839	0.71	
tapping (3-4)	2.547	2.587	2.554	2.27	
tapping (4-5)	2.945	2.962	2.995	2.88	
tapping (5-6)	1.005	1.034	1.06	1.07	
tapping (6-out)	2.08	2.08	2.08	2.08	
sum	11.704	11.734	11.827	10.396	
leachate strength	100%				
date	19/04/1999	14/12/1999	05/09/2000	10/04/2002	26/08/2002
g VFA / l.p.v.	21.41	33.16	56.45	115.86	129.95
tapping (1-2)	1.307	1.185	1.03	0.933	0.942
tapping (2-3)	0.667	0.633	0.635	0.647	0.662
tapping (3-4)	2.31	2.119	2.122	2.224	2.238
tapping (4-5)	2.796	2.81	2.86	2.79	2.826
tapping (5-6)	1.07	1.072	1.046	1.057	1.06
tapping (6-out)	2.208	2.114	2.21	2.201	2.195
sum	10.358	9.933	9.903	9.852	9.923

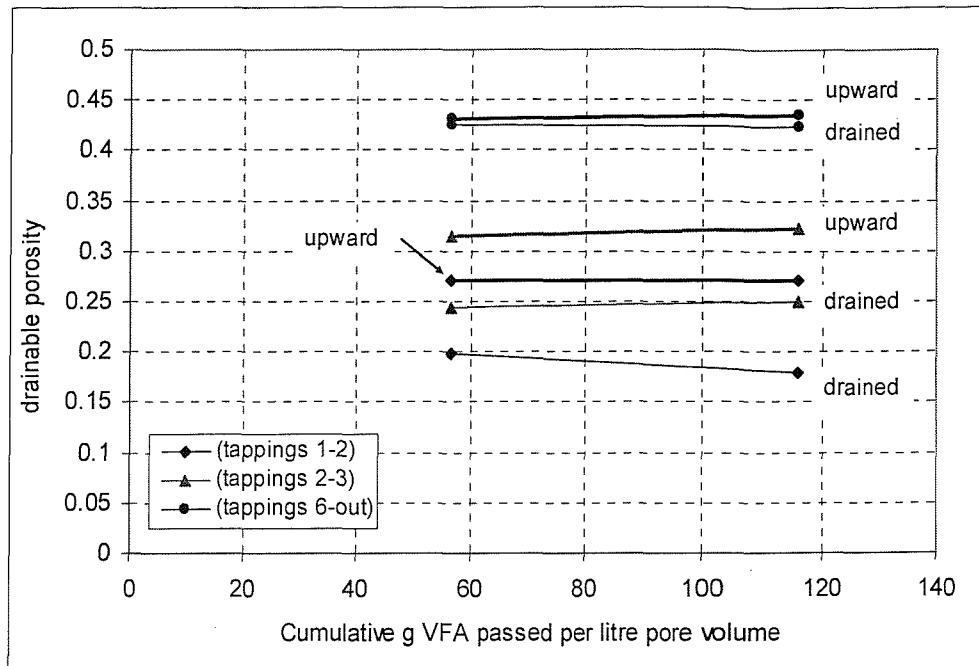
Table 6-2: Drainable pore volumes on draining column 2

The occasional increase in measured porosity for the section between tappings 3-4 and 2-3 during the experiment could be due to biofilm loss as a result of its dying and shearing. This was observed by Cullimore (1993) who noted that biofilm growth is followed by its death, sloughing and subsequent further growth. This periodic phenomenon continues with a decreased difference between the “peak” and “slough” values and a general trend towards decreased porosity.

A. Gas as a clogging agent

Owing to the method of measurement, at least some of the reductions in drainable pore volumes will be due to the presence of gas. The effect of the gas was deduced by comparing the drainable pore volumes on draining and refilling the column from the bottom up, as explained in section 4.4. This technique was adopted after a total of 56.44 g of VFA had passed through the column and the data are presented in Figure 6-12. Gas bubbles made the greatest contribution to the reduction of the drainable porosity (7-9%) in the uppermost sections of the columns where the microbial growth was most pronounced and consequently gas production was most intense. In addition, the 2% reduction in the drainable porosity (97 ml) between 56.4 and 115.8 g VFA passed per litre pore volume

was mainly due to gas as suggested by the constant value for the porosity on filling the column from the bottom up.



Note: The thicker line represents the drainable porosities measured during filling the column in upward flow and the thin line represents the drainable porosities measured on draining the column.

Figure 6-12: The effect of gas bubbles on the drainable porosity in column 2, 100% strength

A smaller absolute reduction in the porosity due to gas bubbles (6-7%) was observed between tappings 2-3 and 3-4. Gas bubbles did not affect the measurements in the lower sections of the column (tappings 4-out). This was to be expected because no microbial activity and consequently no gas production were detected in these sections, as was shown in sections 5.1.1. and Figure 6-9.

The presence in a porous medium of gas bubbles sufficiently large to become trapped in the network of pores causes a reduction in the permeability, leading to clogging because the bubbles decrease the size of the water conducting pores in the same manner as solid particles (Orlob and Radhakrishna, 1958). In fact, gas bubbles need not be larger than the aggregate pore diameters to accumulate in the pores. They can adhere to surfaces, possibly at hydrophobic sites, or they can become entrapped in the matrix of exopolysaccharides that often surround sessile bacteria (Battesby *et al.*, 1985).

Similarly, the values for the drainable porosity plotted in Figure 6-12 were calculated by dividing the measured drainable pore volume on filling the column in upward flow (Table 6-3) by the total volume for each section.

Date	05/09/2000	10/04/2002
Regime	upward flow	upward flow
Tapping (1-2)	1.405	1.41
Tapping (2-3)	0.817	0.837
Tapping (3-4)	2.673	2.663
Tapping (4-5)	2.863	2.786
Tapping (5-6)	1.073	1.057
Tapping (6-out)	2.235	2.259
Sum	11.066	11.012

Table 6-3: Drainable pore volumes on filling column 2 in upward flow

B. Steady state of microbiological growth

A fast initial porosity decrease was measured in the top sections, followed by an almost negligible reduction after 56 g VFA per litre pore volume (395 days since introduction of 100% strength leachate). It is possible that the initial porosity decrease was a result of rapid microbiological growth associated with the exponential stage of bacterial cell growth. The number of newly generated bacterial cells gradually reduced to reach steady state with time, where there was equilibrium between reproduction and death, resulting in zero net growth (Figure 6-13).

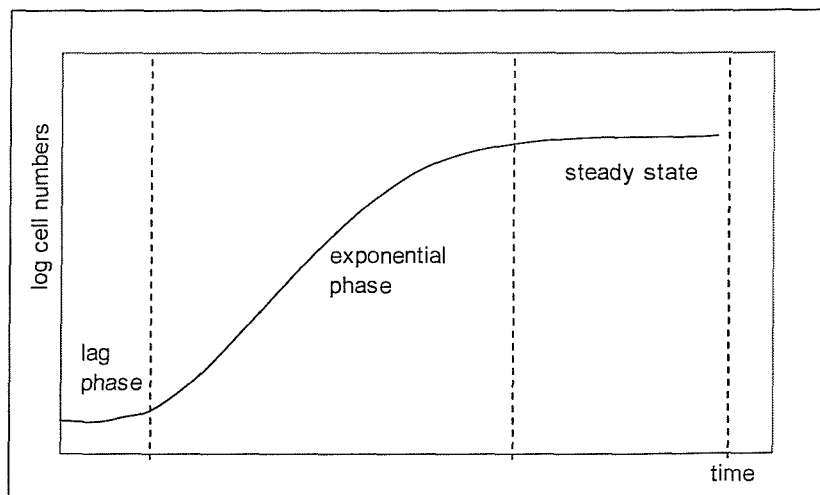


Figure 6-13: Growth curve of a bacterial culture (from Schlegel, 1987)

In addition, the initial accumulation of gas bubbles prior to a steady state being reached, where the volume of gas bubbles generated and released into the column headspace were in balance, may also have contributed to the fast initial porosity reduction.

The small decreases in porosity observed after 56 g VFA per litre pore volume had passed may have been due to the build up of inorganic precipitates, whose contribution to the clogging process in this experimental column was relatively less important, as discussed in section 6.1.4.

6.2. Column supplied with leachate with high VFA (1988 mg/l) and low SO_4^{2-} (36 mg/l) concentrations – column 1, 200 % strength

The leachate strength in column 1 was doubled in order to investigate the effects that the higher concentrations of organic and inorganic substances could have on the clogging of the drainage aggregate.

6.2.1. VFA removal from the leachate

The data shown in Figure 6-14 show that doubling the acetate concentration on switching from 100% to 200% strength leachate did not inhibit/kill the population of acetate utilising bacteria as previously observed on switching from 50% to 100% strength leachate.

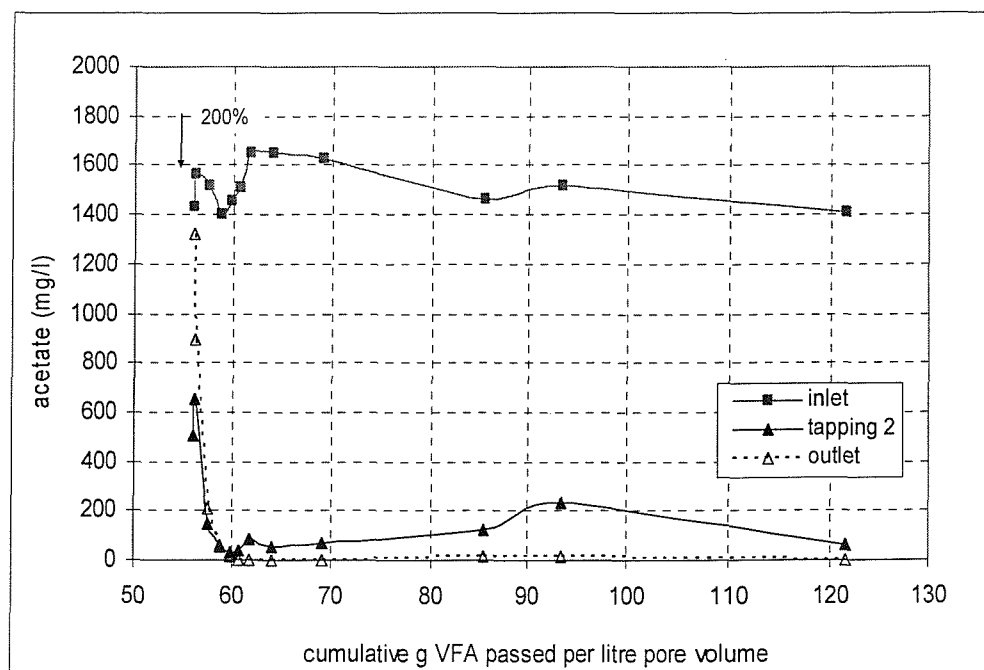


Figure 6-14: Acetate removal in column 1 since introduction of 200% strength leachate

Initially the acetate utilising bacteria were removing 770 mg/l (the amount supplied at 100% strength leachate), which rapidly increased to reach a value of 1540 mg/l, which corresponds to the amount introduced with the 200 % strength leachate. Complete removal of the acetate by the column outlet occurred after the passage of only approximately 6-7 g VFAs per litre pore volume. This is considerably faster than the 14 g VFAs per litre pore volume required by the bacteria on switching from 50% to 100% strength leachate. This could have been due to the enhanced adaptability of the bacterial population as a result of previous substrate increase (50% to 100% strength leachate) leading to faster growth rates or a more active cell metabolism.

The acetate was removed mainly in the section between the inlet and tapping 2. This indicates that the acetate utilising bacteria in the top sections may have become acclimatised to the increased acetate concentrations due to increased biomass or more active cell metabolism. The bacterial population in the lower sections still did not develop, probably for reasons previously explained in section 6.1.1. This observation is consistent with the fact that there was almost no reduction in drainable porosity in the lower sections (section 6.2.6, Figure 6-21). The outlet concentrations immediately after the introduction of full strength leachate were higher than the concentrations at tapping two due to the nature of the experimental procedure (section 6.1.1).

Figure 6-15 shows the propionic acid concentrations at different tappings along the height of the column since the introduction of 200% strength leachate. It appears that the propionate utilising bacteria were not inhibited as previously observed on switching from 50% to 100% strength leachate (section 6.1.1). Initially, the bacterial population was able to remove 95 mg/l (the amount supplied with 100% strength leachate), which rapidly increased until all the propionate supplied with the 200% strength leachate was utilised (190 mg/l). The data show that the propionate utilising bacteria were able to utilise the doubled propionate concentrations after the passage of 5-7 g VFA per litre pore volume, compared with more than 14 g VFA per litre pore volume on switching from 50% to 100% strength leachate.

The majority of the propionate was removed between the inlet and tapping 2 with small amounts (up to 50 mg/l) removed in the other column sections between tapping 2 and the outlet. The high propionate concentration at tapping 2 after a total of 59 g VFA per litre

pore volume had passed could be due to degradation of valeric acid, which would produce propionate as an intermediate product. The high propionate concentration at tapping 2, after a total of 95 g VFA per litre pore volume had passed, could be due to higher inlet concentrations. The variation in the inlet propionate concentrations was probably caused by bacterial activity within the storage container and inlet tubing.

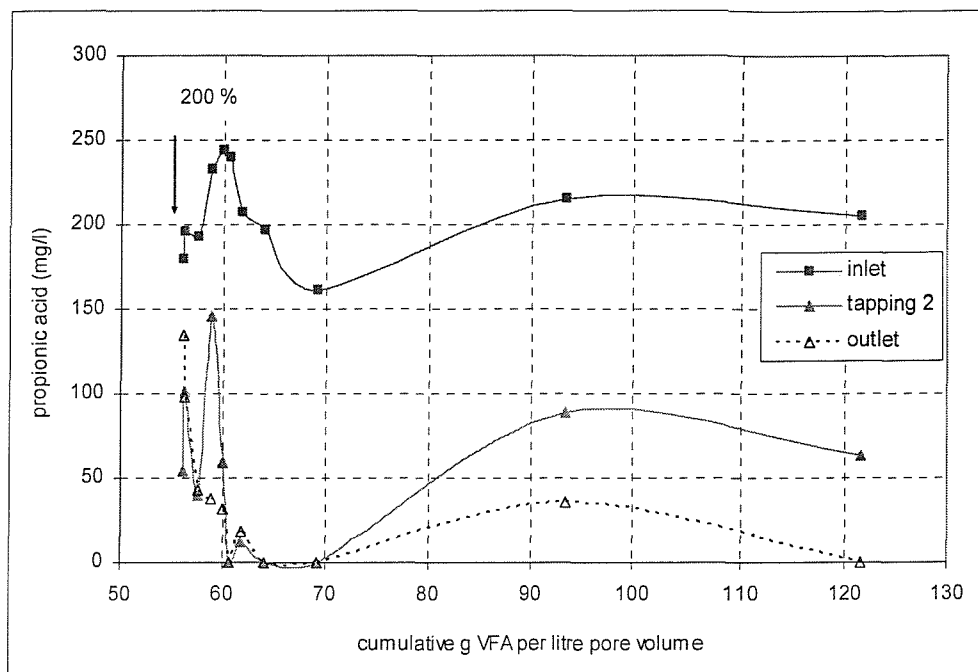


Figure 6-15: Propionic acid removal in column 1, 200% strength leachate

6.2.2. Sulphate reduction

Chemical analysis of leachate samples collected from the different tappings along the height of the columns shows that 39 mg $\text{SO}_4^{2-}/\text{l}$ was removed following the introduction of 200% strength leachate, all in the uppermost section of the column (inlet - tapping 2) (Figure 6-16). This accounts for a total mass of sulphur removed of 11.27 g S^{2-} ($39 \text{ mg } \text{SO}_4^{2-}/\text{l} \times 865.44 \text{ litres} \times 0.334 \text{ S}/\text{SO}_4^{2-} = 11.27 \text{ g } \text{S}^{2-}$) since introduction of 200% strength leachate. The dissolved iron species were not measured. If we assume a solubility similar to when 100% leachate was utilised with an average concentration of dissolved iron of 8.25 mg/l, then the total iron removed would be 7.13 g Fe (865.44 litres passed). If we make the assumption that the sulphur was precipitated mainly in the form of FeS, the available Fe would react with 4.10 g S^{2-} resulting in formation of 11.24 g or 7.03 ml of FeS precipitates, assuming a bulk (wet) density of the clog material of 1.6 g/cm³ as previously explained (section 6.1.4). This accounts for 2.1% of the total volume of

accumulated clog material, which was 340 ml. If the sulphur was precipitated as FeS_2 , then the available iron would react with 8.19 g S^{2-} to form 15.32 g or 9.57 ml of FeS_2 . The calculation again suggests that FeS or FeS_2 precipitates had relatively small contribution to the clogging processes taking place in experimental column 1.

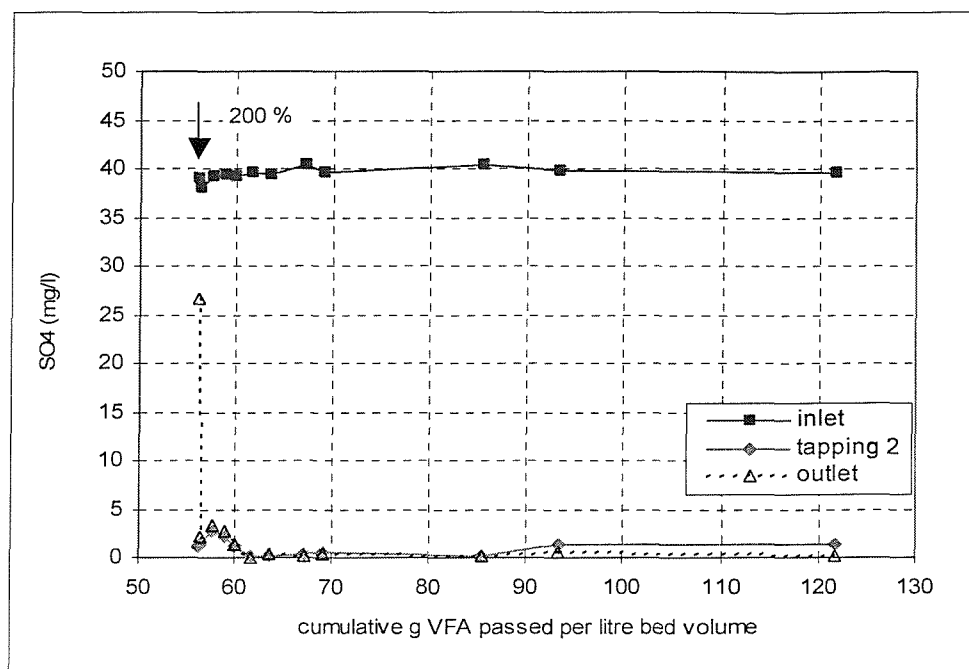


Figure 6-16: Sulphate removal in column 1, 200% strength leachate

6.2.3. Calcium concentrations

Figure 6-17 shows that between 50 mg/l and 100 mg/l of Ca was removed during operation of the column with 200% strength leachate. The concentration of Ca removed is considerably higher than the negligible amounts removed during the passage of 100% strength leachate. This is thought to be due to the higher concentration of Ca, which exceeds the maximum solubility of 233 mgCa/l (section 6.1.5) assuming that the pH of the leachate was 7.6, similar to when 100% strength leachate was supplied. Based on Figure 6-17, the total amount of Ca removed since introduction of 200% strength leachate was 60.52 g ($70 \text{ mgCa/l} \times 865.44 \text{ litres}$), which accounts for the formation of 151.30 g CaCO_3 . Assuming a bulk (wet) density of the clog material of 1.6 g/cm^3 gives a volume of 94.56 ml , which represents 27.8 % of the total volume of accumulated clog material. This calculation indicates that CaCO_3 precipitates had a significant contribution to the clogging process and resulted in cementation of the clog material as observed on column dismantling (section 6-10).

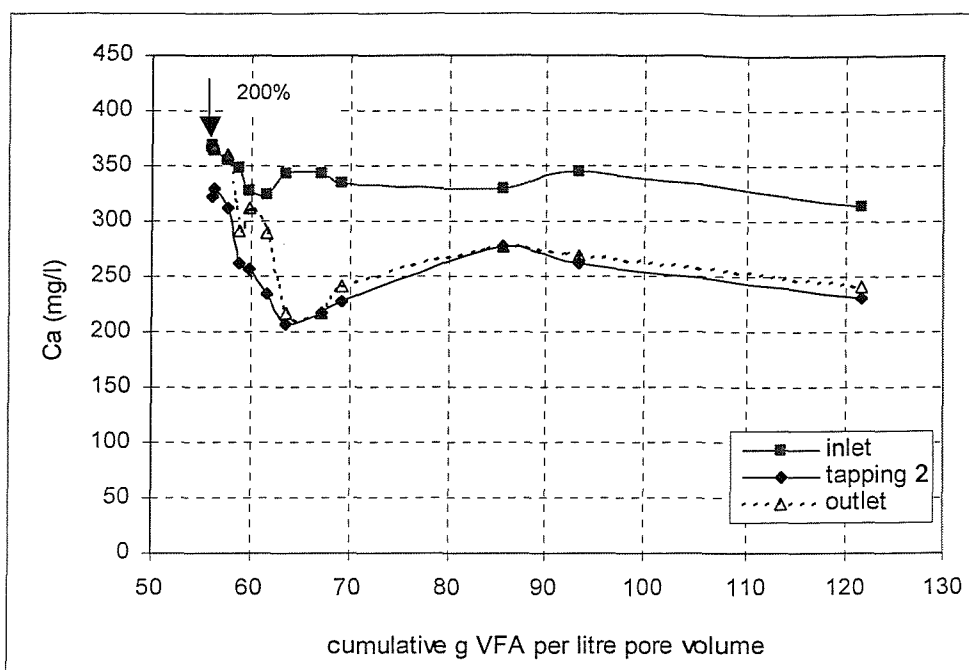


Figure 6-17: Calcium concentrations in column 1 since introduction of 200% strength leachate.

6.2.4. Gas volume

The cumulative volume of gas produced since the introduction of 200% strength leachate is shown in Figure 6-18.

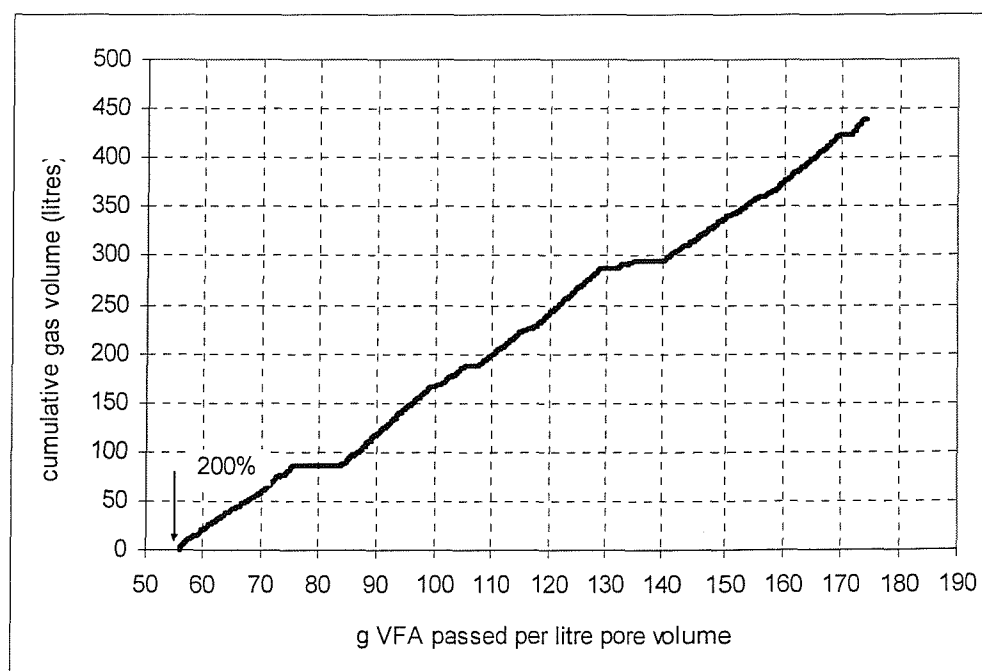


Figure 6-18: Gas production in column 1 since introduction of 200% strength leachate

The daily volume of gas produced apparently varied between zero and 1.5 litres (Figure 6-19). The reason for this apparent variation has already been explained in section 6.1.6.

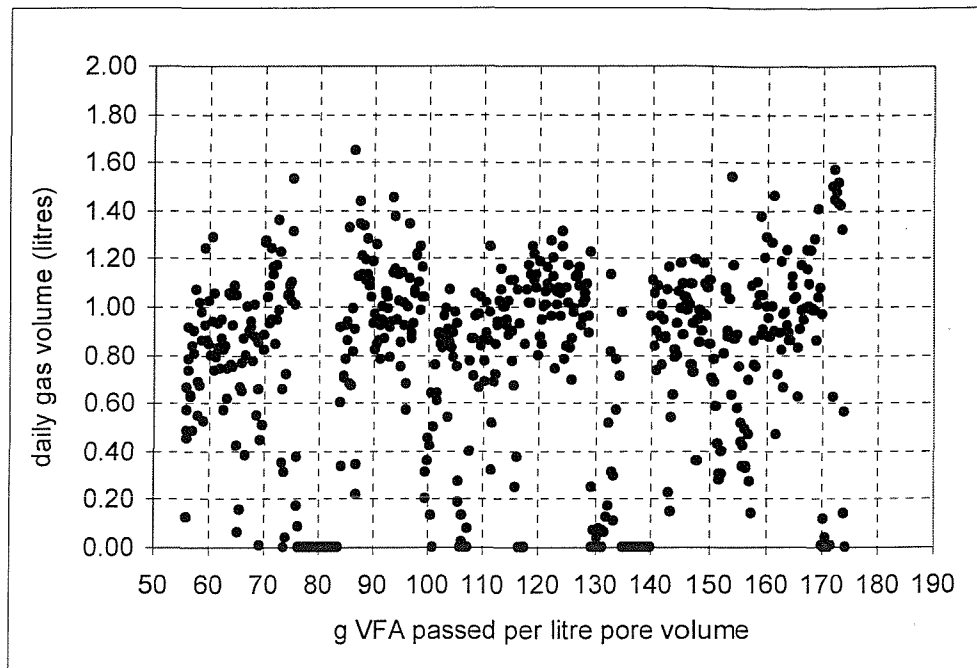


Figure 6-19: Daily gas production in column 1 since introduction of 200% strength leachate

6.2.5. Calculating the expected rate of gas generation on the basis of acetate and propionate degradation.

Detailed calculations of the theoretical volume of gas produced on the basis of the actual concentrations of acetate and propionate being removed are shown in Appendix B (Tables 4, 5 and 6). The total expected gas volumes are 586.99 litres of CH_4 and 560.21 litres of CO_2 , accounting for a total volume of gas of 1147.20 litres as shown on Figure 6-20. The difference between the measured and calculated gas volumes has been explained in section 6.1.8 and is further discussed in sections 5.5. and 5.6. In addition, some of the carbon has been precipitated as CaCO_3 .

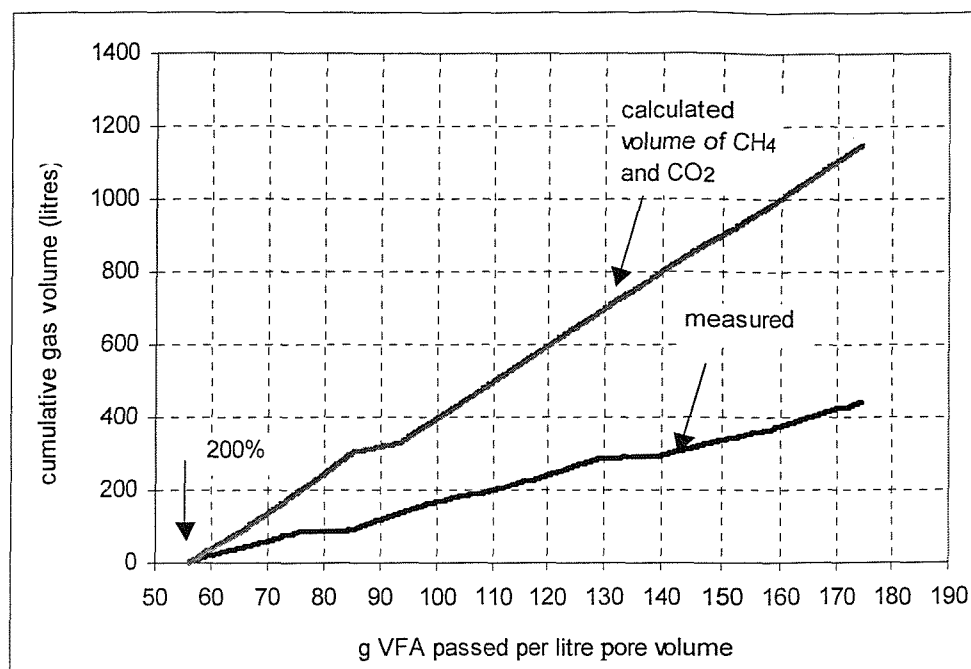


Figure 6-20: Volume of calculated and measured cumulative volume of gas in column 1 since introduction of 200% strength leachate

6.2.6. Reduction in drainable porosity

A further reduction in the drainable porosity of up to 6% occurred in the very top section of the column (inlet-tapping 2) (Figure 6-21) following introduction of 200% strength leachate. This reduction was considered to have been due to microbial growth and the accumulation of exopolysaccharides, precipitates (mainly CaCO_3) and gas bubbles within the pore space. Microbial activity was evidenced by the removal of VFA from the synthetic leachate, as discussed in section 5.2.1, and the observed production of gas, reported in section 5.2.4. The precipitation of CaCO_3 was suggested by the removal of Ca from the leachate and was discussed in section 6.2.3. The contribution of the gas bubbles to the clogging process is discussed later in this section. This reduction was comparable to that with 100% strength leachate although it occurred after the passage of half as many litres of leachate due to the doubled leachate concentration. Detailed data on the cumulative g VFA passed per litre pore volume are given in Appendix C, Table 2.

Almost no reduction in porosity occurred in the lower sections (tappings 2-3, 3-4, 4-5, 5-6 and 6-out). This was probably due to the decreasing concentrations of nutrients being unable to sustain the development of significant microbial population in the lower parts of the columns. Precipitation of CaCO_3 did not occur in these column sections either as indicated by the Ca concentrations (Figure 6-17, section 6.2.3) where the outlet concentrations at the outlet are similar to that at tapping 2.

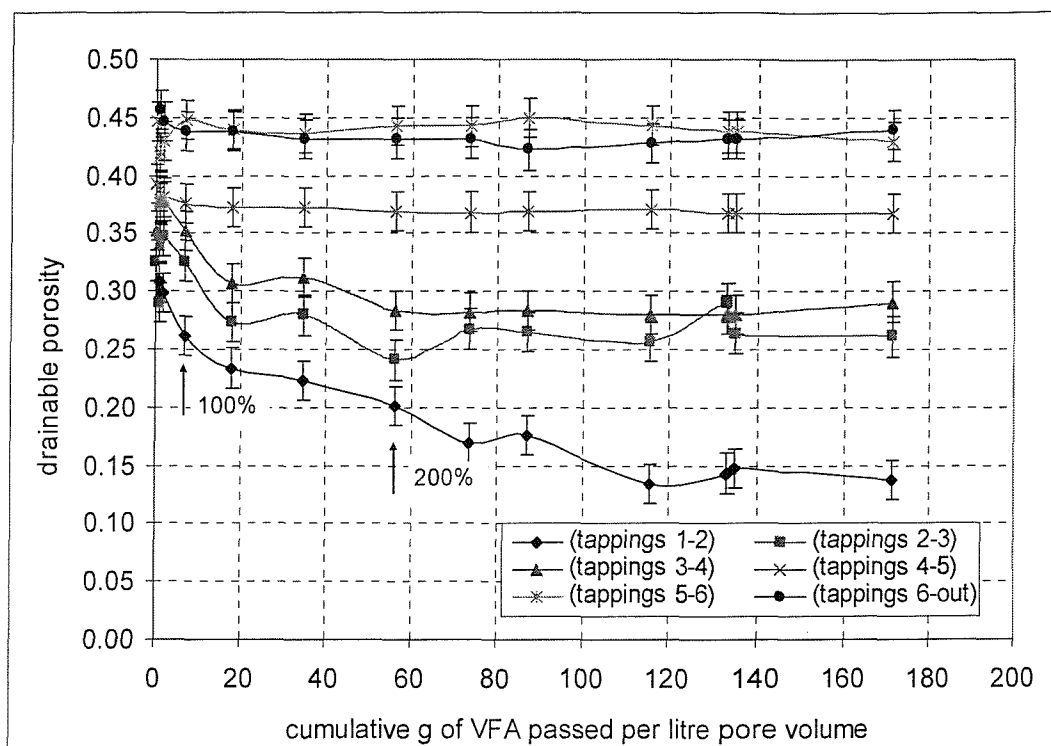


Figure 6-21: Drainable porosity in column 1

The measured drainable pore volumes, used to calculate the drainable porosity in Figure 6-21, are given in Table 6-4.

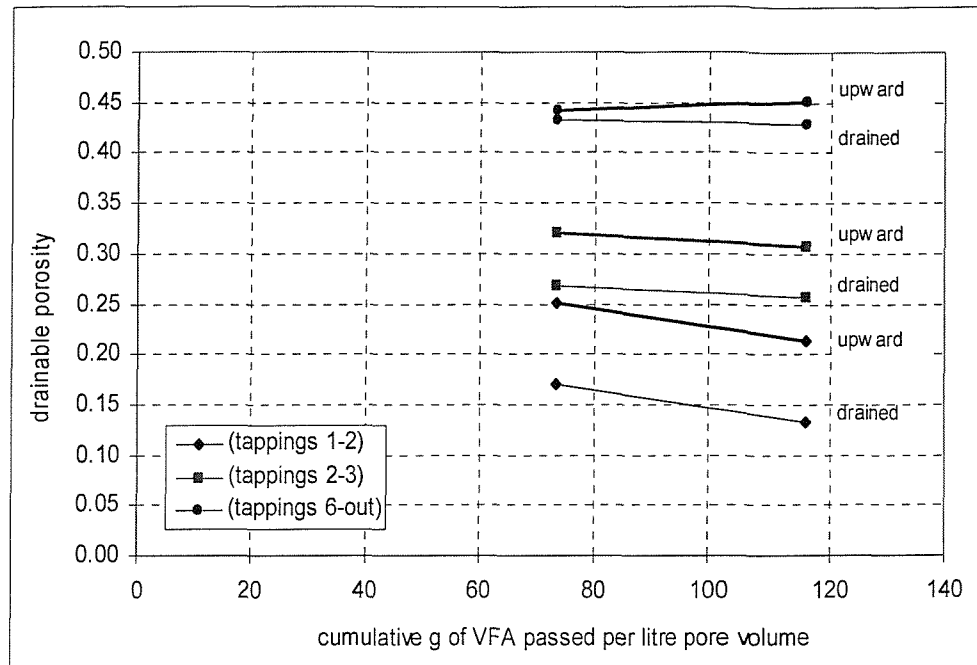
leach. strength	25%	50%				100%		
date	20/03/1998	28/04/1998	09/09/1998	01/11/1998	03/12/1998	05/05/1999	12/12/1999	04/09/2000
g VFA / l.p.v.		0.125	0.656	0.976	1.567	6.833	17.8	34.798
tapping (1-2)	2.328	1.876	1.745	1.598	1.548	1.358	1.214	1.156
tapping (2-3)	0.782	0.846	0.754	0.9	0.9	0.846	0.708	0.725
tapping (3-4)	2.521	2.737	2.65	2.94	2.938	2.745	2.386	2.428
tapping (4-5)	3.07	3.059	3.01	2.92	2.96	2.922	2.9	2.897
tapping (5-6)	1.127	1.159	1.089	1.08	1.115	1.163	1.14	1.133
tapping (6-out)	2.37	2.37	2.37	2.37	2.315	2.271	2.27	2.234
sum	12.198	12.047	11.618	11.808	11.776	11.305	10.618	10.573
leach. strength	200%							
date	01/06/2001	03/09/2001	14/11/2001	09/04/2002	05/07/2002	15/07/2002	09/01/2003	
g VFA / l.p.v.	56.108	73.533	86.877	115.842	133.339	135.369	171.506	
tapping (1-2)	1.043	0.882	0.915	0.694	0.744	0.769	0.716	
tapping (2-3)	0.625	0.694	0.689	0.666	0.672	0.685	0.678	
tapping (3-4)	2.21	2.196	2.205	2.181	2.182	2.182	2.262	
tapping (4-5)	2.872	2.865	2.871	2.889	2.859	2.859	2.865	
tapping (5-6)	1.149	1.147	1.165	1.148	1.134	1.134	1.112	
tapping (6-out)	2.24	2.24	2.189	2.221	2.237	2.237	2.277	
sum	10.139	10.024	10.034	9.799	9.828	9.866	9.910	

Table 6-4: Drainable pore volumes on draining column 1

A. Gas as a clogging agent

Gas bubbles made the greatest contribution to the reduction of the drainable porosity (8% expressed in terms of drainable porosity) in the uppermost sections of the columns where the microbial growth was most pronounced and consequently gas production was most intense (Figure 6-22). The observed reduction in the drainable porosity between 73.5 and 115.8 g VFA passed per litre pore volume was most likely due to microbial growth and accumulation of polysaccharides and precipitates as suggested by the parallel lines for the porosity at draining and filling the column from the bottom up. A smaller absolute reduction in the porosity due to gas bubbles (4-5%) was observed between tappings 2-3 and 3-4. It appears that gas bubbles made a similar contribution to the clogging process to when 100% strength leachate was supplied to the column, despite the larger volume of gas produced as a result of the higher organic content of the 200% strength leachate. It could be that the column matrix was already saturated with gas and that any extra gas bubbles merged together and escaped into the column headspace. Gas bubbles did not affect the measurements in the lower sections of the column (tappings 4-out). This was to be

expected because no microbial activity and consequently no gas production were detected in these sections (section 6.2.4.).



Note: The thicker line represents the drainable porosity measured at upward flow and the thin line represents the drainable porosity measured at draining the column.

Figure 6-22: Effect of gas bubbles on the drainable porosity in column 1 following introduction of 200% strength leachate

Similarly, the measured drainable pore volumes on filling the column in upward flow, used to calculate the drainable porosity in Figure 6-22, are given in Table 6-5.

date	04/09/2000	03/09/2001	09/04/2002
regime	upward flow	upward flow	upward flow
tapping (1-2)	1.18	1.297	1.112
tapping (2-3)	0.846	0.833	0.795
tapping (3-4)	2.726	2.705	2.705
tapping (4-5)	2.901	2.881	2.866
tapping (5-6)	1.141	1.138	1.103
tapping (6-out)	2.258	2.297	2.342
sum	11.052	11.151	10.923

Table 6-5: Drainable pore volumes on filling column 1 in upward flow

6.3. Columns supplied with leachate with low VFA (182 mg/l) and high SO_4^{2-} (1120 mg/l) concentrations (columns 3 and 4)

This section addresses the tests carried out using low VFA and high SO_4^{2-} type leachate. Towards the end of the experiment in column 3, a test was initiated where radionuclide analogues simulating the behaviour of radioelements, likely to be encountered in the Drigg drainage system, were introduced in the leachate medium. Their effects on the clogging by their potential to both absorb onto the biofilm and to precipitate was evaluated. This test is referred to as clogging test with radionuclide analogues. Data for the duplicate column (column 4) are given in Appendix A (Figure 7 to Figure 10).

6.3.1. VFA removal from the leachate

Three species of VFA were supplied to column 3 – acetic (CH_3COOH), propionic ($\text{CH}_3\text{CH}_2\text{COOH}$) and iso-valeric acids ($\text{CH}_3\text{CH}(\text{CH}_3)\text{CH}_2\text{COOH}$). Acetic acid concentrations since the introduction of 50% strength leachate are shown in Figure 6-23.

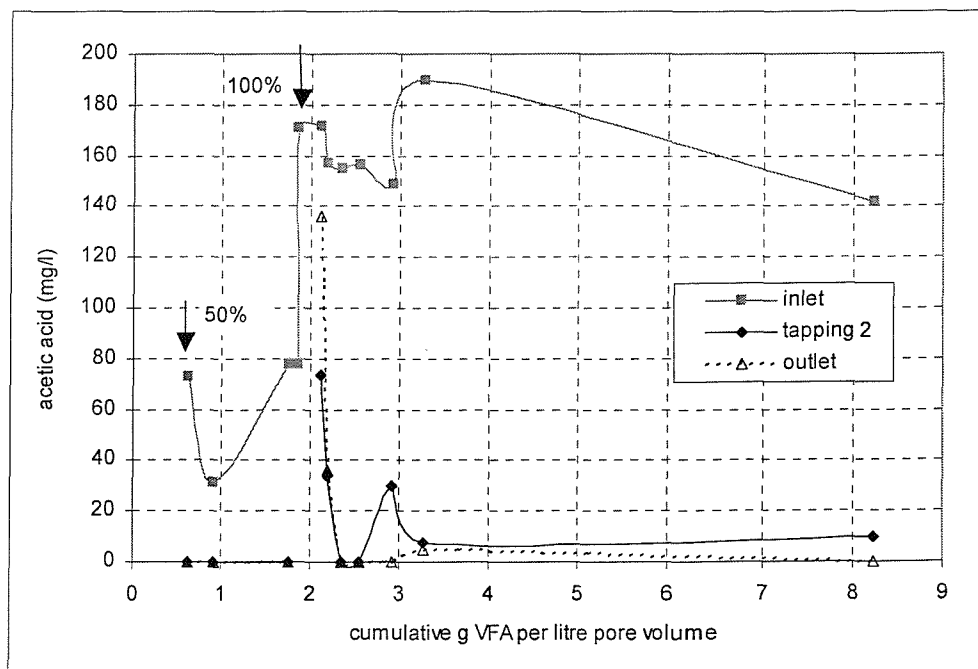


Figure 6-23: Acetic acid concentrations measured at the column inlet, tapping 2 and the column outlet since introduction of 50% strength leachate in column 3.

Only small concentrations of propionic (5 mg/l) and iso-valeric acids (7 mg/l) were supplied to these columns and figures showing the concentrations of these acids at different tappings along the height of the column are not presented owing to the difficulty of making reliable measurements at the concentrations levels utilised.

Immediately following the introduction of full strength leachate, the SRB were initially able to remove 80-90 mg/l of acetate, the same amount (in mg/l) as removed at 50% strength leachate. This was followed by a rapid acclimatisation, which probably involved bacterial growth. The SRB were able to remove completely the doubled acetate concentration after only 0.5 g VFA per litre pore volume had been passed (compared with 14 g VFA per pore volume in columns 1 and 2). It appears that the bacterial population was not inhibited by the increased nutrient concentration. This could be due either to the rather lower concentrations of organic substrate (full strength leachate - 182 mg total VFA/l compared with 994 mg total VFA /l for columns 1 and 2) or to SRB rather than the methanogenic bacteria being the predominant population in this column. It could be that the SRB are metabolically more able to adapt to increased concentrations of acetic acid than the methanogenic bacteria.

It is evident from the increased nutrient removal rates that the bacterial population in the top layer developed/adapted rapidly to the increased leachate strength. As a result, the microbial population in the lower layers received negligible amounts of nutrients throughout the experiment and probably did not develop as previously explained. The outlet concentrations immediately after the introduction of full strength leachate were higher than the concentrations at tapping two due to the nature of the experimental procedure, as already explained for columns 1 and 2 (section 5.1.1.). On switching to the 100% strength leachate the column was initially instantly saturated with the full strength leachate medium. The bacteria at the bottom sections were not very active or had not developed at all, and were therefore unable to remove any acetate.

6.3.2. pH measurements

Figure 6-24 shows the pH at different tappings along the column after VFA removal and that sulphate reduction had reached a steady state. The measurement was carried out after

a total of 20.5 g VFA per litre pore volume had passed through the column, which corresponds to day 513 after the introduction of the full strength leachate.

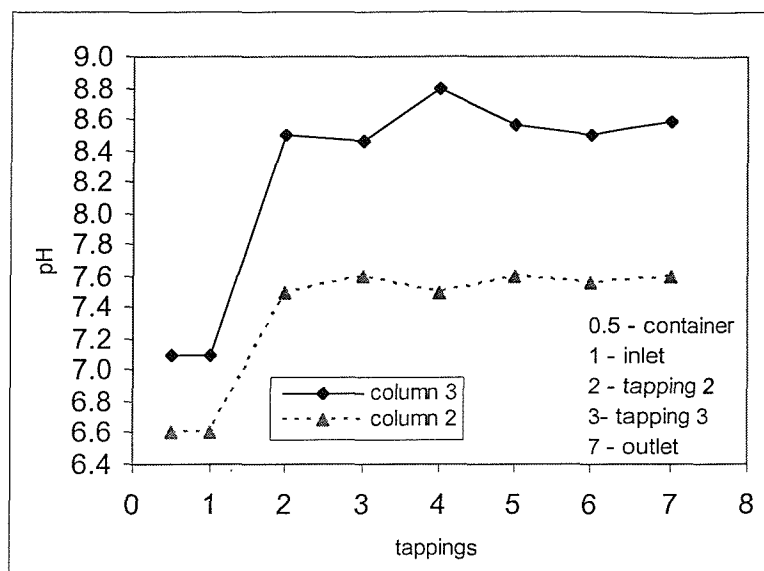


Figure 6-24: pH measurements in columns 3 and 2.

The pH of the simulated leachate medium increased (i.e. it became less acidic) between the inlet and tapping 2 as a result of the utilisation of VFA by the SRB for the reduction of sulphate to sulphide. The pH levels measured at tappings 2 to 7 were between 8.4 and 8.6, considerably higher than in column 2. This could be due to the higher initial pH in column 3 and possibly lower generation rates of CO_2 (as a result of the lower organic content of the leachate), leading to availability of less carbonic acid (H_2CO_3) and hence a higher pH.

6.3.3. Iron measurements

25 g of iron filings were introduced in the 25 litre inlet container where the simulated leachate medium was kept. This resulted in a gradually increasing dissolved iron concentration in the inlet container which reached a max value of 8.6 mg Fe/l (Figure 6-25). The 25 litre container was kept at 4°C and retained sufficient leachate to supply the experimental column for 14 days, which is why the concentration of Fe is shown for this period of time.

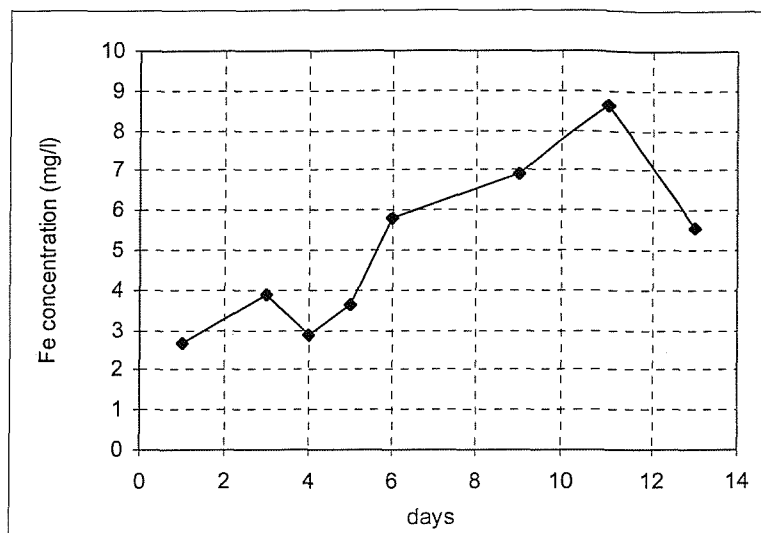


Figure 6-25: Iron concentrations in the inlet container for column 3, 100% strength leachate

The iron concentrations in samples collected from the column outlet were below 1 mg/l, indicating almost complete removal of the dissolved iron species within the column. Taking the average amount of Fe available as 5.2 mg/l gives a total mass of iron removed since introduction of 100% strength leachate of 8.66g Fe ($5.2 \text{ mg/l} \times 1664.64 \text{ litres} = 8.66 \text{ g Fe}$).

6.3.4. Radionuclide concentrations

Additional metal species in the form of the following radionuclide analogues (Cs, Ni, Co, Ba, Eu, Ce, Rb, Ru) were introduced into the leachate medium after a total of 13.7 g VFA per litre pore volume had passed through the column. Their concentration was increased in steps from 20 $\mu\text{g/l}$ to 200 $\mu\text{g/l}$ to 2000 $\mu\text{g/l}$.

The concentrations of the radionuclide analogues in samples collected at the outlet of column 3 following the introduction of the cocktail of 20 $\mu\text{g/l}$, 200 $\mu\text{g/l}$, 2000 $\mu\text{g/l}$ of each radionuclide in the simulated leachate medium are shown in Figure 6-26, Figure 6-27 and Figure 6-28, respectively.

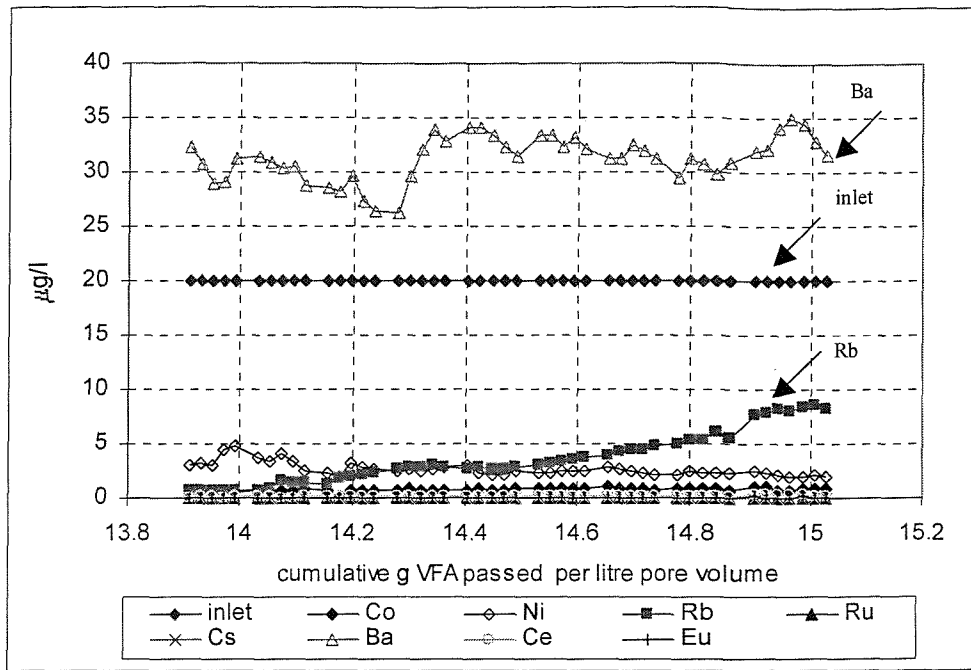


Figure 6-26: Radionuclide concentration at column outlet at 20 $\mu\text{g/l}$

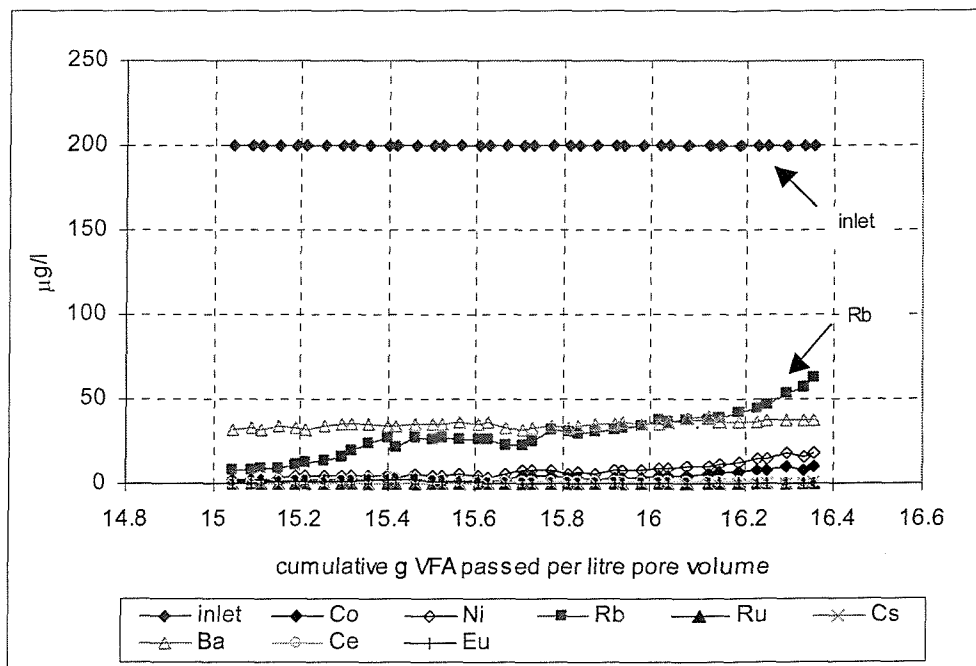


Figure 6-27: Radionuclide concentration at column outlet at 200 $\mu\text{g/l}$

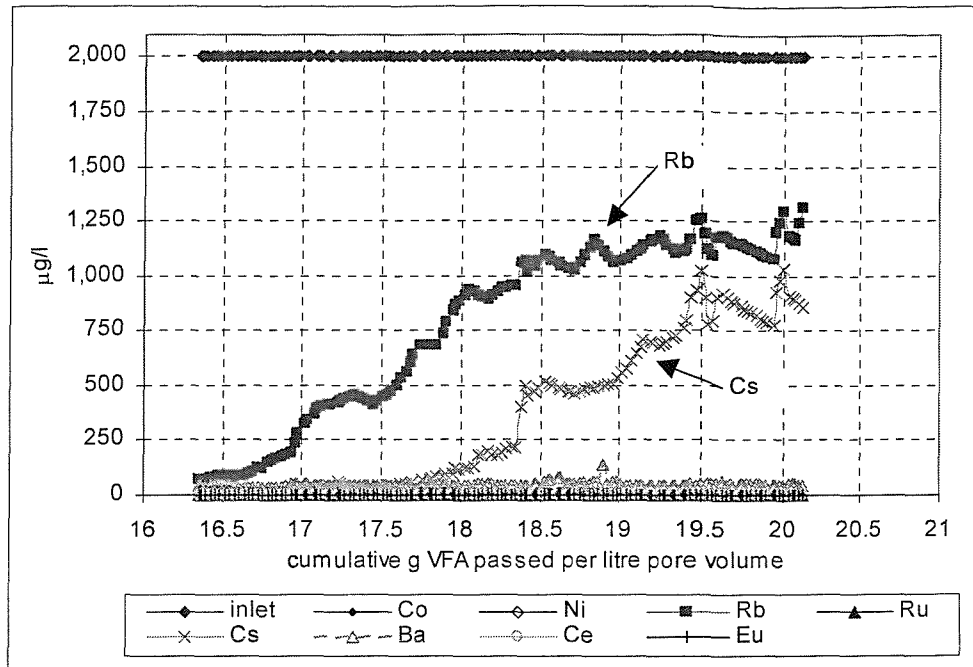


Figure 6-28: Radionuclide concentration at column outlet at 2000 $\mu\text{g/l}$

The results indicate a breakthrough for Rb and Cs, suggesting that the sorption capacity for these two elements has been reached. In addition, the data suggest that Ni, Co, Eu, Ce and Ru are being strongly sorbed and longer periods or higher concentrations are required to reach their sorption capacity within the column. The radionuclide elements with the exception of Rb and Cs could also be retained in the column by means of precipitation.

On the basis of Figure 6-26, Figure 6-27, Figure 6-28 the masses of the radionuclide analogues (mg) removed from the leachate following the introduction of 20 $\mu\text{g/l}$, 200 $\mu\text{g/l}$ and 2000 $\mu\text{g/l}$ are the following:

Co	Ni	Rb	Ru	Cs	Ba	Ce	Eu
1.77	1.60	1.51	1.84	1.84	-	1.83	1.84

Table 6-6: Masses of radionuclide analogues in mg removed at 20 $\mu\text{g/l}$

Co	Ni	Rb	Ru	Cs	Ba	Ce	Eu
18.09	17.76	15.78	18.43	18.41	15.21	18.31	18.37

Table 6-7: Masses of radionuclide analogues in mg removed at 200 $\mu\text{g/l}$

Co	Ni	Rb	Ru	Cs	Ba	Ce	Eu
1182.59	1180.36	719.71	1183.57	965.69	1155.78	1183.26	1183.37

Table 6-8: Masses of radionuclide analogues in mg removed at 2000 μ g/l

Detailed calculations are shown in Appendix D, Tables 1, 2 and 3. These cumulative amounts will be used for calculating the amounts of the respective MeS species (section 6.3.5).

6.3.5. Sulphate reduction

Chemical analysis showed that 270 mg of SO_4^{2-} were reduced per litre of leachate passed. This accounts for only 25% of the total sulphate supplied to the columns (Figure 6-29). The processes of sulphate reduction and VFA degradation were again confined to the top sections of the columns. Theoretical stoichiometric calculations on the basis of Eq. 2-16 show that all the VFAs supplied with the leachate were needed for the reduction of 270 mg/l SO_4^{2-} , indicating that there were not sufficient nutrients to reduce sulphate concentrations further.

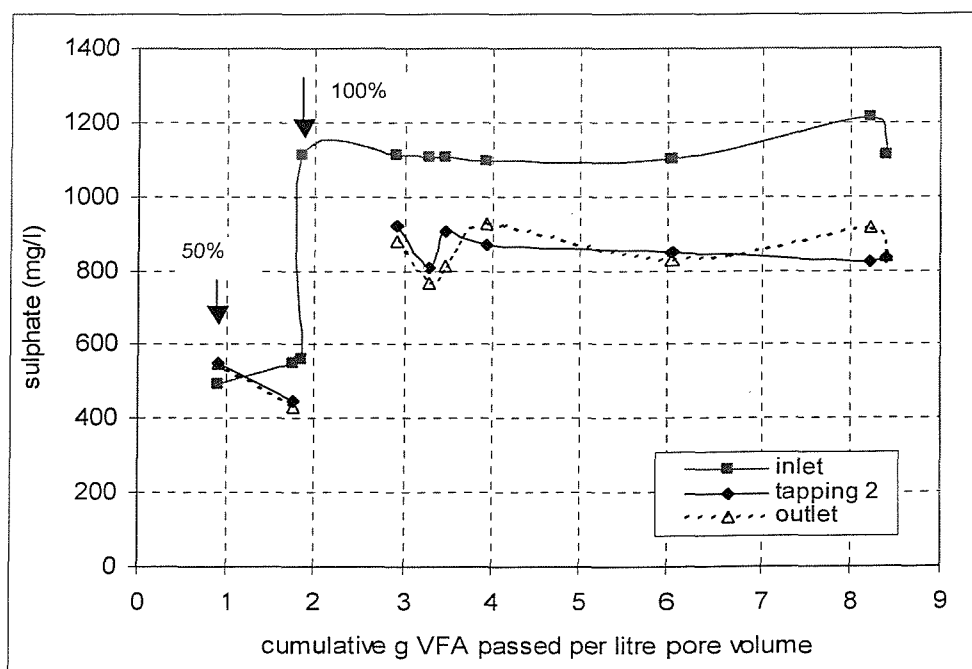


Figure 6-29: Sulphate concentrations measured at the column inlet, tapping 2 and column outlet since the introduction of 50% strength leachate in column 3.

Black deposits started to develop on the surface of the aggregate as soon as the 25% strength leachate was supplied. The black deposits appeared first in the top liquid layer overlying the aggregate, spread into the filter layer and then downwards to occupy the whole column giving it an intense black appearance. The nature of these deposits was analysed on dismantling the columns by means of XRF analysis (section 6-10).

Based on Eq. 5-12, section 6.3.7, 1.9×10^{-3} moles/litre of dissolved H_2S species were present in the leachate which was equivalent to 62.73 mg S^{2-} /l. On the basis of this, the theoretical mass of sulphur removed would be 100.72 g S^{2-} since the introduction of 100% strength leachate bearing in mind that 1664.6 litres had passed. This calculation is more precise than deriving the amount of S^{2-} from the SO_4^{2-} removed, because the latter does not take into account the S species lost as H_2S gas.

If we assume that the sulphur was precipitated mainly in the form of FeS , 175.46 g of Fe would be required or 109.27 mg Fe/l, leading to the formation of 276.18 g of FeS (172.61 ml). However, as shown in section 6.3.3, the total iron removed since introduction of 100% strength leachate was 8.66 g Fe. The available Fe reacted with 4.97 g S^{2-} leading to the formation of 13.63 g FeS or 8.52 ml FeS , assuming a bulk (wet) density of the clog material of 1.6 g/cm^3 . This accounts for 4.4 % of the total volume of accumulated clog material, which was 193 ml. If FeS_2 was formed, 9.94 g S^{2-} would be required leading to the formation 18.60 g or 11.63 ml of FeS_2 .

Additional amounts of metal sulphides would be expected to be formed after commencement of the test with radionuclide analogues. Assuming that the main mechanism by which the radionuclide analogues were removed from the leachate was by their precipitation as low solubility sulphide salts (Table 6-9) then the volume of these MeS would be 7.28 ml. This represents only 0.8 % of the volume of the accumulated clog material since introduction of radionuclide species, which was 917 ml.

	CoS	NiS	Rb ₂ S	Ru ₂ S ₃	Cs ₂ S	BaS	Ce ₂ S ₃	Eu ₂ S ₃
20 µg/l	2.73	2.46	1.79	2.43	2.06	0.00	2.04	2.42
200µg/l	27.93	27.45	18.74	24.28	20.63	18.75	20.40	24.18
200 µg/l	1825.96	1824.93	854.69	1559.00	1082.16	1425.57	1318.63	1557.91
Total (mg)	1856.62	1854.85	875.22	1585.70	1104.85	1444.33	1341.07	1584.51
Theoretical Volume (ml)	1.16	1.16	0.55	0.99	0.69	0.90	0.84	0.99

Table 6-9: Amounts in mg of radionuclide sulphides formed at each operational regime - 20 µg/l, 200µg/l and 2000 µg/l of radionuclide analogues in column 3

6.3.6. Calcium concentrations

Almost no removal of Ca from the synthetic leachate was observed, similar to when 100% strength high VFA, low SO₄²⁻ type leachate was utilised. The maximum solubility of Ca at pH 8.0 is only 44 mg/l (section 6.1.5). However, removal of Ca did not occur probably due to unavailability of dissolved carbonate species (section 6.3.7).

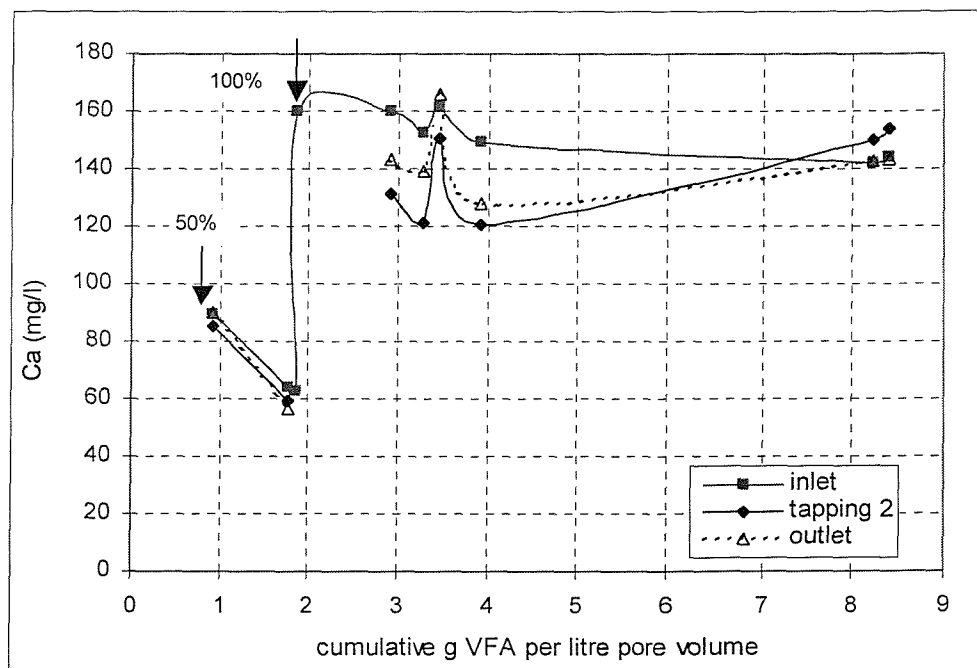


Figure 6-30: Total calcium concentrations measured at the column inlet, tapping 2 and column outlet since the introduction of 50% strength leachate in column 3.

6.3.7. Gas volume and composition

No methane production was detected in these columns because the SRB utilised all the available carbon substrate in the sulphate reduction process, as shown in Figure 6-29. Carbon dioxide and hydrogen sulphide gases were expected to be generated but were measured at very low levels in the columns headspace presumably due to their dissolution and precipitation respectively in the leachate.

CH ₄ (%)	CO ₂ (%)	N ₂ (%)	H ₂ S (%)
1.2	3.7	93.4	1.7

Table 6-10: Headspace gas composition in columns 3 and 4.

Knowing the partial pressure of the H₂S in the gas space the concentration of the dissolved H₂S species (HS⁻_{aqueous}, S²⁻_{aqueous}) can be calculated using Henry's law (section 6.1.7). The partial pressure of H₂S is 1.7/100 = 0.017 atm. The Henry's law constant for H₂S at 20°C is 483 atm (Tchobanoglous, 2002). Thus, the equilibrium molar concentration of H₂S in water is:

$$x_g = \frac{1}{483} 0.017 = 3.52 \times 10^{-5} \text{ mole gas species / mole water} \quad (\text{Eq. 5-12})$$

$$x_g = \frac{n_g}{n_g + 55.6} = 3.52 \times 10^{-5} \quad (\text{Eq. 5-13})$$

$$n_g \approx 55.6 \times 3.52 \times 10^{-5} \quad (\text{Eq. 5-14})$$

$$n_g \approx 1.9 \times 10^{-3} \text{ mole H}_2\text{S/litre} \quad (\text{Eq. 5-15})$$

At the pH measured in the experimental column the dissolved H₂S species are mainly in the form of HS⁻ (section 6.1.4., Figure 6-5) Multiplying by the molecular weigh of HS⁻ (33 g/mol), gives the saturation concentration of H₂S gas in water as 64.57 mgHS⁻/l.

Similarly the saturation concentration of CO₂ in water can be calculated, knowing that the Henry's law constant for CO₂ at 20°C is 1420 atm (Tchobanoglous, 2002).

$$x_g = \frac{1}{1420} 0.037 = 2.61 \times 10^{-5} \text{ mole gas species / mole water} \quad (\text{Eq. 5-16})$$

$$n_g \approx 55.6 \times 2.61 \times 10^{-5} = 1.4 \times 10^{-3} \text{ mole CO}_2\text{/litre} = 63.74 \text{ mg CO}_2\text{/litre} \quad (\text{Eq. 5-17})$$

At the pH range measured in the column the dissolved CO_2 species will be mainly in the form of HCO_3^- (Figure 6-31, Sawyer and McCarty, 1978).

Performing the same calculations for CH_4 ($p_g = 0.012$, $H = 37\,600$ atm) gives a saturation concentration in water of 0.283 mg CH_4 /litre.

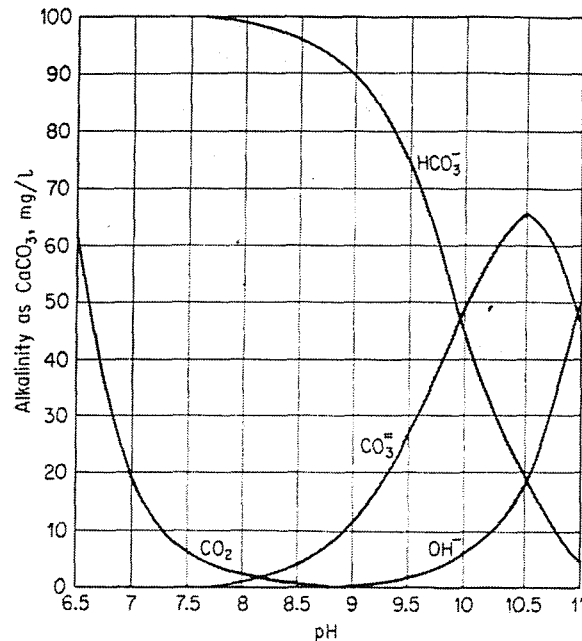


Figure 6-31: Relationship between CO_2 and the three forms of alkalinity at various pH levels (Sawyer and McCarty, 1978)

6.3.8. Changes in hydraulic conductivity

No apparent head losses with depth within the columns were observed throughout the period of operation. This was indicative that clogging was not sufficient to affect significantly the permeability of the drainage media as with columns 1 and 2 (section 5.1.8.)

6.3.9. Reduction in drainable porosity

Figure 6-32 shows the change in drainable porosity in the columns supplied with leachate with low VFAs and high SO_4^{2-} concentrations (columns 3 and 4). As mentioned earlier a test using additional metal species, referred to as radionuclide analogues, was initiated in column 3: this is marked as radionuclide analogues on Figure 6-32. The results will be discussed in two separate parts, relating to the conventional clogging test and the clogging

test with radionuclide analogues. Detailed data on the cumulative g VFA passed per litre pore volume are given in Appendix C, Table 3.

A. Conventional clogging test.

A porosity decrease of 2-3% was evident in the top sections (tappings 1-2) on Figure 6-32. This was probably caused by growth of SRB, as evidenced by the VFA and sulphate removal (see sections 5.2.1. and 5.2.3.) and the development of black deposits on the surface of the aggregate material, which are thought to be predominantly metal sulphides. The accumulation of exopolysaccharides may also have contributed to the observed reductions in the porosity. Generally little porosity change was apparent in the lower sections of the columns (tappings 2-3, 3-4, 4-5, 5-6, 6-out).

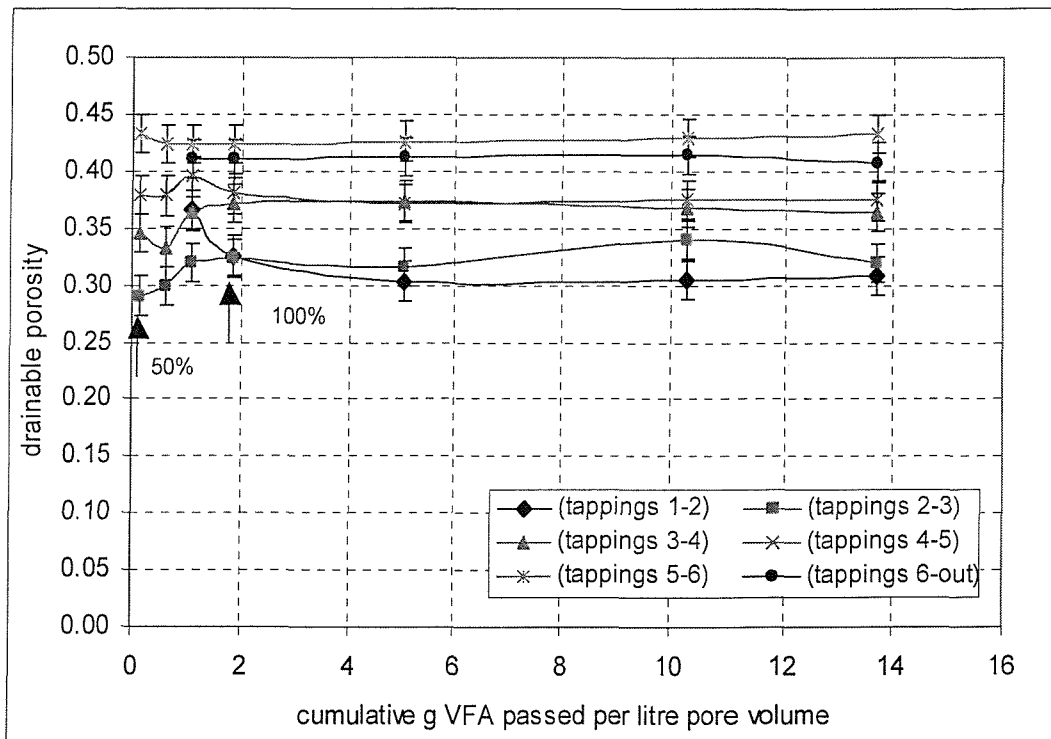


Figure 6-32: Drainable porosity in column 3.

The steady state observed after a total of 5 g VFA per unit volume had passed through the column was due to the low organic loading rate resulting in no net growth of bacterial cells as discussed in section 6.1.10.B. The precipitation of metal sulphides should have resulted in a continuous reduction of the drainable porosity. However, this was not observed because there were not sufficient metal species to react with all the available sulphide species. The amounts of FeS were small and further reductions in drainable

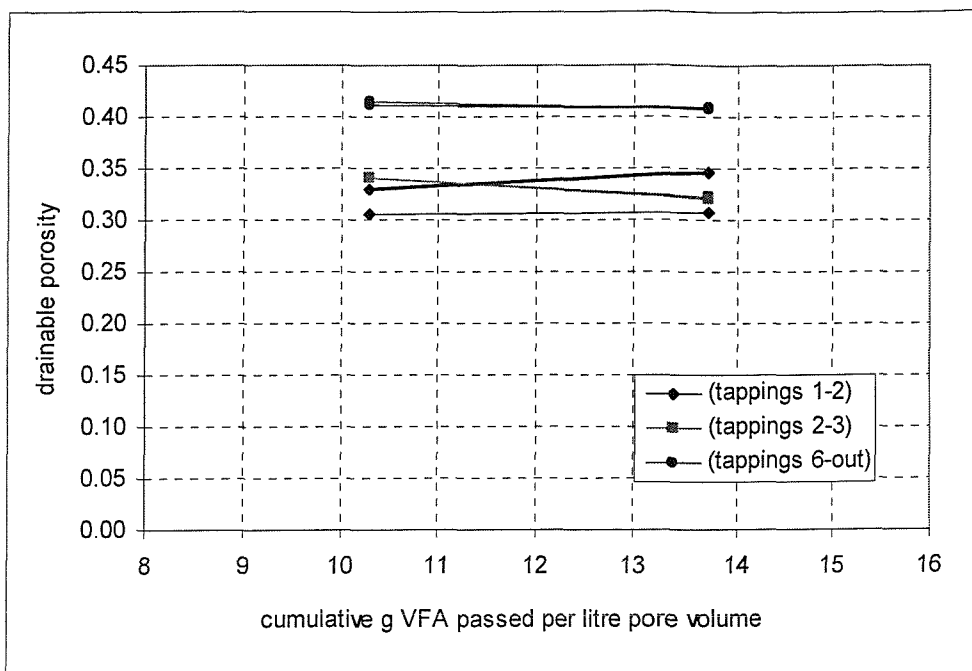
porosity could not be measured within the time scale investigated.

The measured drainable pore volumes, which were used to calculate the drainable porosity, are given in Table 6-11.

Leachate strength	25%	50%			
date	20/03/1998	29/04/1998	09/09/1998	14/12/1998	
g VFA / l.p.v.		0.152	0.625	1.101	
tapping (1-2)	2.883	2.888	2.854	1.896	
tapping (2-3)	0.733	0.754	0.775	0.83	
tapping (3-4)	2.589	2.685	2.595	2.84	
tapping (4-5)	2.911	2.95	2.944	3.075	
tapping (5-6)	1.106	1.122	1.099	1.1	
tapping (6-out)	2.132	2.132	2.132	2.132	
sum	12.354	12.531	12.399	11.873	
Leachate strength	100%				
date	20/04/1999	15/12/1999	20/09/2000	06/03/2001	27/08/2002
g VFA / l.p.v.	1.877	5.057	10.296	13.701	24.869
tapping (1-2)	1.691	1.576	1.581	1.599	0.988
tapping (2-3)	0.838	0.818	0.883	0.829	0.644
tapping (3-4)	2.897	2.913	2.865	2.835	2.614
tapping (4-5)	2.958	2.897	2.923	2.915	2.961
tapping (5-6)	1.1	1.106	1.114	1.125	1.115
tapping (6-out)	2.128	2.142	2.149	2.116	2.18
sum	11.612	11.452	11.515	11.419	10.502

Table 6-11: Drainable pore volumes on draining the column 3

The apparent reduction in the drainable porosity due to gas bubbles ranged from 2-3% of the drainable porosity in the top section to approximately zero in the lower sections, which lay within the experimental error of the method. Bubbles would not have been expected to affect these measurements because no gas production was detected in the columns (Figure 6-33).



Note:

The thicker line represents the drainable porosity measured at upward flow and the thin line represents the drainable porosity measured at draining the column.

Figure 6-33: Effect of gas bubbles in column 3

The drainable pore volumes measured on filling the column in upward flow and used to calculate the drainable porosity are given in Table 6-12.

date	20/09/2000	06/03/2001
regime	upward flow	upward flow
tapping (1-2)	1.712	1.954
tapping (2-3)	0.883	0.837
tapping (3-4)	2.815	2.794
tapping (4-5)	2.924	2.911
tapping (5-6)	1.119	1.074
tapping (6-out)	2.138	2.125
sum	11.591	11.695

Table 6-12: Drainable pore volumes on filling column 3 in upward flow

B. Clogging test with radionuclide analogues

After introducing the cocktail of radionuclide analogues (Co, Ni, Rb, Ru, Cs, Ba, Ce and Eu) in the leachate medium, the porosity of top section reduced by a further 10%, a further 6% reduction in section 2-3, 2-3% in section 3-4 and almost negligible reduction in the

bottom sections. The fast reduction in the drainable porosity in the top sections was thought to be due to the availability of extra metal species which reacted with the sulphide ions present and formed deposits of MeS. However, calculations carried out in section 6.3.5, Table 6-9 suggest that the additional metal sulphides could not have caused the measured reduction in the drainable porosity. It is difficult to speculate about the reasons causing the extensive occlusion of the pore space. It is possible that as some of the radionuclide analogues (Co, Ni) are required by the bacterial cells in trace quantities their introduction stimulated bacterial growth. However, further investigations are required to be able to draw more definite conclusions.

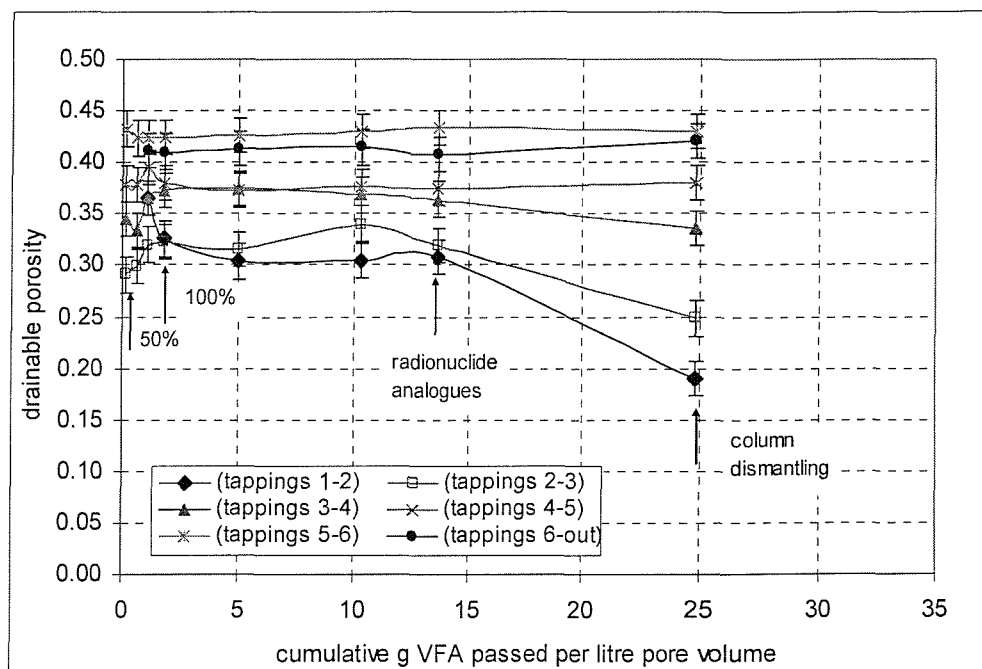


Figure 6-34: Cumulative g VFA passed per litre pore volume required to clog the top section of columns 3 and 4

6.4. Column supplied with leachate with high VFA (994 mg/l) and high SO_4^{2-} (1120 mg/l) concentrations - column 4

This section addresses the test carried out using high VFA and high SO_4^{2-} type leachate and investigates the interaction of VFA and SO_4^{2-} , by comparing the performance of columns supplied with high VFA/high SO_4^{2-} and high VFA/low SO_4^{2-} (column 4 and column 2), and columns supplied with high VFA/high SO_4^{2-} and low VFA/high SO_4^{2-} (column 4 and column 3).

6.4.1. VFA removal from the leachate

Originally, three species of VFA were supplied to column 4 – acetic ($C_2H_4O_2$), propionic ($C_3H_6O_2$) and iso-valeric acids ($C_5H_{10}O_2$). On switching from a low VFA type leachate to a high VFA type leachate, the acetate concentration was increased 4.5 times, the propionate - 19 times and the iso-valeric acid - 5 times. Furthermore, 5 additional acids were added, namely n-butyric, iso-butyric, n-valeric, n-caproic and caprylic acids. Graphs showing the removal rates of only acetic and propionic acids are shown here.

Acetic acid removal in column 4, following the introduction of high VFA type leachate, is shown in Figure 6-35. Immediately after the introduction of high VFA type leachate, the bacterial population was able to remove only 80-90 mg/l of acetate between 15 and 17 g VFA per litre pore volume, which represented only 50% of the amount removed when low VFA type leachate was used (170 mg acetate/litre). This suggests an initial inhibition/death of the acetate utilising bacteria. The measured increase in the drainable porosity (section 6.4.6, Figure 6-42) indicates that this inhibition/death probably resulted in biofilm slough and its subsequent transportation out of the column.

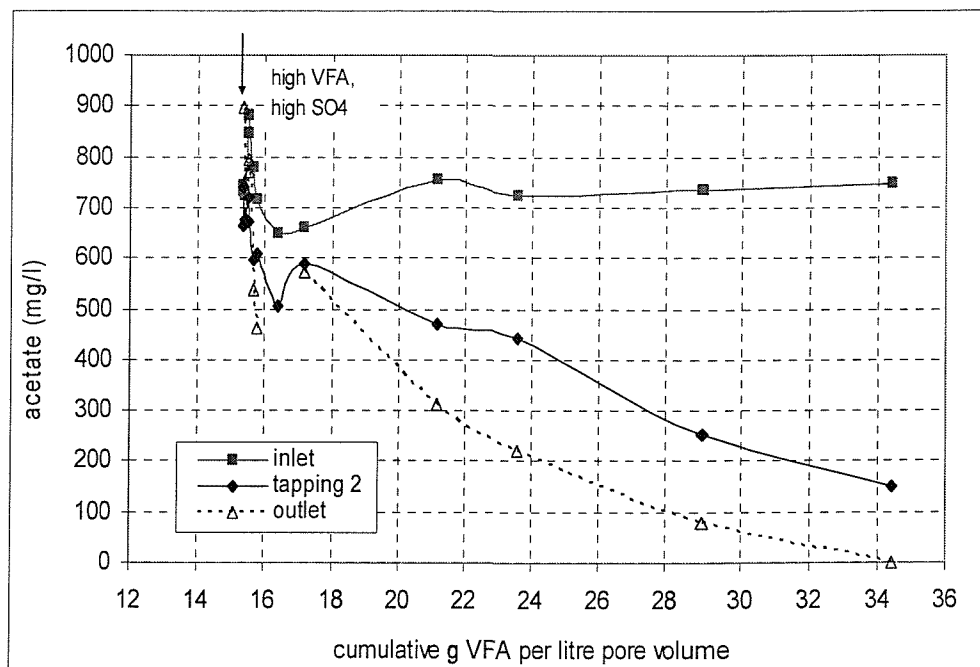


Figure 6-35: Acetic acid removal in column 4 since introduction of leachate containing high VFA, high SO_4^{2-} concentrations

It emerges that the 450% higher acetate concentrations caused extensive inhibition/death of the bacterial population which has not been observed previously on switching from 50% to 100% strength low VFA, high SO_4^{2-} type leachate. It is possible that additional inhibition/death could be due to the high hydrogen sulphide concentrations released, bearing in mind that almost all the sulphate (1100 mg/l) was reduced to sulphide (section 6.4.3.) This was followed by acclimatisation, where the bacterial population was able to remove completely the 4.5 times higher acetate concentration (770 mg acetate/litre) after 20 g VFA per litre pore volume had passed. The process of adaptation of the bacterial population is further discussed in section 6.7.

It is evident that the bacterial population in the top layer developed/adapted to the increased leachate strength, resulting in increasing nutrients removal rates and high clogging rates (Figure 6-42). The bacterial population in the lower sections (2-3 and 3-4) initially was not very active, but apparently gradually developed and was able to remove in total up to 150 mg/l of acetate. This resulted in a reduction in the drainable porosity in these sections between 20 and 30 g VFA per litre pore volume (Figure 6-42).

In theory, additional acetate would be expected to be generated by the degradation of the longer chain fatty acids introduced in the synthetic leachate:

- 81.79 mg/l of acetate from the degradation the 60 mg/l butyric acid, on the basis of Eq. 2-4.
- 24.70 mg/l acetate and 30.47 mg/l propionate from the degradation of 42 mg/l valeric acid (Eq. 2-5). The further degradation of propionate will result in the generation of an extra 24.70 mg/l of acetate (Eq. 2-6).
- 10.8 mg/l from the degradation of 7 mg/l n-caproic acid (Eq. 2-4).
- 33.4 mg/l of acetate from the degradation of 20 mg/l caprylic acid (Eq. 2-4).

The total amount of acetate that would be expected to be generated from the breakdown of the higher chain fatty acids is therefore 175.39 mg/l. Apparently the bacterial population was able to remove this extra acetate.

Figure 6-36 shows the propionic acid concentrations at different tappings along the height of the column since the introduction of high VFA, high SO_4^{2-} type leachate. The data show that the propionate utilising bacteria were able to utilise the 19 times higher propionate

concentrations. It appears that there was no inhibition as previously observed (section 6.1.1 and 6.2.1). This could be due to SRB, rather than the methanogenic bacteria, being the predominant population in this column as a result of the high SO_4^{2-} concentrations in the leachate supplied to this column. It could be that the SRB are metabolically more adaptable than the methanogenic bacteria. The variation in the inlet propionate concentrations was probably caused by bacterial activity within the storage container and the inlet tubing.

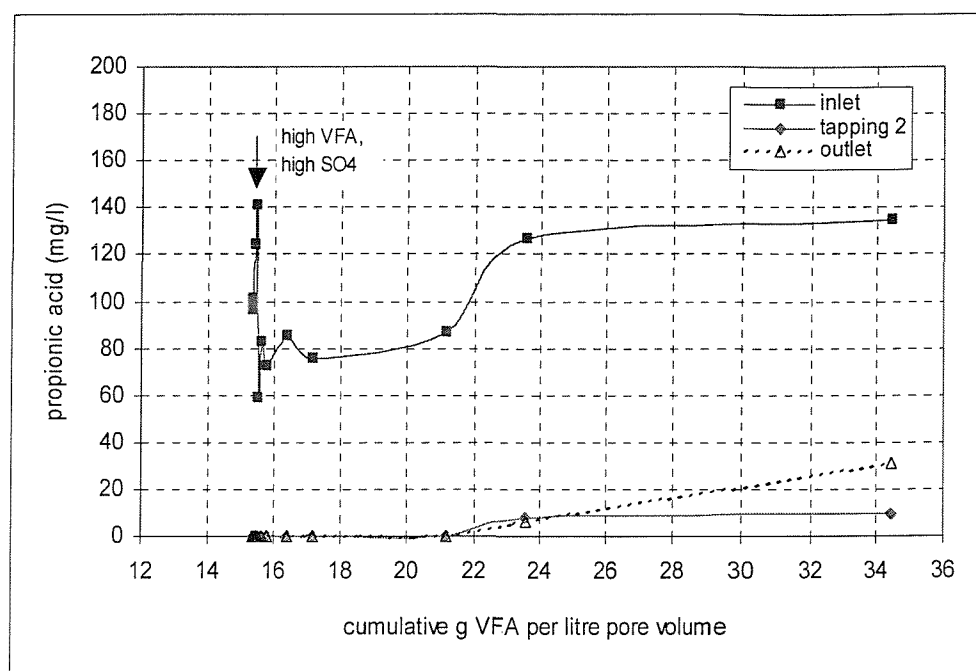


Figure 6-36: Propionic acid removal in column 4 since introduction of leachate containing high VFA, high SO_4^{2-} concentrations

6.4.2. pH measurements

Figure 6-37 shows the pH at different tappings along the column after VFA removal and sulphate reduction had reached a steady state. The measurement was carried out after a total of 55 g VFA had passed per litre pore volume. The pH of the simulated leachate medium increased between the inlet and tapping 2 as a result of the utilisation of VFA.

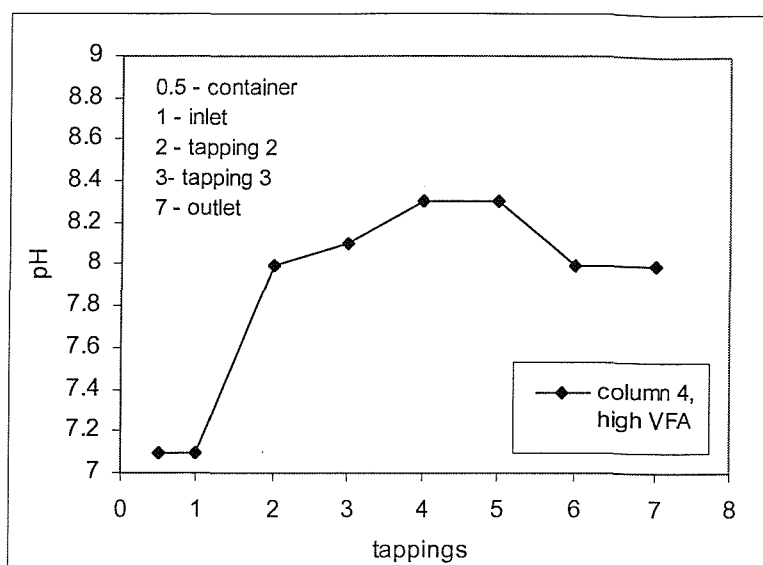


Figure 6-37: pH measurements in column 4 since introduction of high VFA, high SO_4^{2-} type leachate.

6.4.3. Sulphate reduction

Figure 6-38 shows that the sulphate concentration removed from the leachate gradually increased to reach 1100 mg/l of SO_4^{2-} reduced compared with 270 mg/l of SO_4^{2-} when low VFA, high SO_4^{2-} type leachate was supplied to column 4.

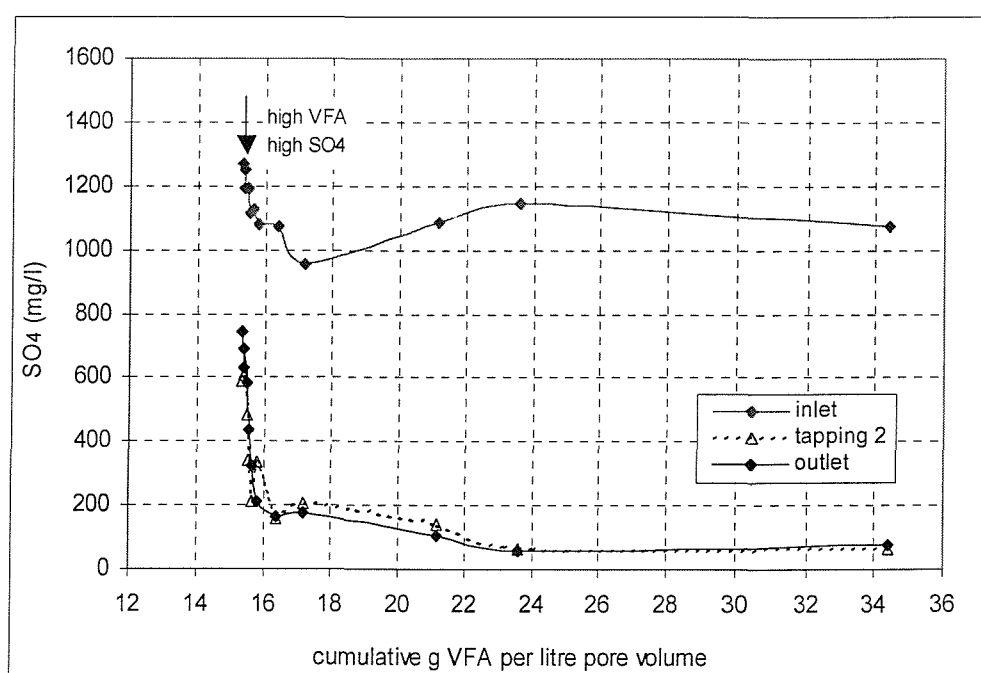


Figure 6-38: Sulphate removal in column 4 since introduction of leachate containing high VFA, high SO_4^{2-} concentrations

Although the inlet sulphate concentration remained the same, the SRB were able to reduce higher sulphate concentrations due to the higher VFA concentrations supplied with the leachate. After a total of 16 g VFA per litre pore volume had been passed through the column, 800 mg $\text{SO}_4^{2-}/\text{l}$ was reduced, which would have required 396 mg/l of acetate on the basis of theoretical stoichiometric calculations (section 6.1.4). The data in Figure 6-35 show removal of only 150 mg/l of acetate. An additional 175.39 mg/l would result from the degradation of longer chain fatty acids (section 6.4.1) but it is not obvious where the additional 71 mg/l of acetate required would have come from. After a total of 24 g VFA per litre pore volume had passed through the column, 1100 mg/l SO_4^{2-} was reduced. The acetate removed in the top section at this time was 300 mg/l and with the additional 175.39 mg acetate/l from degradation of longer chain fatty acids gave 475.39 mg/l while 682 mg/l of acetate were needed. It is not obvious where the additional 206.61 (682 mg/l - 475.39 mg/l) mg/l of acetate originated from. The data suggest that there is deficiency of acetate.

The presence of bacterial populations other than SRB is suggested by the data presented in Figure 6-35 which shows a removal of acetate between tapping 2 and the outlet and a further increase in VFA removal after a total of 24 g VFA per litre pore volume had passed when no further reduction of the sulphate concentrations was observed. Possibly this acetate was utilised by methanogenic bacteria for methane production.

Based on Figure 6-38, the total mass of sulphur removed was 271.79 g since the introduction of high VFA, high SO_4^{2-} type leachate. The dissolved iron species were not measured. If we assume a solubility similar to when low VFA, high SO_4^{2-} type leachate was utilised with an average concentration of dissolved iron of 5.2 mg/l, then the total iron removed would be 4.42 g Fe (849.6 litres passed). If we make the further assumption that the sulphur was precipitated mainly in the form of FeS then the available Fe reacted with 2.52 g S^{2-} resulting in formation of 6.96 g of FeS precipitates or 4.35 ml. This accounts for only 0.3 % of the total volume of accumulated clog material, which was 1.324 litres. If the sulphur was precipitated as FeS_2 then 5.08 g S^{2-} was required leading to the formation of 9.50 g or 5.04 ml of FeS_2 . These calculations suggests that FeS or FeS_2 precipitates made only a very small contribution to the clogging processes taking place in experimental column 4.

6.4.4. Calcium concentrations

Figure 6-39 shows that Ca removal increased gradually to 80 mg/l of Ca removed during the operation of the column with high VFA and high SO_4^{2-} type leachate. This is thought to be because the maximum solubility of Ca at pH 8.0 is only 44 mg/l (section 6.1.5).

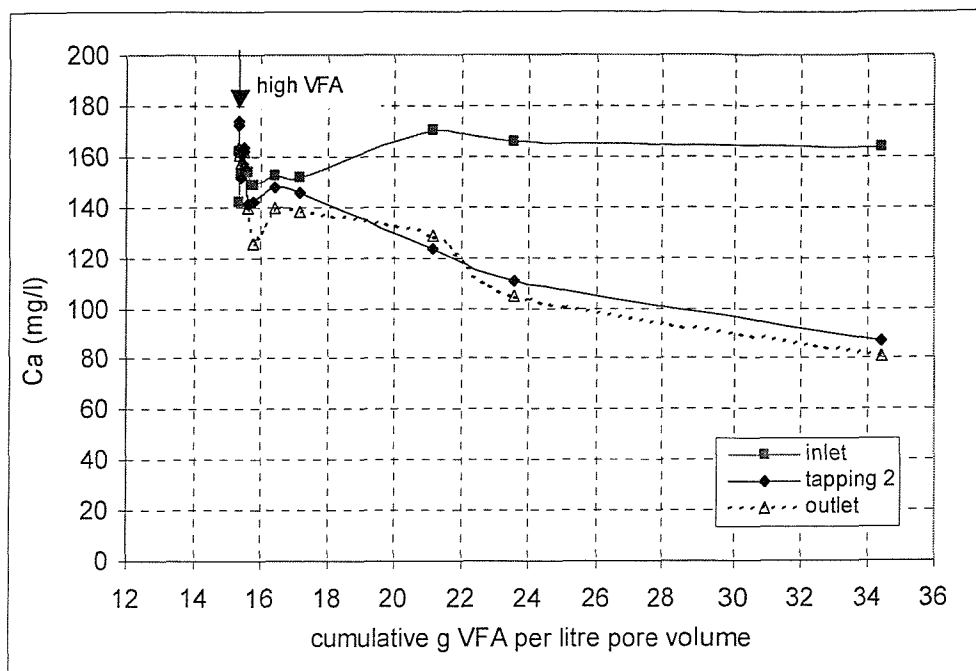


Figure 6-39: Calcium removal in column 4 since introduction of leachate containing high VFA, high SO_4^{2-} concentrations.

Based on Figure 6-39, the total mass of Ca removed was 50.98 g ($60 \text{ mg Ca/l} \times 849.6 \text{ litres}$) since introduction of 200% strength leachate, which would give rise to 127.45 g CaCO_3 . Assuming a bulk (wet) density of the clog material of 1.6 g/cm^3 gives a volume of 79.66 ml, which represents 6.0 % of the total volume of accumulated clog material 1.324 litres.

6.4.5. Gas volume

The cumulative volume of gas produced since the introduction of high VFA, high SO_4^{2-} type leachate is shown in Figure 6-40. Due to the corrosive properties of the H_2S gas produced the transducer used for measuring the headspace pressure build up started to give unreliable results and a new method for measuring the gas was adopted after 45 g VFA per litre pore volume had passed through the column (30/08/2002). The new method involved a graduated inverted pipette submerged in water. The water level in the inverted

pipette was raised by means of vacuum pump. The column gas outlet tubing was introduced beneath the inverted pipette and kept below the water level. Any gas produced bubbled through and replaced the water in the graduated pipette. The pH of the water was kept acidic (pH=4) to prevent the CO₂ and H₂S gas from dissolving (Figure 6-41).

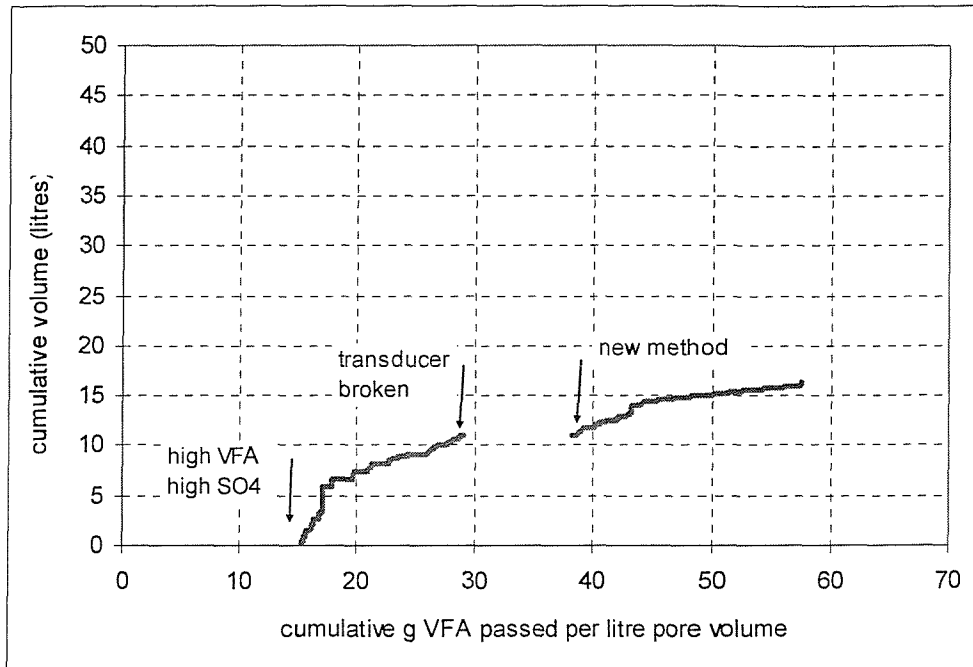


Figure 6-40: Gas production in column 4, high VFA, high SO₄²⁻- type leachate.

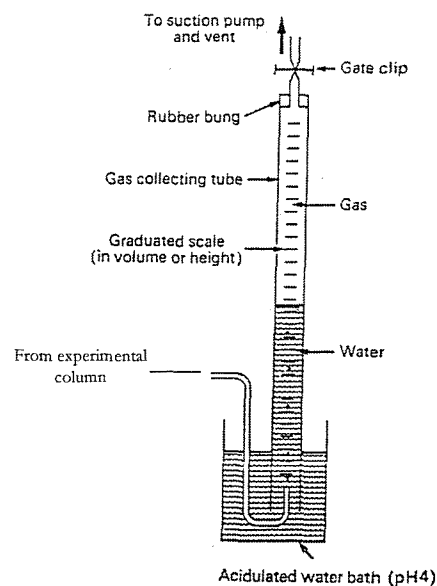


Figure 6-41: Inverted pipette method for gas measurements

Assuming that the 200 mg/l of acetate removed after a total of 24 g VFA per litre pore volume had passed when no further removal of SO_4^{2-} was observed (Figure 6-35) were utilised by methanogenic bacteria gives theoretical production volumes of 22.44 litres of CH_4 and 22.44 litres of CO_2 . The difference between the measured and above calculated values is probably due to the fact that some carbon is utilised by the bacteria for cell growth and polysaccharide production (discussed in section 6.8 and 5.6.) rather than gas generation, and that some is dissolved in the leachate or precipitated as CaCO_3 . In addition, H_2S gas was produced.

6.4.6. Reduction in drainable porosity

The DPV data indicate an initial increase of the drainable porosity of up to 5% in the top column section (tappings 1-2, Figure 6-42) following the introduction of the high VFA, high SO_4^{2-} type leachate. This was most probably due to a shock loading of VFA as a result of the switch from a low VFA to a high VFA type leachate involving a six fold increase in the total VFA concentration. This shock loading may have initially caused the inhibition and death of the bacterial biofilm in the top section followed by its shearing and transportation towards the bottom sections and out of the column. This phenomenon occurred only in the very top section of the column where the bacterial population was most likely to be most numerous and active. A rapid reduction of the drainable porosity of up to 12% followed as a result of accumulation of gas bubbles (Figure 6-42), bacterial re-growth as suggested by the VFA removal (section 6.4.1.) and gas generation (section 6.4.5.) and deposition of low solubility inorganic salts (CaCO_3) indicated by the removal of Ca concentration from the leachate (section 6.4.4.)

Reductions in the drainable porosity of up to 7-8% were measured in the middle sections (2-3, 3-4) of the column. No reduction in the drainable porosity was measured at the bottom sections, probably due to lack of nutrients reaching these sections. Detailed data on the cumulative g VFA passed per litre pore volume are given in Appendix C, Table 4.

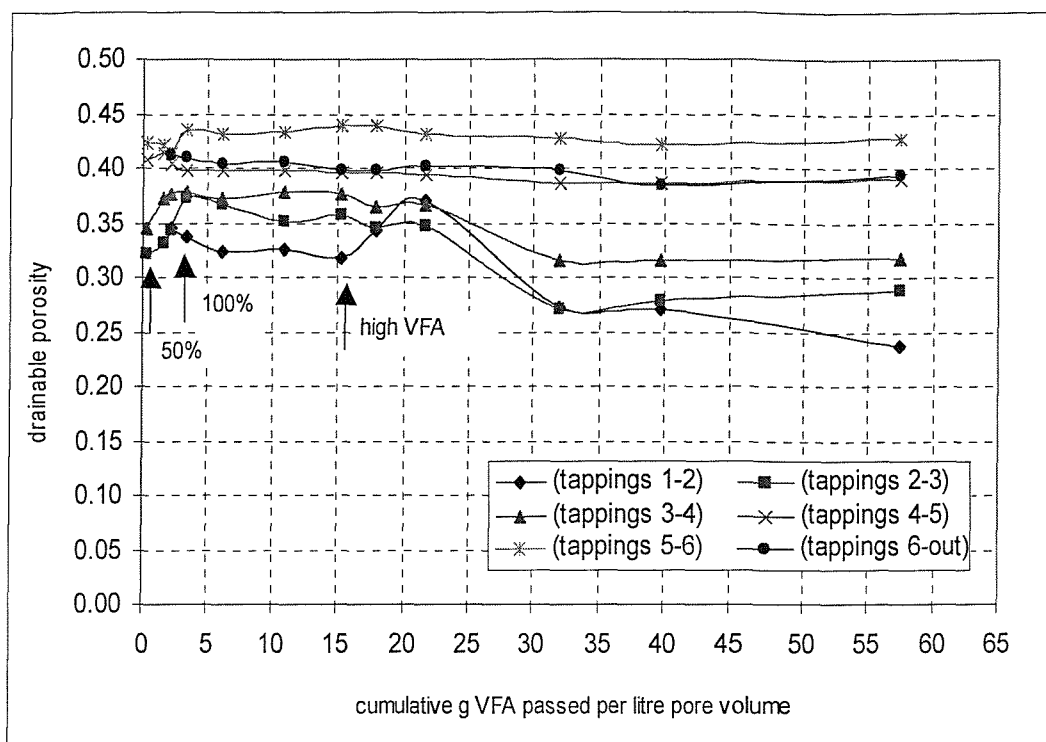


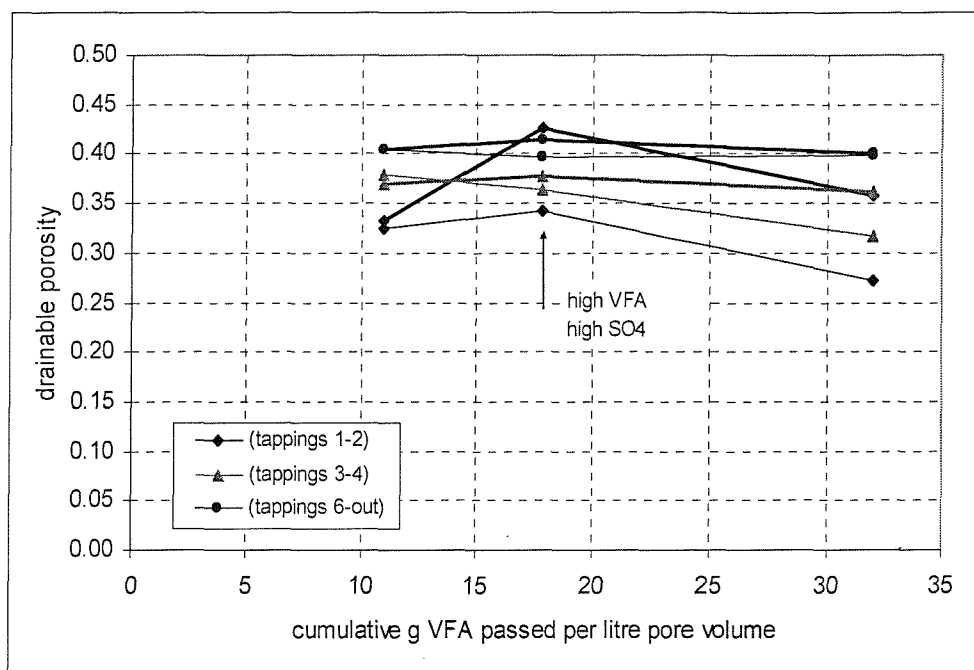
Figure 6-42: Reduction in drainable porosity in column 4 since introduction of leachate containing high VFA, high SO_4^{2-} concentrations

The measured drainable pore volumes, used to calculate the drainable porosity, are given in Table 6-13.

Leach. strength	25%	50%			100%		
date	20/03/1998	30/04/1998	09/09/1998	15/12/1998	04/05/1999	16/12/1999	22/09/2000
g VFA / l.p.v.		0.3239	1.569	2.1673	3.2725	6.1573	10.9387
tapping (1-2)	2.689	2.625	2.99	1.786	1.747	1.675	1.689
tapping (2-3)	0.977	0.835	0.86	0.89	0.964	0.952	0.91
tapping (3-4)	2.514	2.687	2.905	2.93	2.945	2.896	2.946
tapping (4-5)	3.178	3.177	3.215	3.14	3.093	3.093	3.094
tapping (5-6)	1.086	1.1	1.096	1.074	1.131	1.119	1.125
tapping (6-out)	2.14	2.14	2.14	2.14	2.126	2.096	2.101
sum	12.584	12.564	13.206	11.96	12.006	11.831	11.865
Leach. strength	High VFA						
date	30/05/2001	04/09/2001	15/11/2001	11/04/2002	04/07/2002	10/01/2003	
g VFA / l.p.v.	15.3269	17.8817	21.6267	32.0344	39.6968	57.4057	
tapping (1-2)	1.646	1.779	1.926	1.416	1.408	1.227	
tapping (2-3)	0.927	0.894	0.9	0.703	0.724	0.748	
tapping (3-4)	2.933	2.834	2.852	2.461	2.453	2.464	
tapping (4-5)	3.084	3.077	3.065	3.006	3.006	3.03	
tapping (5-6)	1.141	1.139	1.12	1.107	1.095	1.107	
tapping (6-out)	2.067	2.062	2.083	2.066	1.998	2.046	
sum	11.798	11.785	11.946	10.759	10.684	10.622	

Table 6-13: Drainable pore volumes on draining column 4

Gas bubbles made the highest contribution to the drainable porosity reduction (8%) in the upper most column section (Figure 6-43). In addition, the 8% reduction in the drainable porosity between total 17 and 32 g VFA per litre pore volume had passed through the column was mainly due to microbial growth, polysaccharide accumulation and precipitation of inorganic salts as suggested by the parallel curves for the drainable porosity at draining and filling up the column from the bottom up. A smaller absolute reduction in drainable porosity due to gas bubbles (2-3%) was observed in the middle column section (3-4). The reduction in drainable porosity measured there (section 3-4), at draining the column between total 17 and 32 g VFA per litre pore volume had passed through the column, was mainly due to gas, as suggested by the constant value for the porosity on filling the column from the bottom up.



Note: The thicker line represents the drainable porosity measured at upward flow and the thin line represents the drainable porosity measured at draining the column.

Figure 6-43: Effect of gas bubbles on the drainable porosity in column 4, high VFA, high SO_4^{2-} type leachate

Similarly, the drainable pore volumes measured on filling the column in upward flow and used to calculate the drainable porosity are given in Table 6-14.

date	22/09/2000	04/09/2001	11/04/2002
regime	upward flow	upward flow	upward flow
tapping (1-2)	1.725	2.309	1.861
tapping (2-3)	0.903	0.874	0.984
tapping (3-4)	2.875	2.931	2.822
tapping (4-5)	3.075	3.067	3.05
tapping (5-6)	1.116	1.094	1.087
tapping (6-out)	2.103	2.148	2.082
sum	11.797	12.423	11.886

Table 6-14: Drainable pore volumes on filling column 4 in upward flow

6.4.7. Comparison with the columns supplied with high VFA/low SO_4^{2-} and low VFA/high SO_4^{2-} type leachate.

This section addresses the test carried out using high VFA and high SO_4^{2-} type leachate and investigates the interaction of VFA and SO_4^{2-} , by comparing the performance of columns supplied with high VFA/high SO_4^{2-} and high VFA/low SO_4^{2-} (column 4 and column 2), and columns supplied with high VFA/high SO_4^{2-} and low VFA/high SO_4^{2-} (column 4 and column 3).

A. High VFA and high SO_4^{2-} (column 4) versus high VFA and low SO_4^{2-} (column 2) type leachate.

Comparison between the columns supplied with high VFA, high SO_4^{2-} (column 4) and high VFA, low SO_4^{2-} (column 2) type leachate allowed investigation of the effect of SO_4^{2-} on the clogging process. Even though the higher organic content of the leachate resulted in a greater concentration of SO_4^{2-} being reduced to sulphide (S^{2-}) (section 6.4.3), the volume of MeS deposited was small (4.35 ml) because there were not enough dissolved metal species in the leachate to react with the available sulphur. That is why the contribution of the MeS to the clogging process is not significant under the operational conditions employed.

Pages 152 is
missing from
volume

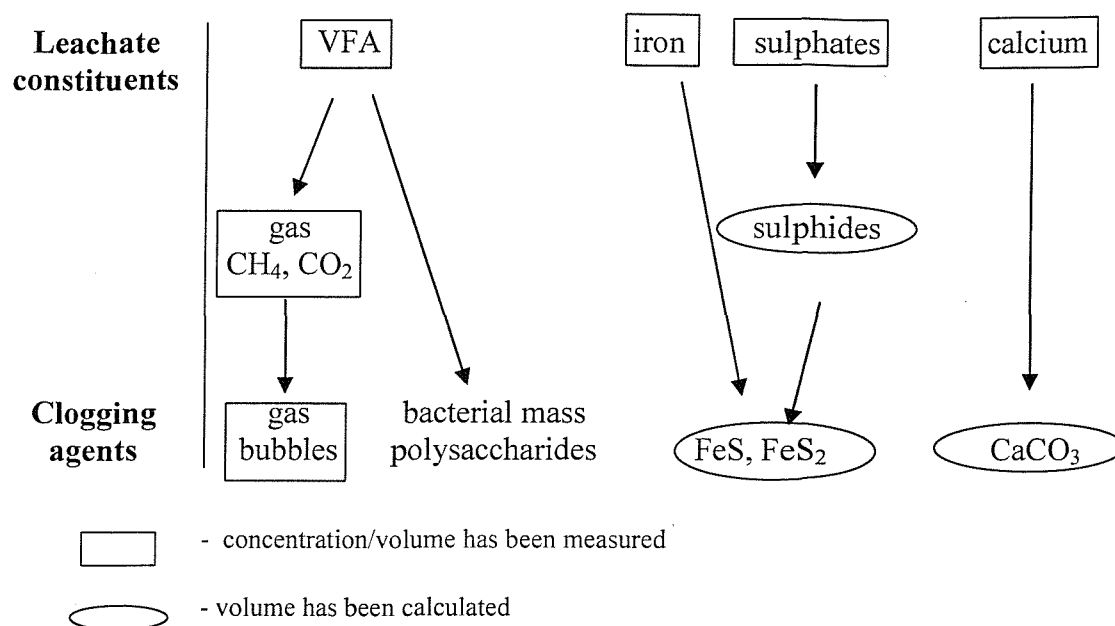


Figure 6-44: Schematic diagram showing the measured and calculated species

	Fe ²⁺	SO ₄ ²⁻	Ca ²⁺
High VFA, low SO₄²⁻, 100%			
Concentration in the leachate (mg/l)	8.25	18.00 (as SO ₄ ²⁻)	170.00
Concentration removed (mg/l)	8.25	18.00 (as SO ₄ ²⁻)	-
Litres passed	1605.60	1605.60	1605.60
Total amount removed (g)	13.25 section 6.1.3	9.30 (as S ²⁻) section 6.1.4	- section 6.1.5
High VFA, low SO₄²⁻, 200%			
Concentration in the leachate (mg/l)	8.25	39.00 (as SO ₄ ²⁻)	340.00
Concentration removed (mg/l)	8.25	39.00 (as SO ₄ ²⁻)	70.00
Litres passed	865.44	865.44	865.44
Total amount removed (g)	7.13 section 6.2.2	11.27 (as S ²⁻) section 6.2.2	60.52 section 6.2.3
Low VFA, high SO₄²⁻			
Concentration in the leachate (mg/l)	5.20	1120.00	160.00
Concentration removed (mg/l)	5.20	270.00	-
Litres passed	1664.64	1664.64	1664.64
Total amount removed (g)	8.66 section 6.3.3	100.72 section 6.3.5	- section 6.3.6
High VFA, high SO₄²⁻			
Concentration in the leachate (mg/l)	8.25	1120.00	160.00
Concentration removed (mg/l)	8.25	1100.00	60.00
Litres passed	849.60	849.60	849.60
Total amount removed (g)	4.42 section 6.4.3	271.79 section 6.4.3	50.58 section 6.4.4

Table 6-15: Concentration of inorganic constituents and amounts removed from the leachate.

6.5.2. Measured organic constituents

Table 6-16 summarises the mass balance between the carbon that has entered the column and the carbon that has escaped in the form of gas, dissolved gas species or deposited as CaCO₃. The difference between these two values gives the carbon trapped as organic clog material.

	Carbon in the leachate (as acetate and propionate)	Gas escaped in the form of gas or dissolved in the leachate	C as CaCO ₃	Carbon trapped as organic clog material (C _{leachate} - C _{gas} - C _{CaCO₃})
	measured	measured/calculated	calculated	calculated
High VFA, low SO₄²⁻, 100%				
Concentration in the leachate (mg/l)	354.22	323.19 l CH ₄ = 13.40 moles = 160.79 g C 109.53 l CO ₂ = 4.54 moles = 54.49 g C (section 5.1.7.)		
Concentration removed (mg/l)	see appendix C			
Litres passed	1605.60			
Total amount removed (g)	537.37 g C see appendix C	215.28 g C		322.09 g C
High VFA, low SO₄²⁻, 200%				
Concentration in the leachate (mg/l)	708.43	438.58 litres = (section 5.2.4.) 18.18 moles =	151.30 mg CaCO ₃ × 12 C / 100 CaCO ₃ (section 5.2.3.) =	
Concentration removed (mg/l)	see appendix C			
Litres passed	865.44			
Total amount removed (g)	593.61 g C see appendix C	218.20 g C*	18.15 g C	357.26 g C*
Low VFA, high SO₄²⁻				
Concentration in the leachate (mg/l)	68.00	1.4 × 10 ⁻³ mole CO ₂ /litre × 1664.64 = 2.33 mole (section 6.3.7) =		
Concentration removed (mg/l)	see appendix C			
Litres passed	1664.64			
Total amount removed (g)	113.65 g C see appendix C	27.96 g C		85.69 g C
High VFA, high SO₄²⁻				
Concentration in the leachate (mg/l)	354.22	15 litres gas = 0.62 moles (section 6.4.5) =	127.45 mg CaCO ₃ × 12 C / 100 CaCO ₃ (section 5.4.5.) =	
Concentration removed (mg/l)	see appendix C			
Litres passed	849.60			
Total amount removed (g)	295.48 g C see appendix C	7.46 g C*	15.29 g C	272.73 g C*

Note: * - The dissolved species of CO₂ and CH₄ were not taken into account because the gas composition was not measured.

Table 6-16: Summary of changes in concentration of the organic constituents

6.5.3. Volume of clog material

Table 6-17 summarises the contribution of each of the clogging agents to the total amount of clog material.

Operational regime	Total litres passed	Total C passed (g)	V_{clog} since the start of the operational regime	$V_{\text{FeS}}/V_{\text{FeS}_2}$	V_{CaCO_3}	V_{gas} accumulated during the operational regime	Volume of organic clog ($V_{\text{clog}} - V_{\text{FeS}} - V_{\text{CaCO}_3} - V_{\text{gas}}$)	Volume of gas before the start of the operational regime	Total volume of clog material
			measured	calculated	calculated	measured	calculated	measured	
High VFA, low SO_4^{2-} (100%) (Column 2)	1605.60	537.37	435 ml	13.04 ml / 10.88 ml	-	97 ml	324.96 ml	1160 ml	1595 ml
High VFA, low SO_4^{2-} (200%) (Column 1)	865.44	593.61*	340 ml	7.03 ml / 9.57 ml	94.56 ml	-	238.41 ml	1127 ml	1467 ml
Low VFA, high SO_4^{2-} (Column 3)	1664.64	113.65	193 ml	8.52 ml / 11.63 ml	-	76 ml	117.00 ml	-	193 ml
High VFA, high SO_4^{2-} (Column 4)	849.60	295.48*	1324 ml	4.35 ml / 5.04 ml	79.66 ml	1127 ml	112.99 ml	-	1324 ml

Note: * - The actual value could be less than the calculated because the dissolved species of CO_2 and CH_4 were not subtracted as gas composition data were not available.
 - Density of clog material - 1.6 g/cm^3 .

Table 6-17: Volumes of the clog material

6.5.4. Comparison between the different operational regimes

Generally the reduction in the drainable porosity in all the columns was greater in the top sections (tappings 1-4) than further down. This reduction is considered to be due to microbiological growth, accumulation of exopolysaccharides and precipitates, and entrapment of gas bubbles. Bacterial populations almost certainly did not develop in the lower sections (tappings 4-outlet) due to depletion of organic nutrients or other essential growth nutrient, resulting in almost no reduction in drainable porosity and no gas production.

The rate of clogging is directly proportional to the VFA content of the leachate. This was suggested by the 15% reduction of the drainable porosity in the column supplied with high VFA and low SO_4^{2-} content leachate (8% since introduction of 100% strength + additional 7% due to accumulation of gas bubbles) compared with only 5% for the columns supplied with low VFA and high SO_4^{2-} content leachate after comparable litres of leachate had passed. This hypothesis is further supported when comparing the performance of columns supplied with high VFA/high SO_4^{2-} and low VFA/high SO_4^{2-} type leachate (section 6.4.7.B).

The chemical clogging due to precipitation of MeS was not significant in the short term as suggested by the calculated volumes of MeS, which were negligible compared with the total volume of the clog material in all the columns. This was because there were not sufficient metal species to react with the available sulphide concentrations and form precipitates of MeS. When the metal content was increased by introduction of radionuclide analogues, a more rapid reduction in the drainable porosity occurred. Although this reduction could not be simply explained with accumulation of MeS and additional experiments are required to further investigate the effect of the radionuclide analogues on the clogging.

Gas bubbles decreased the size of the water conducting pores and thus acted as a clogging agent. The gas bubbles had a similar contribution to the clogging when 100% and 200% strength leachate was supplied to the columns despite the larger volume of gas produced when 200% strength leachate was supplied. It could be that the column matrix became saturated with gas and any extra gas bubbles merged together and escaped into the column headspace. This implies that a steady state of the accumulation of gas bubbles occurred.

Gas bubbles did not affect the measurements in the lower sections of the column (tappings 4-out). This was to be expected because no microbial activity and consequently no gas production were detected in these sections.

The reduction in the drainable porosity reached a steady state when 100% high VFA/low SO_4^{2-} and low VFA/high SO_4^{2-} type leachate was utilised. These operational conditions involved low organic and inorganic loading where the calcium concentrations were below the aqueous solubility limit for CaCO_3 . The clogging due to bacterial growth and accumulation of gas bubbles reached a steady state where there was equilibrium between reproduction and death and a balance between the gas bubbles generated and released into the column headspace. The effect of the chemical clogging was negligible and although continual accumulation of MeS may lead to porosity reduction in the long-term, its effect in the short-term was minor.

6.6. Summary of results regarding the competition between SRB and methanogenic bacteria.

The literature review showed that, there was uncertainty regarding the competition between SRB and methanogenic bacteria when acetate was utilised. The experiments described in this thesis showed that the sulphate reduction preceded the methanogenesis when acetate is used as organic substrate. In the columns supplied with leachate containing low VFA but high SO_4^{2-} concentrations only 25% of the total sulphate supplied to the columns was removed. There was insufficient organic substrate for the SRB to reduce all the sulphate supplied and for the methanogenic bacteria to produce methane. When high VFA, high SO_4^{2-} type leachate was used 99% of the sulphate supplied with the leachate was reduced due to the higher concentrations of acetate available for the SRB. The sulphate reduction was confined to the top section where the bacterial populations were most active.

6.7. Summary of results regarding the adaptation of the bacterial populations to the increased nutrient concentrations

The bacterial populations in all the columns were inhibited on increasing the leachate strength from 50% to 100% and from 100% to 200% leachate strength. The SRB are

metabolically more adaptable than the methanogenic bacteria as suggested by the shorter adaptation period of only 0.5 g VFA per litre pore volume required to utilise the doubled acetate concentrations on switching from 50% to 100% low VFA, high SO_4^{2-} type leachate compared with 14 g VFA per litre pore volume for the methanogenic bacteria (high VFA, low SO_4^{2-} type leachate) (Table 6-18).

Operational regime	Acetate length of adaptation period (conc. increase from to)	Propionate length of adaptation period (conc. increase from to)	Type of bacteria present
High VFA, low SO_4^{2-} (50% to 100%)	14 g VFA per l.p.v. (from 385 mg/l to 770 mg/l)	more than 14 g VFA per l.p.v. (from 47.5 mg/l to 95 mg/l)	mainly methanogenic and acetogenic bacteria
High VFA, low SO_4^{2-} (100% to 200%)	7 g VFA per l.p.v. (from 770 mg/l to 1540 mg/l)	7 g VFA per l.p.v. (from 95 mg/l to 190 mg/l)	mainly methanogenic and acetogenic bacteria
Low VFA, high SO_4^{2-} (50% to 100%)	0.5 g VFA per l.p.v. (from 85 mg/l to 170 mg/l)	No inhibition (from 2.5 mg/l to 5 mg/l)	mainly sulphate-reducing bacteria
High VFA, high SO_4^{2-} (low VFA to high VFA)	20g VFA per l.p.v. (from 170 mg/l to 770 mg/l)	No inhibition (from 5 mg/l to 95 mg/l)	mainly sulphate-reducing bacteria

Note: l.p.v. – litre pore volume

Table 6-18: Adaptation of the bacterial population

An inhibition of the SRB occurred when the leachate type was changed from low to high VFA type. This is suggested by the considerably long adaptation period for the acetate utilizing SRB, which lasted 20 g VFA per litre pore volume. This could have been as a result of the inhibitory effect of the high concentration of hydrogen sulphide bearing in mind that almost all the sulphate (1100 mg/l) was reduced to sulphide. However, the fact that the propionate utilizing SRB were not inhibited indicates that a substrate accelerated death caused by the high acetate concentrations could have been the cause of the inhibition.

6.8. Comparison of the clogging rates with data from other researchers

The data reported in section 6.1 and 6.3 of this thesis are compared with those reported in the literature. To facilitate comparison only saturated conditions and columns packed with 6 mm particle sizes were considered. Two authors fulfilled these conditions – Rowe *et al.*, (2000a, 2001b), who carried out tests using real and synthetic leachate, and Paksy *et al.* (1998). Experimental details and leachate characteristics are shown in Table 6-19.

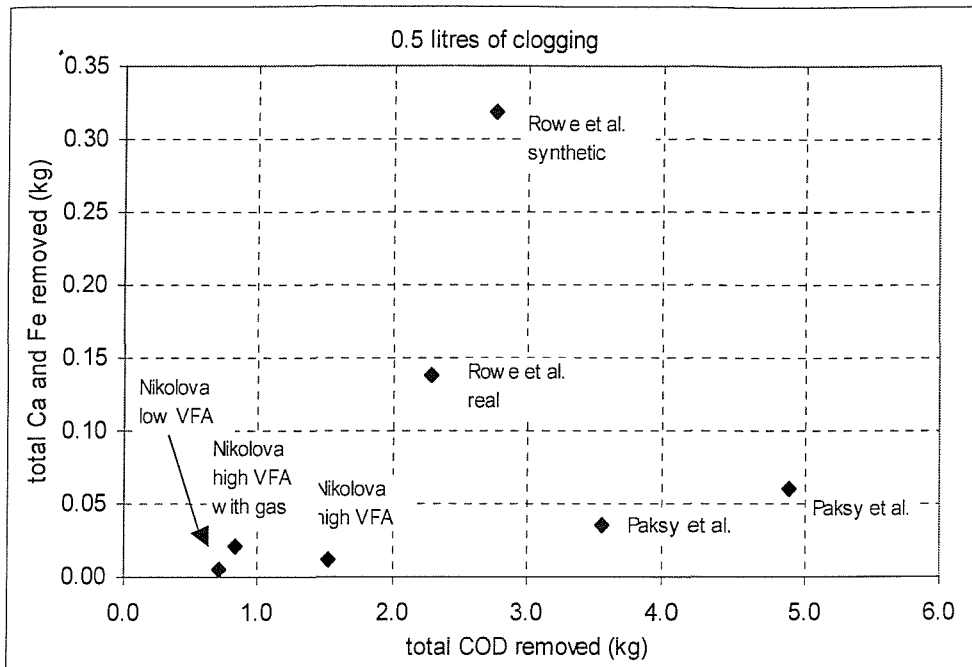
	Rowe <i>et al.</i> real	Rowe <i>et al.</i> synt.	Paksy <i>et al.</i>	Paksy <i>et al.</i>	Nikolova low VFA (100%)	Nikolova high VFA (100%)
Particle size (mm)	6	6	5-10	5-10	6	6
Bed dimensions i.d. × height (cm)	5×59.1	5×63.7	22×91	23×60	25.7×60	25×60
Cross sectional area of the column (cm ²)	19.63	19.63	380.13	415.48	518.75	518.75
Volume of the column (litres)	1.160	1.25	34.59	24.93	15.56	15.56
Initial pore volume	0.441	0.475	12.43	10.55	11.28	11.28
Flow rate (litre/day)	1	1	1.15	1.28	1.44	1.44
Litres passed	176	327.20	587.46	479.58	629.28	627.84
Volume of the clog material (litres)	0.306	0.300	1.164	0.556	0.163	0.228
Period over which it was observed	259	355	510	409	437	436
COD in leachate (mg/l)	10756	16860	20012	20211	205	1227
Total COD removed (kg)	1.40	1.65	8.29	5.44	0.129	0.693
Organic loading rate by volume (mgCOD/cm³.day)	6.859	4.044	0.470	0.582	0.027	0.102
Organic loading rate by pore volume (mgCOD/cm³.day)	18.059	10.647	1.307	1.374	0.037	0.141
Ca concentration in the leachate mg/l	536	1040	200	200	160	170
Ca removed in mg/l	396.64	582.4	100	100	0	0
Fe concentration in the leachate mg/l	205	0.735	100	100	5.2	8.25
Fe removed in mg/l	82	0.294	40	40	5.2	8.25
Total inorganic passed (Ca and Fe) (kg)	0.08	0.19	0.08	0.07	0.0046	0.0051
Total inorganic loading rate by volume (mg/cm³.day)	0.412	0.466	0.005	0.007	0.0007	0.0008
Total inorganic loading rate by pore volume (mg/cm³.day)	1.086	1.227	0.013	0.017	0.0009	0.0011
Hydraulic surface loading (ml/cm ² .day)	50.93	50.93	3.03	3.08	2.78	2.78
Hydraulic volumetric loading (ml/cm ³ .day)	0.862	0.800	0.033	0.051	0.093	0.093
Hydraulic pore volumetric loading (ml/cm ³ .day)	2.269	2.105	0.093	0.121	0.128	0.128

Note: Rowe real stands for experiments carried out using real leachate, Rowe synt. – synthetic leachate, Nikolova low – low VFA, high SO₄²⁻ type leachate, Nikolova high – high VFA, low SO₄²⁻ type leachate.

Table 6-19: Comparison between the leachate compositions, organic and inorganic load employed by Rowe *et al.* (2000a), Paksy *et al.* (1999) and this thesis.

Table 6-19 shows that the lowest organic and inorganic loading rates resulted from the experiments presented in this thesis. The organic loading rate was 10 times lower than that used by Paksy *et al.* (1999) and 100 times lower than Rowe *et al.* (2000a). It is therefore not surprising that the microbiological clogging in these tests reached a steady state where there was no significant further reduction in porosity.

Figure 6-45 shows the amount of COD and inorganic substances required to obtain 0.5 litres of clogging in each of the different studies. The data suggest that the column tests described in this thesis accumulated 0.5 litres of clog material after relatively lower quantities of COD and inorganic substances had passed.



Note: **Nikolova high VFA** – refers to columns 1 and 2, supplied with leachate with high VFA and low sulphate concentrations and the volume of the gas bubbles was subtracted from the volume of the clog material, **Nikolova high VFA with gas** – refers again to columns 1 and 2 and the effect of the gas was taken into account, **Nikolova low VFA** – refers to columns 3 and 4, supplied with leachate with low VFA and high sulphate concentrations.

Figure 6-45: Amount of COD and inorganic substances needed to obtain 0.5 litres of clogging.

To investigate this apparent discrepancy a more careful consideration of the nutrient requirements for bacterial growth, namely the presence of carbon, nitrogen and phosphorus, is required. Typical values for the composition of prokaryotic cells are: 50% carbon, 22% oxygen, 12% nitrogen, 9% hydrogen and 2% phosphorus (Tchobanoglous *et al.*, 2002). On this basis the optimal ratio between carbon, nitrogen and phosphorus for cell growth would be 100:24:4. However, data reported by Rowe *et al.* (2002b) revealed C:N:P ratio measured in the clog material of 100:9:2. Other researchers have reported C:N:P values for heterotrophic organisms equal to 100:10:1 (Momba *et al.*, 2000). The data in Table 6-20 show that the C:N:P ratio for the two types of leachate supplied to the experimental columns described in this thesis are significantly below the lowest reported values, suggesting that the bacterial population is nitrogen and phosphorus limited.

When an essential microbial growth nutrient like nitrogen or phosphorus is limiting, bacterial cells tend to produce and accumulate polysaccharides, which requires the availability of only carbon, hydrogen and oxygen. In such a system the number of

bacterial cells per unit volume would be considerably lower, resulting in the production of less final degradation products such as CO₂ and CH₄ gas. This would imply that less carbon would be lost in the form of gas and more carbon will become trapped in the form of polysaccharides, causing clogging after the passage of relatively smaller quantities of organic substances. Measurement of the polysaccharide content in the material retrieved from the column on dismantling was carried out to validate this hypothesis (chapter 6).

Leachate type	Carbon (g)	Nitrogen (g)	Phosphorus (g)	C:N:P
Leachate A	429.2	4.5	0	100 : 1 : 0
Leachate B	74.5	3.6	0	100 : 4.8 : 0

Table 6-20: Ratio between carbon, nitrogen and phosphorus in the leachate medium used in this study.

A. Effect of gas bubbles

The contribution of the gas bubbles to the clogging process has not been recognised by either of the researchers who carried out experimental studies on the clogging of the leachate drainage systems. Rowe *et al.* (2000a) carried out their experiments in upward hydraulic flow conditions where gas bubbles will tend to escape and will not contribute to the clogging process. Paksy *et al.* (1998) mentioned the presence of gas but referred to it as a shortcoming of their method of drainable porosity measurement. They quantified the effect of gas by comparing the drainable porosity in a non-gassing column, which was not supplied with leachate for two weeks, with a column after nitrogen gas had been bubbled through the base for a period of 24h (Paksy *et al.*, 1998). The measurement showed that the presence of gas bubbles could result in an average error of 0.57% (maximum 1.12%) in the measured drainable porosity. However, the non-gassing column cannot be considered as a control column because it may already have had gas trapped, making the comparison not very reliable. In addition, it could be that no significant accumulation of gas bubbles occurred in the tests carried out by Paksy *et al.* (1998) because of the vigorous gas production expected as a result of the relatively high organic content of their leachate. Large quantities of small bubbles will tend to merge together to form bigger ones and escape into the headspace. However, the gas bubbles could act as a clogging agent and contribute significantly to the measured reduction in the porosity in the experiments as described in this thesis (sections 6.1.10, 6.2.6 and 6.4.6). It could be that under low gas generation rates, due to the small organic content of the leachate, relatively small

quantities of gas bubbles would be generated which do not merge together and would remain trapped in the column.

6.9. Dismantling of Column 3

This section provides data on the dismantling of columns 3 and on the chemical and microbiological composition of the clog material retrieved from these columns.

6.9.1. Dismantling procedure

The aims of the column dismantling were to obtain undisturbed aggregate samples from the experimental column and gain information on the chemical and microbiological composition of the clog material. The main challenge at the initial stage of column dismantling was to achieve segregation between the aggregate sections along the height of the column. The method for column dismantling involved unbolting the bottom platen and lifting the column, section by section with the aid of a portable crane (Figure 6-46a). A metal sheet with a diameter slightly larger than the column, was introduced after each lift to prevent the remaining aggregate escaping the column and to separate the different aggregate sections (Figure 6-46b).

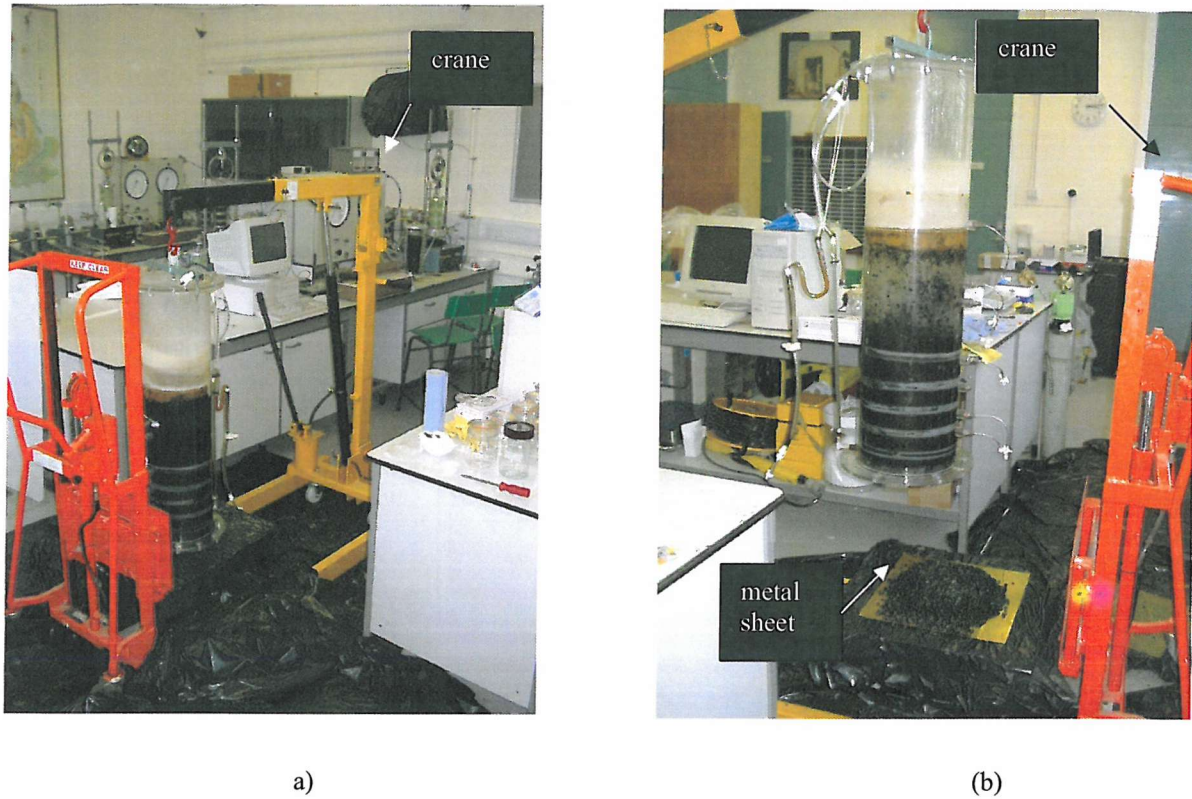


Figure 6-46: Set up for column dismantling

The aggregate particles that were removed from the filter layer (6 mm aggregate) and main drainage layer (40 mm aggregate) of the column were covered with a moist, black film and were not cemented to each other in any way (Figure 6-47 and Figure 6-48).



Figure 6-47: 6 mm aggregate



Figure 6-48: 40 mm aggregate

Four samples were taken from each column section. Two of these samples were for microbiological analysis of the clog material and were stored at 4°C whilst maintaining anaerobic conditions in the storage bottle. Anaerobic conditions were achieved by means of an anaerobic atmosphere generation kit (AnaeroGen 2.5 litres, Oxoid Ltd) that consists of ascorbic acid which rapidly absorbs the air with a simultaneous generation of carbon dioxide. The other two samples, for chemical analysis and for BNFL to archive, were placed in a freezer after purging the headspace of the storage bottle with nitrogen gas. Leachate from each section was kept and reintroduced to the samples kept for BNFL. A detailed description of the samples taken is given in Table 6-21. The remaining aggregate from each section was stored in sealed plastic boxes at 4°C, maintaining anaerobic conditions using AnaeroGen sachets.

Samples	Purpose
1 storage bottle + anaerobic generation atmosphere kit, keep at 4°C	Microbiological analysis
1 Glass Jar + anaerobic generation atmosphere kit, keep at 4°C	Microbiological analysis
1 Glass Jar + flush with N ₂ and freeze	Chemical analysis (XRF)
1 Glass Jar + flush with N ₂ and freeze	BNFL

Note: XRF – stands for X-ray Fluorescence

Table 6-21: Samples taken at dismantling of column 3

6.9.2. Chemical analysis of the clog material

X-Ray Fluorescence analysis was carried out at the Southampton Oceanography Centre. This analysis provided information for the chemical composition of the clog material. This was determined by subtracting the values for each element for the clean aggregate (blank sample) from the respective values for the coated aggregate samples. Triplicate samples of the coated aggregate retrieved from the first column section and duplicate samples from the following sections were analysed. The elemental composition of 10 blank samples was measured to obtain representative average values. Detailed data for each column section are given in Appendix E, Table 1.

The results, presented in terms of the average mg of each element deposited, on the basis of the triplicate or duplicate samples, per kg of drainage aggregate are shown in Table 6-22. The data indicate the presence of high quantities of Fe and S and smaller quantities of Ni, Co, Ba, Rb and Ce. The highest amounts of Fe, S, Ni and Ce were deposited on the aggregate from the top column sections, with gradually decreasing amounts towards the column outlet. It appears that Co was retained in all column sections while Ba was deposited mainly between tappings 4-5 and 5-6. High amounts of Ca and P were found on the aggregate between tappings 2-3 and 3-4.

Section	Ni mg/kg	Co mg/kg	Ba mg/kg	Rb mg/kg	Ce mg/kg	Fe mg/kg	S mg/kg	Ca mg/kg	P mg/kg
top -2	115.07	94.23	0.00	5.03	108.93	4416.30	2213.33	0.00	0.00
tappings 2-3	99.40	359.40	20.75	6.10	197.88	1181.39	7268.50	3425.00	33.45
tappings 3-4	5.70	199.25	0.00	5.10	0.00	2702.67	1474.55	447.86	109.82
tappings 4-5	0.00	112.35	389.40	3.20	0.00	0.00	561.15	0.00	0.00
tappings 5-6	17.60	104.95	221.55	106.00	21.53	0.00	184.00	0.00	0.00
tapping 6-out	0.00	146.60	5.00	2.90	0.00	0.00	407.50	0.00	0.00

Table 6-22: Amounts mg/kg of elements deposited on the drainage aggregate in column 3

Mass balance calculations based on the same data, but recalculated to show the concentration in mmoles (Table 6-23), indicate good correlation between the mmoles of iron, radionuclide analogues (Ni, Co, Ba, Ce) and sulphur in the top column section (top-2) suggesting that the iron and the radionuclide analogues were present mainly in the form of their sulphide salts (FeS, NiS, CoS, BaS and Ce₂S₃). The slightly higher number of mmoles of iron compared to sulphur suggests the formation of other low-solubility iron salt possibly siderite (FeCO₃). The results from samples collected between tappings 2-3

show surprisingly little removal of Fe although high concentrations of Ca and S are precipitated. It is possible that CaSO_4 precipitates were formed. The data for section 3-4 suggest formation of FeS_2 . Elevated levels of S were detected in the bottom column section (tappings 4-out).

Section	Ni mmol/ kg	Co mmol/ kg	Ba mmol/ kg	Rb mmol/ kg	Ce mmol/ kg	Fe mmol/ kg	S mmol/ kg	Ca mmol/ kg	P mmol/ kg
top -2	2.00	1.60	0.00	0.10	0.80	79.10	69.00	0.00	0.00
tappings 2-3	1.69	6.10	0.15	0.07	0.68	21.15	226.69	85.45	1.08
tappings 3-4	0.10	3.38	0.00	0.06	0.00	48.39	45.99	11.17	3.55
tappings 4-5	0.00	1.91	2.84	0.04	0.00	0.00	17.50	0.00	0.00
tappings 5-6	0.30	1.78	1.61	1.24	0.15	0.00	5.74	0.00	0.00
tapping 6-out	0.00	2.49	0.04	0.03	0.00	0.00	12.71	0.00	0.00

Table 6-23: Amounts in mmol of elements deposited per kg of aggregate in column 3

The total amounts of the radionuclide analogues deposited for the whole column are shown in Table 6-24, bearing in mind the following amounts of aggregates for each column section - 6.99 kg for section top-2, 3.49kg for section 2-3, 10.48 kg for section 3-4, 10.73 kg for section 4-5, 3.58 kg for section 5-6 and 7.16 kg for section 6-out.

A good correlation exists between the total amounts of Ni, Rb and Ce deposited for all sections of column 3 and the total amounts removed from the leachate (Table 6-24). Surprisingly high quantities of Co, Ba and Fe were also deposited. It is possible that these were available and leached out from the waste inoculum while it was placed above the drainage aggregate in the experimental column.

Element section	Total amount deposited (mg)							Theoretical amount (mg)*
	top-2	2-3	3-4	4-5	5-6	6-out	Total	
Ni	803.78	347.17	59.72	0.00	62.97	0.00	1273.64	1199.72
Co	658.25	1255.26	2087.74	1205.96	375.51	1049.07	6631.79	1202.45
Ba	0.00	72.47	0.00	4179.82	792.71	35.78	5080.78	1170.99
Rb	35.16	21.31	53.44	34.35	379.27	20.75	544.28	737.00
Ce	760.94	334.71	0.00	0.00	77.05	0.00	1172.70	1203.40
Fe	20422.63	0.00	12678.64	0.00	0.00	0.00	33101.27	12460.03
S	15251.31	25281.67	15135.99	5701.36	551.01	2701.39	64622.73	100000.72^
Ca	0.00	11962.38	4692.65	0.00	0.00	0.00	16655.03	
P	0.00	116.82	383.57	0.00	0.00	0.00	500.39	

Note: * the theoretical amount is calculated on the basis of the amount removed from the leachate.

^ represents the sulphate reduced to S^{2-} and not necessarily the S^{2-} removed from the leachate due to lack of metal species

Table 6-24: Amounts of metals retained for the whole column 3

6.9.3. Optical images of fully hydrated biofilm

A. Optical images of samples located between the inlet section and tapping 2

Optical images have been taken using an Episcopic Differential Interference Contrast (EDIC) microscope in combination with Epifluorescence (EF) microscopy. The traditional DIC microscopy is commonly used with transmitted light and is therefore unsuitable to viewing biofilms on opaque materials such as rocks. However, Keevil and Walker (1992) were able to adapt and reconfigure a Nikon Labophot-2 microscope. The modifications allowed the observation of curved specimens containing live, fully hydrated biofilms and more details on this technique can be found in Keevil and Walker (1992) and Keevil (2003). The images revealed a biofilm structure consisting of bacterial stacks which covered the aggregate surface and these formed a series of fingers extending from the basal layer (Figure 6-49). These structures consisted of what is presumed to be a polysaccharide matrix in which a relatively low number of microorganisms are embedded (section 6.8). The polysaccharide matrix facilitates attachment to surfaces and other microorganisms. Channels were observed to penetrate the structure (Figure 6-50 and Figure 6-51) and these have been postulated as a mechanism by which the transport of nutrients can be enhanced throughout the biofilm (Costerton *et al.*, 1995). This is consistent with the conceptual model illustrated in Figure 6-52.

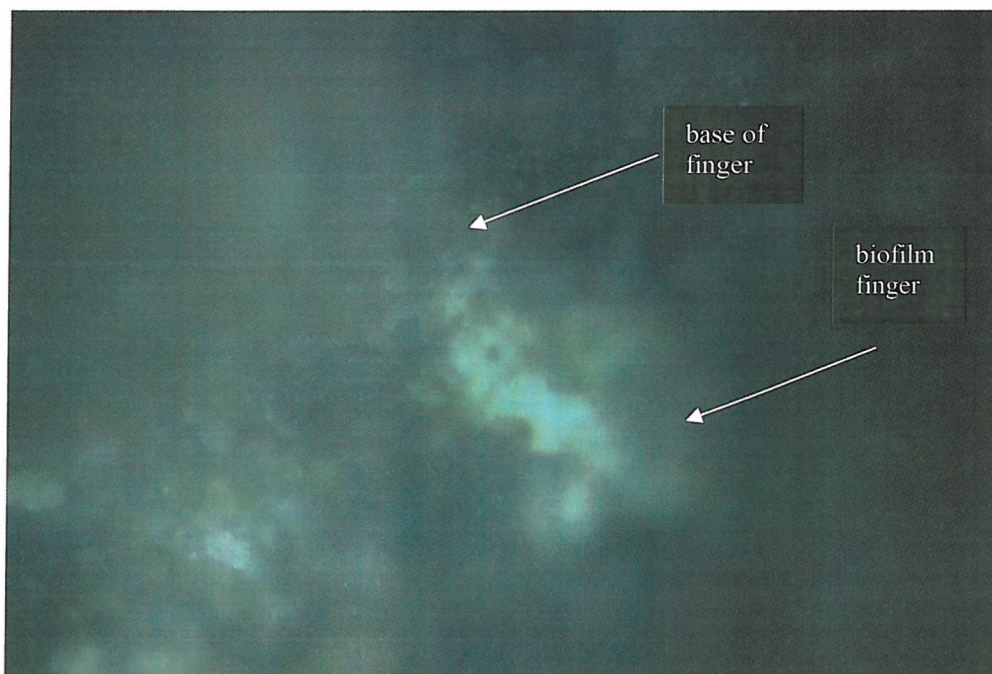


Figure 6-49: Biofilm structure

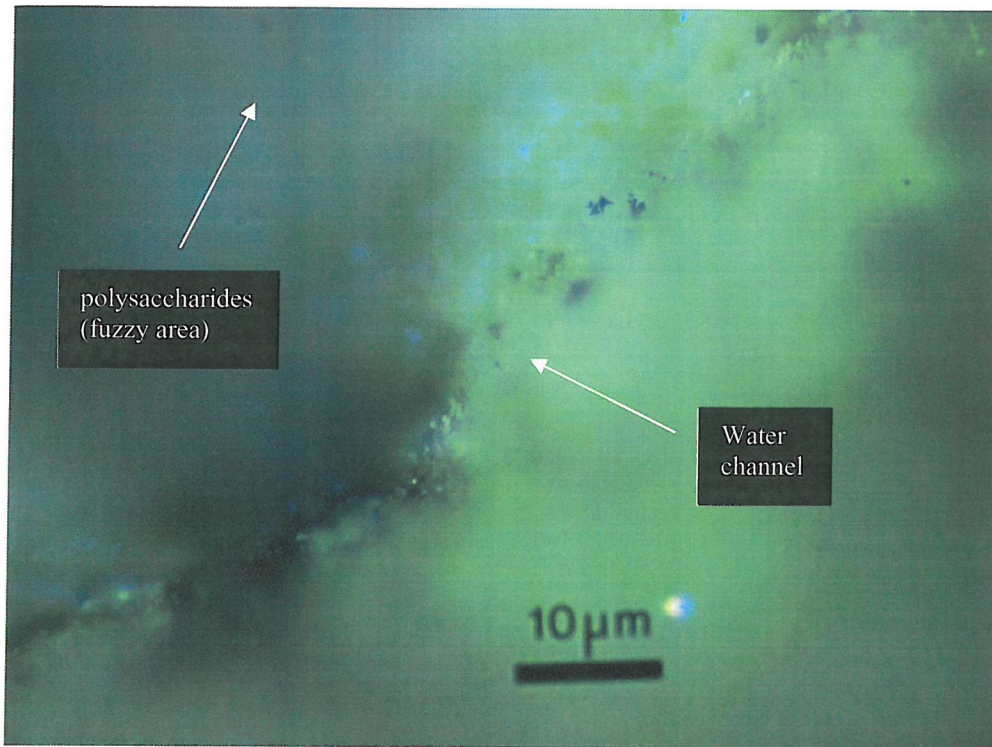


Figure 6-50: Water channel

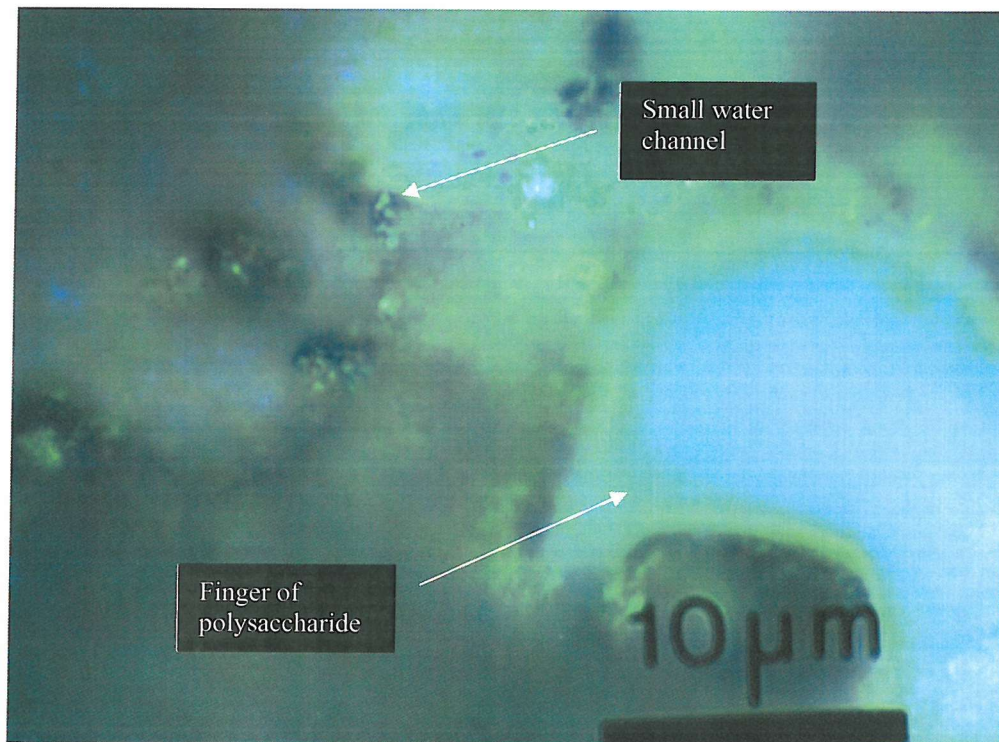


Figure 6-51: Finger of polysaccharide

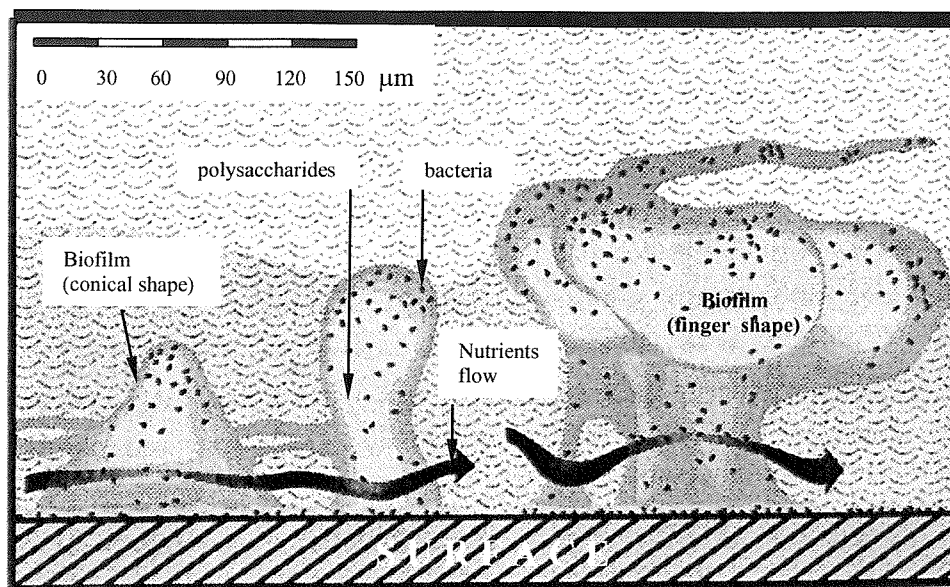


Figure 6-52: Conceptual model of the architecture of single-species biofilm (From Costerton *et al.*, 1995)

A LIVE/DEAD *BacLight* Bacterial Viability Kit (L-7012, Molecular Probes) was used to visualize live and dead bacteria in the biofilm structure. The kit consisted of mixtures of two stains – a green fluorescent nucleic acid stain (SYTO 9) and a red-fluorescent nucleic stain, propidium iodide. These stains differ both in their spectral characteristics and in their ability to penetrate healthy bacterial cells. When used alone the green fluorescent stain generally labels all bacteria in a population – those with intact membranes and those with damaged membranes. In contrast, propidium iodide penetrates only bacteria with damaged membranes, causing a reduction in the green fluorescent dye when both dyes are present. Thus, with an appropriate mixture of the green fluorescent and propidium iodide stains, bacteria with intact cells membranes stain fluorescent green (Figure 6-53), whereas bacteria with damaged membranes stain fluorescent red (Figure 6-54). The merged image (Figure 6-55) allows discrimination between the live and dead cells.

The mixture of SYTO 9 and propidium iodide stain was prepared by mixing equal volumes of each stain and dissolving 3 μl of the dye mixture in 1 ml of filter-sterilized dH_2O . The solution was applied to the colonised with biofilm drainage aggregate and incubated at room temperature in the dark for 15 min.

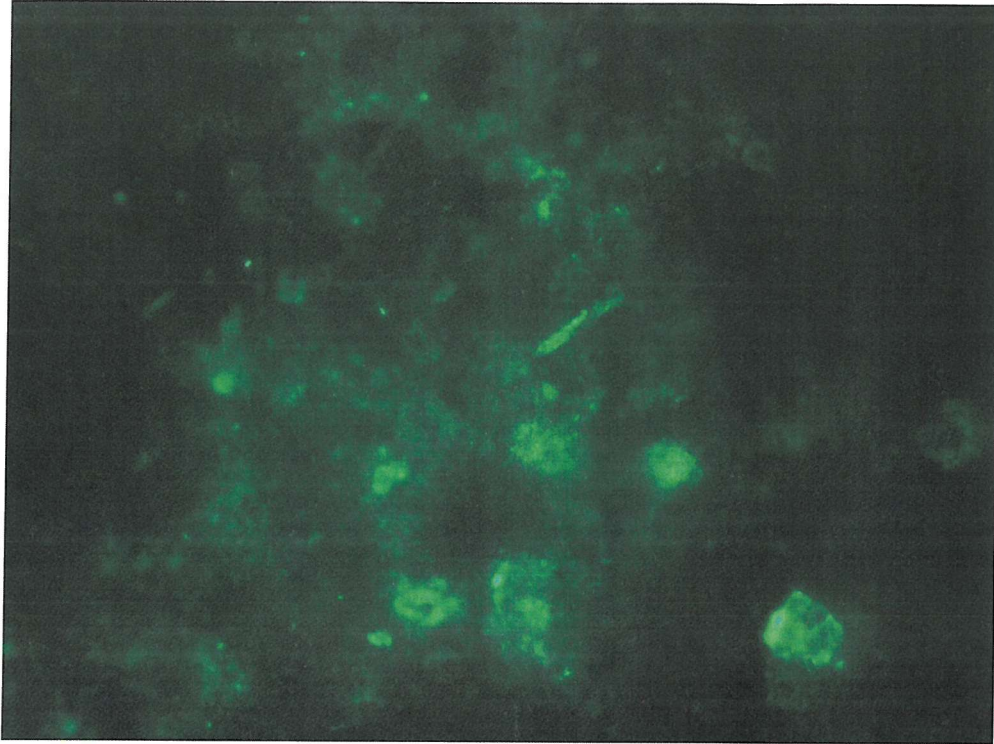


Figure 6-53: Live bacteria cells

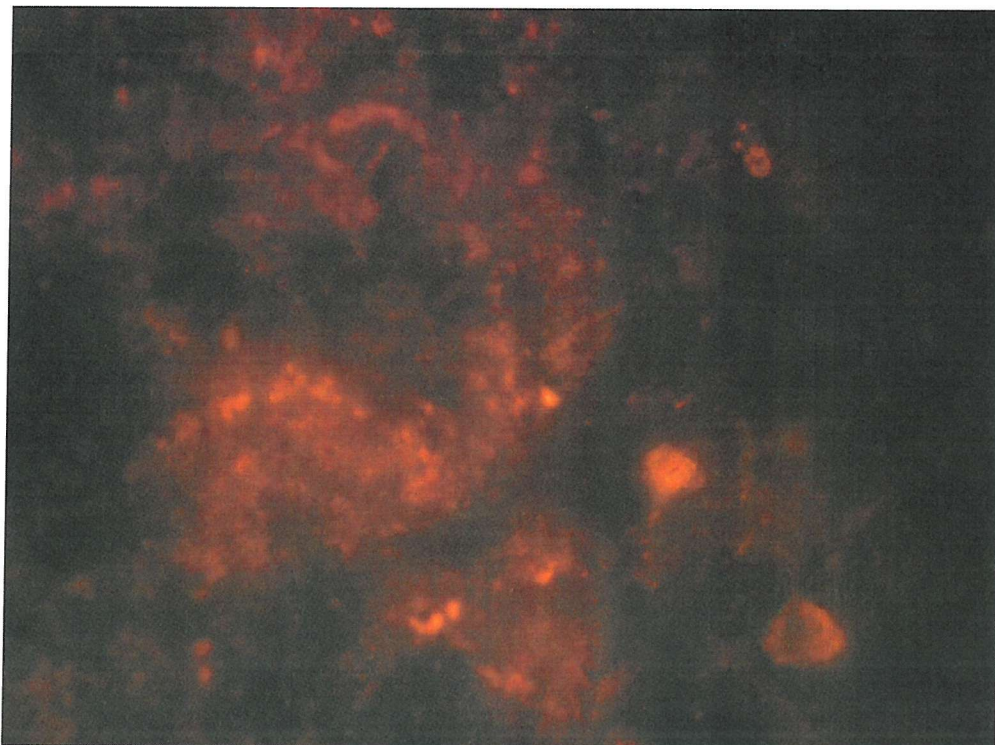


Figure 6-54: Dead bacterial cells

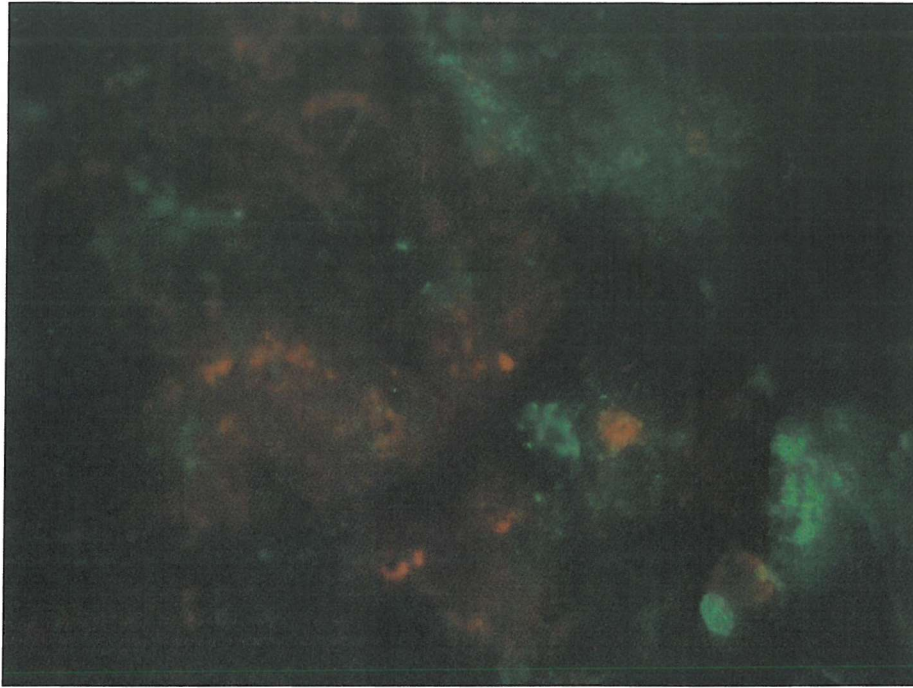


Figure 6-55: Live/Dead merged image

B. Optical images of samples located between tapping 2 – tapping 3

Nodules of precipitations, possibly of iron sulphide, were observed (Figure 6-56) together with water channels (Figure 6-57 and Figure 6-58). The water channels were clearer and visible than the previous column section, due to the reduced thickness of the polysaccharide layer.

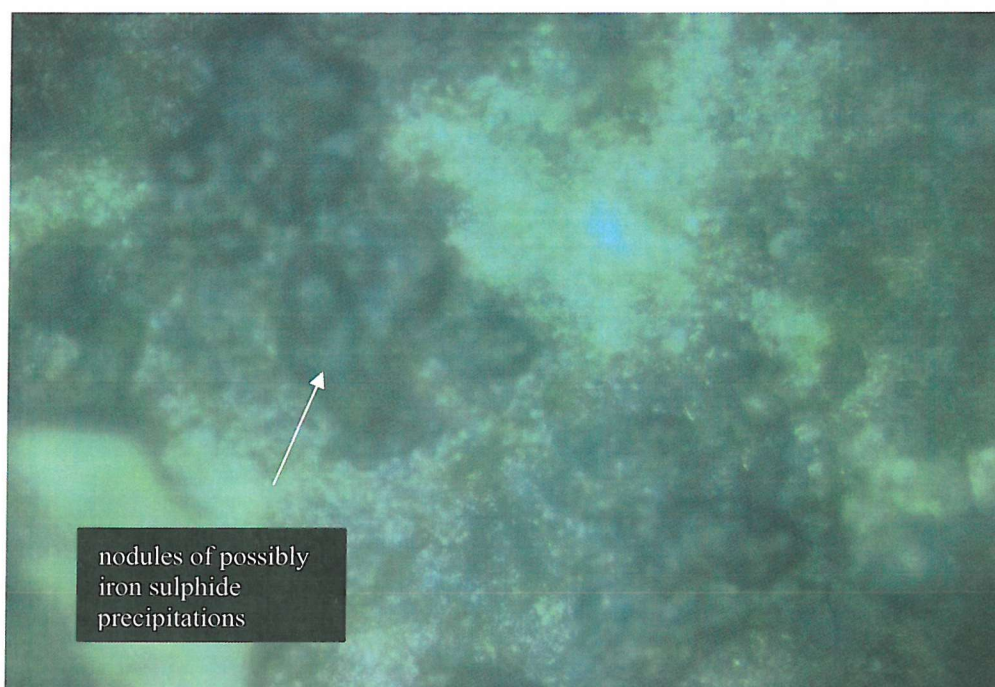


Figure 6-56: Nodules of precipitates

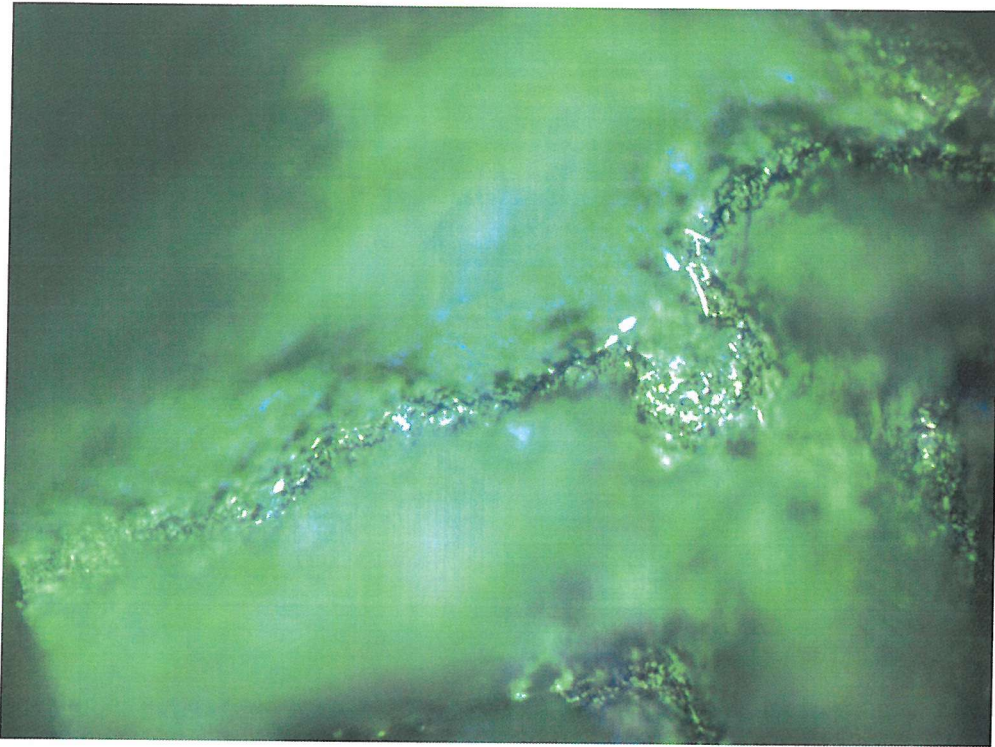


Figure 6-57: Water channels

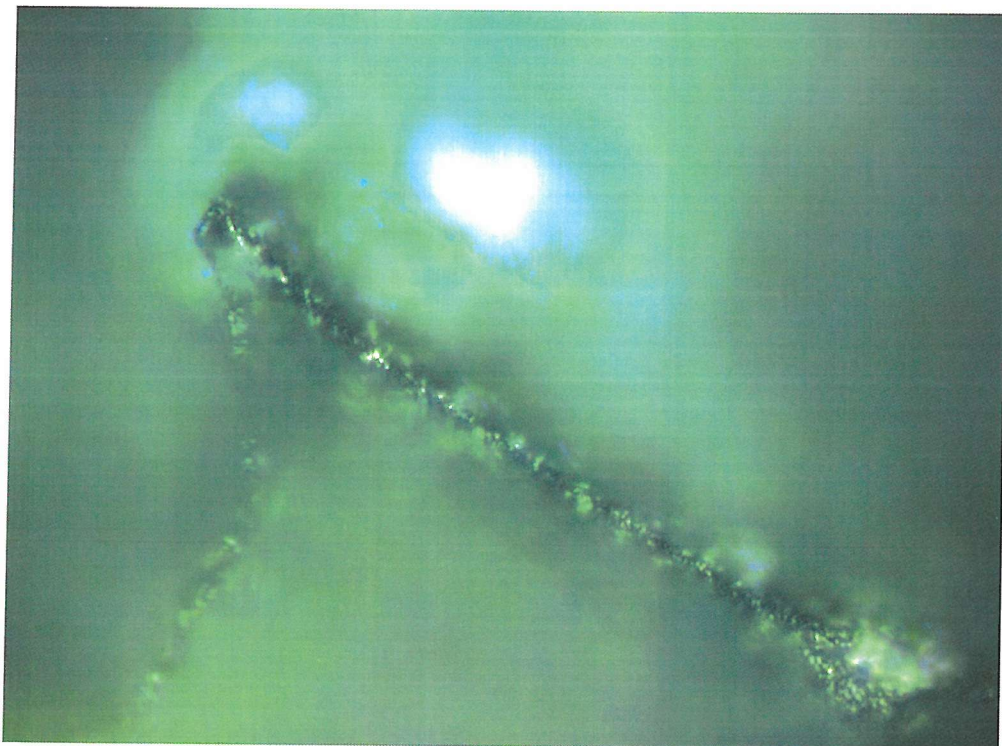


Figure 6-58: Water channels

C. Optical images of samples located between tapping 3 - tapping 4

Optical images revealed a reduced accumulation of polysaccharides and a thinner biofilm. This is consistent with the negligible reduction in drainable porosity and acetic acid degradation observed in this layer.

D. Optical images of samples located between tapping 4 -tapping 5

The optical images for this section revealed the presence of single rod-shaped and oval-shaped bacteria. The polysaccharide layer was less well established (Figure 6-59). Again, this is consistent with the negligible reduction in the drainable porosity and acetic acid removal measured in this layer.

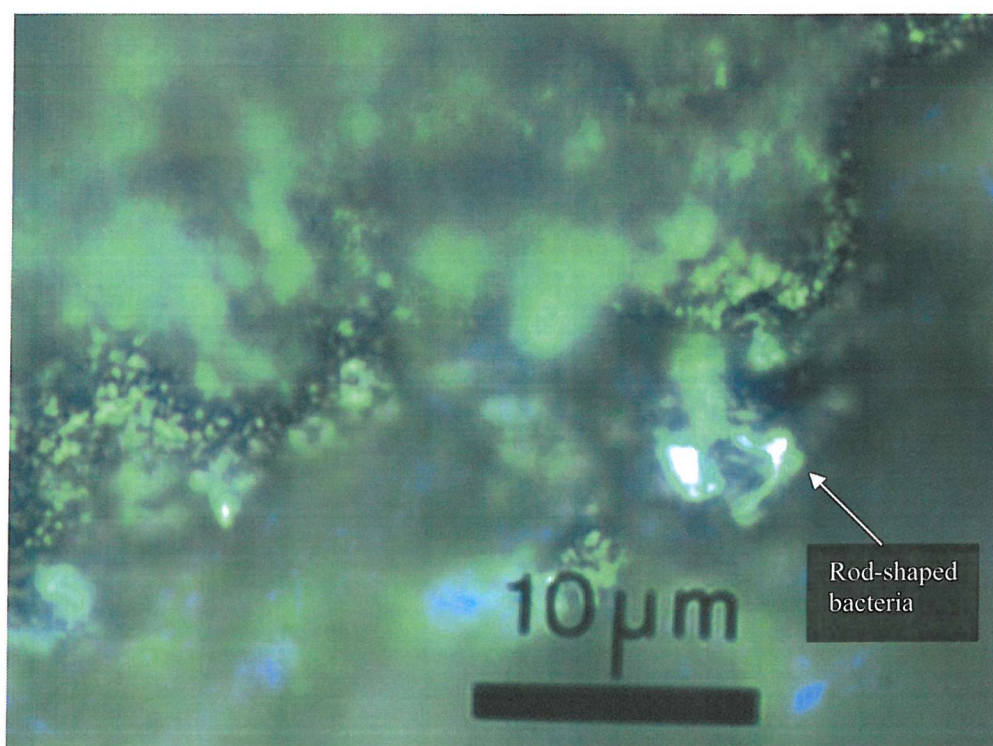


Figure 6-59: Water channels and individual bacterial cells

6.9.4. Polysaccharide and carbon analysis

Determination of the polysaccharide content of the biofilm that colonised the drainage aggregate was considered important to support the theory outlined in section 5.7. Known quantities of aggregate samples (18.8 g dry weight for sections top-2, 2-3 and 3-4, 30.36 g dry weight for section 4-5, 28.88 g for section 5-6 and 38.45 g for section 6-out) were placed in beakers containing 15 ml H₂O acid and the biofilm was detached by ultra-sound treatment for 800 s to allow extraction of the biofilm material attached to the aggregate

(Alves *et al.*, 2002). Up to 5 successive leaching tests were carried out on the sample from the top column section (inlet-2) where more extensive accumulation of biofilm had occurred. The polysaccharide content was determined using the phenol–sulphuric method as described by Dubois *et al.* (1956) and explained in section 4.7.8.

Table 6-25 shows the total polysaccharide content in mg, which was expressed in terms of total carbon to allow easy comparison with the total carbon content of the leached samples. The data suggest that the highest accumulation of polysaccharides had occurred in the top column sections (top-2 and 2-3) with considerably smaller amounts in the other sections.

	I leaching mg	II leaching mg	III leaching Mg	IV leaching mg	V leaching mg	Total mg
top - 2	2.239	0.627	1.256	0.455	0.328	4.906
top - 2	1.730	2.085	0.635	0.344	0.450	5.243
top - 2	1.921	0.528	0.381	0.174	0.176	3.180
2-3	0.755	0.263	0.367	0.235	0.395	2.015
2-3 dupl.	1.367		0.340	0.164	0.312	2.183
3-4	0.127	0.185				0.312
3-4 dupl.	0.136	0.055				0.191
4-5	0.053					0.053
4-5 dupl.	0.000					0.000
5-6	0.000					0.000
5-6 dupl.	0.000					0.000
6-out	0.085					0.085
6-out dupl.	0.036					0.036

Note: 20 g wet weight material was used which had 6% moisture corresponding to 18.8 g dry weight

Table 6-25: Total polysaccharide content expressed in terms of carbon (mg)

The total carbon contents for the same samples were measured and the results are presented in Table 6-26. The mg C deposited per g of aggregate that is shown in the last column of Table 6-26 was calculated by dividing the average amount of carbon in mg by the weights of the aggregate samples as reported above.

	I leach. mg	II leach. Mg	III leach. mg	IV leach. mg	V leach. mg	Total mg	Average mg	mgC/g of aggregate
top - 2	18.68	5.42	5.52			29.62		
top - 2	13.79	5.41	3.91	1.66	1.36	26.12		
top - 2	6.17	2.29	2.11	0.83	0.79	12.19	27.87	1.48
2-3	4.19	1.75	2.32	0.92	1.56	10.75		
2-3 dupl.	9.41		1.29	0.89	1.14	12.72	11.74	0.62
3-4	1.18	1.28				2.45		
3-4 dupl.	1.72	0.59				2.31	2.38	0.13
4-5	0.22					0.22		
4-5 dupl.							0.22	0.01
5-6	0.38					0.38		
5-6 dupl.	0.18					0.18	0.28	0.01
6-out	1.00					1.00		
6-out dupl.	0.46					0.46	0.73	0.02

Table 6-26: Total amount of carbon in 15 ml extracted material

On the basis of Table 6-25 and Table 6-26 the percentage of polysaccharide was calculated and is shown in Table 6-27. The data indicate a significant percentage of polysaccharide in the biofilm, further confirming the theory suggested in section 5.5.

	I leaching %	II leaching %	III leaching %	IV leaching %	V leaching %	Total %	Average %
top - 2	11.99	11.57	22.77			16.56	
top - 2	12.54	38.54	16.26	20.71	33.14	20.07	
top - 2	31.12	23.07	18.09	20.84	22.16	26.07	20.90
2-3	18.02	14.98	15.79	25.45	25.39	18.75	
2-3 dupl.	14.52		26.31	18.58	27.44	17.15	17.95
3-4	10.75	14.53				12.72	
3-4 dupl.	7.89	9.28				8.25	10.48
4-5							
4-5 dupl.							
5-6	0.00					0.00	
5-6 dupl.	0.00					0.00	
6-out	8.47					8.47	
6-out dupl.	7.80					7.80	8.13

Table 6-27: Percent of polysaccharides

6.10. Dismantling of Column 1

This section provides data on the dismantling of columns 1 and on the chemical and microbiological composition of the clog material retrieved from these columns.

6.10.1. Dismantling procedure

Column 1 was dismantled following the same procedure as for column 3. Similarly, the aggregate removed from the column was coated in a moist, black material with the only difference being that the aggregate particles in the top column section were cemented to each other and the column walls and did not fall under the influence of gravity on column dismantling (Figure 6-60).



Figure 6-60: Cementation of the top column section (top-2)



Figure 6-61: Close-up of the top column section

6.10.2. Chemical analysis of the clog material

The chemical analysis of the clog material was carried out following the same procedure as for column 3 (section 6.9.2.). The data indicate the presence of high quantities of Ca and S in the top column section with gradually decreasing amounts towards the column outlet. Although no additional quantities of Ni, Co, Ba, Rb and Ce were dissolved in the leachate, still some quantities of Ni, Ba, Rb and Ce were deposited on the drainage aggregate. This could be due to their presence as impurities in the inorganic salts used for preparation of the synthetic leachate medium. Surprisingly high quantities of Co were deposited on the drainage aggregate in all column sections.

Section	Ni mg/kg	Co mg/kg	Ba mg/kg	Rb mg/kg	Ce mg/kg	Fe mg/kg	S mg/kg	Ca mg/kg	P mg/kg
tapping top -2	9.55	100.90	0.00	0.20	0.00	0.00	1568.50	33505.00	53.09
tappings 2-3	0.00	141.75	15.10	6.00	0.00	0.00	629.5	390.71	31.27
tappings 3-4	0.85	95.60	26.80	0.50	4.63	870.80	284.00	0.00	66.18
tappings 4-out	0.00	201.35	0.00	0.00	0.00	0.00	56.50	0.00	0.00

Table 6-28: Amounts mg/kg of elements deposited on the drainage aggregate in column 1

The above data were recalculated to show the concentration in mmoles (Table 6-29). The results from samples collected between tappings top-3 suggest formation of a salt of Ca and S, most probably CaSO_4 . Much higher quantities of Ca were deposited in section top – 2 indicating the deposition of another Ca salt, most probably CaCO_3 . Precipitates of low solubility FeS and possibly FeCO_3 salts were deposited in section 3-4.

Section	Ni mmol/ kg	Co mmol/ kg	Ba mmol/ kg	Rb mmol/ kg	Ce mmol/ kg	Fe mmol/ kg	S mmol/ kg	Ca mmol/ kg	P mmol/ kg
tapping top -2	0.16	1.71	0.00	0.002	0.00	0.00	48.92	835.95	1.72
tappings 2-3	0.00	2.41	0.11	0.07	0.00	0.00	19.63	9.75	1.01
tappings 3-4	0.01	1.62	0.20	0.006	0.033	15.59	8.86	0.00	2.14
tappings 4-out	0.00	3.42	0.00	0.00	0.00	0.00	1.76	0.00	0.00

Table 6-29: Amounts in mmol of elements deposited per kg of aggregate in column 1

6.10.3. Findings from dismantling of columns 1 and 3

The major findings from the column dismantling were the following:

- The chemical analysis of the clog material suggested that metal species dissolved in the leachate precipitated under anaerobic conditions and formed low solubility salts - MeS/MeS_2 or FeCO_3 . Calcium also precipitated most probably in the forms of its insoluble salts - CaCO_3 and/or CaSO_4
- The optical images and polysaccharide analysis indicated the high concentration of polysaccharides in the biofilm structure
- The optical images also showed the presence of live and dead bacterial cells suggesting a cycle of bacterial growth and decay.

6.11. Conceptual model of clogging observed in the laboratory experiments

A conceptual model of the clogging mechanisms observed in the column tests described in this thesis is illustrated in Figure 6-62. Bacterial populations develop and attach to the drainage medium by means of extra-cellular polysaccharides. The amount of bacterial biomass formed would be expected to be related to the flux of organics (VFA) supplied in the leachate. A cycle of bacterial growth, biofilm formation and subsequent decay, release of the organic matter of dead bacterial cells and utilization by the live bacterial cells took place, leading to a steady state where no further reduction of the drainage aggregate porosity was observed. When an essential microbial growth nutrient like nitrogen or phosphorus is missing, bacterial cells can be expected to produce and accumulate polysaccharides (Schlegel, 1987). In such a system there will be less carbon lost in the form of CO_2 and CH_4 gas, with most of it being trapped as polysaccharides. This indicates that clogging develops after the passage of relatively smaller quantities of organic substances as explained in section 5.3.

If concentrations of sulphate are present in the leachate, the SRB will reduce the sulphate to hydrogen sulphide, which can then evolve as gas or be precipitated as insoluble FeS as suggested by the XRD analysis. Precipitates of calcium carbonate (CaCO_3) and calcium sulphate (CaSO_4) were formed and confirmed by the XRD analysis. Optical images, which were taken using a Differential Interference Contrast (DIC) microscope, have

suggested that the inorganic precipitates do not form a uniform layer but nodules, as marked with "2" on Figure 6-62. Gas bubbles also acted as a clogging agent.

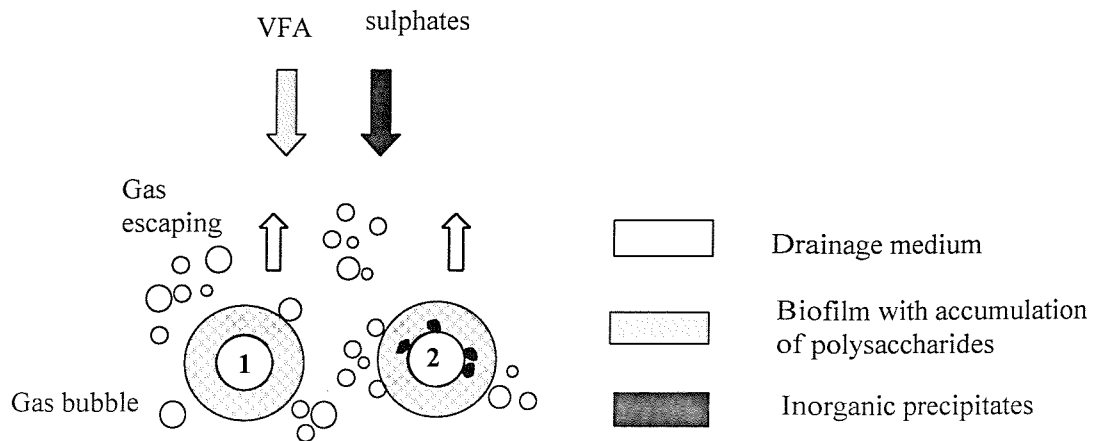


Figure 6-62: Conceptual model

Chapter 7

Conclusions

This chapter presents the key conclusions drawn from the work and outlines areas of future research.

The work described in this thesis had shown that the clogging of the drainage aggregate when permeated with leachates representative of those emanating from low level radioactive waste disposal sites was due to microbiological activity causing formation of bacterial mass and polysaccharides (microbiological clogging), due to precipitation of low solubility inorganic salts such as FeS and CaCO₃ (chemical clogging) and the entrapment of gas bubbles. This was demonstrated in laboratory columns where the microbiological activity was evidenced by the removal of VFA and the concurrent production of CH₄ and CO₂ gases, the precipitation of low solubility salts - by the removal of iron, sulphate and calcium from the leachate and the clogging - by the reduction of the porosity of the drainage aggregate.

The clogging process in the experimental columns reached a steady state and complete clogging did not occur. A key role in this process was played by the concentration of the organics in the leachate. Their low concentration accounted for a low organic loading and governed the development of bacterial mass, polysaccharides and gas bubbles, which accumulation reached a steady state.

The chemical clogging due to precipitation of low solubility salts (FeS, CaCO₃) can be significant but only in the long term due to the low rate of formation and accumulation of these precipitates. The accumulation of FeS is influenced by the availability of iron

species and was negligible at the low iron concentrations in the leachate used in the current experiments. The accumulation of CaCO_3 precipitates was significant but only occurred for Ca concentrations exceeding the aqueous solubility limit of the CaCO_3 salt.

Leachates with a low concentration of organics and a negligible concentration of iron, will not induce a measurable reduction in the permeability despite the reduction in the drainable porosity of the drainage aggregate of up to 15%.

The clogging of the drainage aggregate concentrated in the sections by the leachate inlet even when the mass loading was doubled by increasing the concentration of the leachate constituents. This seems to indicate that the clogging will not spread downwards, provided that the flow rate is kept the same.

Polysaccharides, produced by the bacterial populations under nitrogen and phosphorus limited conditions, played a significant role in the clogging of the pore space. Nitrogen and phosphorus are essential elements for bacterial growth and their unavailability leads to the production of storage material if carbon, hydrogen and oxygen are available. In these conditions, the number of bacterial cells per unit volume would be considerably reduced, with the generation of extra polysaccharides resulting in the production of less final degradation products such as CO_2 and CH_4 gases. This would imply that less carbon will be lost in the form of gas and more carbon will become trapped in the form of polysaccharides, causing the build up of a given volume of clog material after relatively smaller quantities of organic substances have passed through the column.

Gas bubbles influenced the clogging process by decreasing the size of the water conducting pores and hence acting as a clogging agent. Gas bubbles accumulated mainly in the top column sections, where the microbiological activity was most pronounced and consequently the gas production most vigorous. This accumulation would depend on the pore water pressure at the bottom of waste disposal site. A higher pore water pressure would result in an increased solubility of the gases in the leachate and consequently less accumulation of gas bubbles.

The laboratory tests investigated the competition between the sulphate reducing and methanogenic bacteria. The results indicated that sulphate reduction preceded

methanogenesis when acetate was used as organic substrate. Sulphate reduction was confined to the top section where the bacterial populations were most active.

The experiments described in this thesis studied the adaptability of the bacterial populations to doubling the VFA concentration on switching from 50% to 100% and from 100% to 200% leachate strength. The bacterial populations were inhibited by the sudden increase of nutrient concentration. The adaptation period for the SRB was shorter than that for the acetogenic and methanogenic bacteria indicating that the SRB were metabolically more adaptable under the conditions utilised in these experiments.

Column dismantling revealed that the clog remains relatively porous and permeable when its nature is mainly biological but becomes cemented and impermeable if accumulation of CaCO_3 precipitates has occurred.

The significance of two main factors, the organic content of the leachate (COD) and the particle size of the drainage aggregate, on microbial clogging of the drainage systems in general was investigated. Previous laboratory column test data obtained by other researchers were reviewed in an attempt to establish a common framework that draws general conclusions despite differences in column sizes, organic and inorganic loading rates, upward and downward hydraulic flows and presence or absence of suspended solids. A correlation between the amount of COD removed from the leachate and the volume of clog material that developed was found to exist. This correlation did not appear to depend on the particle size of the drainage aggregate, indicating that the total volume of the clog material will depend mainly on the amount of organics removed from the leachate. However, the particle size has been shown to play a major role in the distribution pattern of the clogging. Rowe *et al.* (2000a) suggested that clogging occurred over a similar surface area – the top layers (20 cm) for the small particles (4, 6 mm diameter particles) and over the entire column (70 cm) for the larger particles (15 mm diameter particles). After similar amounts of COD had been removed the columns packed with small particles clogged faster because the clogging occurred in a small section near the column inlet. The larger particles allowed a more uniform distribution of the clogging throughout the experimental reactor thus providing a larger pore space resulting in a longer period of time over which the system is permeable.

This research has investigated the mechanisms and the potential for biological and chemical clogging of leachates representative of those emanating from low level radioactive waste disposal sites. The results showed that the clog material will be mainly organic in nature with the entrapment of gas bubbles, and its volume will reach a steady state leaving the drainage system relatively permeable. However, the operational conditions employed were limited in terms of their physico-chemistry and further experiments could be required to assess the effect of higher dissolved metal concentrations and presence of suspended solids in the leachate on the clogging rates.

References

- Alves C.F., Melo L.F. and Vieira M.J. (2002) Influence of medium composition on the characteristics of a denitrifying biofilm formed by *Alcaligenes denitrificans* in a fluidised bed reactor, *Process Biochemistry*, vol. 37, pp. 837-845
- Archer D., (1988) A basic study of Landfill Microbiology and Biochemistry. *Contractor Report ETCU B 1159. ARFC Institute for Food Research*. UK, pp.6-14, 25-47
- Bailey J.E. and Ollis D.F. (1977) *Biochemical Engineering Fundamentals*. McGraw-Hill, pp. 337-356
- Banfield F.S., Meek D.M. and Lowden G.F. (1978) Manual and automated gas-chromatograph procedures for the determination of volatile fatty acids. Technical report TR 76, Laboratory Services Division, Water Research Centre
- Battesby N.S., Stewart D.J. and Sharma A.P. (1985) Microbiological problems in the offshore oil and gas industries. *Journal of Bacteriology*, Symposium Suppl, pp. 227S-235S.
- Barone F.S., Costa J.M.A. and Ciardullo L. (1997) Temperatures at the base of a municipal solid waste landfill. *50th Canadian Geotechnical Conference*, Ottawa, Canada.
- Baveye P., Vandevivere P, Hoyle B.L., DeLeo P.C. and Lozada D.S. (1998) Environmental impact and mechanisms of the biological clogging of saturated soils and aquifer materials. *Critical Reviews in Environmental Science and Technology*, vol. 28, No .2, pp. 123-191.
- Bedient P., Rifai H. and Newell C. (1994) *Groundwater Contamination. Transport and remediation*. First edition, Prentice Hall PTR, New Jersey, USA, pp. 165-187
- Bialkowski Stephen, Utah State University, Use of acid distribution in solubility problems, <http://www.chem.usu.edu/faculty/~sbialkow/Classes/3600/Alpha/alpha3.html>, last updated 31 October 2000

- British Nuclear Fuels Ltd. (2002) Drigg Post Closure Safety Case: engineering design
- Bordier C. and Zimmer D. (1999) Clogging of leachate collection systems: preliminary results of a column study. *Proceedings Sardinia 99, Seventh International Landfill Symposium*, CISA publisher, Cagliari, Italy, pp.261-268.
- Brune M., Ramke H.G., Collins H.J., and Hanert H.H. (1991) Incrustation process in drainage systems of sanitary landfill. *Proceedings Sardinia 91, Third International Landfill Symposium*, CISA publisher, Cagliari, Italy, pp. 999-1035.
- Buswell A.M. and Haftfield W.D. (1939) Anaerobic fermentation. *Illinois State Water Survey Bulletin*. Vol. 32, pp. 1-193.
- Clark R.B. (1997) *Marine Pollution*. Fourth edition, Oxford University Press, Oxford, pp.97-108
- Costerton J.W., Lewandowski Z., Caldwell D.E., Korber D.R. and Lappin-Scott H.M. (1995) Microbial biofilms. *Annual Review of Microbiology*, vol. 49. pp. 711-745
- Cullimore D.R. (1993) *Practical manual of Groundwater Microbiology*. Lewis Publishers. Chelsea, Michigan, USA.
- Davies J.N. and Coultier J.P. (1995) UK DoE Technical guidance for landfill design, construction and operational practice. *Proceedings Sardinia 95, Fifth International Landfill Symposium*, CISA publisher, Cagliari, Italy, vol. 3, pp. 93-104.
- Daniel D.E. (1993) *Geotechnical Practice for Waste Disposal*. First edition. Chapman & Hall, USA, pp. 97-112, 187-214
- Department for Environment, Food & Rural Affairs. (2000) *Waste Strategy 2000 for England & Wales*.
- Department of the Environment (1995) *Waste Management Paper 26B, Landfill Design, Construction and Operational Practice*, HMSO
- Dubois M., Gilles K.A., Hamilton J.K., Rebers P.A. and Smith F (1956) Colorimetric method for determination of sugars and related substances. *Analytical Chemistry*, vol. 28, pp. 350-356
- Fleming I.R., Rowe R.K. and Cullimore D.R. (1999) Field observations of clogging in a landfill leachate collection systems. *Canadian Geotechnical Journal*, vol. 36, pp. 685-707.
- Harper S.R. and Surdan M.T. (1991) Anaerobic Treatment Kinetics. *Water Science and Technology*, vol. 24, No. 8.

- Hoeks F.W.J.M.M., Ten Hoopen H.J.G., Roels JA and Kuenen J.G. (1984) Anaerobic treatment of acid water (methane production in sulphate rich environment). *Progr. Ind. Microbiol.* vol.20, pp. 113-119
- Hudson, A.; Beaven, R. P.; Powrie, W. (2001) Interaction of Water and Gas in Saturated Household Waste in a Large Scale Compression Cell. *Proceedings Sardinia 2001, Eight International Landfill Symposium*, CISA publisher, Cagliari, Italy, vol. 3, pp.585-594.
- Humphreys P.N. *et al*, (1996) Microbial aspects of LLW disposal at the UK low level radioactive waste disposal site. *NATO Advanced Research Workshop on Microbial degradation Processes in Radioactive Waste Repository and in Nuclear Fuel Storage Areas*, Budapest, Hungary, pp. 217-232.
- Kalyuzhnyi S., Fedorovich V., Lens P., Hulshoff Pol L and Lettinga G. (1998) Mathematical modelling as a tool to study population dynamics between sulphate reducing and methanogenic bacteria. *Biodegradation.* vol. 9, pp. 187-199.
- Keevil C.W. and Walker J.T. (1993) Nomarski DIC microscopy and image analysis of biofilms. *Binary*, vol. 4, pp. 93-95
- Keevil, C.W. (2003). Rapid detection of biofilms and adherent pathogens using scanning confocal laser microscopy and episcopic differential interference contrast microscopy. *Water Science and Technology*, vol. 47, pp. 105-116.
- Kiely G. (1996) *Environmental Engineering*. McGraw-Hill, pp. 678-682
- King K.S., Quigley R.M., Fernandez F., Reades D.W. and Bacopoulos A. (1993) Hydraulic conductivity and diffusion monitoring of the Keele Valley Landfill liner, Maple, Ontario. *Canadian Geotechnical Journal*, vol. 30, No. 1, pp. 124-134
- McCarty P.L., Rittmann B.E. and Bouwer E.J. (1984) Microbial processes affecting chemical transformations in groundwater. *Groundwater Pollution Microbiology.* pp.89-115.
- McIsaac R.S., Rowe R.K., Fleming I.R. and Armstrong M.D. (2000) Leachate collection system design and clog development. Sixth Environmental Engineering Specialty Conference of the CSCE & Second Spring Conference of the Geotechnical Division of the Canadian Geotechnical Society, London, Ontario, Canada, pp.66-73.
- Momba M.N.B., Kfir R., Venter S.N., Cloete T.E. (2000) An overview of biofilm formation in distribution systems and its impact on the deterioration of water quality. *Water SA*, vol. 26, No. 1, pp. 59-66
- Mulder A. (1984) The effect of high sulphate concentrations on the methane fermentation of waste water. *Progress in Industrial Microbiology.* vol. 20, pp.133-143

- Nazaroff W.W. and Alvarez-Cohen L. (2001) *Environmental Engineering Science*. John Wiley & Sons, USA
- Nikolova R. (1997) *Utilisation of tannery waste for biogas production*. MSc thesis. University of Chemical Technology and Metallurgy, Sofia, Bulgaria.
- Omil F., Lens P., Hulshoff Pol L. and Lettinga G. (1996) Effect of upward velocity and sulphate concentration on volatile fatty acids degradation in a sulphidogenic granular sludge reactor. *Process Biochemistry*. vol. 31, No 7, pp. 699-710.
- Omil F., Lens P., Hulshoff Pol L. and Lettinga G. (1997) Characterisation of biomass from a sulphidogenic volatile fatty acids-degrading granular sludge reactor. *Enzyme and Microbial Technology*. vol. 20, pp. 229-236.
- Orlob G.T. and Radhakrishna G.N. (1958) The effect of entrapped gasses on the hydraulic characteristics of porous media. *Transactions, American Geophysical Union*. vol. 39, pp. 648-659.
- Oude Elferik S.J.W.H., Visser A., Hulshoff Pol L. and Stams AJM. (1994) Sulphate reduction in methanogenic bioreactors. *FEMS Microbiological Review*, vol. 15, pp.119-136
- Paksy A., Peeling L., Robinson J.P., Powrie W., and White J.K. (1995) Landfill drainage as a fixed bed bioreactor. *Proceedings Sardinia 95, Fifth International Landfill Symposium*, CISA publisher, Cagliari, Italy, pp.681-690.
- Paksy A., Powrie W., Robinson J.P. and Peeling L. (1998) A laboratory investigation of anaerobic clogging in granular drainage media. *Geotechnique*, vol. 48, No. 3, pp. 389-401.
- Paksy (2002) Microbial clogging of landfill drainage systems – experimental and theoretical studies. PhD thesis. Queen Mary and Westfield College, University of London
- Peeling L., Paksy A., Powrie W. and Robinson J.P. (1999) Removal of volatile fatty acids from synthetic landfill leachate by anaerobic biofilms on drainage aggregates: a laboratory study. *Waste Management and Research*, vol. 17, pp.141-149
- Powrie W., Paksy A., Robinson J.P., Peeling L. (1997) Pilot scale field trials of landfill drainage systems. *Proceedings Sardinia 97, Sixth International Landfill Symposium*, CISA publisher, Cagliari, Italy, pp.373-382.
- Powrie W. (1999) Preface. *Proceedings of the Institution of Civil Engineers, Geotechnical Engineering*, vol. 137, pp. 179-180

- Powrie W. and Robinson J.P. (2000) The sustainable landfill bioreactor – a flexible approach to solid waste management. *Sustainable Solid Waste Management in the Southern Black Sea Region*. Kluwer Academic Publishers, Printed in the Netherlands, pp. 113-240.
- Rittmann B.E. and McCarty P.L. (1980) A model of steady-state biofilm kinetics. *Biotechnology and Bioengineering*, vol. 22, pp. 2343-2357.
- Rittmann B.E., Fleming I.R. and Rowe K.R. (1996) Leachate chemistry: Its implication for Clogging. *North American Water and Environment Congress*, Anaheim, California, paper 4 (CD ROM), Session GW-1, Biological processes in groundwater quality
- Roberts T.O.L. (1988) *Seepage in shallow unconfined aquifers: permeability limits for gravity drainage*. PhD dissertation, University of London (King's College)
- Robinson J.P. and Sturtz H.C. (1993) A basic study of landfill microbiology and biochemistry. *Renewable Energy Research and Development Programme, Energy Technology Support Unit (ETSU)*, Contract No. ETSU B 1271.
- Rovers F.A. and Farquhar G.I. (1972) Sanitary landfill study final report: Effect of season on landfill leachate and gas production. Waterloo Research Institute, Report 8083, vol. 11.
- Rowe K.R. (1998) From the past to the future of the landfill engineering through case histories. *Proceedings: Fourth International Conference on Case Histories in Geotechnical Engineering*, St. Louis, Missouri, 9-12 March 1998. pp. 145-166
- Rowe R.K., Fleming I.R., Cullimore D.R., Kosaric N., Quigley R.M. (1995) *A research study of clogging and encrustation in leachate collection systems at municipal solid waste landfills*. Submitted to Interim Waste Authority.
- Rowe K.R., Fleming I.R., Armstrong M.D. Cooke A.J., Cullimore D.R., Rittmann B.E., Bennett P and Longstaffe F.J. (1997) Recent advances in understanding the clogging of leachate collection systems. *Proceedings Sardinia 97, Sixth International Landfill Symposium*, CISA publisher, Cagliari, Italy, pp. 383-390
- Rowe K.R. and Fleming I.R. (1998) Estimating the time for clogging of leachate collection systems, *3rd International Congress on Environmental Geosynthetics*, Lisbon, vol. 1, pp. 23-28
- Rowe K.R., Armstrong M.D. and Cullimore D.R. (2000a) Particle size and clogging of granular drainage media permeated with leachate. *Journal of Geotechnical and Geoenvironmental Engineering*, Vol. 126, No 9, pp. 775-786

- Rowe K.R., Armstrong M.D. and Cullimore R.D. (2000b) Mass loading and the rate of clogging due to municipal solid waste leachate, *Canadian Geotechnical Journal*, vol. 37(2), pp. 355-370
- Rowe K.R. and VanGulck J. (2001a) Clogging of leachate collection systems: From laboratory and field study to modelling and precipitation. *GeoEnvironment Conference*, Smith, Futyus & Allman.
- Rowe K.R., VanGulck J.F. and Millward S.C. (2001b) Biologically induced clogging of a granular media permeated with synthetic leachate (in preparation)
- Rowe K.R., Southen J., VanGulck J., Moore I.D., Sangam H.P. and Krol M. (2001c) *Review of the state-of-the-art of landfill site design*. Submitted to Ontario Ministry of Environment
- Sawyer C.N. and McCarty P.L. (1978) *Chemistry for environmental engineering*. Third edition, McGraw-Hill Inc, USA.
- Schlegel H.G. (1987) *General Microbiology*. Cambridge University Press, pp. 65-69
- Scott, J.D. (1980) The filtration permeability test. *Proceeding of the first Canadian Symposium on Geotextiles*. Alberta, Canada, pp.175-186
- Somerville, S.H. (1986) Control of groundwater for temporary works. CIRIA Report 113. Construction Industry Research and Information Association, London
- Stumm W. and Morgan J.J. (1996) *Aquatic Chemistry*. Third edition, John Wiley & Sons, Inc. New York, USA, pp. 473-478.
- Suflita, J.M., Gerba C.P., Ham R.K., Palmisano A.S., Ratje W.L. and Robinson J.P. (1992) The World's largest landfill – a multidisciplinary investigation. *Environmental Science and Technology*, Vol. 26, No 8, pp.1486-1494
- Tchobanoglous G., Burton F.L. and Stensel H.D. (2002) *Waste Water Engineering treatment and Reuse*, McGraw Hill, pp. 684
- Thorne, M.C. (1992) Development Priorities for the Drigg Technical Programme. Electrowatt Engineering Services (UK) Ltd, Report Ref. No. WMDTC/P(92)29
- Visser A., Beeksma I., Van der Zee F., Stams A.J.M. and Lettinga G. (1993) Anaerobic degradation of volatile fatty acids at different sulphate concentrations. *Applied Microbiology and Technology*. Vol. 40, pp. 549-556
- Waste Management Paper 26B, Landfill Design, Construction and Operational Practice. (1995) Department of the Environment. HMSO.

APPENDICES

Appendix A

VFA, SO₄, Ca, gas and drainable pore volume data for columns 1 and 4 (duplicates)

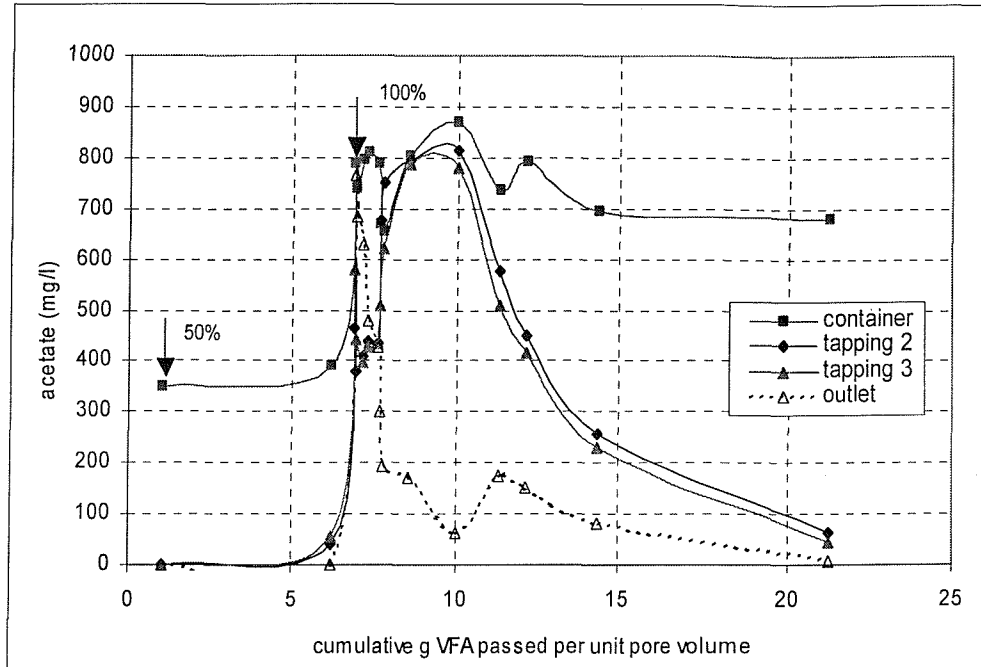


Figure 1: Acetate removal in column 1, 100% strength

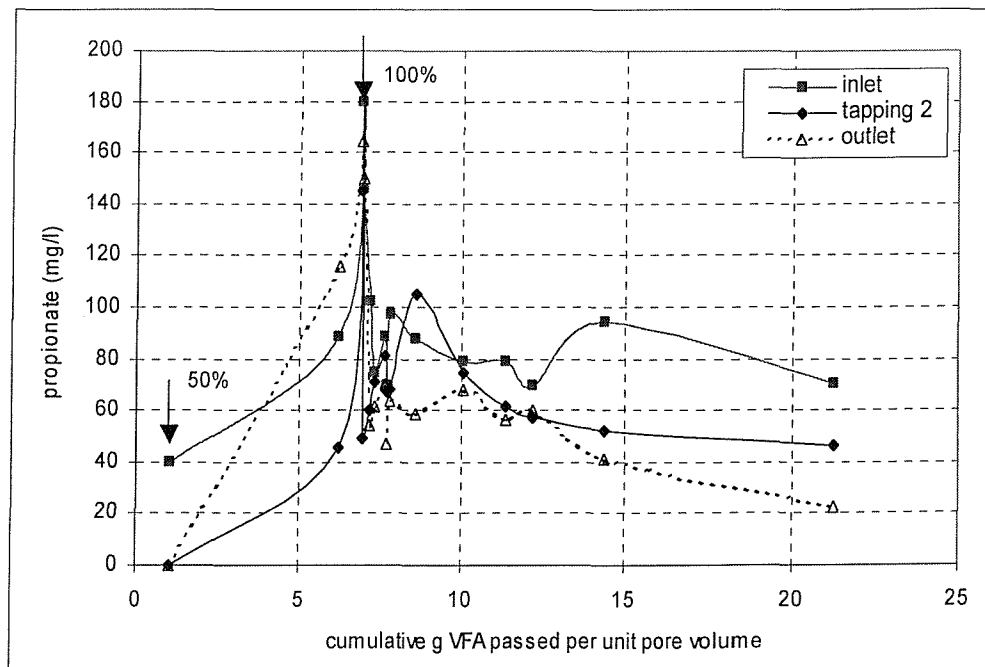


Figure 2: Propionate removal in column 1, 100% strength

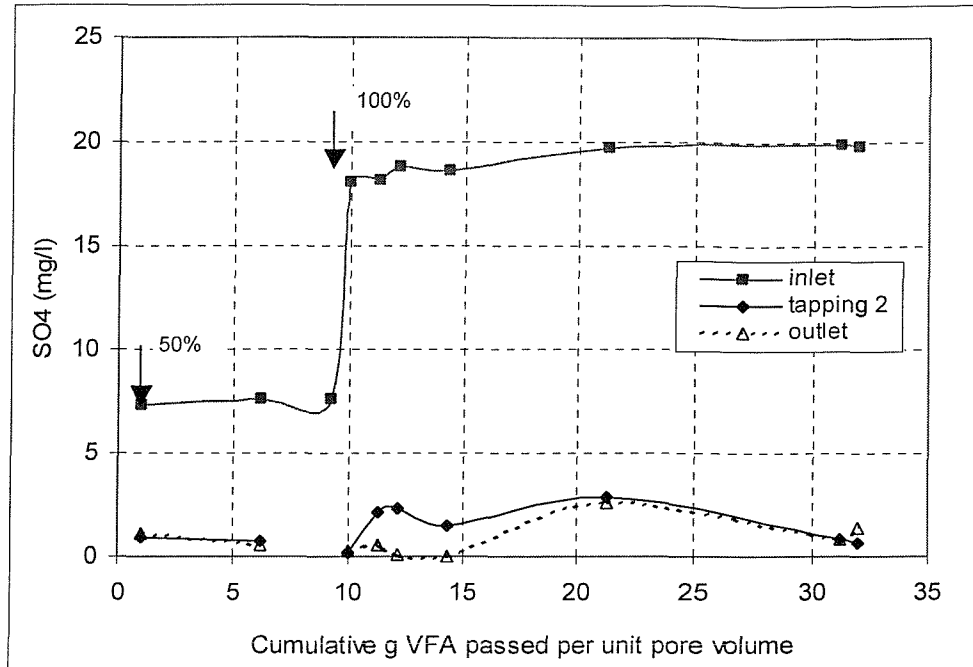


Figure 3: Sulphate removal in column 1, 100% strength

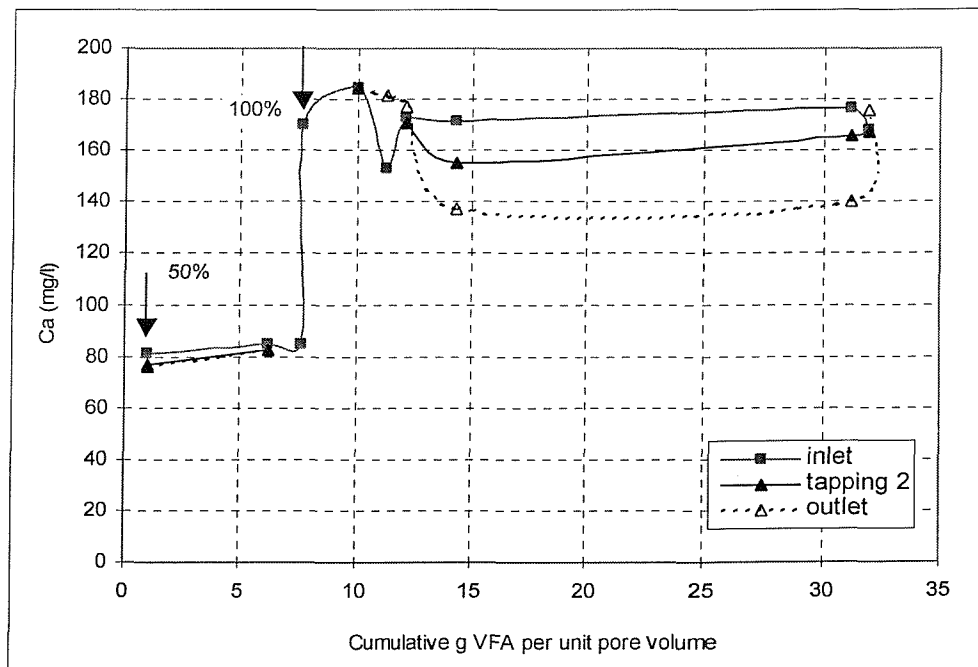


Figure 4: Calcium concentrations in column 1, 100% strength

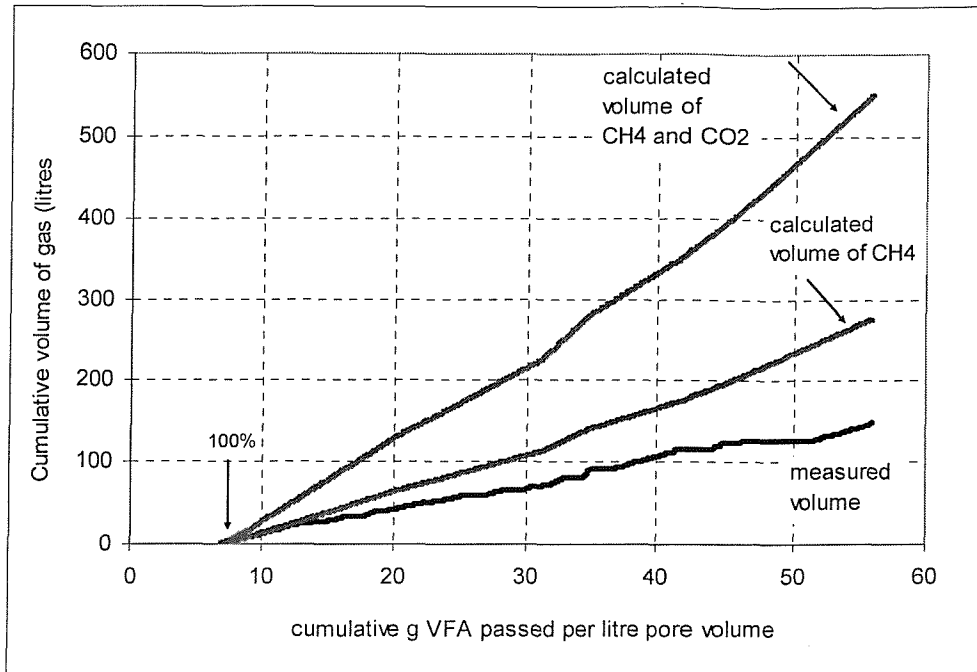


Figure 5: Volume of the theoretical and measured gas production in column 1, 100% strength leachate

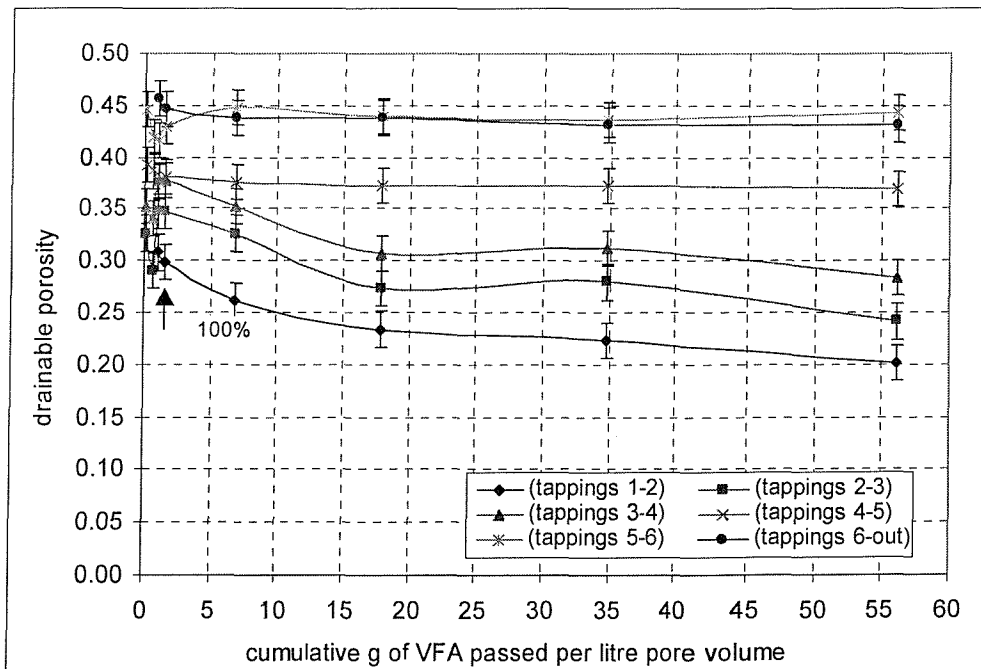


Figure 6: Drainable porosity in column 1, 100% strength leachate

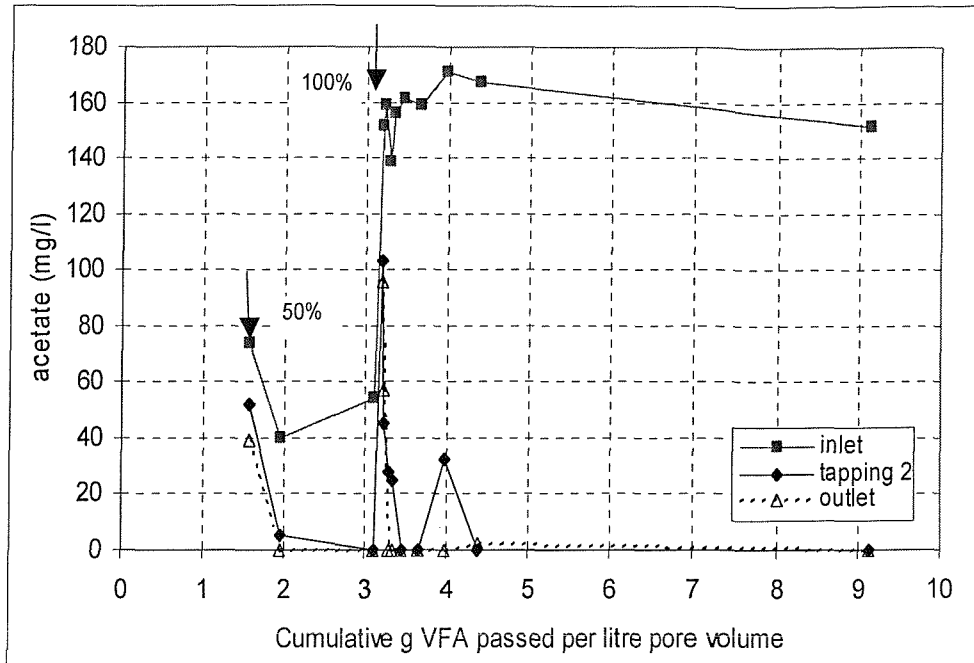


Figure 7: Acetate removal in column 4, 100% strength leachate

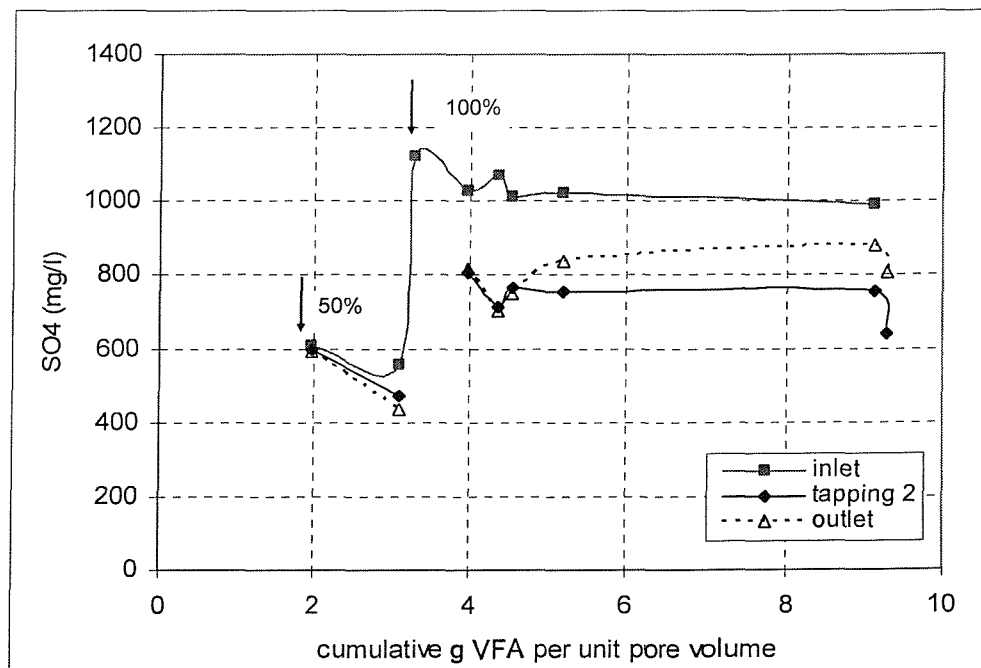


Figure 8: Sulphate removal in column 4, 100% strength leachate

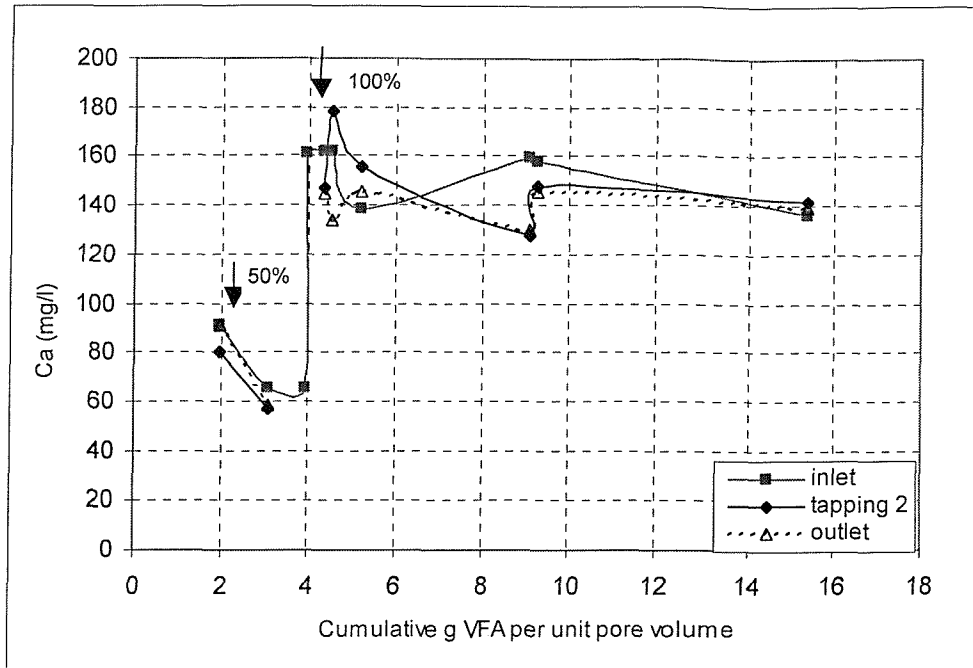


Figure 9: Calcium concentrations in column 4, 100% strength leachate

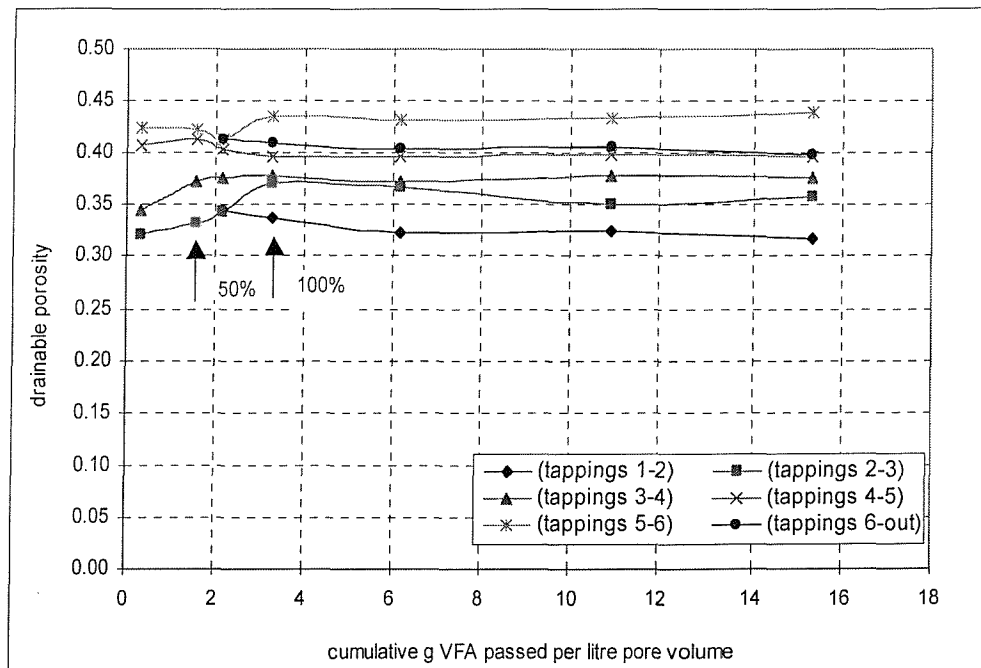


Figure 10: Drainable porosity in column 4, 100% strength leachate

Appendix B

Total gas production (acetate removed) in column 2

date	days	days between samples	conc. acetate removed	moles of acetate removed	moles CH ₄	ml of CH ₄ per day	ml of CH ₄ total	moles CO ₂	ml of CO ₂	ml of CO ₂ total	total ml CH ₄ + CO ₂ per day
A	B	C	D	E	F	G	H	J	K	L	M
		B _i -B _{i+1}		D*1.44 / (1000*60.05)	E*1.0	F*24.12*1000	((G _i +G _{i+1})/2)C _i	E*1.0	I*24.12*1000	((J _i +J _{i+1})/2)C _i	(H _i +K _i)
19/04/1999											
21/04/1999	2	2	21.7	0.00052	0.00052	12.55124	25.10247	0.00052	12.55124	25.10247	50.2049
22/04/1999	3	1	56.15	0.00135	0.00135	32.47705	22.51414	0.00135	32.47705	22.51414	45.0283
27/04/1999	8	5	166.02	0.00398	0.00398	96.02564	321.25671	0.00398	96.02564	321.25671	642.5134
30/04/1999	11	3	327.32	0.00785	0.00785	189.32123	428.02031	0.00785	189.32123	428.02031	856.0406
07/05/1999	18	7	358.69	0.00860	0.00860	207.46558	1388.75385	0.00860	207.46558	1388.75385	2777.5077
12/05/1999	23	5	368.82	0.00884	0.00884	213.32475	1066.62375	0.00884	213.32475	1066.62375	2133.2475
20/05/1999	31	8	462.09	0.01108	0.01108	267.27193	1922.38673	0.01108	267.27193	1922.38673	3844.77347
03/06/1999	45	14	634.45	0.01521	0.01521	366.96461	4439.65581	0.01521	366.96461	4439.65581	8879.3116
22/06/1999	64	19	804.97	0.01930	0.01930	465.59304	7909.29769	0.01930	465.59304	7909.29769	15818.5954
12/07/1999	84	20	560.36	0.01344	0.01344	324.11110	7897.04144	0.01344	324.11110	7897.04144	15794.0829
22/07/1999	94	10	638.7	0.01532	0.01532	369.42280	3467.66954	0.01532	369.42280	3467.66954	6935.3391
25/09/1999	128	34	614.24	0.01473	0.01473	355.27519	12319.86587	0.01473	355.27519	12319.86587	24639.7317
16/02/2000	193	65	673.06	0.01614	0.01614	389.29656	24198.58180	0.01614	389.29656	24198.58180	48397.1636
01/01/2001	513	320	770	0.01846	0.01846	445.36646	133546.08325	0.01846	445.36646	133546.08325	267092.1665
01/06/2001	664	151	770	0.01846	0.01846	445.36646	67250.33565	0.01846	445.36646	67250.33565	134500.6713
27/08/2002	1115	451	770	0.01846	0.01846	445.36646	200860.27404	0.01846	445.36646	200860.27404	401720.5481
TOTAL							467063.46304			467063.46304	934126.9261

Table 1: Theoretical gas production on the basis of the actual amounts of acetate removed in column 2

Appendix B

Total gas production (propionate removed) in column 2

date	days	days between samples	conc. propionate removed	moles of propionate removed	moles CH ₄	ml of CH ₄ per day	ml of CH ₄ total	moles CO ₂	ml of CO ₂	ml of CO ₂ total	total ml CH ₄ + CO ₂ per day
A	B	C	D	E	F	G	H	J	K	L	M
		B _i -B _{i+1}		D*1.44 / (1000*74.08)	E*1.75	F*24.12*1000	((G _i +G _{i+1})/2)C _i	E*1.25	I*24.12*1000	((J _i +J _{i+1})/2)C _i	(H _i +K _i)
21/04/1999	2	2	13.06	0.00025	0.00044	10.71569	21.43138	0.00032	7.65406	15.30813	36.73950
22/04/1999	3	1	15.35	0.00030	0.00052	12.59463	11.65516	0.00037	8.99616	8.32511	19.98027
27/04/1999	8	5	48.76	0.00095	0.00166	40.00742	131.50512	0.00118	28.57673	93.93223	225.43735
30/04/1999	11	3	49.8	0.00097	0.00169	40.86074	121.30224	0.00121	29.18624	86.64446	207.94670
07/05/1999	18	7	33.71	0.00066	0.00115	27.65895	239.81890	0.00082	19.75639	171.29921	411.11811
12/05/1999	23	5	31.79	0.00062	0.00108	26.08359	134.35634	0.00077	18.63114	95.96882	230.32516
20/05/1999	31	8	12.84	0.00025	0.00044	10.53518	146.47508	0.00031	7.52513	104.62506	251.10014
03/06/1999	45	14	55.35	0.00108	0.00188	45.41450	391.64772	0.00134	32.43893	279.74837	671.39609
22/06/1999	64	19	33.56	0.00065	0.00114	27.53587	693.02849	0.00082	19.66848	495.02035	1188.04883
12/07/1999	84	20	3.9	0.00008	0.00013	3.19994	307.35809	0.00009	2.28567	219.54149	526.89958
22/07/1999	94	10	10.39	0.00020	0.00035	8.52496	58.62449	0.00025	6.08926	41.87464	100.49913
25/09/1999	128	34	42.19	0.00082	0.00144	34.61676	733.40923	0.00103	24.72626	523.86374	1257.27297
16/02/2000	193	65	39.56	0.00077	0.00135	32.45885	2179.95733	0.00096	23.18489	1557.11238	3737.06971
01/01/2001	513	320	47.95	0.00093	0.00163	39.34282	11488.26744	0.00117	28.10201	8205.90531	19694.17275
01/06/2001	664	151	47.95	0.00093	0.00163	39.34282	5940.76577	0.00117	28.10201	4243.40412	10184.16989
27/08/2002	1115	451	95	0.00185	0.00323	77.94719	26448.89768	0.00231	55.67657	18892.06977	45340.96745
TOTAL							49048.50045			35034.64318	84083.14362

Table 2: Theoretical gas production on the basis of the actual amounts of propionate removed in column 2

Appendix B

Total gas production (acetate and propionate removed) in column 2

total ml CH ₄ + CO ₂ due to Ac. +Pr. (L _i +L _i)	cumulative CH ₄ + CO ₂ due to Ac. +Pr.	date
86.94445	86.94445	21/04/1999
65.00855	151.95300	22/04/1999
867.95077	1019.90377	27/04/1999
1063.98731	2083.89107	30/04/1999
3188.62580	5272.51687	07/05/1999
2363.57267	7636.08955	12/05/1999
4095.87361	11731.96315	20/05/1999
9550.70772	21282.67087	03/06/1999
17006.64421	38289.31508	22/06/1999
16320.98245	54610.29753	12/07/1999
7035.83821	61646.13574	22/07/1999
25897.00471	87543.14045	25/09/1999
52134.23330	139677.3737	16/02/2000
286786.33924	426463.713	01/01/2001
144684.84119	571148.554	01/06/2001
447061.51553	1018210.070	27/08/2002
1018210.06971		TOTAL

Table 3: Total gas production on the basis of the actual amounts of acetate and propionate removed in column 2

Appendix B

Total gas production (acetate removed) in column 1 since introduction of 200% strength leachate

date	days	days between samples	conc. acetate removed	moles of acetate removed	moles CH ₄	ml of CH ₄ per day	ml of CH ₄ total	moles CO ₂	ml of CO ₂	ml of CO ₂ total	total ml CH ₄ + CO ₂ per day
A	B	C	D	E	F	G	H	J	K	L	M
		Bi-Bi+1		D*1.44 / (1000*60.05)	E*1.0	F*24.12*1000	((Gi+Gi+1)/2)Ci	E*1.0	I*24.12*1000	((Ji+Ji+1)/2)Ci	(Hi+Ki)
05/06/2001	4	4	106	0.00254	0.0025419	61.310	245.241	0.00254	61.31019	245.241	490.482
07/06/2001	6	2	666	0.01597	0.0159707	385.213	446.523	0.01597	385.21307	446.523	893.047
15/06/2001	14	8	1302	0.03122	0.0312220	753.074	4553.149	0.03122	753.07420	4553.149	9106.298
02/07/2001	31	17	1510	0.03621	0.0362098	873.381	13824.869	0.03621	873.38098	13824.869	27649.738
07/07/2001	36	5	1653	0.03964	0.0396390	956.092	4573.682	0.03964	956.09190	4573.682	9147.364
18/07/2001	47	7	1647	0.03950	0.0394951	952.622	6680.497	0.03950	952.62151	6668.351	13348.847
12/08/2001	72	25	1630	0.03909	0.0390874	942.789	23692.628	0.03909	942.78874	23692.628	47385.256
07/11/2001	159	87	1450	0.03477	0.0347710	838.677	77493.764	0.03477	838.67710	77493.764	154987.529
18/12/2001	200	7	1498	0.03592	0.0359221	866.440	5967.911	0.03592	866.44021	5967.911	11935.821
09/04/2002	312	112	1540	0.03693	0.0369292	890.733	98401.695	0.03693	890.73292	98401.695	196803.390
08/05/2002	341	29	1540	0.03693	0.0369292	890.733	25831.255	0.03693	890.73292	25831.255	51662.510
05/07/2002	399	58	1540	0.03693	0.0369292	890.733	51662.510	0.03693	890.73292	51662.510	103325.019
15/07/2002	409	10	1540	0.03693	0.0369292	890.733	8907.329	0.03693	890.73292	8907.329	17814.658
09/01/2003	587	178	1540	0.03693	0.0369292	890.733	158550.460	0.03693	890.73292	158550.460	317100.920
23/01/2003	601	14	1540	0.03693	0.0369292	890.733	12470.261	0.03693	890.73292	12470.261	24940.522
TOTAL							493301.774			493289.628	986591.402

Table 4: Total gas production on the basis of the actual amounts of acetate removed in column 1 since introduction of 200% strength leachate

Appendix B

Total gas production (propionate removed) in column 1 since introduction of 200% strength leachate

date	days	days between samples	conc. propionate removed	moles of propionate removed	moles CH ₄	ml of CH ₄ per day	ml of CH ₄ total	moles CO ₂	ml of CO ₂	ml of CO ₂ total	total ml CH ₄ + CO ₂ per day
A	B	C	D	E	F	G	H	J	K	L	M
		Bi-Bi+1		D*1.44 / (1000*74.08)	E*1.75	F*24.12*1000	((Gi+Gi+1)/2)Ci	E*1.25	I*24.12*1000	((Ji+Ji+1)/2)Ci	(Hi+Ki)
05/06/2001	4	4	190	0.00369	0.00646	155.89438	623.578	0.00462	111.35313	445.413	1068.990
07/06/2001	6	2	190	0.00369	0.00646	155.89438	311.789	0.00462	111.35313	222.706	534.495
15/06/2001	14	8	190	0.00369	0.00646	155.89438	1247.155	0.00462	111.35313	890.825	2137.980
02/07/2001	31	17	190	0.00369	0.00646	155.89438	2650.205	0.00462	111.35313	1893.003	4543.208
07/07/2001	36	5	190	0.00369	0.00646	155.89438	779.472	0.00462	111.35313	556.766	1336.238
18/07/2001	47	11	190	0.00369	0.00646	155.89438	1714.838	0.00462	111.35313	1224.884	2939.723
12/08/2001	72	25	190	0.00369	0.00646	155.89438	3897.360	0.00462	111.35313	2783.828	6681.188
07/11/2001	159	87	190	0.00369	0.00646	155.89438	13562.811	0.00462	111.35313	9687.722	23250.534
18/12/2001	200	41	190	0.00369	0.00646	155.89438	6391.670	0.00462	111.35313	4565.478	10957.148
09/04/2002	312	112	190	0.00369	0.00646	155.89438	17460.171	0.00462	111.35313	12471.551	29931.722
08/05/2002	341	29	190	0.00369	0.00646	155.89438	4520.937	0.00462	111.35313	3229.241	7750.178
05/07/2002	399	58	190	0.00369	0.00646	155.89438	9041.874	0.00462	111.35313	6458.482	15500.356
15/07/2002	409	10	190	0.00369	0.00646	155.89438	1558.944	0.00462	111.35313	1113.531	2672.475
09/01/2003	587	178	190	0.00369	0.00646	155.89438	27749.200	0.00462	111.35313	19820.857	47570.058
23/01/2003	601	14	190	0.00369	0.00646	155.89438	2182.521	0.00462	111.35313	1558.944	3741.465
TOTAL							93692.525			66923.232	160615.757

Table 5: Total gas production on the basis of the actual amounts of propionate removed in column 1 since introduction of 200% strength leachate

Appendix B

Total gas production (acetate and propionate removed) in column 1 since introduction of 200% strength leachate

total ml CH ₄ + CO ₂ due to Ac. +Pr. (L _i +L _i)	cumulative CH ₄ + CO ₂ due to Ac. +Pr.	date
1559.472	1559.472	05/06/2001
1427.542	2987.013	07/06/2001
11244.278	14231.291	15/06/2001
32192.946	46424.237	02/07/2001
10483.602	56907.839	07/07/2001
16288.570	73196.409	18/07/2001
54066.444	127262.854	12/08/2001
178238.062	305500.916	07/11/2001
22892.969	328393.885	18/12/2001
226735.112	555128.998	09/04/2002
59412.687	614541.685	08/05/2002
118825.375	733367.060	05/07/2002
20487.134	753854.194	15/07/2002
364670.978	1118525.172	09/01/2003
28681.987	1147207.159	23/01/2003
1147207.159		TOTAL

Table 6: Total gas production on the basis of the actual amounts of acetate and propionate removed in column 1 since introduction of 200% strength leachate

Appendix C

Cumulative g VFA passed per litre pore volume in column 1

Operational regime	Date	Total days	Days after change to 1 ml/min	Litres passed	Litres passed since 200%	g VFA passed per litre pore volume	Total acetate passed (g)	Total propionate passed (g)	Acetate removed from leachate (g/l)	Propionate removed from leachate (g/l)
	01/05/1996									
	29/07/1996	89	since	64.08						
	25/02/1997	300	introduction	216.00						
	25/11/1997	573	of 25%	412.56						
25% strength	30/11/1997	578	0	416.16						
	20/03/1998	688	110	574.56						
50% strength	27/03/1998	695	117	584.64						
	28/04/1998	727	149	630.72		0.12538948	1.52064	1.93536		
	09/09/1998	861	283	823.68		0.65602948	7.88832	10.03968	0.033	0.042
	01/11/1998	914	336	900.00		0.97686876	11.7260712	12.3815592		
	04/11/1998	917	339	904.32		0.99502948	11.9433024	12.5141184		
	10/11/1998	923	345	912.96		1.04383606	12.5271072	12.6814752	0.06757	0.01937
	03/12/1998	946	368	946.08		1.56731519	18.77256216	13.7226024		
	06/04/1999	1070	492	1124.64		6.20050118	74.04955992	21.4899624	0.309571	0.0435
100% strength	05/05/1999	1099	521	1166.40		6.83335923	81.5434128	22.4218368		
	12/05/1999	1106	528	1176.48		6.87535183	82.0406592	22.4332272	0.04933	0.00113
	20/05/1999	1114	536	1188.00		6.97152949	83.1795264	22.651992	0.09886	0.01899
	03/06/1999	1128	550	1208.16		7.76485172	92.5734816	23.4519408	0.46597	0.03968
	22/06/1999	1147	569	1235.52		9.23434472	109.974168	24.1208928	0.63599	0.02445
	12/07/1999	1167	589	1264.32		10.5350197	125.375832	24.5315808	0.53478	0.01426
	22/07/1999	1177	599	1278.72		11.3708465	135.273096	24.8725728	0.68731	0.02368
	25/09/1999	1242	627	1319.04		13.5601312	161.1970416	25.5733344	0.642955	0.01738
	12/12/1999	1320	681	1396.80		17.8006528	210.7618488	28.8446976		
	16/02/2000	1386	715	1445.76		20.4473737	241.6977144	32.1132672	0.63186	0.06676
	10/06/2000	1501	830	1611.36		30.3780961	357.7717224	45.5069952		
	19/06/2000	1510	839	1624.32		31.1552831	366.8557752	46.5552		
	04/09/2000	1587	877	1679.04		34.7987266	408.9901752	51.7536	0.77	0.095

	02/12/2000	1676	916	1735.20		38.5380502	452.2333752	57.0888	0.77	0.095
	01/01/2001	1706	946	1778.40		38.5380502	452.2333752	57.0888		
	01/06/2001	1857	1097	1995.84		56.1089272	652.9261752	81.8496	0.77	0.095
200% strength	05/06/2001	1861	1101	2001.6	5.76	56.1623824	653.5367352	82.10592	0.106	0.0445
	07/06/2001	1863	1103	2004.48	8.64	56.3303124	655.4548152	82.3873536	0.666	0.09772
	15/06/2001	1871	1111	2016.00	20.16	57.643495	670.4538552	84.120192	1.302	0.15042
	22/06/2001	1878	1118	2026.08	30.24	58.8843113	684.0618552	86.0874048	1.350	0.19516
	28/06/2001	1884	1124	2034.72	38.88	59.9478682	696.4948152	87.9280704	1.439	0.21304
	02/07/2001	1888	1128	2040.48	44.64	60.7093527	705.1924152	89.3104704	1.51	0.24
	07/07/2001	1893	1133	2047.68	51.84	61.751351	717.0940152	90.6673824	1.653	0.18846
	16/07/2001	1902	1142	2060.64	64.8	63.6235439	738.4780152	93.1677552		
	18/07/2001	1904	1144	2063.52	67.68	64.0388303	743.2213752	93.7362672	1.647	0.1974
	02/08/2001	1919	1159	2085.12	89.28	67.1374041	778.6129752	97.6069872		
	12/08/2001	1929	1169	2099.52	103.68	69.2138362	802.0849752	99.9253872	1.63	0.161
	03/09/2001	1951	1191	2131.20	135.36	73.5332683	850.8721752	102.4756272		
	07/11/2001	2016	1256	2224.80	228.96	85.5493979	986.5921752	102.4756272	1.45	
	14/11/2001	2023	1263	2234.88	239.04	86.8772131	1001.450095	103.3821216		
	18/12/2001	2057	1297	2283.84	288	93.4316116	1074.792175	112.1880672	1.498	0.17986
	09/04/2002	2169	1409	2445.12	449.28	115.842184	1323.163375	143.6376672	1.54	0.195
	08/05/2002	2198	1438	2486.88	491.04	121.644921	1387.473775	151.7808672	1.54	0.195
	05/07/2002	2256	1496	2570.40	574.56	133.338936	1516.094575	168.0672672	1.54	0.195
	15/07/2002	2266	1506	2584.80	588.96	135.369086	1538.270575	170.8752672	1.54	0.195
	09/01/2003	2444	1684	2841.12	845.28	171.505747	1933.003375	220.8576672	1.54	0.195
	23/01/2003	2458	1698	2861.28	865.44	174.347957	1964.049775	224.7888672	1.54	0.195
						Total C	228.3542064	28.90526244		
							524.205216	69.41332566		

The total C passed was calculated using the following formula: $C = \frac{\sum acetate \times 24}{60} + \frac{\sum propionate \times 36}{74}$

Table 1: Number of pore volumes passed in column 1

Appendix C

Cumulative g VFA passed per litre pore volume in column 2

Operational regime	Date	Total days	Days after change to 1 ml/min	Litres passed	g VFA passed per litre pore volume	Total acetate passed (g)	Total propionate passed (g)	Acetate removed from leachate (g/l)	Propionate removed from leachate (g/l)
	07/05/1996								
	16/09/1996	132		95.04					
	25/02/1997	294		211.68					
	27/11/1997	569		409.68					
25% strength	30/11/1997	572	0	411.84					
	20/03/1998	682	110	570.24					
50% strength	27/03/1998	689	117	580.32					
	29/04/1998	722	150	627.84	1.7116	20.0059			
	09/09/1998	855	283	819.36	8.5893	100.6358		0.421	
	04/11/1998	911	339	900.00	11.2411	131.7234			
	10/11/1998	917	345	908.64	13.6488	159.9490		0.350	
	10/12/1998	947	375	951.84	15.0423	175.9153			
	06/04/1999	1064	492	1120.32	20.7646	241.4809		0.389	
100% strength	19/04/1999	1077	505	1139.04	21.4084	248.7660			
	21/04/1999	1079	507	1141.92	21.41390	248.82852	0.03744	0.022	0.013
	22/04/1999	1080	508	1143.36	21.42107	248.90937	0.05904	0.056	0.015
	27/04/1999	1085	513	1150.56	21.52709	250.10472	0.41011	0.166	0.049
	30/04/1999	1088	516	1154.88	21.65251	251.51874	0.62525	0.327	0.050
	07/05/1999	1095	523	1164.96	21.97320	255.13433	0.96504	0.359	0.034
	10/05/1999	1098	526	1169.28	22.04192	255.90910	1.03786		
	12/05/1999	1100	528	1172.16	22.13613	256.97130	1.12941	0.369	0.032
	20/05/1999	1108	536	1183.68	22.60828	262.29458	1.27733	0.462	0.013
	03/06/1999	1122	550	1203.84	23.74275	275.08509	2.39319	0.634	0.055
	22/06/1999	1141	569	1231.20	25.69618	297.10907	3.36611	0.805	0.036
	12/07/1999	1161	589	1260.00	27.12758	313.24744	3.47843	0.560	0.004
	22/07/1999	1171	599	1274.40	27.94334	322.44472	3.62804	0.639	0.010

	Date	Total days	Days after change to 1 ml/min	Litres passed	g VFA passed per litre pore volume	Total acetate passed (g)	Total propionate passed (g)	Acetate removed from leachate (g/l)	Propionate removed from leachate (g/l)
	25/09/1999	1205	633	1323.36	30.61071	352.51791	5.69367	0.614	0.042
	14/12/1999	1236	664	1368.00	33.2032	381.2504	7.5183		
	16/02/2000	1270	698	1416.96	36.1766	414.2035	9.4552	0.673	0.040
	10/06/2000	1385	813	1582.56	47.6819	541.7155	16.0792		
	19/06/2000	1394	822	1595.52	48.5823	551.6947	17.3104		
	05/09/2000	1472	900	1707.84	56.5631	638.9673	27.9808		
	01/01/2001	1590	1018	1877.76	68.6365	770.9951	44.1232		
	01/06/2001	1741	1169	2095.20	84.0865	939.9460	64.7800		
	10/04/2002	2054	1482	2545.92	116.1331	1285.4783	107.5984		
	26/08/2002	2192	1620	2744.64	130.2593	1438.4927	126.4768		
						475.8656918	61.5110322	0.770	0.095

The total C passed was calculated using the following formula: $C = \frac{\sum acetate \times 24}{60} + \frac{\sum propionate \times 36}{74}$

Table 2: Number of pore volumes passed in column 2

Appendix C

Cumulative g VFA passed per litre pore volume in Column 3

Column 3									
Date	Total days	Days after change to 1 ml/min	Litres passed	Litres passed since 200% strength	g VFA passed per litre pore volume	Total acetate passed (g)	Total propionate passed (g)	Total n-valeric acid Passed (g)	Acetate removed from leachate (g/l)
03/06/1996									
02/09/1996	91		131.04						
25/02/1997	267		384.48						
27/11/1997	542		780.48						
20/03/1998	655	113	943.20						
27/03/1998	662	120	953.28			1.93536			
29/04/1998	695	153	1000.8		0.15197484	3.83616			
09/09/1998	828	286	1192.32		0.62465552	11.49696			0.04
04/11/1998	884	342	1272.96		0.88879792	14.7935232			
10/11/1998	890	348	1281.60	328.32	0.91770811	15.1543296			0.04176
14/12/1998	924	382	1330.56		1.10156363	17.4265632			
06/04/1999	1037	495	1493.28	211.68	1.77383628	25.7350464			0.05106
19/04/1999	1050	508	1512.00		1.86930846	26.914968	1.278	1.7892	
20/04/1999	1051	509	1513.44		1.87672719	27.0057312			
22/04/1999	1053	511	1516.32		1.89438242	27.2217312			0.075
27/04/1999	1058	516	1523.52		1.95376874	27.9482832			0.10091
07/05/1999	1068	526	1537.92		2.12268224	30.0148272			0.14351
12/05/1999	1073	531	1545.12		2.19611035	30.9131712			0.12477
20/05/1999	1081	539	1556.64		2.34554424	32.7413952			0.1587
03/06/1999	1095	553	1576.8		2.55452099	35.2980864			0.12682
22/06/1999	1114	572	1604.16	110.88	2.91356368	39.6907344			0.16055
12/07/1999	1134	592	1632.96	28.8	3.27526054	44.1158544			0.15365
22/07/1999	1144	602	1647.36	14.4	3.459846	46.3741344			
25/09/1999	1169	627	1683.36	36	3.92130964	52.0198344			

Date	Total days	Days after change to 1 ml/min	Litres passed	Litres passed since 200% strength	g VFA passed per litre pore volume	Total acetate passed (g)	Total propionate passed (g)	Total n-valeric acid Passed (g)	Acetate removed from leachate (g/l)
15/12/1999	1230	688	1771.20		5.05766162	65.7953424			
16/02/2000	1283	741	1847.52	164.16	6.04498383	77.7642264			
10/06/2000	1398	856	2013.12	165.6	8.23065872	104.2602264			0.16
19/06/2000	1407	865	2026.08	12.96	8.40705694	106.3986264			
20/09/2000	1500	958	2160.00		10.2969141	129.1650264			0.17
02/12/2000	1573	1031	2265.12		11.7803503	129.1650264			0.17
06/03/2001	1667	1125	2400.48	374.4	13.701651	152.176226			0.17
09/05/2001	1731	1189	2492.64	92.16	15.009770	167.843426			0.17
12/07/2001	1795	1253	2584.80	92.16	16.317889	183.510626			0.17
27/08/2002	2206	1664	3176.64	591.84	24.718468	284.123426	8.316	11.6424	0.17
			2223.36		Total C	113.6493706	4.66735135	7.900941176	

The total C passed was calculated using the following formula:
$$C = \frac{\sum \text{acetate} \times 24}{60} + \frac{\sum \text{propionate} \times 36}{74} + \frac{\sum \text{iso-valeric} \times 60}{102}$$

Table 3: Number of pore volumes passed in Column 3

Appendix C

Cumulative g VFA passed per litre pore volume in Column 4

Column 4									
Date	Total days	Days after change to 1 ml/min	Litres passed	Litres passed since 200%	g VFA passed per litre pore volume	Total acetate passed (g)	Total propionate passed (g)	Acetate removed from leachate (g/l)	Propionate removed from leachate (g/l)
06/06/1996									
09/09/1996	95	since	136.8						
25/02/1997	264	introduction	380.16						
28/11/1997	540	of 25%	777.6						
20/03/1998	652	112	938.88						
27/03/1998	659	119	948.96						
30/04/1998	693	153	997.92		0.323940452				
09/09/1998	825	285	1188		1.569078775			0.084	
04/11/1998	881	341	1268.64		1.935294079				
10/11/1998	887	347	1277.28		1.957171591			0.03247	
15/12/1998	922	382	1327.68		2.167347551				
06/04/1999	1034	494	1488.96		3.09852008			0.07304	
04/05/1999	1062	522	1529.28		3.27255307	2.1829248			
07/05/1999	1065	525	1533.6		3.284690101	2.3351616		0.03524	
12/05/1999	1070	530	1540.8		3.340074201	3.0298536		0.096485	
20/05/1999	1078	538	1552.32		3.454556297	4.4658216		0.12465	
03/06/1999	1092	552	1572.48		3.654899963	6.9787656		0.12465	
22/06/1999	1111	571	1599.84		3.959862952	10.8039672		0.13981	
12/07/1999	1131	591	1628.64		4.355315244	15.7641912		0.17223	
22/07/1999	1141	601	1643.04		4.540280975	18.0842472			
25/09/1999	1206	636	1693.44		5.187661036	26.2044432			
16/12/1999	1288	688	1768.32		6.157348008	38.2687344			
16/02/2000	1350	740	1843.2		7.12703498	50.3330256			
10/06/2000	1465	855	2008.8		9.123590268	75.1730256		0.15	
19/06/2000	1474	864	2021.76		9.279842421	75.1730256		0.15	

Date	Total days	Days after change to 1 ml/min	Litres passed	Litres passed since 200%	g VFA passed per litre pore volume	Total acetate passed (g)	Total propionate passed (g)	Acetate removed from leachate (g/l)	Propionate removed from leachate (g/l)
22/09/2000	1569	959	2158.56		10.9387783	95.6930256		0.15	
30/05/2001	1819	1209	2518.56		15.32696091	149.6930256		0.15	high VFA, high SO4
05/06/2001	1825	1215	2527.2	8.64	15.35644923	150.0559056	0.6912		
07/06/2001	1827	1217	2530.08	2.88	15.36627876	150.1768656	0.9216		
15/06/2001	1835	1225	2541.6	11.52	15.40559652	150.6607056	1.8432	0.042	0.08
22/06/2001	1842	1232	2551.68	10.08	15.49406148	151.7493456	2.6496	0.108	0.08
28/06/2001	1848	1238	2560.32	8.64	15.52916662	152.1813456	3.3408	0.05	0.08
02/07/2001	1852	1242	2566.08		15.64243922	153.5752656	3.8016	0.242	0.08
07/07/2001	1857	1247	2573.28	12.96	15.78988083	155.3896656	4.3776	0.252	0.08
16/07/2001	1866	1256	2586.24	12.96	16.26327369	161.2151856	5.4144		
18/07/2001	1868	1258	2589.12		16.41469388	163.0785456	5.6448	0.647	0.08
02/08/2001	1883	1273	2610.72	24.48	17.06150615	171.0381456	7.3728		
12/08/2001	1893	1283	2625.12	14.4	17.16682159	172.3341456	8.5248	0.09	0.08
04/09/2001	1916	1306	2658.24		17.88172145	181.0943856	11.1744		
07/11/2001	1980	1370	2750.4	125.28	21.18341073	221.5526256	18.5472	0.439	0.08
15/11/2001	1988	1378	2761.92		21.62674793	226.9727856	19.4688		
18/12/2001	2021	1411	2809.44	59.04	23.57794985	250.8278256	23.2704	0.502	0.08
11/04/2002	2135	1525	2973.6		32.03443395	353.1815856	36.4032		
08/05/2002	2162	1552	3012.48	203.04	34.42757648	382.1471856	39.5136	0.745	0.08
04/07/2002	2219	1609	3094.56		39.69684223	445.3487856	46.08	0.77	0.08
10/01/2003	2409	1799	3368.16	355.68	57.40579274	656.0207856	67.968	0.77	0.08
						59.87721024			
						262.4083142	33.06551351		

The total C passed was calculated using the following formula: $C = \frac{\sum acetate \times 24}{60} + \frac{\sum propionate \times 36}{74}$

Table 4: Number of pore volumes passed in Column 4

Appendix D

Concentration of radionuclide analogues removed, inlet concentration - 20 µg/l

Inlet (µg/l)	cumulative g VFA	Co (µg/l)	Ni (µg/l)	Rb (µg/l)	Ru (µg/l)	Cs (µg/l)	Ba (µg/l)	Ce (µg/l)	Eu (µg/l)
20	13.91	19.47	16.92	19.25	20.00	19.99	-12.36	19.93	19.99
20	13.93	19.40	16.83	19.29	20.00	19.99	-10.73	19.91	19.99
20	13.95	19.46	16.99	19.32	20.00	19.99	-8.95	19.90	19.99
20	13.97	19.30	15.59	19.33	20.00	19.99	-9.12	19.91	19.98
20	13.99	19.40	15.19	19.30	20.00	20.00	-11.28	19.91	19.99
20	14.03	19.35	16.23	19.26	20.00	20.00	-11.51	19.90	19.98
20	14.05	19.30	16.60	19.02	19.99	19.99	-10.93	19.89	19.98
20	14.07	19.24	15.93	18.48	19.99	19.99	-10.41	19.91	19.98
20	14.09	19.21	16.54	18.53	19.99	19.99	-10.58	19.92	19.98
20	14.12	19.19	17.46	18.52	19.99	20.00	-8.77	19.89	19.98
20	14.16	19.22	17.68	18.68	19.99	20.00	-8.64	19.89	19.98
20	14.18	20.02	17.97	18.22	19.99	20.00	-8.19	19.90	19.98
20	14.20	19.23	16.78	18.07	19.99	19.99	-9.58	19.89	19.98
20	14.22	19.27	17.19	17.83	19.98	19.99	-7.32	19.91	19.98
20	14.24	19.23	17.37	17.61	19.98	20.00	-6.42	19.89	19.98
20	14.28	19.27	17.49	17.34	19.98	20.00	-6.19	19.89	19.98
20	14.30	19.18	17.38	17.13	19.98	20.00	-9.65	19.88	19.97
20	14.32	19.25	17.42	17.11	19.97	20.00	-12.09	19.89	19.97
20	14.34	19.24	17.33	16.89	19.97	19.99	-13.94	19.85	19.97
20	14.36	19.23	17.22	17.09	19.97	19.99	-12.89	19.84	19.96
20	14.41	19.21	17.04	17.23	19.98	20.00	-14.08	19.85	19.96
20	14.43	19.19	17.64	17.19	19.97	20.00	-14.14	19.87	19.97
20	14.45	19.21	17.82	17.25	19.98	20.00	-13.46	19.86	19.96
20	14.47	19.21	17.88	17.27	19.96	20.00	-12.26	19.85	19.96
20	14.49	19.08	17.50	17.11	19.98	19.99	-11.37	19.87	19.96
20	14.53	19.10	17.69	17.00	19.98	19.99	-13.47	19.87	19.96
20	14.55	19.13	17.60	16.81	19.98	19.99	-13.35	19.88	19.96
20	14.57	19.09	17.54	16.67	19.95	19.99	-12.26	19.86	19.96
20	14.59	19.08	17.56	16.35	19.97	19.99	-13.14	19.83	19.95
20	14.61	19.06	17.49	16.18	19.98	20.00	-12.12	19.87	19.96
20	14.65	18.98	17.20	16.10	19.99	19.99	-11.24	19.83	19.94
20	14.67	19.15	17.41	15.80	19.98	20.00	-11.21	19.86	19.96
20	14.70	19.16	17.56	15.50	19.99	19.99	-12.49	19.83	19.95
20	14.72	19.18	17.61	15.61	19.99	19.99	-12.04	19.83	19.95
20	14.74	19.27	17.81	15.12	19.99	19.99	-11.23	19.85	19.96
20	14.78	19.17	17.78	15.08	19.99	19.99	-9.53	19.87	19.96
20	14.80	19.17	17.49	14.58	19.97	19.99	-11.26	19.81	19.94
20	14.82	19.12	17.62	14.58	19.97	19.99	-10.74	19.83	19.95
20	14.84	19.16	17.73	14.01	19.98	19.99	-9.88	19.79	19.94
20	14.86	19.24	17.68	14.38	19.98	19.99	-10.95	19.77	19.93
20	14.90	18.99	17.56	12.36	19.96	19.99	-12.01	19.71	19.91
20	14.92	18.98	17.65	12.13	19.99	19.99	-12.20	19.72	19.91
20	14.94	19.24	17.84	11.72	19.99	19.99	-14.07	19.72	19.92
20	14.96	19.22	18.03	11.89	19.99	19.99	-14.93	19.71	19.92
20	14.99	19.17	17.96	11.54	19.99	19.99	-14.48	19.65	19.90

Inlet (µg/l)	cumulative g VFA	Co (mg/l)	Ni (mg/l)	Rb (mg/l)	Ru (mg/l)	Cs (mg/l)	Ba (mg/l)	Ce (mg/l)	Eu (mg/l)
20	15.01	19.08	17.90	11.48	19.99	19.99	-12.86	19.78	19.94
20	15.03	19.15	17.96	11.82	19.99	19.98	-11.58	19.74	19.92
aver. remov (microg/l)		19.22	17.33	16.36	19.98	19.99	-11.32	19.85	19.96
removed (mg)		1.77	1.60	1.51	1.84	1.84		1.83	1.84
molecular weight		58.93	58.71	170.94	101.07	265.82	137.34	280.24	303.92
molecular weight MeS		90.99	90.77	203.00	133.13	297.88	169.40	312.30	400.11
removed MeS (mg)		2.73	2.47	1.79	2.43	2.06		2.04	2.42

Table 1: Concentration of radionuclide analogues removed form the leachate, inlet concentration - 20 µg/l

Appendix D

Concentration of radionuclide analogues removed, inlet concentration - 200 µg/l

Inlet (µg/l)	cumulative g VFA	Co (µg/l)	Ni (µg/l)	Rb (µg/l)	Ru (µg/l)	Cs (µg/l)	Ba (µg/l)	Ce (µg/l)	Eu (µg/l)
200	15.05	198.95	197.47	191.59	199.99	199.98	167.92	199.53	199.88
200	15.09	199.05	197.79	191.79	199.99	199.99	167.36	199.51	199.78
200	15.11	199.02	197.60	191.39	199.98	199.98	168.72	196.91	198.14
200	15.15	198.42	196.95	190.71	199.97	199.98	166.43	197.21	198.45
200	15.19	197.64	195.49	188.24	199.97	199.96	167.40	197.53	198.74
200	15.21	197.72	195.75	187.38	199.96	199.92	168.25	198.12	199.09
200	15.25	197.88	195.77	186.38	199.97	199.94	165.67	198.30	199.23
200	15.30	197.58	195.45	183.90	199.95	199.93	164.58	198.05	199.13
200	15.32	197.78	195.46	180.20	199.95	199.86	164.38	197.71	198.93
200	15.36	197.94	195.66	176.23	199.96	199.76	164.73	196.69	198.22
200	15.40	197.73	195.77	172.32	199.94	199.65	165.76	195.80	197.58
200	15.42	198.17	196.19	178.00	199.96	199.82	166.17	196.64	198.08
200	15.46	198.08	194.47	173.19	199.95	199.71	165.21	196.69	198.14
200	15.50	198.00	195.56	173.76	199.95	199.77	164.80	197.39	198.58
200	15.52	198.33	195.80	172.54	199.95	199.70	164.86	198.15	199.05
200	15.57	198.38	194.83	174.10	199.95	199.77	164.09	198.74	199.41
200	15.61	198.16	195.20	173.96	199.96	199.79	164.64	198.70	199.36
200	15.63	198.43	196.43	174.06	199.96	199.78	163.88	198.88	199.49
200	15.67	197.77	194.77	177.44	199.99	199.80	166.97	199.32	199.68
200	15.71	195.58	192.36	177.54	199.98	199.84	168.46	199.34	199.68
200	15.73	196.02	192.28	175.48	199.98	199.79	166.67	199.41	199.74
200	15.77	195.56	191.89	168.73	199.98	199.65	166.20	199.38	199.70
200	15.81	197.14	194.26	169.52	199.99	199.73	166.66	199.39	199.72
200	15.84	196.47	192.85	170.80	199.99	199.81	165.83	199.34	199.65
200	15.88	198.12	194.30	169.37	199.99	199.83	164.93	199.24	199.54
200	15.92	196.28	192.08	168.01	199.99	199.83	164.72	199.40	199.65
200	15.94	196.30	192.53	166.85	199.99	199.80	163.69	199.40	199.65
200	15.98	196.25	192.16	165.98	199.99	199.83	164.61	199.43	199.66
200	16.02	195.35	190.89	163.01	199.98	199.76	164.91	199.32	199.56
200	16.04	195.54	190.93	163.64	199.99	199.78	163.98	199.43	199.62
200	16.08	195.09	190.25	162.97	199.98	199.79	161.81	199.39	199.59
200	16.13	194.66	189.49	162.90	199.98	199.79	160.72	199.41	199.62
200	16.15	193.65	188.41	161.43	199.97	199.79	163.26	199.33	199.47
200	16.19	193.28	187.55	157.59	199.98	199.72	163.13	199.39	199.58
200	16.23	191.85	185.31	155.12	199.98	199.77	163.44	199.41	199.61
200	16.25	191.97	185.75	153.43	199.98	199.62	163.01	199.44	199.64
200	16.29	189.59	181.78	146.94	199.98	199.49	163.01	199.58	199.73
200	16.33	192.23	184.57	143.06	199.98	199.56	162.57	199.55	199.74
200	16.35	190.17	181.99	137.23	199.98	199.20	162.36	199.54	199.74
aver. remov (microg/l)		196.31	192.67	171.20	199.97	199.78	165.02	198.67	199.28
removed (mg)		18.09	17.76	15.78	18.43	18.41	15.21	18.31	18.37
molecular weight		58.93	58.71	170.94	101.07	265.82	137.34	280.24	303.92
molecular weight MeS		90.99	90.77	203.00	133.13	297.88	169.40	312.30	400.11
removed MeS (mg)		27.93	27.45	18.74	24.28	20.63	18.76	20.40	24.18

Table 2: Concentration of radionuclide analogues removed from the leachate, inlet concentration - 200 µg/l

Appendix D

Concentration of radionuclide analogues removed, inlet concentration - 2000 µg/l

Inlet (µg/l)	cumulative g VFA	Co (µg/l)	Ni (µg/l)	Rb (µg/l)	Ru (µg/l)	Cs (µg/l)	Ba (µg/l)	Ce (µg/l)	Eu (µg/l)
2,000.00	16.35	1,991.06	1,983.44	1,933.96	1,999.90	1,998.65	1,959.68	1,999.37	1,999.65
2,000.00	16.37	1,990.57	1,983.06	1,930.57	1,999.88	1,997.68	1,960.46	1,999.38	1,999.65
2,000.00	16.39	1,988.36	1,981.15	1,926.37	1,999.89	1,997.12	1,960.79	1,999.43	1,999.65
2,000.00	16.44	1,987.36	1,979.85	1,921.96	1,999.90	1,996.11	1,959.85	1,999.40	1,999.64
2,000.00	16.46	1,988.27	1,980.47	1,919.07	1,999.91	1,996.15	1,957.35	1,999.35	1,999.63
2,000.00	16.48	1,987.92	1,980.53	1,909.36	1,999.87	1,995.04	1,953.79	1,999.33	1,999.60
2,000.00	16.52	1,990.01	1,983.32	1,909.81	1,999.89	1,994.90	1,956.83	1,999.35	1,999.62
2,000.00	16.54	1,991.26	1,985.21	1,916.57	1,999.92	1,996.42	1,959.34	1,999.32	1,999.62
2,000.00	16.58	1,993.18	1,987.96	1,917.70	1,999.93	1,996.54	1,960.64	1,999.22	1,999.55
2,000.00	16.60	1,996.27	1,992.40	1,915.22	1,999.01	1,997.76	1,966.49	1,999.46	1,999.63
2,000.00	16.64	1,996.64	1,993.14	1,908.42	1,998.93	1,997.28	1,965.98	1,999.45	1,999.62
2,000.00	16.66	1,996.75	1,993.18	1,903.34	1,998.84	1,997.25	1,964.03	1,999.45	1,999.61
2,000.00	16.68	1,996.56	1,992.71	1,895.57	1,998.92	1,996.74	1,964.62	1,999.44	1,999.62
2,000.00	16.73	1,996.96	1,993.30	1,881.54	1,999.10	1,996.17	1,965.40	1,999.44	1,999.61
2,000.00	16.75	1,997.29	1,993.64	1,874.67	1,999.22	1,995.98	1,963.07	1,999.43	1,999.61
2,000.00	16.79	1,997.51	1,993.83	1,849.92	1,999.23	1,995.37	1,965.04	1,999.45	1,999.61
2,000.00	16.81	1,997.58	1,994.02	1,846.43	1,999.30	1,994.87	1,965.81	1,999.48	1,999.63
2,000.00	16.83	1,997.90	1,994.38	1,835.83	1,999.37	1,995.15	1,964.95	1,999.48	1,999.63
2,000.00	16.87	1,998.19	1,994.94	1,827.38	1,999.38	1,993.77	1,964.62	1,999.49	1,999.64
2,000.00	16.89	1,997.70	1,992.81	1,818.93	1,999.44	1,987.13	1,953.00	1,999.32	1,999.53
2,000.00	16.93	1,997.41	1,991.68	1,810.47	1,999.52	1,980.89	1,945.34	1,999.16	1,999.43
2,000.00	16.95	1,997.55	1,991.86	1,766.87	1,999.65	1,972.29	1,943.14	1,999.13	1,999.39
2,000.00	16.97	1,997.64	1,992.19	1,723.27	1,999.76	1,966.37	1,943.91	1,999.11	1,999.36
2,000.00	17.02	1,997.76	1,992.44	1,679.67	1,999.84	1,972.79	1,945.08	1,999.16	1,999.38
2,000.00	17.04	1,997.93	1,992.98	1,655.18	1,999.92	1,966.07	1,945.84	1,999.18	1,999.37
2,000.00	17.08	1,998.40	1,993.89	1,630.69	1,999.99	1,972.05	1,959.27	1,999.40	1,999.58
2,000.00	17.10	1,998.33	1,993.89	1,606.21	1,999.99	1,963.91	1,957.94	1,999.43	1,999.58
2,000.00	17.12	1,998.37	1,993.82	1,599.58	1,999.99	1,969.06	1,956.53	1,999.43	1,999.59
2,000.00	17.16	1,998.39	1,993.75	1,592.95	1,999.99	1,959.22	1,955.69	1,999.44	1,999.60
2,000.00	17.18	1,998.40	1,993.89	1,586.32	1,999.99	1,954.98	1,955.51	1,999.42	1,999.59
2,000.00	17.22	1,998.41	1,993.92	1,579.69	1,999.97	1,941.48	1,955.71	1,999.38	1,999.56
2,000.00	17.24	1,998.57	1,994.28	1,573.06	1,999.96	1,950.44	1,958.10	1,999.40	1,999.59
2,000.00	17.26	1,998.48	1,994.13	1,562.72	1,999.96	1,954.71	1,957.44	1,999.40	1,999.61
2,000.00	17.31	1,998.53	1,994.20	1,552.39	1,999.96	1,956.78	1,956.53	1,999.41	1,999.61
2,000.00	17.33	1,998.54	1,994.35	1,542.05	1,999.95	1,959.01	1,957.40	1,999.40	1,999.61
2,000.00	17.37	1,998.51	1,994.29	1,553.19	1,999.94	1,959.91	1,956.68	1,999.41	1,999.62
2,000.00	17.39	1,998.51	1,994.31	1,564.33	1,999.93	1,961.61	1,957.57	1,999.42	1,999.63
2,000.00	17.41	1,998.56	1,994.35	1,575.47	1,999.92	1,962.59	1,957.62	1,999.38	1,999.61
2,000.00	17.45	1,998.57	1,994.31	1,586.60	1,999.89	1,963.83	1,958.37	1,999.32	1,999.59
2,000.00	17.47	1,998.53	1,994.17	1,571.78	1,999.87	1,965.30	1,958.07	1,999.32	1,999.59
2,000.00	17.51	1,998.54	1,994.15	1,556.96	1,999.87	1,965.01	1,957.78	1,999.34	1,999.61
2,000.00	17.53	1,998.61	1,994.36	1,542.15	1,999.84	1,959.14	1,956.98	1,999.27	1,999.55
2,000.00	17.55	1,998.61	1,994.19	1,527.33	1,999.83	1,959.60	1,957.38	1,999.26	1,999.55
2,000.00	17.60	1,998.73	1,994.79	1,498.53	1,999.89	1,960.90	1,960.98	1,999.32	1,999.58
2,000.00	17.62	1,998.73	1,994.56	1,469.74	1,999.88	1,947.19	1,959.81	1,999.30	1,999.57
2,000.00	17.66	1,998.82	1,994.97	1,440.95	1,999.86	1,950.69	1,960.86	1,999.28	1,999.54
2,000.00	17.68	1,998.82	1,994.68	1,400.02	1,999.85	1,947.79	1,960.80	1,999.24	1,999.50

Inlet (µg/l)	cumulative g VFA	Co (µg/l)	Ni (µg/l)	Rb (µg/l)	Ru (µg/l)	Cs (µg/l)	Ba (µg/l)	Ce (µg/l)	Eu (µg/l)
2,000.00	17.70	1,998.82	1,994.79	1,359.09	1,999.86	1,941.92	1,960.71	1,999.24	1,999.52
2,000.00	17.74	1,998.81	1,994.89	1,318.16	1,999.86	1,944.92	1,961.34	1,999.28	1,999.51
2,000.00	17.76	1,998.72	1,994.57	1,318.73	1,999.69	1,933.98	1,956.68	1,999.17	1,999.44
2,000.00	17.80	1,998.81	1,994.64	1,319.29	1,999.77	1,929.08	1,956.67	1,999.27	1,999.49
2,000.00	17.82	1,998.80	1,994.45	1,319.86	1,999.83	1,922.82	1,956.23	1,999.28	1,999.49
2,000.00	17.84	1,998.79	1,994.47	1,320.42	1,999.86	1,916.47	1,954.85	1,999.29	1,999.49
2,000.00	17.89	1,998.76	1,994.39	1,267.89	1,999.88	1,912.28	1,954.10	1,999.25	1,999.44
2,000.00	17.91	1,998.78	1,994.42	1,215.35	1,999.89	1,903.45	1,954.74	1,999.23	1,999.46
2,000.00	17.95	1,998.74	1,994.49	1,162.81	1,999.91	1,900.03	1,954.28	1,999.24	1,999.42
2,000.00	17.97	1,998.78	1,994.58	1,137.79	1,999.91	1,878.54	1,953.24	1,999.25	1,999.43
2,000.00	17.99	1,998.83	1,994.53	1,112.77	1,999.91	1,884.34	1,955.89	1,999.31	1,999.49
2,000.00	18.03	1,998.83	1,994.62	1,087.75	1,999.90	1,879.63	1,955.78	1,999.30	1,999.48
2,000.00	18.05	1,998.79	1,994.46	1,062.73	1,999.88	1,874.50	1,955.38	1,999.25	1,999.41
2,000.00	18.09	1,998.77	1,994.38	1,074.29	1,999.87	1,864.41	1,954.23	1,999.19	1,999.38
2,000.00	18.11	1,998.78	1,994.40	1,085.85	1,999.88	1,817.29	1,951.44	1,999.17	1,999.39
2,000.00	18.14	1,998.73	1,994.37	1,097.42	1,999.88	1,815.62	1,949.97	1,999.17	1,999.34
2,000.00	18.18	1,998.75	1,994.38	1,108.98	1,999.89	1,797.83	1,950.31	1,999.17	1,999.36
2,000.00	18.20	1,998.80	1,994.43	1,091.45	1,999.90	1,818.04	1,951.17	1,999.20	1,999.40
2,000.00	18.24	1,998.80	1,994.66	1,073.92	1,999.91	1,816.17	1,951.98	1,999.25	1,999.41
2,000.00	18.26	1,998.80	1,994.78	1,056.40	1,999.91	1,804.40	1,952.98	1,999.26	1,999.42
2,000.00	18.28	1,998.75	1,994.68	1,052.13	1,999.90	1,788.61	1,952.24	1,999.25	1,999.43
2,000.00	18.32	1,999.02	1,996.31	1,047.87	1,999.30	1,785.00	1,955.73	1,999.43	1,999.59
2,000.00	18.34	1,998.99	1,996.01	1,043.61	1,999.42	1,780.14	1,955.49	1,999.44	1,999.60
2,000.00	18.38	1,998.92	1,995.79	945.16	1,999.50	1,600.06	1,955.46	1,999.43	1,999.60
2,000.00	18.40	1,998.89	1,995.44	933.08	1,999.56	1,497.68	1,955.70	1,999.44	1,999.61
2,000.00	18.43	1,998.87	1,995.12	986.20	1,999.65	1,547.51	1,956.31	1,999.46	1,999.63
2,000.00	18.47	1,999.23	1,997.28	958.38	1,999.59	1,527.06	1,949.52	1,999.34	1,999.53
2,000.00	18.49	1,998.64	1,993.75	930.55	1,999.67	1,506.60	1,943.56	1,999.08	1,999.35
2,000.00	18.53	1,998.61	1,993.46	902.73	1,999.76	1,486.15	1,938.91	1,999.13	1,999.37
2,000.00	18.55	1,998.54	1,992.80	916.56	1,999.81	1,495.07	1,932.78	1,999.07	1,999.29
2,000.00	18.57	1,998.42	1,992.55	930.39	1,999.85	1,503.99	1,928.88	1,998.87	1,999.18
2,000.00	18.61	1,998.42	1,992.28	944.22	1,999.91	1,512.91	1,925.17	1,998.87	1,999.17
2,000.00	18.63	1,998.41	1,992.56	958.05	1,999.93	1,521.83	1,922.71	1,998.86	1,999.14
2,000.00	18.67	1,998.86	1,994.29	964.30	1,999.97	1,526.23	1,944.54	1,999.17	1,999.39
2,000.00	18.69	1,998.82	1,994.08	970.54	1,999.97	1,530.63	1,943.26	1,999.18	1,999.39
2,000.00	18.72	1,998.80	1,993.98	976.78	1,999.97	1,535.03	1,943.52	1,999.22	1,999.41
2,000.00	18.76	1,998.82	1,993.88	942.28	1,999.98	1,528.11	1,944.59	1,999.23	1,999.42
2,000.00	18.78	1,998.84	1,994.16	907.78	1,999.98	1,521.19	1,941.65	1,999.15	1,999.37
2,000.00	18.82	1,997.74	1,991.97	873.29	1,999.97	1,514.27	1,945.14	1,998.83	1,999.24
2,000.00	18.84	1,998.85	1,994.19	838.79	1,999.98	1,507.35	1,940.11	1,999.05	1,999.31
2,000.00	18.86	1,998.81	1,993.99	863.68	1,999.98	1,502.54	1,941.38	1,999.03	1,999.29
2,000.00	18.90	1,998.33	1,993.64	888.58	1,999.95	1,497.74	1,862.54	1,997.61	1,998.30
2,000.00	18.92	1,998.79	1,994.18	913.47	1,999.98	1,492.94	1,946.36	1,999.13	1,999.38
2,000.00	18.96	1,998.76	1,993.72	938.37	1,999.99	1,488.14	1,942.22	1,999.12	1,999.35
2,000.00	18.98	1,998.75	1,993.75	934.10	1,999.99	1,465.03	1,942.81	1,999.14	1,999.39
2,000.00	19.01	1,998.85	1,994.02	929.84	1,999.99	1,441.93	1,948.17	1,999.22	1,999.47
2,000.00	19.05	1,998.89	1,994.30	925.57	1,999.99	1,418.82	1,952.23	1,999.31	1,999.51
2,000.00	19.07	1,999.46	1,997.87	909.26	1,999.86	1,387.47	1,958.06	1,999.47	1,999.60
2,000.00	19.11	1,999.44	1,997.70	892.95	1,999.85	1,356.12	1,954.95	1,999.37	1,999.50
2,000.00	19.13	1,999.46	1,997.71	876.64	1,999.85	1,324.76	1,958.34	1,999.42	1,999.54
2,000.00	19.15	1,999.46	1,997.79	847.37	1,999.85	1,302.22	1,955.60	1,999.41	1,999.54
2,000.00	19.19	1,999.47	1,997.68	860.33	1,999.85	1,293.41	1,956.32	1,999.40	1,999.51
2,000.00	19.21	1,999.49	1,997.74	834.42	1,999.85	1,311.04	1,955.61	1,999.41	1,999.54

Inlet (µg/l)	cumulative g VFA	Co (µg/l)	Ni (µg/l)	Rb (µg/l)	Ru (µg/l)	Cs (µg/l)	Ba (µg/l)	Ce (µg/l)	Eu (µg/l)
2,000.00	19.25	1,999.53	1,997.83	840.52	1,999.86	1,307.99	1,956.86	1,999.47	1,999.57
2,000.00	19.27	1,999.51	1,998.14	859.57	1,999.85	1,296.12	1,956.81	1,999.45	1,999.56
2,000.00	19.30	1,999.52	1,998.16	878.62	1,999.85	1,284.26	1,957.87	1,999.48	1,999.59
2,000.00	19.34	1,999.50	1,997.94	897.67	1,999.85	1,272.39	1,955.76	1,999.43	1,999.54
2,000.00	19.36	1,999.51	1,997.86	890.53	1,999.84	1,236.16	1,955.04	1,999.46	1,999.57
2,000.00	19.40	1,999.49	1,997.56	883.39	1,999.87	1,199.94	1,956.13	1,999.50	1,999.59
2,000.00	19.42	1,999.45	1,997.50	839.36	1,999.87	1,096.91	1,949.49	1,999.44	1,999.55
2,000.00	19.44	1,999.44	1,997.47	746.48	1,999.90	1,065.14	1,953.83	1,999.49	1,999.59
2,000.00	19.48	1,999.29	1,997.05	742.98	1,999.90	973.78	1,948.00	1,999.22	1,999.41
2,000.00	19.50	2,000.00	2,000.00	812.98	2,000.00	1,098.49	2,000.00	2,000.00	2,000.00
2,000.00	19.52	1,999.41	1,997.21	882.98	1,999.95	1,223.19	1,946.64	1,999.40	1,999.51
2,000.00	19.54	1,999.38	1,997.71	907.53	1,999.98	1,203.80	1,951.40	1,999.39	1,999.50
2,000.00	19.56	1,999.38	1,997.11	823.98	1,999.97	1,102.11	1,951.18	1,999.33	1,999.46
2,000.00	19.59	1,999.45	1,997.72	817.00	1,999.98	1,082.00	1,937.98	1,999.88	1,999.86
2,000.00	19.63	1,999.38	1,997.66	825.97	1,999.96	1,096.45	1,956.05	1,999.38	1,999.48
2,000.00	19.65	1,999.48	1,997.91	842.06	1,999.95	1,115.12	1,951.83	1,999.28	1,999.37
2,000.00	19.67	1,999.41	1,997.78	849.86	1,999.95	1,126.15	1,951.91	1,999.24	1,999.34
2,000.00	19.69	1,999.34	1,997.59	857.66	1,999.94	1,137.18	1,948.99	1,999.11	1,999.24
2,000.00	19.73	1,999.32	1,997.35	865.46	1,999.94	1,148.21	1,948.93	1,999.21	1,999.35
2,000.00	19.75	1,999.31	1,997.39	873.26	1,999.93	1,159.25	1,943.79	1,999.15	1,999.28
2,000.00	19.77	1,999.36	1,997.46	881.07	1,999.94	1,170.28	1,948.31	1,999.17	1,999.32
2,000.00	19.79	1,999.36	1,997.47	888.87	1,999.94	1,181.31	1,948.18	1,999.20	1,999.31
2,000.00	19.83	1,999.34	1,997.42	896.67	1,999.94	1,192.35	1,949.32	1,999.24	1,999.38
2,000.00	19.85	1,999.47	1,997.93	904.47	1,999.94	1,203.38	1,957.78	1,999.33	1,999.43
2,000.00	19.88	1,999.43	1,997.84	912.28	1,999.93	1,214.41	1,952.73	1,999.24	1,999.40
2,000.00	19.90	1,999.44	1,997.90	920.08	1,999.94	1,225.44	1,954.54	1,999.30	1,999.41
2,000.00	19.94	1,999.44	1,997.79	798.51	1,999.94	1,071.78	1,956.69	1,999.37	1,999.43
2,000.00	19.96	1,999.44	1,997.75	753.79	1,999.85	1,019.58	1,953.46	1,999.28	1,999.36
2,000.00	19.98	1,999.48	1,998.01	709.07	1,999.72	967.39	1,957.71	1,999.27	1,999.34
2,000.00	20.00	1,999.11	1,996.25	819.38	1,999.44	1,091.63	1,947.27	1,999.21	1,999.37
2,000.00	20.04	1,999.06	1,996.35	831.30	1,999.53	1,100.05	1,949.09	1,999.17	1,999.34
2,000.00	20.06	1,999.20	1,996.55	832.05	1,999.48	1,108.75	1,950.59	1,999.33	1,999.46
2,000.00	20.08	1,999.40	1,996.88	757.97	1,999.48	1,127.11	1,952.50	1,999.40	1,999.48
2,000.00	20.10	1,999.43	1,997.62	683.89	1,999.94	1,145.47	1,953.49	1,999.45	1,999.54
aver. remov (microg/l)		20.12	1,994.39	1,216.06	1,999.81	1,631.68	1,952.85	1,999.29	1,999.48
removed (mg)		1,182.59	1,180.36	719.71	1,183.57	965.69	1,155.78	1,183.26	1,183.37
molecular weight		58.93	58.71	170.94	101.07	265.82	137.34	280.24	303.92
molecular weight MeS		90.99	90.77	203.00	133.13	297.88	169.40	312.30	400.11
removed MeS (mg)		1,825.96	1,824.93	854.69	1,559.00	1,082.16	1,425.57	1,318.63	1,557.91
20 microg		2.73	2.47	1.79	2.43	2.06		2.04	2.42
200 microg		27.93	27.45	18.74	24.28	20.63	18.76	20.4	24.18
Total (gram)		1,856.62	1,854.85	875.22	1,585.71	1,104.85	1,444.33	1,341.07	1,584.51
Volume		1.16	1.16	0.55	0.99	0.69	0.90	0.84	0.99

Table 3: Concentration of radionuclide analogues removed form the leachate, inlet concentration - 2000 µg/l

Appendix E

XRF data for 10 samples of clean aggregate, representing the filter layer

Compound	Units	Sample 1	Sample 2	Sample 3	Sample 4	Sample 5	Sample 6	Sample 7	Sample 8	Sample 9	Sample 10	Average	Stand. Deviation
SiO ₂	(%)	98.88	98.75	97.99	96.88	98.27	97.11	98.11	97.69	97.88	96.55	97.81	0.8
TiO ₂	(%)	0.13	0.13	0.13	0.14	0.13	0.13	0.13	0.13	0.14	0.13	0.13	2.4
Al ₂ O ₃	(%)	0.73	0.88	0.82	0.86	0.94	0.79	0.85	1.09	0.99	1.18	0.91	15.2
Fe ₂ O ₃	(%)	0.94	0.89	1.13	2.34	2.20	1.41	0.79	1.03	0.85	1.10	1.27	43.9
MnO	(%)	0.01	0.01	0.01	0.01	0.01	0.01	0.01	0.01	0.01	0.01	0.01	11.2
MgO	(%)	0.02	0.04	0.03	0.03	0.03	0.03	0.04	0.09	0.06	0.12	0.05	63.5
CaO	(%)	0.16	0.17	0.17	0.17	0.18	0.18	0.17	0.19	0.18	0.20	0.18	6.6
K ₂ O	(%)	< 0.01	< 0.01	< 0.01	< 0.01	< 0.01	< 0.01	< 0.01	< 0.01	< 0.01	< 0.01		
Na ₂ O	(%)	0.15	0.16	0.15	0.16	0.16	0.16	0.16	0.18	0.16	0.18	0.16	6.1
P ₂ O ₅	(%)	0.04	0.03	0.04	0.07	0.07	0.04	0.04	0.04	0.04	0.05	0.04	27.8
Sum	(%)	101.1	101.0	100.5	100.6	102.0	99.9	100.3	100.5	100.3	99.5	100.56	0.7
Co	(ppm)	98	148	107	120	141	160	164	150	123	133	134.40	16.5
Cr	(ppm)	53	36	52	80	57	47	43	42	58	48	51.51	23.3
V	(ppm)	18	11	15	32	27	19	5	13	8	19	16.70	48.6
Ni	(ppm)	6	6	7	12	17	9	6	6	6	9	8.34	43.5
Cu	(ppm)	<2	<2	<2	<2	<2	<2	<2	<2	<2	<2		
Zn	(ppm)	220	199	232	414	361	240	182	193	167	216	242.40	33.3
As	(ppm)	3	3	3	7	6	4	2	3	2	4	3.52	49.0
Pb	(ppm)	5	6	5	5	5	5	7	5	7	6	5.54	13.7
Ba	(ppm)	138	154	126	134	143	143	128	122	159	92	133.90	14.0
Rb	(ppm)	<2	<2	<2	<2	<2	<2	<2	<2	<2	<2		
Sr	(ppm)	14	16	14	15	16	17	19	14	21	14	15.95	13.8
Ce	(ppm)	<5	<5	14	<5	14	<5	8	16	<5	15	13.12	23.2
S	(ppm)	<20	<20	<20	<20	<20	<20	<20	<20	<20	<20		
Cl	(%)	0.009	0.016	0.011	0.018	0.017	0.016	0.016	0.019	0.023	0.021	0.02	25.3

Table 1: XRF data for 10 samples of clean aggregate, representing the filter layer, 6 mm size particles